Synthesis of perfluoroalkylated monomers for speciality coating applications

ROBERT ALAN GOODWILL

Durham University

A Thesis Entitled

Synthesis of perfluoroalkylated monomers for speciality coating applications

By

ROBERT ALAN GOODWILL

(Van Mildert College)

A candidate for the degree of Doctor of Philosophy

Department of Chemistry, Durham University

2014

Abstract

This thesis is concerned with the synthesis of a range of perfluoroalkylated monomers that can be used as 'drop in' additives in commercial paint coatings, with the aim of improving coating lifetime and performance. The potential of 1*H*,1*H*,2*H*,2*H*-perfluorooctyl iodide as a building block for the creation of side chain fluorinated monomers was investigated through reaction of 1*H*,1*H*,2*H*,2*H*-perfluorooctyl iodide with oxygen and nitrogen nucleophiles, where $E2_{CB}$ elimination competes with nucleophilic substitution.

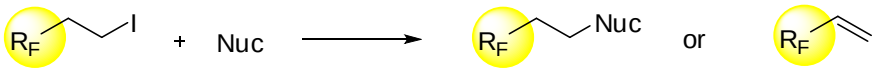

Other potential 'side chain' monomers synthesised include perfluoroalkylated anhydride systems and perfluoroalkylated epoxides, formed via reaction of perfluoroalkylated alcohols with epichlorohydrin.

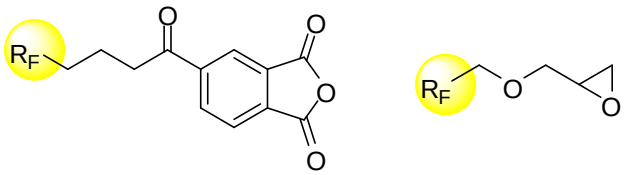

'Main chain' fluorinated epoxides are also potentially useful coating additives and were synthesised in good yield by reaction of 2,2,3,3,4,4,5,5-octafluorohexane-1,6-diol with either epichlorohydrin or by a two-step process involving reaction with allyl bromide and subsequent oxidation of the alkene. Synthesised monomers were introduced into existing paint coating formulations as 'drop-in' additives and the effect of incorporating a perfluoroalkyl group upon the lifetime, colour and stability of a coating system was analysed.

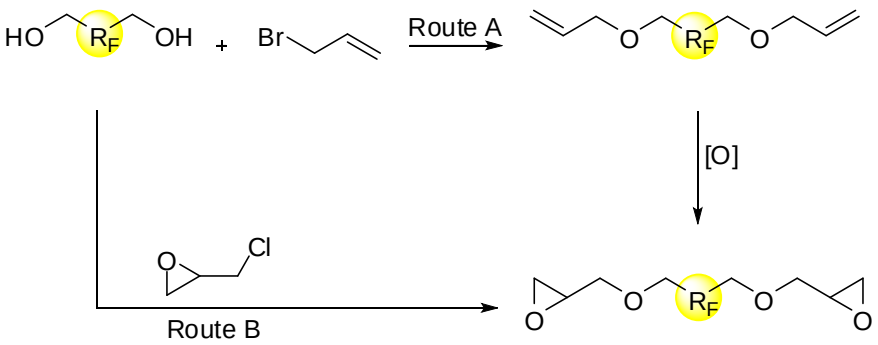

Acknowledgements

Primarily, thanks must go to my supervisor, Graham Sandford, for his helpful comments and support throughout this period of work. I would also like to thank; Dr. Alison Parry, Dr. Doug Beaumont, Mr. Laurent Mialon, Dr. David Ring, Dr. Tom Straw and Dr. Trevor Wills from AkzoNobel for insightful discussion into the background, synthesis and testing of paint coatings as well as supervising work undertaken at the Felling site and providing funding for this PhD.

This research would not have been possible without the input and help of analytical and technical staff at Durham, who are; Mrs. Catherine Heffernan, Dr. Alan Kenwright, Mr. Ian McKeag, Dr Juan Malavia (NMR); Dr Jackie Mosley, Dr David Parker, Mr Peter Stokes (Mass spectrometry); Miss Judith Magee (Elemental analysis) and Dr Dmitri Yufit (X-ray crystallography). Finally, I would like to thank all members of the Durham Fluorine group with whom I have shared a laboratory over the past few years for making this an enjoyable period.

Memorandum

The work in this thesis was carried out at Durham University between October 2010 and December 2013. This thesis is the work of the author, except where acknowledged by reference, and has not been submitted for any other degree. The copyright of this thesis rests with the author. No quotation from it can be published without prior written consent and information derived from it should be acknowledged.

Nomenclature and abbreviations

Analytical / General

ASAP	Atmospheric solids analysis probe
AV	Acid value
BDE	Bond dissociation energy
DFT	Dry film thickness
DSC	Differential scanning calorimetry
ΔE	Colour difference
EEW	Epoxy equivalent weight
EW	Equivalent weight
ESI	Electrospray ionisation
FG	Functional group
FT-IR	Fourier transform infra-red spectroscopy
GC-MS	Gas chromatography-Mass spectra
GPC	Gel permeation chromatography
HOMO	Highest occupied molecular orbital
HRMS	High resolution mass spectrum
LUMO	Lowest unoccupied molecular orbital
M_n	Number average molecular mass
M_w	Mass average molar mass
NHEW	Amine equivalent weight
NMR	Nuclear magnetic resonance
Nu	Nucleophile
pK_a	Acid dissociation content
PDI	Polydispersity index
PSI	Pounds per square inch
PVC	Pigment volume concentration
R_F	Perfluoroalkyl group
RT	Ambient temperature
SE	Surface energy
SOMO	Singly occupied molecular orbital
T_g	Glass transition temperature
UV	Ultraviolet
VOC	Volatile organic components
XRD	X-ray diffraction

Chemical

BGE	Butyl glycidyl ether
Bis-A	Bisphenol-A
DIAD	Diisopropyl azodicarboxylate
DMF	*N*,*N*-dimethylformamide
DMPU	1,3-Dimethyl-3,4,5,6-tetrahydro-2-pyrimidinone
DMSO	Dimethyl sulfoxide
HDDGE	Hexanediol diglycidyl ether
HG-II	Hoveyda-Grubbs 2nd generation catalyst
HMPA	Hexamethylphosphoramide
IPA	Isophthalic acid
Me	Methyl
MeCN	Acetonitrile
MAK	Methyl amyl ketone
MEK	Methyl ethyl ketone
Mes	Mesitylene
MIBK	Methyl *iso*-butyl ketone
NMF	*N*-methyl formamide
NPG	Neopentyl glycol
Phen	1,10-Phenantroline
TBAB	Tetrabutylammonium bromide
TBAF	Tetrabutylammonium fluoride
TCICA	Trichloroisocyanuric acid
TDAE	Tetrakis(diamino)ethylene
THF	Tetrahydrofuran
TMA	Trimellitic anhydride
TMA-Cl	Trimellitic anhydride chloride
TMS	Trimethlysilyl

Contents

1. Perfluoroalkyl systems for paint formulations

1.1 Introduction

Paint is encountered in everyday life by any person of the Western world and over 7.5 million tonnes of paint and related coatings are produced annually. [1] Coatings are used for a number of reasons, sometimes aesthetic but also as protective barriers to prolong lifetime of the substrate underneath. In terms of protection, paint is used to prevent corrosion, alter physical properties i.e. reduce drag/increase slip resistance, and to impart hygienic properties such as bacterial or fouling resistance on a range of surfaces including wood, plaster, concrete and steel. [2]

The purpose of this thesis is to explore the impact of adding molecules bearing perfluoroalkyl groups, whether as part of a polymer side chain or within a polymeric molecular backbone, to paint formulations and to explore how addition of such perfluoroalkyl units affect the UV degradation, surface energy and coating performance. Therefore, this review will comment briefly on the basic components and properties of paint and discuss the synthesis of organic systems bearing perfluoroalkyl groups, to provide background to the experimental work described in this thesis.

1.2 Key aspects of paint formulations

1.2.1 Paint composition

Paint is any substance that when applied to a substrate will convert into a solid adhesive film which is formed either by drying, with loss of water or solvent, or by chemical reaction of the binding components, frequently caused by heating or by oxidation in air. [3]

All paints contain a 'binder', the material that forms the solid film, and many formulations also have the following components; solvent, pigment, and various 'additives' that give paint the particular properties for specific applications

The binder is the only requirement for a paint system and it is the binder, or binding materials, that coalesce to form the polymeric film and account for the majority of the properties exhibited by the paint. Binders are often monomers or oligomers that react together upon application to give a solid, reasonably chemically stable film.

The solvent is a key component of wet paint coatings, many of which form films upon evaporation of the solvent. The solvent is not present after application of the paint coating and is primarily present in paint to enhance the ease of application by lowering viscosity of the formulation and enabling a more even flow during application of the coating to a substrate surface. [4] A range of solvents have been used in paint, from water to organic solvents such as ketones and aromatic systems such as xylene. Generally, reasonably volatile organic components (VOCs) are used to enable evaporation on a reasonable timescale.

Pigments are added to paint mainly to influence colour and visual appearance but they can also enhance other features such as adhesion and durability of the coating system, and alter physical properties such as viscosity by 'filling' the paint system. [5] Some of the most common pigments include calcium carbonate (talcum powder) and titanium dioxide, which both give a white colour not easily achieved with organic compounds and slow UV degradation of the paint. [6]

Various additives are generally present in paint in smaller amounts than the binder, solvent and pigment but can play a significant role in the physical properties of the final film coating. Additives include everything from catalysts, to speed chemical film formation, to biocides to prevent biological growth and

fouling. Surfactants are also used to promote dispersion and miscibility of two non-compatible components.

1.2.2 Failure of polymer based paint coatings

Despite the large scale use of paint as a coating system, various paint products can fail to protect the substrate in the long term by a variety of mechanisms. Research into increasing the performance and lifetime of paint films has focused on three of the most important defects; failure of the coating by UV degradation, damage to the substrate by poor barrier properties of the coating and bio-fouling of the substrate. These topics are discussed below to provide an overview of the reasons for incorporation of fluorinated alkyl units into paint coatings, which potentially may lead to improved paint performance, explored in this thesis.

1.2.2.1 Effect of UV light on polymer coating systems

Long wave UV light (300 – 380 nm) has sufficient energy to break covalent organic bonds. Upon irradiation with UV light, organic molecules can be excited to a higher energy state and dissipation of this energy can occur by several pathways of which one is bond cleavage and radical generation. [7]

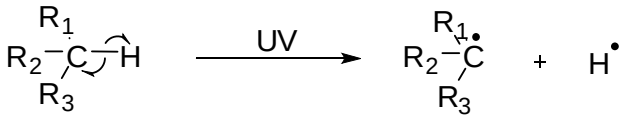

Figure 1.1: Homolytic cleavage of a C-H bond to give a carbon centred radical

Once a radical centre is generated, there are several ways it can react. One is to transfer the radical to another alkyl chain, as shown in figure 1.2. An alternative process is the reaction of the radical with molecular oxygen initially generating a peroxy radical which can then form a hyperperoxide as in figure 1.3. Other transformations include radical combination leading to the formation of a new

crosslinking bond between two alkyl chains, as in figure 1.4, and the formation of alkenes by elimination of a hydride radical.

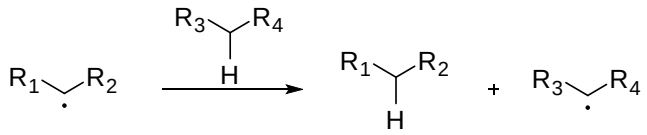

Figure 1.2: A radical chain transfer process

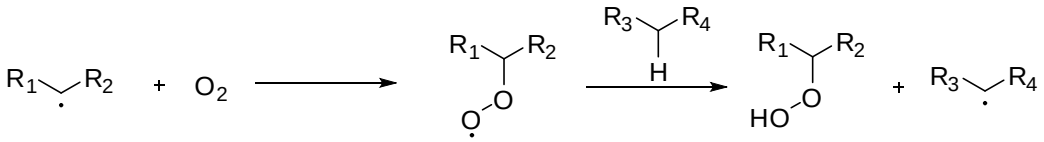

Figure 1.3: Propagation of a radical centre by incorporation of oxygen to give a peroxy radical and further reaction

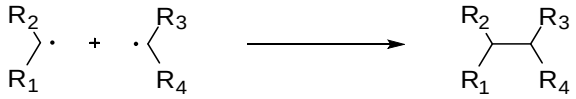

Figure 1.4: Combination of two radicals on adjacent parts of a polymer backbone giving rise to a new crosslink

While crosslinking is a problem, of greater influence on polymer stability is chain scission, which arises when a radical is formed at one of the polymer linkages (Figure 1.5). [8] Given the stability of radicals formed at carbonyl centres, this is particularly of concern in amide, polyester and isocyanate systems. Fission of C-C bonds upon UV irradiation is also potentially possible at any point of the polymer backbone.

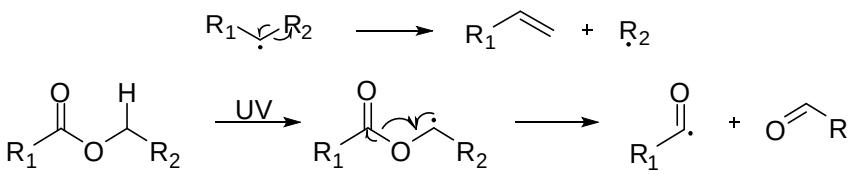

Figure 1.5: C-C bond cleavage, and chain scission of a polymer

Clearly, methods for preventing free radical formation and cleavage of polymers would lead to higher performance coatings.

1.2.2.2 Barrier properties of polymer coatings

The protective nature of a paint coating is linked to its barrier properties and its ability to prevent attack of water and other chemicals on the protected substrate surface beneath. [9] The flow of gases through a coating has been shown to involve three main processes; dissolution of the permeating species into the film, diffusion through the film and evaporation of the permeating species onto the substrate surface. [5] All permeation processes can damage the structure of the polymer, as in the case of blistering caused by passage of water, or lead to degradation of the substrate beneath.

Flow of water through a liquid is often modelled using Fick's First Law of diffusion, which was derived from studying the behaviours of gases but adequately models diffusion of water vapour and liquid water assuming that the flow is in steady state, the concentration gradient through the paint coating is linear and that diffusion takes place in only one direction. [10]

Fick's Law states that the flow of diffusing fluid will be proportional to the concentration gradient. While this is true, paint coating design can do nothing to alter the concentration of water at the surface of the coating. Fick's first law states nothing more unexpected than liquid will take longer to penetrate a thicker solid system, but this is because the law does not account for molecular interactions between water and the paint coating prior to the steady state equilibrium being reached. Fick's Second Law does represent this pre equilibrium state, and shows that the rate of change of concentration, the amount of fluid absorbed into the coating, is equal to the amount of fluid retained per unit volume of coating. This suggests coatings with good barrier properties to water are those which are hydrophobic or feature a hydrophobic surface, and thus repel water from entering the paint coating. Paint systems with hydrophilic groups, such as alcohols and amines, form hydrogen bonds with water molecules and, consequently, increase

the amount of water absorbed per unit volume of the coating.

Fick's Second Law of diffusion also shows that improved barrier properties (decreased permeability) arise when minimising fluid retention in the coating. The incorporation of hydrophobic groups decreases the free volume of the coating and also helps to prevent the absorbtion of water into a coating. Decreasing the 'free space' in a given coating for absorbed molecules can be achieved by greater crosslinking density or by incorporation of a pigment to occupy the volume. Paint coating systems can also be designed to have minimal free volume, for example, by excluding *para*-disubstitutedbenzene units which give rise to a large free volume due to less effective packing in the polymer matrix. [11]

1.2.2.3 Biofouling of coating surfaces

Biofouling starts with the physical adsorbtion of organic molecules, such as polysaccharides, upon which monocellular bacteria grow and produce a biofilm that adheres to the coating via polar electrostatic forces. The collection of electrostatically bonded bacteria on a surface provides the site of adhesion for larger bacteria and algae. [12] Build-up of biofilms, and adhesion of higher level organisms, is unsightly but also increases the rate of deterioration of the surface. If the paint coating is on a moveable object, such as a ship, then the biofouling leads to an increase in drag, and thus an increase in the energy required to propel the vessel and a subsequent increase in fuel consumption and cost of journey. [13]

Hence, it is imperative that coatings used in marine environments can withstand or reduce biofouling. [14] Brady has catalogued the key features a coating requires to resist biofilm formation; low elastic modulus, a smooth surface, surface active side chains, physical/chemical stability and a polymer backbone that is not involved in unfavourable interactions that lead to accumulation of polysaccharides and proteins and initiate biofilm formation. [15]

Recently, toxic organotin compounds, mainly tributyl- and triphenyltin derivatives have been used as additives in coating systems acting as biocides by inhibiting oxidative phosphorylation. [16] As one approach to reducing biofilm formation, tin species exhibit biocidal activity against a broad range of fouling organisms, including molluscs and dog whelks, while not interacting in redox processes that give rise to galvanic corrosion of aluminium. The choice of organotin species also allows for tuning of water solubility. Triphenyltin fluoride leaches out of a coating in an aqueous environment around an order of magnitude slower than tributyltin. [17] However, use of biocides in marine paint is either banned, since 1991 for tributyltin containing systems in Japan, and 2003 in the case of lead systems worldwide, or is likely to be phased out. A more contemporary approach to the preparation of environmentally benign antifouling coatings is to utilise non-stick, fouling-release coatings. In this case, a smooth, low-energy surface that will form a weak interaction with an algae biofilm, preventing binding and allowing lower energy removal of the surface since adhesion of biofouling increases as a linear function of surface energy. [18] This is the approach taken with the Intersleek 900 coating from AkzoNobel. [19]

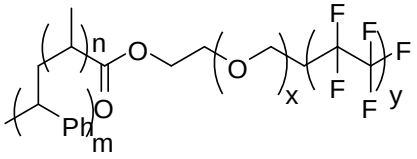

Figure 1.6: Block copolymer featuring semifluorinated sidechain

A useful class of low energy surface coatings are block copolymers featuring fluoroalkyl end groups (Figure 1.6). [20] The block copolymer (Figure 1.6) is a useful agent for anti-biofouling purposes as it presents a hydrophobic, low energy surface to incoming organisms that cannot adhere either by electrostatic interactions due to the low energy nature of the surface or by mechanical interactions due to the smoothness of the surface.

Despite having a low energy surface, of around 4 $mJ.m^{-2}$, [20] the fluorinated block

copolymer (Figure 1.6) will still attract some biomolecular fouling, as will all low energy surfaces immersed in water. However, while biofouling will still occur, biomolecules are attached more weakly and, consequently, are easier to remove. Some of the surfaces formed by fluorinated alkyl units are of low enough energy that removal of biofilms occurs with the shear stress caused by flow of water past the coating at speeds as low as 20 knots (~ 10 $m.s^{-1}$). Part of the advantage of smooth surfaces, such as those formed using Intersleek, [21] is laminar flow past the coating, which helps lift attached bio organisms by shear stress from the hull.

The other use of paint coatings featuring fluorinated alkyl units is to create low energy ambiphilic coatings. Biofilms are composed of a range of organisms which bind through hydrophobic or hydrophilic interactions. Fluorinated block copolymers offer areas of both hydrophobicity and lipophobicity; if the areas are small any incoming foulant will cover a mixture of areas and experience both unfavoured binding and some weak binding with the low energy fluorine rich area. Polymers containing fluorinated monomers are used extensively in commercially significant coatings of this type as they mix readily with other monomers, allowing a tunability of both the size and lipophilic character of amphiphilic coatings. [22]

Thus, there have been various approaches taken to address the three methods by which coatings systems fail and one approach that is pursued in this thesis is the addition of polyfluorinated derivatives to paint formulations due to the changes in physical and chemical properties of perfluoroalkyl containing organic systems.

Consequently, it is necessary to introduce the subject of organofluorine chemistry and briefly discuss the physical properties associated with polymers featuring perfluorinated substituents. Methods for the synthesis of organic systems containing perfluorinated substituents will also be briefly covered.

1.3 Organofluorine chemistry

1.3.1 Fundamental concepts in organofluorine chemistry

Fluorine is the most electronegative element in the Periodic Table with a Pauling electronegativity value of 4.0, more than half a unit greater than the next most electronegative element oxygen. [23] This observation explains why C-F bonds are partially ionic in nature and is one reason why the carbon-fluorine bond is so strong (Table 1.1). [24] Fluorine also has three unbonded pairs of electrons which provide an electrophobic sheath and can thus repel charged species away from the C-F bond, leading to high thermal and chemical stability of perfluorocarbons.

Table 1.1: Bond energies for bonds between sp^3 hybridised carbon centres and selected elements

Bond	Bond Energy / kcal.mol^{-1}
C-F	116
C-Cl	81
C-Br	68
C-C	83
C-H	99

The covalent radius of fluorine in carbon tetrafluoride (1.32 Å) lies between the radius of hydrogen (1.09 Å) and oxygen (1.53 Å) in organic systems [25] and so replacement of hydrogen with fluorine in an organic system imposes little conformational change due to steric reasons. Hence, almost all the difference in molecular properties of organic systems caused by incorporation of fluorine is due to electronic effects.

Since a carbon-fluorine bond is thermodynamically stronger than a carbon-hydrogen bond radical formation should be hindered by lowering the possibility of bond cleavage due to the additional energy this requires. [26] In addition, the

presence of fluorine atoms can affect the strength of C-H bonds at α- and β-positions.

The presence of fluorine atoms at a carbon centre is known to stabilise a carbon centred radical by conjugative effects between the radical SOMO and low lying fluorine HOMO which gives rise to a more planar structure as this allows for greater orbital overlap. [27] Fluorine atoms at the β position to a carbon radical destabilise the radical by electron withdrawal and offer no counteracting orbital overlap or resonance. This trend is best shown by examination of bond dissociation energies for carbon-hydrogen bonds at fluorinated centres. As can be seen in table 1.2, addition of either one or two fluorine atoms at the α carbon offers a slight stabilisation compared to the methyl radical, and hence the carbon-hydrogen bond dissociates at lower energy. However, addition of a third fluorine atom, to create a trifluoromethyl radical, increases bond dissociation energy relative to the methyl radical. The trend of destabilisation with addition of successive α fluorine atoms lies in the less planar structures found for the more substituted systems which lowers the effect of orbital overlap. Incorporation of β fluorine atoms on the ethane systems destabilises the radical, with the magnitude of the effect increasing with the number of β fluorine atoms. Conversely, fluorination of ethene creates a stronger C-C bond as shown in table 1.3.

Table 1.2: Bond dissociation energies of C-H bonds of fluorinated methane and ethane units [28,29,30]

System	BDE / kcal.mol^{-1}
CH_3-H	104.8
CH_2F-H	101.2
CHF_2-H	103.2
CF_3-H	106.7
CH_3CH_2-H	97.7
CH_2FCH_2-H	99.6
CHF_2CH_2-H	101.3
CF_3CH_2-H	102.0

Table 1.3: Bond dissociation energy of C-C bond in ethane and fluorinated ethane analogues [30]

Molecule	C-C BDE / kJ.mol^{-1}
H_3C-CH_3	375
H_2FC-CH_3	380
H_2FC-CH_2F	386
HF_2C-CH_3	408
HF_2C-CH_2F	397
F_3C-CH_3	423
HF_2C-CHF_2	407
F_3C-CH_2F	407
F_3C-CH_2F	397
F_3C-CF_3	407

Large perfluoroalkyl units in organic systems can have a significant effect on the electronic character of a molecule, best shown by values from Hammett linear free energy equations and pK_a data of molecules featuring perfluoroalkyl chains. A list of Hammett substituent values has been calculated for fluorinated systems with selected results shown in the table below. [31]

Table 1.4: Hammett σ values for fluorinated substituents in the m- and p- positions of benzoic acid

Substituent	σ_m	σ_p
H	0.00	0.00
F	0.34	0.06
CF_3	0.43	0.54
C_2F_5	0.47	0.52
n-C_3F_7	0.44	0.48
$C(CF_3)_3$	0.55	0.55
Cyclo-C_4F_7	0.48	0.53

Table 1.4 shows that larger fluorinated straight chain derivatives have a greater effect on the Hammett equilibrium than a single fluorine atom, and exhibit a greater electron withdrawing effect. Electron withdrawing effects of perfluoroalkyl groups can also be assessed by considering the effects on pK_a upon a range of related acid systems (Table 1.5).

Table 1.5: Effect of fluorinated at the α-carbon on the acidity of acetic acid

Acid	K_a
Acetic acid	1.75×10^{-5}
Fluoroacetic acid	1.75×10^{-3}
Difluoroacetic acid	3.50×10^{-2}
Trifluoroacetic acid	1.8

Fluoroacetic acid is one of the few naturally occurring fluorine containing compounds and is 10^2 times more acidic than acetic acid due to the electron withdrawing effect of the fluorine atom. [32] Increasing the degree of fluorination further emphasises this trend (Table 1.5). While no experimental data is available for the effect of incorporating perfluoroalkyl groups into related systems, computational models have calculated estimates of pK_a values of a range of perfluoroalkylated carboxylic acids. Table 1.6 shows that the addition of larger

perfluoroalkyl chains lowers pK_a, through electron withdrawal and stabilisation of the carboxylate anion.

Table 1.6: Computationally derived pKa values of carboxylic acids bearing fluoroalkyl groups [33]

Molecule	Ascribed pK_a value
$F(CF_2)_3COOH$	0.4
$F(CF_2)_7COOH$	-0.1
$F(CF_2)_{11}COOH$	-0.2
$F(CF_2)_2CH_2CH_2COOH$	4.0
$F(CF_2)_6CH_2CH_2COOH$	3.7
$F(CF_2)_{10}CH_2CH_2COOH$	3.6

As well as illustrating the inverse relationship between increase in the size of the fluorinated alkyl group and the lowering of pK_a, table 1.6 shows the 'insulating' effect of a hydrocarbon spacer. In the above table, incorporation of an ethylene group between the acid and fluoroalkyl group dramatically increases the magnitude of the pK_a by lessening the electron withdrawing effect of the perfluoroalkyl group.

Similarly, fluoroalkyl groups lower the basicity and nucleophilicity of amines. [34] This lowering of basicity is shown by pK_a values in DMSO calculated by Bordwell. [35] Trifluoromethylaniline is 3.7 units lower than aniline (from 30.7 to 27.0).

Fluoroalkyl groups also have a unique conformation, in that they exist in a helical twist formation, whereas standard hydrocarbon organic systems have a zig-zag anti-conformation based around the tetrahedral geometry of carbon. [36] For example, polytetrafluoroethylene (PTFE) is different to hydrocarbon systems, with a regular helical twist taking in 13 carbon atoms for every 180 ° rotation as

has been shown by X-ray diffraction. [37] Perfluorocetane, $C_{16}F_{34}$, is very similar in structure, again showing a helical twist, although the distance over which the twist repeats is slightly smaller. The Van der Waal's radius of fluorine is larger than that of hydrogen and, without distortion the fluorine radii would overlap, and so the carbon backbone twists increasing the distance between successive fluorine atoms. It has been speculated that bond-orientation effects may put a limit on the size of the twist and prevent a full anti-configuration, [38] although a competing theory is that the limitation arises as a consequence of repulsion between fluorine atoms and β carbon atoms. [36] In the same study concerning PTFE, the packing of distinct rod like molecules with little or no spacial overlap between perfluoroalkyl systems was noted.

1.3.2 Effects of perfluoroalkylation on physical properties of organic systems

Highly fluorinated alkyl groups, of the type incorporated into coatings as additives, are known to affect physical properties of organic systems imparting high densities, low surface tensions [39] and immiscibility with both polar organic solvents and water, [40] which gives fluorinated coatings a low wettability. [41] A discussion as to why these effects arise will now be given, with fundamental properties related to the use of perfluoroalkyl moieties in paint coatings.

1.3.2.1 Effect on intermolecular bonding

As a consequence of having a high electronegativity, fluorine is relatively non-polarisable. [42] In perfluoroalkyl groups the whole chain is relatively immune to induced dipoles and so Van der Waals type electrostatic forces are negligible. Consequently perfluoroalkyl groups show little intermolecular bonding, which gives organic systems incorporating perfluoroalkyl units a low boiling point relative to their size and atomic mass. As an example, perfluorohexyl-1-iodide

boils at 117 °C (atomic mass 446.0) [43] which is far less than the boiling point for 1-iodohexane (179 °C, atomic mass 212.1).

This near absence of Van der Waals type interactions has two distinct manifestations in the physical properties of molecules bearing perfluoroalkyl units. Firstly, fluorocarbons have a high compressibility due to the large space between discrete molecules, which arises from a lack of attractive intermolecular bonding and, in addition, organic systems, particularly polymers bearing fluorinated pendant chains, exhibit a low surface energy. These properties are discussed as they have particular relevance in providing 'non-stick' low energy coatings that prevent biofilm accumulation.

Many commercially available low energy antifouling coatings are manufactured and feature a variety of fluorinated subunits arising from reaction of fluorinated acrylates, [44] polyurethanes [45] and poly(ethyleneglycol)-fluoroethylene copolymers. [46]

Poly(1*H*,1*H*,2*H*,2*H*-perfluorodecanoyl diisocyanate) (Figure 1.7) showed only limited anti-fouling capability due to reorientation of the system so that the fluorinated groups were orientated inwards, away from the aqueous environment. [44] However, a highly crosslinked copolymer, formed from 1*H*,1*H*,2*H*,2*H*-heptadecafluorodecyl acrylate and acrylic acid linked with a copolymer of poly(2-isopropenyl-2-oxazoline) and methyl methacrylate gave a system where chain reorientation could not occur. [47] This not only produced a low surface energy coating that biofilms could only weakly adhere to but also created a polymer with little free volume limiting diffusion of water molecules into the coating.

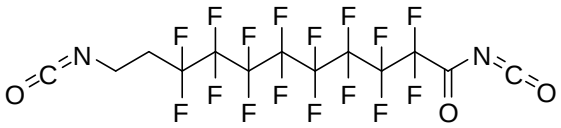

Figure 1.7: Structure of 1H,1H,2H,2H-perfluorodecanoyl diisocyanate

1.3.2.2 Effect on wettability

Wettability is primarily determined by the molecular interactions between a surface and liquid and is often measured with reference to contact angle, an easily obtained experimental parameter. Contact angle data relies merely on analysis of the shape of a droplet on a surface from which the angle between the droplet and planar surface can be obtained. Young's equation (Equation (1)) relates the equilibrium contact angle θ_c to the interfacial free energy change of wetting [48] and shows that for theoretical total wetting, $\theta = 0\,°$, γ_{SL} must be less than the interfacial tension of the solid-gas interface. [49]

$$\gamma_{SG} = \gamma_{SL} + \gamma_{LG} \cos\theta_C \quad (1)$$

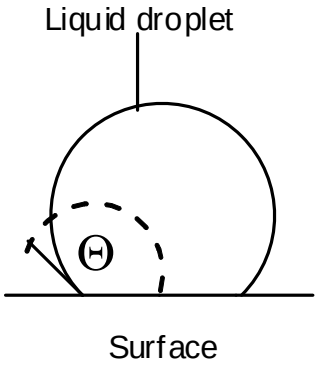

Figure 1.8: A sessile drop showing θ_c as the angle between solid-liquid and liquid-gas interfaces

Contact angle measurements can be related to surface energy (Equation (2)) by combining Young's equation (Equation (1)) with Goods' equation. The commonly used OWRK (Owens-Wendt-Rabel-Kaelble) method [50, 51] is a two drop method that takes the contact angle of two different liquids and allows not only the total energy of a solid surface to be calculated but also the relative contributions to surface energy from polar and dispersive interactions.

$$\frac{\sigma_L(\cos\theta_C+1)}{2\sqrt{\sigma_L^D}} = \frac{\sqrt{\sigma_S^P}\sqrt{\sigma_L^P}}{\sqrt{\sigma_L^D}} + \sqrt{\sigma_S^D} \quad (2)$$

In equation (2), σ_S^D and σ_S^P are the dispersive and polar components of the solid surface energy, which account for dispersion interactions at the surface and polar, hydrogen bonding and acid-base type interactions respectively. σ_L is the total surface energy of the liquid.

Equation (2) shows that contact angle, a measure of wettability, is dependent on the surface energy which has both a polar and dispersive component. Since systems bearing perfluoroalkyl groups have lower surface tensions than corresponding alkyl groups of similar length, they are less prone to wetting, due to a lowering of polar forces. [52] PTFE is well known for its low wettability, and has a surface energy of 21 $mJ.m^{-2}$ compared to 35.7 $mJ.m^{-2}$ for poly(ethylene).

A low wettability surface does not improve the barrier properties of a paint coating system but does hinder the absorbtion and diffusion of water through a coating and onto the substrate beneath. Low surface energy PTFE has a water contact angle of 111.9 °, [53] indicative of low adhesion between water and surface. The low wettability allows water to slide off the surface at low energies rather than stay attached to the surface and penetrate the system. However, this mechanism fails when the coating is submerged in water due to saturation of the surface. [54]

It is known that water uptake by coatings often results in water molecules sitting at polar sites. Reducing the number of such sites should lower water uptake and slow diffusion of water through a coating. [55] Since perfluorinated chains are non-polarisable and have an electrophilic sheath that repels charged, polar molecules such as water, they can potentially prevent water sitting in the coating between fluorinated chains, resulting in improved barrier properties according to Fick's

Second Law.

The reasons for incorporation of fluorinated units into paint coatings have been discussed and some commercial examples given based on perfluoroalkyl moieties in paint coatings. However, application of paint coatings that have low surface energy is difficult due to low adhesion between coating and substrate. This project aims to create fluorinated monomers that can be included in existing coating formulations as additives to alter surface properties and the stability of coatings to UV degradation but leave many bulk properties unchanged. Potentially this would allow for the creation of coatings that do not suffer from low adhesion to substrates.

1.4 Synthesis of organic systems bearing perfluoroalkylated groups

This project focuses on the synthesis of novel monomers bearing fluoroalkyl units and the use of such systems as 'drop in' additives with existing coating formulations at AkzoNobel. Therefore, it is necessary to briefly review how organic molecules bearing perfluoroalkyl groups can be synthesised, to place in context research aimed at developing a suitable synthetic methodology for the creation of fluorinated monomers.

Our research will focus on the use of species with some hydrocarbon (methylene or ethylene) linkers between the fluorinated chain and functional group. This will insulate the functional group from the electron withdrawing effect of the perfluoroalkyl unit and enable rates of polymerisation reactions to be closer to the rates of the unfluorinated analogues within the paint formulation. Hence, this review will focus on methods of synthesising molecules having perfluoroalkyl groups separated from functionality by a methylene (CH_2) or ethylene (CH_2CH_2) section, of the types shown in figure 1.9.

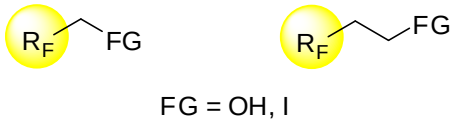

Figure 1.9: Perfluoroalkyl systems considered in this review

The starting point of all fluorocarbon chemistry is the mineral fluorspar, CaF_2, which when treated with concentrated sulfuric acid forms anhydrous hydrogen fluoride, which is isolated by distillation. [32] The synthesis of perfluorinated compounds can be accomplished by perfluorination of hydrocarbon chains by use of metal fluorides, electrochemical fluorination or elemental fluorine gas all of which are in turn synthesised from anhydrous hydrogen fluoride. [56] However, perfluorocarbons are outside the scope of this review since they do not bear any functionality for incorporation into paint systems. An alternative approach is to take small fluorinated telomers, and to build up larger fluoroalkyl chains through telomerisation and radical chemistry which is discussed below.

1.4.1 Synthesis of perfluoroalkylated derivatives by telomerisation

Telomerisation reactions, first utilised in 1942 [57] have displaced the Hunsdiecker reaction [58] as an industrial process and are now the primary way of creating fluorinated organic systems of the type R_FCH_2X and $R_FCH_2CH_2X$ (Figure 1.10). Telomerisation involves reaction of fluoroalkenes with a radical initiator, and creates new carbon-carbon bonds linking together monomeric subunits. [59] As with any polymerisation type process, telomerisation reactions, which lead to low molecular weight telomers, have four key steps; initiation, propagation, chain transfer and termination. [60] Initiation is typically by one of four methods; thermal, by use of a radical initiator, photochemical, or by redox catalysis. [61]

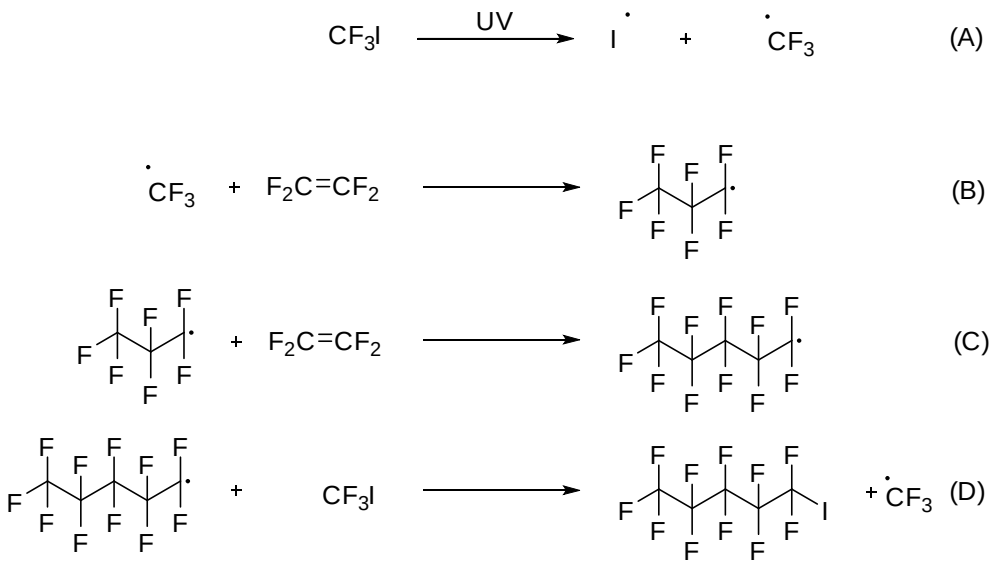

Figure 1.10: Radical reaction showing (A) photolytic initiation, (B) chain activation, (C) propagation/chain transfer and (D) termination [61]

Figure 1.10 shows the four key steps of a telomerisation reaction. In part (A) the telogen, in this example trifluoromethyl iodide, undergoes UV initiated decomposition resulting in the formation of two new radical species. Of the two species formed only the trifluoromethyl radical causes chain activation and leads to a reaction with the fluoroalkene. The chain activation step gives rise to a larger perfluorinated radical which reacts in one of two ways; it can either propagate further by reaction with another molecule of fluoroalkene, resulting in the synthesis of a larger perfluorinated radical system, or it can react with the starting trifluoromethyl iodide in a termination step. While the final step results in termination of the propagating chain it generates a trifluoromethyl radical which can activate another fluoroalkene.

The transfer agent, or telogen, of which there are many types, caps both ends of the alkene unit(s), and, for a general transfer agent X-Y, gives products of the type X-$(M)_n$-Y as summarised below (Figure 1.11). [62]

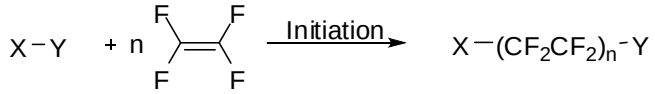

Figure 1.11: Generalised scheme for telomerisation between transfer agent X-Y and tetrafluoroethylene

A specific example of this end capping is the reaction of tetrafluoroethylene with dibromodifluoromethane. [60] Addition of bromine and CF_2Br_2 leads to a symmetrical product, with two terminal carbon-bromine bonds that can undergo nucleophilic substitution reactions. Use of a difluoromethylene derived chain transfer agent creates an odd number of difluoromethylene units in the product, whereas, typically, an even number of difluoromethylene units are found in products arising from telomerisation of tetrafluoroethylene.

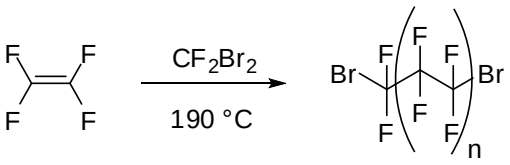

Figure 1.12: Telomerisation of tetrafluoroethylene with CF_2Br_2

Given that the transfer agent forms the terminal groups of the final molecule, it has a large effect on the chemistry of the product. For this reason, many transfer agents have been investigated featuring a range of cleavable bonds including; C-H, S-H, Si-H and C-Hal. Transfer agents that contain a carbon-halogen bond are the most commonly used due to the low bond dissociation energy the of carbon-halogen bonds. [63]

Reaction of fluorinated iodides with dienes, such as 1,3-butadiene, gives rise to branched products due to both 1,2- and 1,4-addition processes. [64] The product distribution shown (Figure 1.13) is evidence that 1,4-addition is clearly favoured and, consequently, the linear product is the major isomer.

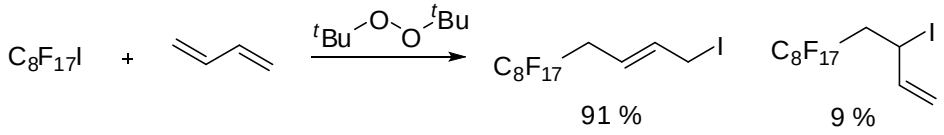

Figure 1.13: Telomerisation reaction between a perfluoroalkyl iodide and 1,3-butadiene

As shown above, fluoroalkyl iodides are not only the products of telomerisation reactions, they are the precursors to further reactions, used to prepare functional perfluoroalkyl systems. One of the most common processes, used to produce molecules of the type $R_FCH_2CH_2I$, is the reaction between fluoroalkyl iodide and ethene by a related free radical process. [65]

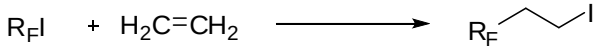

Figure 1.14: Reaction between perfluoroalkyl iodide and ethene

The analogous reaction of perfluoroalkyl iodide with 1,1-difluoroethylene gives exclusively products that arise from initial addition of the perfluoroalkyl radical to the methylene unit (Figure 1.15). [66] One explanation for this observation is a consideration of reactions of electrophilic and nucleophilic radicals. [67] An electrophilic radical, such as a perfluoroalkyl radical, will preferentially react with the most nucleophilic site, which for 1,1-difluoroethene is the methylene unit. The methylene unit is also less sterically hindered than the difluoromethylene unit.

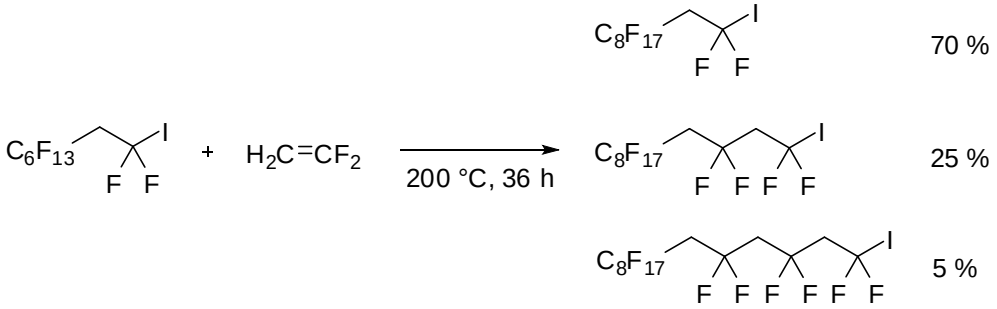

Figure 1.15: Telomerisation reaction between perfluorooctyl iodide and 1,1-difluoroethylene

The rates of reaction between various fluoroalkyl radicals and 1,1-

difluoroethylene have been determined and show that addition to the non-fluorinated carbon is far more likely than addition to the difluoromethylene unit (Table 1.7). [68] Increasing the size of the fluoroalkyl radical increasingly favours reaction at the CH_2 subunit.

Table 1.7: Probability of addition of fluoroalkyl radicals to the CF_2 unit of 1,1-difluoroethylene relative to the CH_2 unit

Radical species	Probability of addition of CF_2 end of alkene
CF_3	0.032
C_2F_5	0.011
n-C_3F_7	0.009
i-C_3F_7	0.001

Along with polyfluoroalkyl iodides, highly fluorinated alcohols may also be generated by telomerisation. Fluorinated alcohols are generated by reaction of an alcohol with a radical initiator and a fluoroalkene (Figure 1.16). [69]

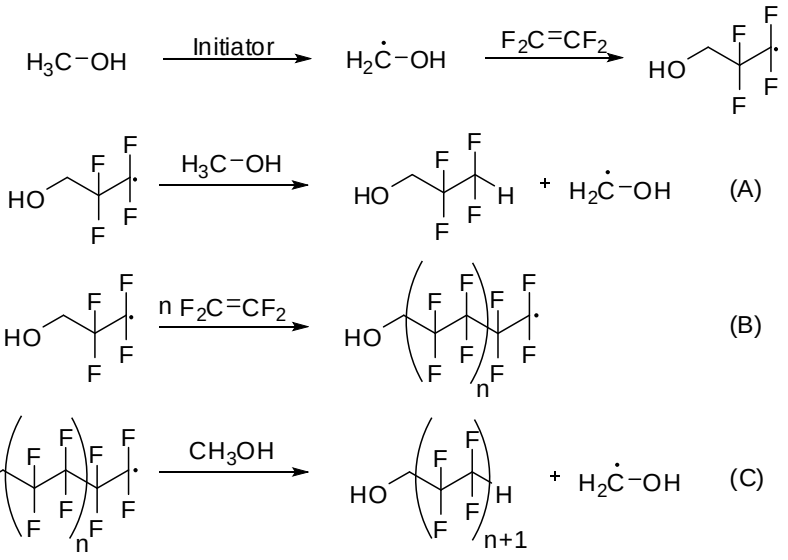

Figure 1.16: Telomerisation reaction between methanol and tetrafluoroethene showing (A) chain transfer, (B) propagation and (C) termination

While reactions of this type give rise to terminal CF_2H groups, use of hexafluoropropene, [70] gives rise to products featuring a terminal trifluoromethyl

group (Figure 1.17).

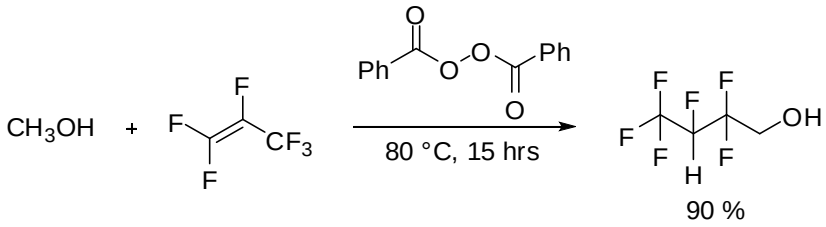

Figure 1.17: Polyfluorinated alcohol with terminal trifluoromethyl group generated by telomerisation

Larger perfluorinated α-alkenes, such as decafluoropent-1-ene, may also give polyfluoroalcohols by the process shown in figure 1.18. As well as giving lower yields, reactions with alcohols other than methanol lead to chain branched products as the radical forms at the α carbon, due to stabilisation of the α carbon radical by the adjacent oxygen atom.

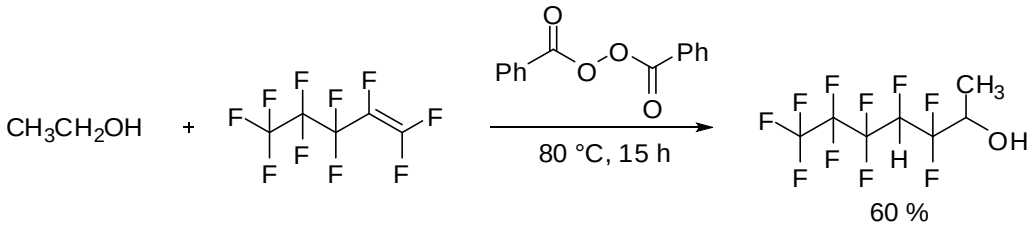

Figure 1.18: Reaction of ethanol with decafluoro-1-ene in a radical reaction initiated by benzoyl peroxide

In order to produce alcohols that do not possess either a CF_2H unit or a fluoromethylene unit amongst the perfluoroalkyl chain it is necessary to functionalise a perfluoroalkyl iodide derivative, synthesised by telomerisation. The transformation of perfluoroalkylethyl iodide into the alcohol derivative is commonly achieved by reaction with fuming sulfuric acid. [71]

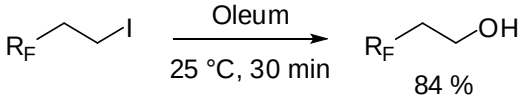

Figure 1.19: Synthesis of perfluoroalkylated alcohols

Consequently, a range of $R_FCH_2CH_2I$, $HCF_2R_FCH_2CH_2I$ and corresponding alcohols can be formed from telomerisation of PTFE with perfluoroalkyl iodides and subsequent reaction. The perfluoroalkyl building blocks can then be used in a variety of functional group transformations described below.

1.5 Reactions of common perfluoroalkylated systems

Molecules featuring a fluorinated alkyl chain adjacent to a CH_2 or CH_2CH_2 alkyl linker are synthesised by telomerisation, [72] and the most common products of these reactions are fluorinated alkyl iodides. As well as iodides, alcohols of similar structure (R_FCH_2OH and $R_FCH_2CH_2OH$) are also readily available due to industrial scale synthesis.

Both perfluoroalkyl iodides and perfluoroalkyl alcohols represent potentially useful building blocks for the creation of perfluoroalkyl monomers which are the focus of this thesis and so a brief review of their chemistry will be presented.

1.5.1 Reactions of polyfluoroalkyl iodides ($R_FCH_2CH_2I$) as an electrophile

Reaction of perfluoroalkyl iodides with ethylene (Figure 1.10) gives substrates bearing a carbon-iodine bond that can undergo nucleophilic substitution reactions as is seen in reactions with water, in both DMF and NMP, [73,74] pyridine [75] and sodium sulfite. [76] Reaction of fluorinated alkyl iodides with pyridine forms a water soluble pyridinium salt, facilitating easy separation of the product from other organic material (Figure 1.20).

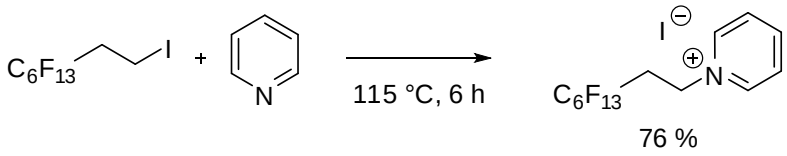

Figure 1.20: Reaction between a polyfluoroalkyl iodide and pyridine nucleophile generating a pyridinium salt [77]

Sodium azide reacts with polyfluoroalkyl iodides, [78] and subsequently a palladium catalysed hydrogenation of the intermediate gives the polyfluoroalkyl amine.

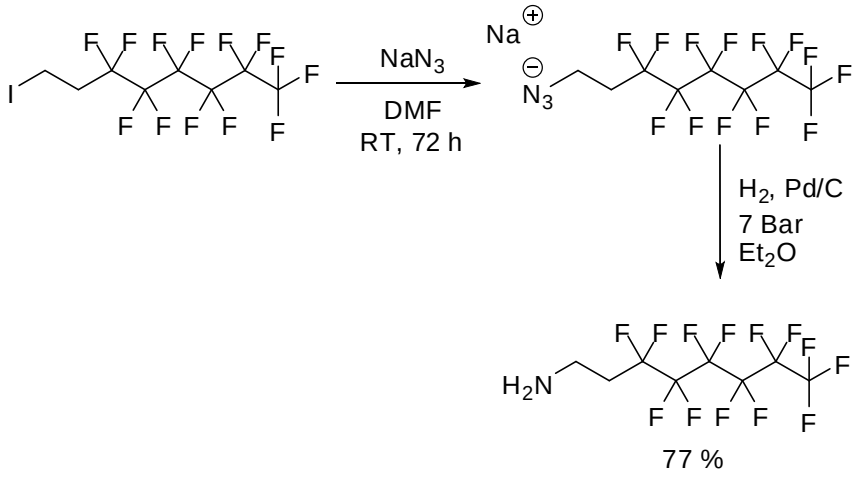

Figure 1.21: Reaction of a polyfluoroalkyl iodide with sodium azide [78]

Further examples of nucleophilic substitution involve cyanide [79] and thiolate [80] salts.

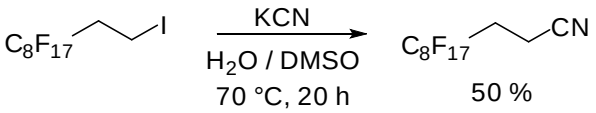

Figure 1.22: Reaction of polyfluoroalkyl iodide with potassium cyanide

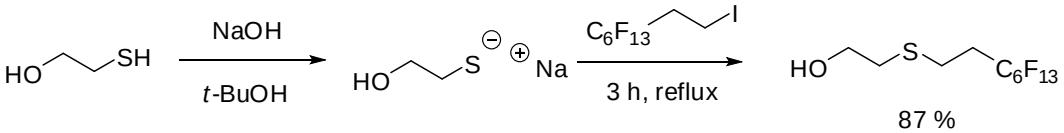

Figure 1.23: Generation, and subsequent use, of a thiolate to give a thioether bearing a fluorinated chain

Phase transfer conditions are often required to allow substitution of iodine by chlorine due to low solubility of $C_8F_{17}CH_2CH_2I$ in organic systems. [81]

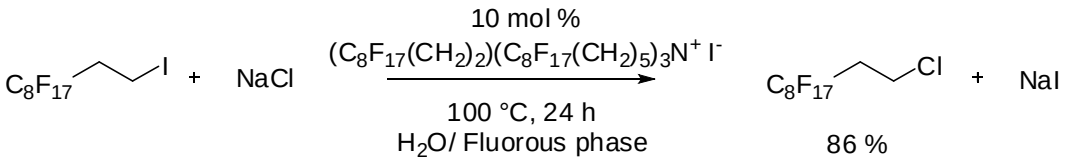

Figure 1.24: Phase transfer catalysed reaction between 1H,1H,2H,2H-perfluorooctyl iodide and an excess of sodium chloride

In principle, reaction of polyfluoroethyl iodides of the type $R_FCH_2CH_2I$ with nucleophiles should offer a route to a range of perfluoroalkylated systems but only a small number of reactions, reviewed above, have been reported, offering scope for further development.

1.5.2 Chemistry of polyfluoroalkyl alcohols ($R_FCH_2CH_2OH$)

1.5.2.1 Synthesis of fluoroalcohols

Telomerisation reactions between tetrafluoroethylene and alcohols are the major method for producing polyfluoroalkyl alcohols (Section 1.4.1). [82] An alternative method is to react polyfluoroalkyl iodides with oxygen nucleophiles. This reaction has been the focus of several studies and two distinct reaction pathways are known. One method involves heating fluorinated iodides with *N*-methyl formamide (NMF) resulting in the formation of an imide salt. The imide salt intermediate reacts with a further molecule of NMF followed by alkoxide elimination (Figure 1.25). [83] This is an attractive method as it does not involve the use of strong acids or oxidising agents.

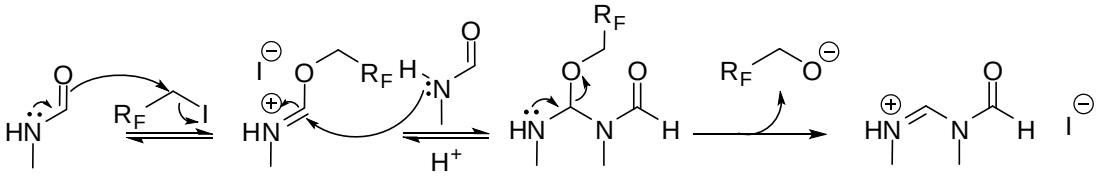

Figure 1.25: Synthesis of fluoroalcohol (R_F=$CF_3(CF_2)_xCH_2$) from a polyfluoroalkyl iodide and N-methylformamide.

A mechanistically simpler, but lower yielding, synthesis focuses around the creation of an alkyl zinc or alkyl copper species (Figure 1.26). [84] The electron rich carbon centre can be oxidised under a flow of oxygen and protonated with an organic/mineral acid mixture.

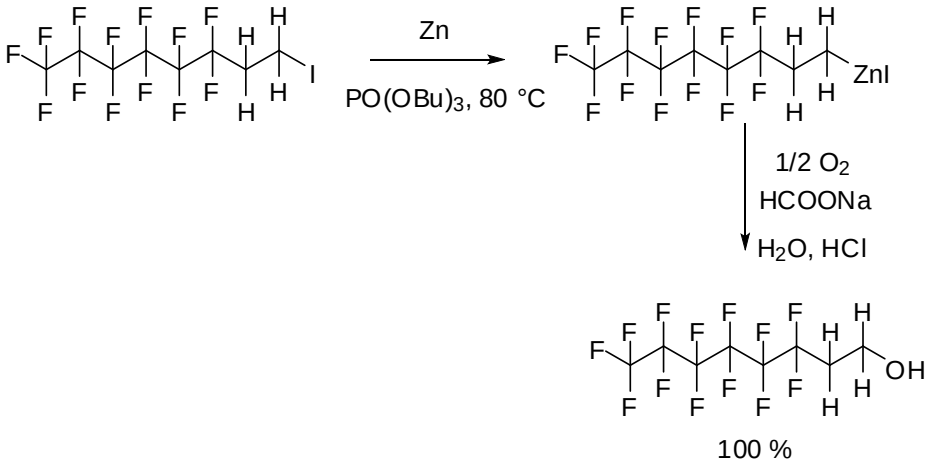

Figure 1.26: Conversion of a fluorinated alkyl iodide to a semi fluorinated alcohol via an organozinc intermediate.

Reaction of 1-perfluoroalkyl-2-iodoalkanes with sulfur trioxide in liquid sulfur dioxide, followed by hydrolysis, is another method for the synthesis of polyfluoroalkyl alcohols from polyfluoroalkyl iodide precursors (Figure 1.27). [85] The key step of the reaction is the condensation of two iodosulfate groups to give the S-O-S bridged compound, which creates a good leaving group and readily undergoes hydrolysis.

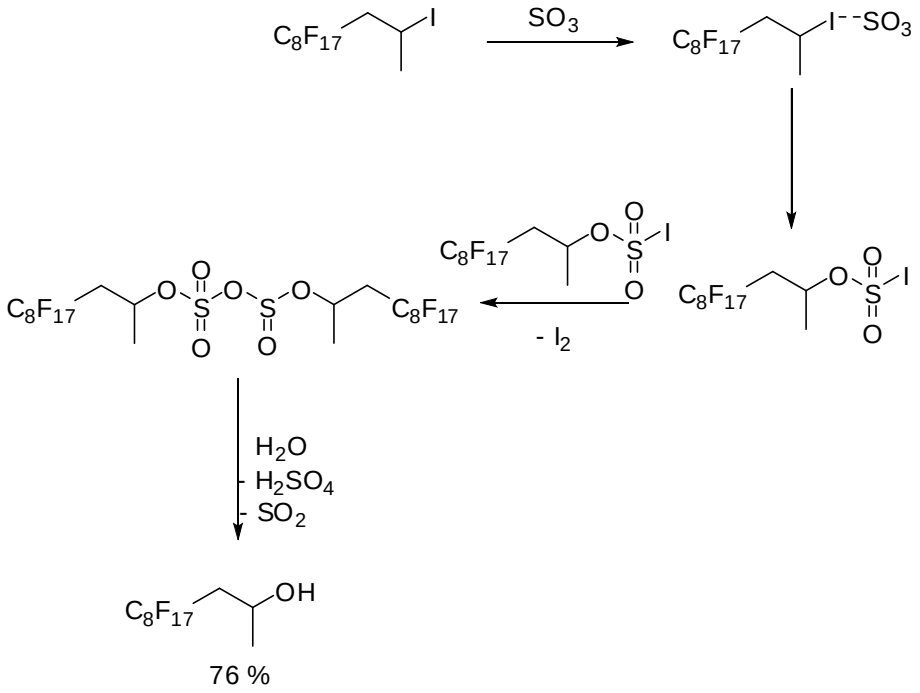

Figure 1.27: Mechanism for the reaction of polyfluoroalkyl iodide with sulfur trioxide

Hydroboration of a fluoroalkene also leads to formation of a polyfluorinated alcohol. Both the primary and secondary alcohols can be produced in a selective fashion, dependent upon the reaction conditions. [86] At room temperature bulky boranes, such as catecholborane, give almost exclusively the kinetic product. This reaction is characterised by an excellent yield which is independent of fluoroalkyl chain size. [87]

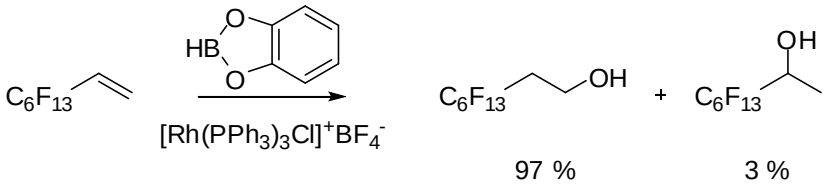

Figure 1.28: Hydroboration of a fluoroalkene

1.5.2.2 Representative reactions of polyfluoroalkyl alcohols ($R_FCH_2CH_2OH$)

One of the most easily acquired fluoroalcohols is 1H,1H,2H,2H-perfluorooctan-1-ol, made commercially in high volume.

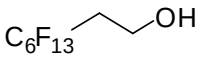

1.5.2.2.1 Reactions with nucleophilic oxygen

The perfluoroalkyl unit of a fluoroalcohol lowers the nucleophilicity of the oxygen atom (Section 1.3.1). Despite this, there are examples of nucleophilic reactions involving fluoroalcohols. Reaction of 2-(perfluorohexyl)ethanol with paraformaldehyde [88] and hydrogen chloride, reaches full conversion in two hours giving an 86 % isolated yield of the ether at room temperature.

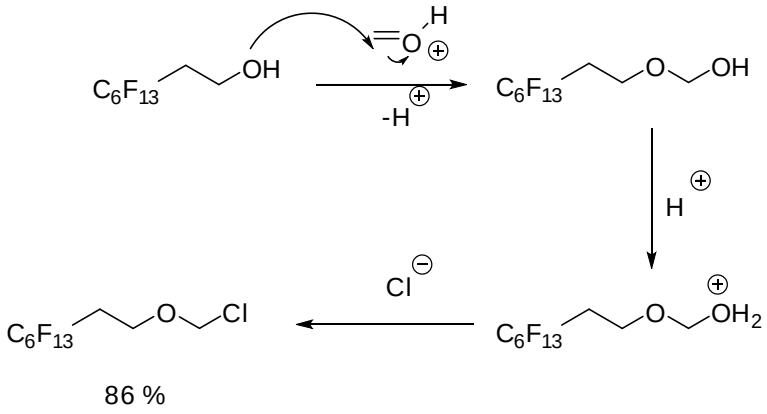

Figure 1.29: Nucleophilic addition of 1H,1H,2H,2H-perfluorooctan-1-ol to formaldehyde

The more classical way of forming ethers is through use of a Williamson ether synthesis, reacting an alcohol and an alkyl halide, and this reaction has been attempted using 1H,1H,2H,2H-perfluorooctan-1-ol (Figure 1.30). [89] The use of an aprotic solvent is necessary to prevent hydrogen bonding between the hydroxyl

group and solvent. The use of larger *n*-alkyl bromides causes a decrease in the yield, whereas altering the size of the R_F chain, between the four, six and eight carbon perfluoroalkyl moieties has little effect on yield.

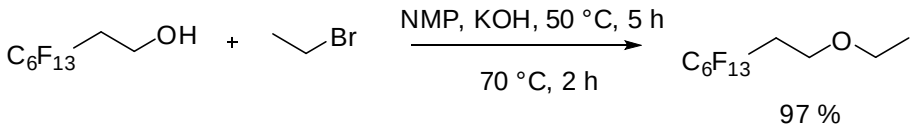

Figure 1.30: Williamson ether type synthesis of an ether bearing a fluorinated substituent

Fluorinated alcohols of the type $R_FCH_2CH_2OH$ react with carboxylic acids to give ester products. [83] Esterification is a common reaction in paint chemistry, used to create polyester linked binders, and so evidence of such reactions involving fluoroalcohols shows potential as a method for the incorporation of fluorinated alcohols into paint coating systems.

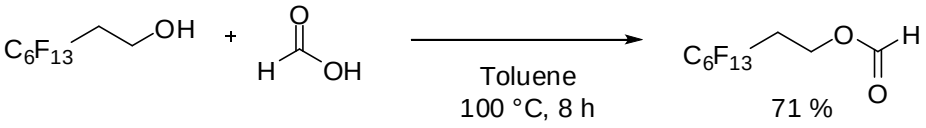

Figure 1.31: Esterification of a fluoroalcohol

The Appel reaction has also been shown to proceed with use of polyfluoroalkyl alcohols. [90] This reaction involves nucleophilic attack of a phosphorus-halogen bond by a polyfluoroalkyl alkoxide.

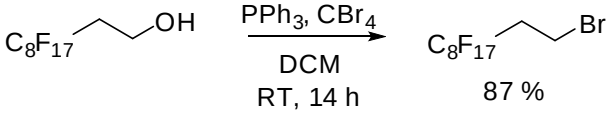

Figure 1.32: Transformation of a fluoroalcohol to a polyfluorinated alkyl bromide

1.5.2.2.2 Reactions catalysed by metal reagents

Fluorinated ethers have been synthesised through use of a copper catalysed cross

coupling reaction between polyfluorinated alkyl alcohols of the type R_FCH_2OH and aryl halides. [91] Commonly, 1,10-phenanthroline is used as a ligand with copper mediated cross coupling reactions but, in this instance, gave a poor yield and so ethyl-2-oxocyclohexanecarboxylate was preferred. The reaction proceeds with larger homologues such as 1H,1H-perfluorooctan-1-ol, but yield decreases as the size of the fluorinated group increases, despite the use of harsher conditions.

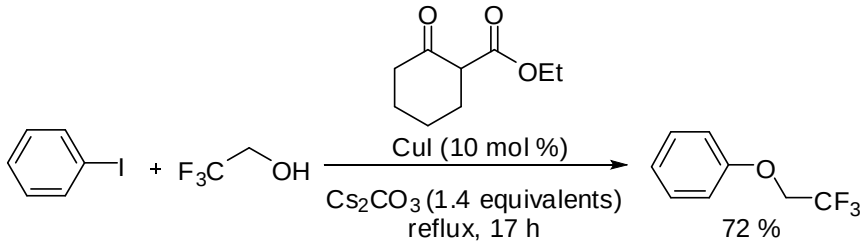

Figure 1.33: Cross-coupling reaction of aryl iodide and fluorous tagged alcohol

Fluorinated acids can be formed by oxidation of fluoroalcohols and this can be achieved with various common oxidants such as the chromium based Jones reagent [92] and periodic acid. [93] The resulting polyfluorocarboxylic acids can be reacted with thionyl chloride to create a stronger electrophile. [94]

1.6 Conclusions

Paint coatings are ubiquitous, used as inert barrier coatings to provide protection to a range of diverse substrates. However, paint coatings can deteriorate via a number of pathways including UV degradation. One possible method of enhancing the UV durability of paint coatings is by addition of perfluoroalkyl units to the formulation.

Molecules featuring perfluoroalkyl chains are produced on a bulk scale by telomerisation reactions. As a consequence, they are readily available in quantities suitable for both research and, if necessary, larger scale production. Both polyfluoroalkyl iodides and polyfluoroalkyl alcohols undergo a range of organic

functional group transformations, which, in principle, can be exploited to create perfluoroalkylated monomers from these building blocks. Such polyfluorinated monomers will be explored in this thesis as 'drop in' additives into existing liquid and powder paint formulations used in the protective coatings industry.

1.7 References to chapter 1

1. Zhuang, Y.; Wang, H.; Zhang, W.; Hao, Z.; Wang, X.; Integrated management strategies for VOC emission control in the paint and coatings sector in China in *Integrated Air Quality Management: Asian Case Studies*; Oanh, N.T.K. Ed.; CRC press: Boca Raton, 2013; Vol. 1, pp 349 – 367.

2. Milne. A.; Economics and the environment: The role of coatings in *The Chemistry and Physics of coatings*; Marrion, A.R. Ed.; RSC publishing: Cambridge, 1994, Vol. 1, pp 1 – 8.

3. Stoye, D.; Freitag, W. (Eds); *Paints, Coatings and Solvents*, Wiley-VCH: Weinheim, 1998, pp 1, 8 – 9.

4. Bentley, J.; Turner, G.P.A.; *Introduction to Paint Chemistry and principles of paint technology*, Chapman and Hall: Bury St Edmonds, 1988.

5. Paul, S.; *Surface Coatings, science and technology*, Wiley: Chichester, 1985.

6. Winkler, J.; *Titanium Dioxide*, Vincentz: Hannover, 2003.

7. Hare, C.H.; *J. Protective Coatings and Linings*, **1992**, 5, 29 – 33.

8. Shin, B.S.; Han, D.H.; Narayan, R.; *J. Polym. Environ.*, **2010**, 18, 558 – 566.

9. Feldman, D.; *J. Polym. Environ.*, **2001**, 9, 49 – 55.

10. Ninnemann, K.W.; Measurement of Physical Properties of Flexible films in *The Science and Technology of polymer films*; Sweeting, O.J. Ed.; Interscience: New York, 1968, Vol. 1, pp 545 – 651.

11. Patterson, D.; *Macromolecules*, **1969**, 6, 672 – 677.

12. Haras, D.; *Mater. Tech.*, **2006**, 93, 27 – 33.

13. Townsin, R.L.; *Biofouling*, **2003**, 19, 9 – 15.

14. Yebra, D.M.; Kill, S.; Dam-Johnson, K.; *Prog. Org. Coat.*, **2004**, 50, 75 – 104.

15. Brady, R.F.; *Prog. Org. Coat.*, **1999**, 35, 31 – 35.

16. Omae, I.; *Appl. Organomet. Chem.*, **2003**, 17, 81 – 105.

17. Evans, C.J.; Karpel, S.; *Organotin compounds in Modern Technology*, Elsevier: Amsterdam, 1985, pp 135.

18. Brady, R.F.: *Prog. Org. Coat.*, **2001**, 43, 188 – 192.

19. Williams, D.N.; Shewring, N.I.E.; Lee, A.J.; Antifouling compositions with a fluorinated alkyl- or alkoxy-containing polymer or oligomer, International Patent WO2002074870, 18 Mar 2002.

20. Krishnan, S.; Ayothi, R.; Hexemer, A.; Finlay, J.A.; Sohn, K.E.; Perry, R.; Ober, C.K.; Kramer, E.J.; Callow, M.E.; Callow, J.A.; Fischer, D.A; *Langmuir*, **2006**, 22, 5075 – 5086.

21. International Marine Coatings.; Intersleek 1100 SR: Groundbreaking patented slime release fluoropolymer technology, *Internet, www.international-marine.com/products/info/intersleek-1100-SR-brochure.pdf*

22. Callow, J.A.; Callow, M.E.; *Nature Commun.*, **2011**, 2, 244 – 244.

23. Pauling, L.; *J. Am. Chem. Soc.*, **1932**, 54(9), 3570 – 3582.

24. O'Hagan, D.; *Chem. Soc. Rev.*, **2008**, 37, 308 – 319.

25. Patrick, C.R.; *Advan. Fluorine Chem.*, **1963**, 3, 117 – 117.

26. Dolbier, W.R.; *Chem. Rev.*, **1996**, 96, 1557 – 1584.

27. Bernardi, F.; Cherry, W.; Shaik, S.; Epiotis, N.D.; *J. Am. Chem. Soc.*, **1978**, 100, 1352 – 1356.

28. McMillen, D.F.; Golden, D.M.; *Ann. Rev. Phys. Chem.*, **1982**, 33, 493 – 532.

29. Lide, D.R.; *CRC Handbook of Chemistry and Physics*, CRC Press: Boca Raton, 1996.

30. Martell, J.M.; Boyd, R.J.; Shi, Z.; *J. Phys. Chem.*, **1993**, 97, 7208 – 7215.

31. Hansch, C.; Leo, A.; Taft, R.W.; *Chem. Rev.*, **1991**, 91, 165 – 195.

32. Chambers, R.D.; *Fluorine in Organic Chemistry*, Blackwell: Oxford, 2004.

33. Goss, K.U.; *Environ. Sci. Technol.*, **2008**, 42, 456 – 458.

34. Henne, A.L.; Stewart, J.J.; *J. Am. Chem. Soc.*, **1955**, 77, 1901 – 1902.

35. Bordwell, F.G.; Algrim, D.J.; *J. Am. Chem. Soc.*, **1988**, 110, 2964 – 2968.

36. Bunn, C.W.; Howells, E.R.; *Nature*, **1954**, 174, 549 – 551.

37. Drobny, J.G.; *Fluoroplastics*, Smithers Rapra Press: Shrewsbury, 2006.

38. Bunn, C.W.; *Proc. Roy. Soc. A.*, **1942**, 180, 67 – 81.

39. Zisman, W.A.; "Relation of the equilibrium contact angle to liquid and solid construction" In *Contact angle, wettability, and adhesion*, Fowkes, F.M. Ed.; ACS 1964; pp 1 – 51.

40. Le Grand, D.G.; Gaines, G.L.; *J. Colloid Interface Sci.*, **1975**, 50, 272 – 279.

41. Fan, C.F.; Cagin, T.; *J. Chem. Phys.*, **1995**, 103, 9053 – 9061.

42. Lemal, D.M.; *J. Org. Chem.*, **2004**, 69, 1 – 11.

43. Anderson, H.H.; *J. Chem. Eng. Data*, **1966**, 11, 117 – 122.

44. Pullin, R.A.; Nevell, T.G.; Tsibouklis, J.; *Mater. Lett.*, **1999**, 39, 142 – 148.

45. Brady, R.F.; Robust nontoxic antifouling elastomers, US patent 5652027, 23 Feb 1996.

46. Krishnan, S.; Wang, N.; Ober, C.K.; Finlay, J.A.; Callow, M.E.; Callow, J.A.; Hexemer, A.; Sohn, K.E.; Kramer, E.J.; Fischer, D.A.; *Biomacromolecules*, **2006**, 7, 1449 – 1462.

47. Schmidt, D.L.; Brady, R.F.; Lam, K.; Schmidt, D.C.; Chaudhury, M.K.; *Langmuir*, **2004**, 20, 2830 – 2836.

48. Dalvi, V.H.; Rossky, P.J.; *Proc. Nat. Acad. Sci.*, **2010**, 107 (31), 13603 – 13607.

49. Yuan, Y.; Lee, T.R.; "Contact angle and wetting properties" In *Surface Science Techniques*, Bracco, G.; Holst, B.; Eds. Springer Berlin Heidelberg, 2013 pp. 3 – 34.

50. Owens, D.K.; Wendt, R.C.; *J. Appl. Poly. Sci.*, **1969**, 13, 1741 – 1747.

51. Kaelbe, D.H.; *J. Adhes.*, **1970**, 2, 66 – 81.

52. Katano, Y.; Tomono, H.; Nakajima, T.; *Macromolecules*, **1994**, 28, 2342 – 2344.

53. Rios, P.F.; Dodiuk, H.; Kenig, S.; McCarthy, S.; Dotan, A.; *J. Adhesion Sci. Technol.*, **2007**, 21, 227 – 241.

54. Griffith, J.R.; Bultman, J.D.; *Ind. Eng. Chem. Prod. Res. Dev.*, **1978**, 17, 8 – 9.

55. Delucchi, M.; Turri, S.; Barbucci, A.; Bassi, M.; Novelli, S.; Cerisola, G.; *J. Polym. Sci. B Polym. Phys.*, **2002**, 40, 52 – 64.

56. Stephens, R.; Tatlow, R.C.; *Quart. Rev.*, **1962**, 16, 44 – 70.

57. E. I. Du Pont De Nemours And Company; Halogenated hydrocarbons and method for their preparation, US Patent 2440800A, 10 Apr 1942.

58. Brace, N.O.; *J. Fluorine Chem.*, **1999**, 93, 1 – 25.

59. E. I. Du Pont De Nemours And Company; Process for the preparation of perfluorocarbon iodides, US Patent 3234294A, 20 Dec 1962.

60. Ameduri, B.; Boutevin, B.; "Telomerisation reactions in fluorinated alkenes" in *Organofluorine chemistry: Fluorinated alkenes and reactive intermediates*, Chambers, R.D. Ed.; Wiley-Verlag: Berlin-Heidelburg, 1997, Vol. 192, pp 165 – 249.

61. Haszeldine, R.N.; *J. Chem. Soc.*, **1949**, 1, 2856 – 2861.

62. Ameduri, B.; Boutevin, B.; Guida-Piestranta, F.; Rousseau, A.; *J. Fluorine. Chem.*, **2001**, 107, 397 – 409.

63. Ameduri, B.; Boutevin, B.; "Telomerisation reactions in fluorinated alkenes" in *Organofluorine chemistry: Fluorinated alkenes and reactive intermediates*, Chambers, R.D. Ed.; Springer, Berlin-Heidelburg, 1997; pp 165 – 234.

64. Lebreton, P.; Ameduri, B.; Boutevin, B.; Corpart, J.; Juhue, D.; *Macromol. Chem. Phys.*, **2000**, 201, 1016 – 1024.

65. Ameduri, B.; Boutevin, B.; Nouiri, M.; Talbi, M.; *J. Fluorine Chem.*, **1995**, 74, 191 – 197.

66. Chambers, R.D.; Hutchinson, J.; Mobbs, R.H.; Musgrave, W.K.R.; *Tetrahedron*, **1964**, 20, 497 – 506.

67. March, J.; *Advances Organic Chemistry*, Wiley: New York, 1992.

68. Ashton, D.S.; Mackay, A.F.; Tedder, J.M.; Tipney, D.C.; Walton, J.C.; *J. Chem. Soc. Chem. Comm.*, **1973**, 14, 496 – 497.

69. Guiot, J.; Alric, J.; Ameduri, B.; Rousseau, A.; Boutevin, B.; *New J. Chem.*, **2001**, 25, 1185 – 1190.

70. Lazerte, J.D.; Koshar, R.J.; *J. Am. Chem. Soc.*, **1955**, 77, 910 – 914.

71. Benefice-Malouet, S.; Blancou, H.; Calas, P.; Commeyras, A.; *J. Fluorine Chem.*, **1988**, 39, 245 – 260.

72. Kostov, G.; Boschet, F.; Ameduri, B.; *J. Fluorine Chem.*, **2009**, 12, 1192 – 1199.

73. Asahi Glass Co. Ltd.; Method of preparing polyfluoroalkyl group containing compounds, US Patent 4001309, 16 Apr 1973.

74. Hoechst Aktiengesellschaft; Process for the manufacture of 2-(perfluoroalkyl)-ethanols, US Patent 4219681, 6 Aug 1979.

75. E. I. Du Pont De Nemours And Company; Perfluoroalkyl substituted ammonium salts, US Patent 3257407, 21 Jun 1966.

76. Prod. Chem. Ugine Kuhlman; Method of preparing polyfluorinated sulphonic acid and derivatives, US patent 3825577, 23 Jul 1974.

77. Quigliotto, P.; Barolo, C.; Barbero, N.; Barni, E.; Compari, C.; Fisicaro, E.; Viscardi, G.; *Eur. J. Org. Chem.*, **2009**, 19, 3167 – 3177.

78. Ortial, S.; Durand, G.; Poeggeler, B.; Polidori, A.; Pappolla, M.A.; Boker, J.; Hardeland, R.; Pucci, B.; *J. Med. Chem.*, **2006**, 49, 2812 – 2820.

79. Moreau, L.; Campins, N.; Grinstaff, M.W.; Barthelemy, P.; *Tet. Lett.*, **2006**, 47, 7117 – 7120.

80. Cirkva, V.; Duchek, J.; Kaplanek, R.; Paleta, O.; Michalek, J.; Pradny, M.; Chmelikova, D.; Wichterlova, J.; *Eur. J. Med. Chem.*, **2006**, 41, 1320 – 1326.

81. Mandal, D.; Gladsyz, J.A.; *Tetrahedron*, **2010**, 66, 1070 – 1077.

82. Lehmler, H.; *Chemosphere,***2005**, 58, 1471 – 1496.

83. Brace, N.O.; *J. Fluorine. Chem.*, **1986**, 31, 151 – 174.

84. Blancou, H.; Benefice, S.; Commeyras, A.; *J. Fluroine Chem.*, **1983**, 23, 57 – 65.

85. Mares, F.; Oxenrider, B.C.; *J. Fluorine. Chem.*, **1976**, 8, 373 – 378.

86. Ramachandran, P.V.; Jennings, M.P.; Brown, H.C.; *Org. Lett.*, **1999,** 1, 1399 – 1402.

87. Segarra, A.M.; Claver, C.; Fernandez, E.; *Chem. Comm.*, **2004**, 4, 464 – 465.

88. Ikeda, K.; Mori, H.; Sato, M.; *Chem. Comm.*, **2006**, 29, 3093 – 3094.

89. Zaggia, A.S.; Conte, L.; Ceretta, F.; *J. Fluorine Chem.*, **2010**, 131, 844 – 851.

90. Emnet, C.; Weber, K.M.; Vidal, J.A.; Consorti, C.S.; Stuart, A.M.; Gladysz, J.A.; *Adv. Synth. Catal.*, **2006**, 348, 1625 – 1634.

91. Vuluga, D.; Legros, J.; Crousse, B.; Bonnet-Delpon, D.; *Eur. J. Org. Chem.*, **2009**, 21, 3513 – 3518.

92. Dobbs, A.P.; Jones, P.; Penny, M.J.; Rigby, S.E; *Tetrahedron*, **2009**, 65, 5271 – 5277.

93. Haridasan, N.K.; Bell, S.L.; Process for preparing fluorinated carboxylic acids by treatment of fluoroalcohols with periodic acid in the presence of optional reaction mechanism, U.S. Patent 20080064900,13 Mar 2008.

94. Filler, R.; Fenner, J.V.; Stokes, C.S.; O'Brien, J.F.; Hauptschein, M.; *J. Am. Chem. Soc.*, **1953**, 75, 2693 – 2695.

2. Reactions of polyfluoroalkyl iodides with nucleophiles

2.1 Background

Paint coatings are a significant commercial market and useful as a means of protecting a variety of substrates from weathering and chemical attack. However, paint coatings fail by a variety of mechanisms, among which is UV degradation which can initially cause a loss of gloss of the coating and lead to delamination. A potential solution to this problem is to incorporate perfluoroalkyl units that may stabilise the polymer systems used in paint coatings to UV attack and slow the rate of biofilm formation.

2.2 Aims and approach

A potential solution to the problems associated with paint coatings is to introduce perfluoroalkylated groups into the paint formulation as part of the polymeric binder. Such perfluoroalkyl containing polymers can be of two types; main chain fluorinated or side chain fluorinated polymers. Main chain fluorinated polymers (Figure 2.1) have the perfluoroalkyl units as part of the polymer backbone whereas side chain fluorinated polymers feature the perfluoroalkyl unit as a side chain (Figure 2.2).

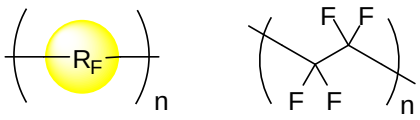

Figure 2.1: Examples of main chain fluorinated polymer

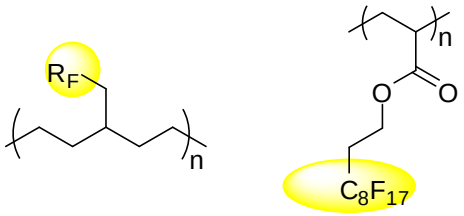

Figure 2.2: Examples of side chain fluorinated polymer

The two contrasting types of fluorinated polymer, in principle, give different surface properties arising from the packing of such systems. A qualitative prediction [1] suggests that while the perfluoroalkyl units in both main and side chain fluorinated systems surface segregate, due to an immiscibility with the other components of a coating system, they are arranged at the surface in different orientations (Figure 2.3). Main chain fluorinated systems lie parallel to the air/paint interface while side chain fluorinated systems have the perfluoroalkyl groups perpendicular to the surface. Differing orientations of perfluoroalkyl groups at the air/paint interface should lead to differences in the surface properties of the coating. In figure 2.3, it is postulated that a greater number of perfluoroalkyl units can position at an interface when the perfluoroalkyl units are part of a side chain, relative to perfluoroalkyl units bound as part of a main chain.

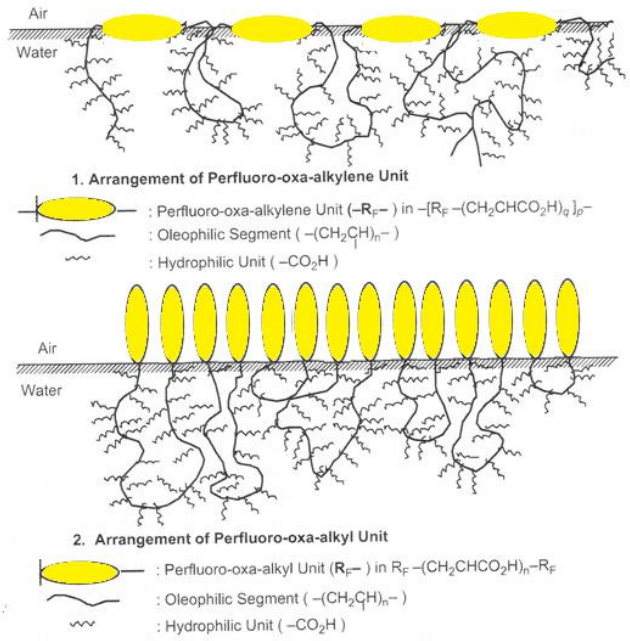

Figure 2.3: Orientation of main chain fluorinated (above) and side chain fluorinated (bottom) units at an air/water interface [1]

Main chain fluorinated polymers are synthesised from monomers with perfluoroalkyl regions as part of the backbone, connected to some functionality that can polymerise. Examples of such systems are shown below (Figure 2.4). Perfluoroalkylated main chain diols are useful as potential paint additives as they are commercially available on a large scale and relatively inexpensive. Bis(epoxy) and diamine monomers are used in many current paint formulations and so the perfluorinated analogues have potential as 'drop in' additives in which a coating containing perfluoroalkyl units can be synthesised by simply replacing one component of the mixture. Our selection of polyfluoroalkyl monomers was informed by the composition of existing paint formulations.[2,3]

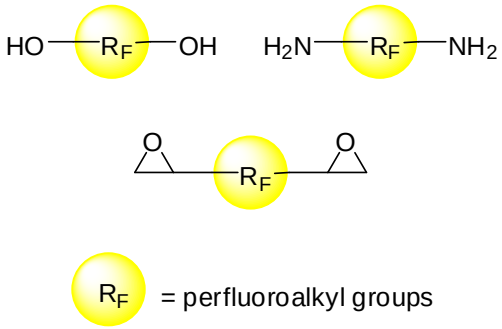

Figure 2.4: Monomers for main chain fluorinated systems

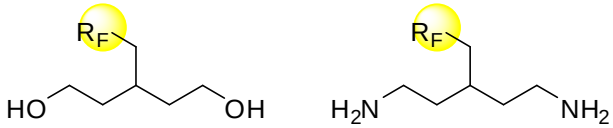

Figure 2.5: Monomers for side chain fluorinated polymers

In this chapter, we describe model reactions of $R_FCH_2CH_2I$ with a range of nucleophiles to assess the potential utility of polyfluoroalkyl iodides for incorporation of perfluoroalkyl groups into paint formulations.

2.3 Reactions of 1*H*,1*H*,2*H*,2*H*-perfluorooctyl iodide ($C_6F_{13}CH_2CH_2I$)

This chapter will focus on our initial attempts to synthesise monomers that could be used to produce side chain fluorinated polymers through use of 1H,1H,2H,2H-perfluorooctyl iodide, **1**, as a building block. **1**, produced by telomerisation of perfluoroethyl iodide, is a potentially useful building block as it is inexpensive and available from a number of suppliers on a large scale.

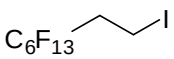

1

2.3.1 Reactions of 1*H*,1*H*,2*H*,2*H*-perfluorooctyl iodide, 1 ($C_6F_{13}CH_2CH_2I$), with oxygen nucleophiles

Model reactions were initially used to assess the viability of **1** as a building block for the creation of more complex organic systems through reaction with nucleophilic substrates such as alcohols. It was hoped that use of more complicated trifunctional nucleophiles would create difunctional products featuring two groups that allow the product of reaction to be used as a perfluoroalkylated monomer in paint formulations.

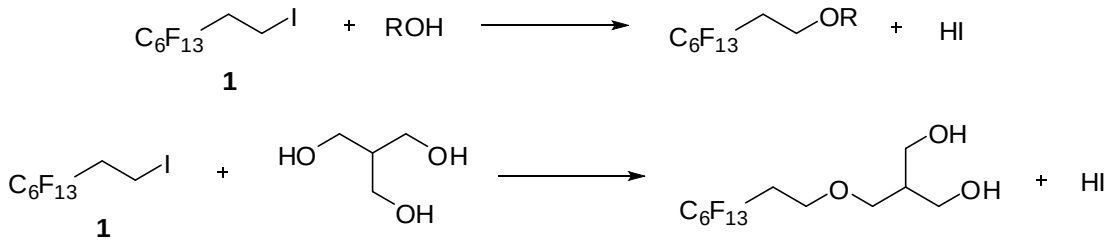

Figure 2.6: Generic reaction scheme for nucleophilic substitution of iodine

Consequently, our initial model experiments studied reactions of primary alcohols with 1*H*,1*H*,2*H*,2*H*-perfluorooctyl iodide with the aim of synthesising perfluoroalkylated ethers. These early reactions were a modified version of the procedure used by Matondo for the reaction of non-fluorinated alkyl bromides with primary alcohols [4] and were studied as initial model processes, with a view to extending the conditions to involve reactions featuring more complex di- and trifunctional alcohols if successful.

Reactions of **1** with 1-octanol (Figure 2.7) and *t*-butanol (Figure 2.8), in DMF and THF, gave, in all attempts, the perfluoroalkene **3** (Table 2.1). NMR analysis of the fluoroalkene product, **3**, shows six fluorine environments, with peak intensities and coupling constants consistent with a perfluorohexyl unit, and two proton environments in a 2:1 ratio with shift values in the alkene region of the spectrum. In the ^{19}F NMR

spectrum of **3** the fluorine atoms attached to the allylic γ-carbon appear at – 114.5 ppm, and are distinct from the position at – 115 ppm observed in the starting material.

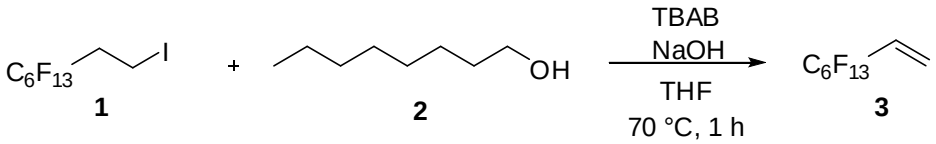

Figure 2.7: Reaction of 1H,1H,2H,2H-perfluorooctyl iodide with 1-octanol

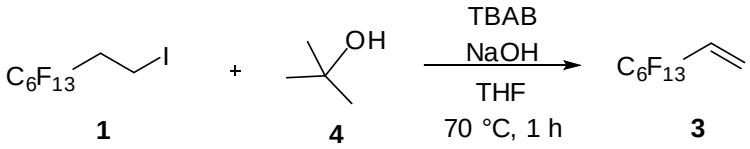

Figure 2.8: Reaction of 1H,1H,2H,2H-perfluorooctyl iodide with t-butanol

Table 2.1: Conditions for reaction of 1H,1H,2H,2H-perfluorooctyl iodide with oxygen nucleophiles

Nucleophile	Solvent	Phase transfer catalyst[a]	Base	Conditions	Product
n-$C_8H_{17}OH$	THF	TBAB	NaOH	70 °C, 1 h	**3**
n-$C_8H_{17}OH$	DMF	TBAB	NaOH	70 °C, 1 h	**3**
t-BuOH	THF	TBAB	NaOH	70 °C, 1 h	**3**
t-BuOH	DMF	TBAB	NaOH	70 °C, 1 h	**3**
$HO(CH_2)_2OH$	DMF	TBAB	KOH	70 °C, 1 h	**3**
$HO(CH_2)_2ONa$	THF	-	-	Ambient temperature, 4 h	**3**

[a] TBAB = Tetrabutylammonium bromide, Bu_4NBr

As noted previously, perfluoroalkyl chains are highly electronegative, which increases the acidity of the protons at the *β*-position of **1** relative to the non-fluorinated analogue 1-iodooctane, enhancing the likelihood of elimination.

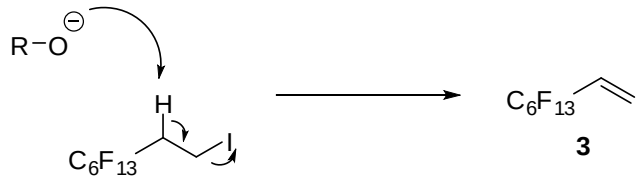

Figure 2.9: $E1_{CB}$ elimination of HI from a perfluoroethyl iodide

From these initial reactions between **1** and oxygen nucleophiles, including both alcohols and sodium alkoxides, it appears that elimination reactions dominate over substitution due to the acidity of the protons at the *β*-carbon, and proximity of a good leaving group. Since it appears that oxygen nucleophiles are too basic to give substitution products reactions between less basic nitrogen nucleophiles and 1*H*,1*H*,2*H*,2*H*-perfluorooctyl iodide were explored.

2.3.2 Reactions of 1*H*,1*H*,2*H*,2*H*-perfluorooctyl iodide with nitrogen nucleophiles

Nitrogen nucleophiles are, generally, less basic than oxygen nucleophiles [5] and the first nitrogen containing compound that we investigated as a model nucleophile was imidazole. This reaction was attempted twice, once using ethyl acetate as solvent at reflux temperature and once using microwave irradiation. In both cases a mixture of starting polyfluoroalkyl iodide **1** and the elimination product **3** were observed in ^{19}F NMR spectra of the crude reaction mixture.

However, reaction between 1*H*,1*H*,2*H*,2*H*-perfluoroalkyl iodide and *N*-methylimidazole under similar conditions with a reaction time of 24 hours, gave the substitution product **6** which was isolated in a 42 % yield (Figure 2.10). [6]

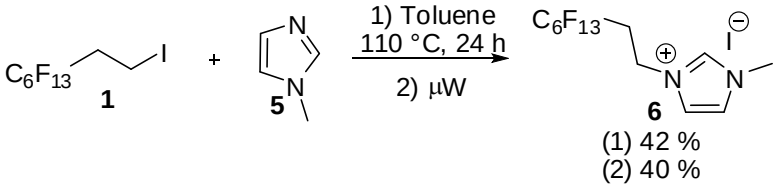

Figure 2.10: Nucleophilic substitution reaction between polyfluorinated alkyl iodide and N-methylimidazole

6 is a water soluble solid, and elemental analysis of the sample is consistent with an empirical formula of $C_{12}H_{10}N_2F_{13}I$. In addition, the ^1H NMR spectrum (acetone-d_6) displays a triplet at 4.78 ppm which is in the region of the spectrum associated with alkyl protons adjacent to a nitrogen atom, and a shift of over one ppm from the corresponding protons in the α-position of the starting perfluoroalkyl iodide.

Given this successful perfluoroalkylation reaction, a series of nitrogen nucleophiles were reacted with **1** to determine the substrate tolerance of the process. Reactions involving nitrogen nucleophiles were screened under microwave conditions in which 500 μmol of nucleophile was combined with a slight excess (~ 502 μmol) of 1*H*, 1*H*, 2*H*, 2*H*-perfluorooctyl iodide in approximately 2 mL of THF and heated to 100 °C for 40 minutes. The outcome of the microwave reactions between amines and **1** under microwave irradiation are tabulated below (Table 2.2).

Table 2.2: Outcome of reaction for nucleophiles with 1H,1H,2H,2H-perfluorooctyl iodide under microwave conditions

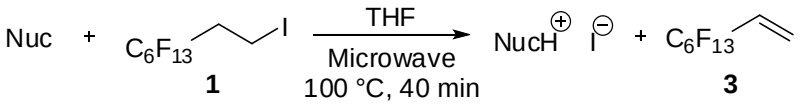

Nucleophile	pK_a	Outcome of reaction (Isolated yield)
Ethylamine	10.6	$EtNH_3I$ (66 %)+ **3**
Isopropylamine	10.6	$^iPrNH_3I$ (60 %) + **3**
Morpholine	8.36	$O(CH_2CH_2)_2NH_2I$ (49 %) + **3**
Diisopropylamine	11.1	$^iPr_2NH_2I$ (27 %)+ **3**
Triethylamine	10.8	Et_3NHI (24 %) + **3**

Unfortunately, as can be seen from table 2.2, each reaction led to the formation of a white salt, which was identified as the iodide salt of the amine conjugate acid, and **3**, formed by the same mechanism as before (Figure 2.9) by amine acting as a base in an $E1_{CB}$ mechanism. The white salts precipitated from the THF reaction solution but were soluble in water and acetone, which enabled analysis of the salts by NMR spectroscopy. ^{1}H NMR spectra of the salts all resemble the NMR spectra of the starting nitrogen bases, due to fast exchange of the most acidic proton in D_2O. ^{19}F NMR spectra of the salts showed no fluorine resonances and mass spectrometry data is consistent with amine.HI salt formation.

In order to minimise the possibility of competing elimination processes, nitrogen nucleophiles with a lower pK_a than *N*-methylimidazole were used. A summary of this work (Table 2.3) is presented, collating the pK_a of nucleophile with the outcome of the reaction.

Table 2.3: Correlation of pK_a data for nitrogen based nucleophiles and product of reaction for the reaction

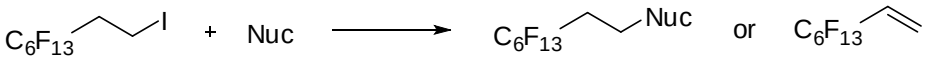

1 **3**

Nucleophile	pK_a	Product obtained
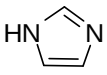	14.50	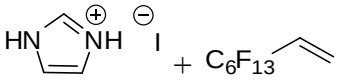 42 %
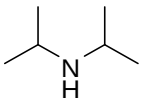	11.05	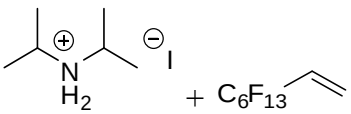 27 %
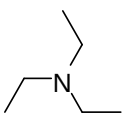	10.78	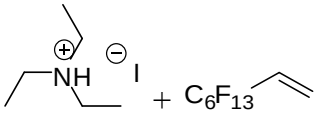

		24 %
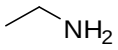	10.63	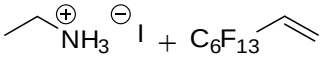 66 %
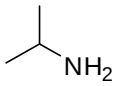	10.63	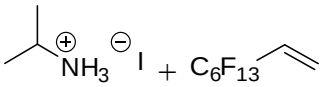 60 %
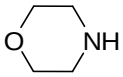	8.36	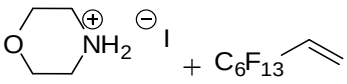 49 %
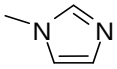	7.40	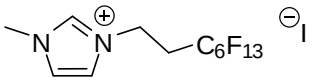 **6** 42 %
	5.25	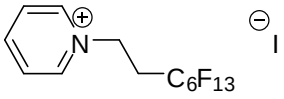 **7** 83 %
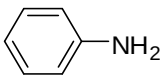	4.70	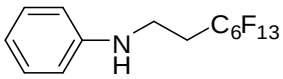 **8** 69 %
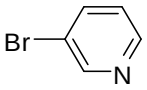	2.84	No reaction

As previously discussed, *N*-methyl imidazole gives predominantly products arising from substitution rather than elimination and is the nucleophile with the highest pK_a for which this is seen. Reaction of pyridine with an excess of 1*H*,1*H*,2*H*,2*H*-perfluorooctyl iodide leads to formation of a *N*-pyridinium salt. As for product **6**, arising from reaction of **1** with *N*-methyl imidazole, the ^{1}H NMR spectra of 1-(3,3,4,4,5,5,6,6,7,7,8,8,8-tridecafluorooctyl)pyridinium iodide, **7**, shows two peaks corresponding to alkyl methylene units. One is a complex multiplet due to H-F

coupling and the other a triplet, shifted by more than 3 ppm relative to the position of the peak in the starting material due to the presence of an adjacent positively charged nitrogen atom. Mass spectrometry (ESI^+) data shows a major peak corresponding to loss of 126.9 from the molecular ion, as would be expected for an iodide salt.

In contrast, reaction of aniline gives **8**. The reaction of aniline with **1** was performed with a four-fold excess of aniline, which can also act as a base and deprotonate any positively charged intermediate. Consequently, the ^1H NMR spectra of product **8** shows three aromatic environments and two alkyl environments with the protons β to the perfluoroalkyl unit less deshielded in **8** than **7** as the adjacent nitrogen atom is less electron deficient. In addition, both elemental analysis and mass spec are consistent with **8**. Attempted reaction of 3-bromopyridine with **1** failed to give either nucleophilic substitution or elimination even after six days at reflux.

The data in tables 2.2 and 2.3 suggests that when a nucleophile is also a reasonably strong base, $pK_a \geq 8.36$, then elimination is favoured due to the presence of a relatively acidic proton attached to the carbon adjacent to the perfluoroalkyl unit. In contrast, for nucleophiles with a pK_a between 7.40 and 4.70, products arising from nucleophilic substitution are obtained because the nucleophile is sufficiently nucleophilic but too weak a base for competing elimination to occur. Nucleophiles with a pK_a lower than 2.84 give no reaction since these are weak nucleophiles as well as weak bases. While basicity does not linearly correlate with nucleophilicity as basicity falls, generally, so too does nucleophilicity, and so unbasic molecules are often poor nucleophiles.

Consequently, perfluoroalkyl containing organic systems can be synthesised by nucleophilic substitution of perfluoroalkylethyl iodides if the nucleophile falls within a narrow pK_a 'window' of between 4.70 and 7.40. This limits the utility of this perfluoroalkyl building block for the synthesis of fluorinated monomers bearing a perfluoroalkyl moiety, but indicates the opportunities for the synthesis of perfluoroalkylated pyridine and imidazolium derivatives.

2.4 Reactions of 1*H*,1*H*,2*H*,2*H*,3*H*,3*H*-perfluorononyl iodide

Results above suggest that a more effective perfluoroalkylating agent would be perfluoroalkylpropyl iodides, such as **9**, where elimination is less likely to compete with the substitution process. Representative examples of reactions of tridecafluorononyl iodide **9** and a short series of nucleophiles were undertaken to assess the use of **9** as a perfluoroalkylated building block (Table 2.4).

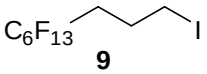

9

Table 2.4: Summary of reactions between nucleophiles and 4,4,5,5,6,6,7,7,8,8,9,9,9 -tridecafluorononyl iodide

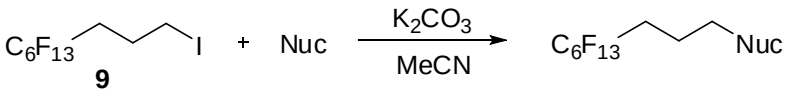

9

Nucleophile	Conditions	Product
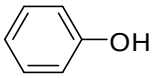	Reflux, 21 hours	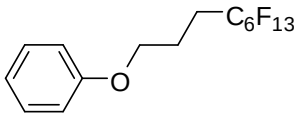 **10** 78 %
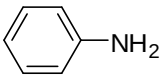	Reflux, 47 hours	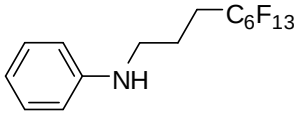 **11** 63 %
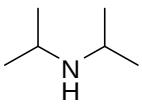	Reflux, 20 hours	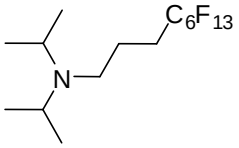 **12** 69 %

Reaction between perfluoroalkylpropyl iodide, **9**, and phenol was conducted under typical Williamson ether conditions involving weak base and a polar, aprotic solvent. These conditions were then extended to the other nucleophiles. [7] In each case the substitution products were observed and the resulting product isolated. ^{1}H NMR spectra of **10-12** all show three alkyl units between 1.50 ppm and 2.80 ppm with the most downfield signal split into a triplet due to only one adjacent methylene unit. **12** also shows a heptet, caused by splitting of a C*H* proton by six adjacent protons that are all chemically and magnetically equivalent. **10** is a semi-crystalline product, and a crystal structure was obtained by XRD (Figure 2.11). Figure 2.11 clearly shows the helical twist found in perfluoroalkyl chains, which was discussed in chapter 1. As a consequence of the helix the distance between C4 and C6 is greater than the distance between C1 and C3.

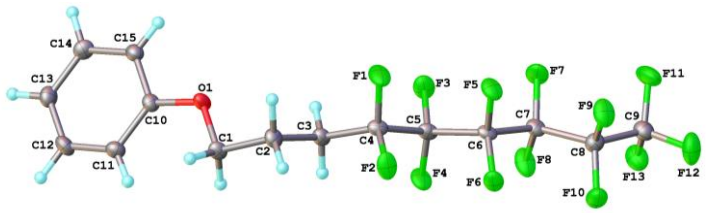

*Figure 2.11: Crystal structure of **10***

2.5 Conclusions

Nucleophilic substitution reactions involving perfluoroalkylethyl iodides, such as **1**, are possible if the nitrogen nucleophile has a pK_a value in the range 7.40 to 4.70 where the correct balance of nucleophilicity and basicity allows substitution to compete effectively with elimination. We have shown that in the presence of oxygen based nucleophiles elimination dominates because the pK_a values of the oxygen based nucleophiles are in excess of 8.36. This creates a limited range of suitable nucleophiles, most of which are nitrogen based, but does allow for the creation of some useful perfluoroalkylated functionalised products. A limited number of reactions of 1*H*,1*H*,2*H*,2*H*-perfluorooctyl iodide and nucleophiles have been reported in the literature but the use of pK_a to predict product outcome has not been discussed

previously.

Perfluoroalkylpropyl iodides are a more promising class of molecule to be utilised as fluorinated building blocks. However, perfluoroalkylpropyl iodides are significantly more expensive than perfluoroalkylethyl iodides, due to the more difficult synthesis, which limits the utility of perfluoroalkylpropyl iodides as building blocks for additives to large scale paint formulations.

2.6 References to chapter 2

1. Sawada, H.; *Prog. Polym. Sci.*, **2007**, 32, 509 – 533.
2. Dougherty, T.K.; Lau, S.E.; Rosales, T.L.; Tunick, S.A.; Amine curing agents and epoxy coatings produced using same, U.S. Patent 6103853A, 29 Jan 1998.
3. Neville, R.G.; Mahoney, J.W.; MacDowell, K.R.; *J. Appl. Polym. Sci.*, **2003** 12, 607 – 618.
4. Matondo, H.; Baboulene, M.; Rico-Lattes, I.; *Appl. Organomet. Chem.*, **2003**, 17, 239 – 243.
5. Bordwell, F.G.; *Acc. Chem. Res.*, **1988**, 21, 456 – 463.
6. Xu, L.; Chen, W.; Bickley, J.F.; Steiner, A.; Xiao, J.; *J. Organomet. Chem.*, **2000**, 598, 409 – 416.
7. Tojino, M.; Mizuno, M.; *Tetrahedron Lett.*, **2008**, 49, 5920 – 5923.

3. Perfluoroalkylated trimellitic anhydride for paint formulations

3.1 Introduction

Trimellitic anhydride (TMA) **13** is a potentially useful building block for the synthesis of side chain fluorinated monomers as the anhydride functionality is a masked diacid unit which can be incorporated into a polymer network by reaction with alcohols, to form ester linkages, or amines, to form amide linkages. In addition to the anhydride ring, TMA contains a carboxylic acid group, an electrophilic site potentially suitable as a site for reaction with fluorinated nucleophiles. TMA is readily used in many powder coating systems due to the low cost and the ease of obtaining TMA on a significant scale. Therefore, synthesis of a perfluoroalkylated analogue of TMA would create a fluorinated monomer that could be used as a 'drop-in' replacement for TMA in current paint formulations.

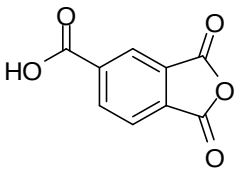

13

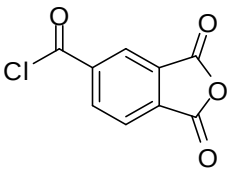

14

We decided to use trimellitic anhydride chloride (TMA-Cl) **14** as a building block due to the greater reactivity of the acid chloride relative to a carboxylic acid, which should lead to an enhanced chemoselectivity in reactions and, therefore, less ring opening during reaction with fluorinated nucleophiles.

3.2 Esterification of trimellitic anhydride chloride (TMA-Cl)

In complementary studies to the reactions of polyfluoroalkyl iodides discussed in

chapter 2, research in this chapter describes the synthesis of side chain perfluoroalkylated monomers synthesised by reaction of polyfluoroalcohols and TMA-Cl **14** through use of nucleophilic addition-elimination processes.

Due to the possibility of competing anhydride ring opening, initial reaction between **14** and 1*H*,1*H*,2*H*,2*H*-perfluorooctan-1-ol **15** was performed without the addition of base to maximise regioselectivity at the acid chloride site by using a weaker nucleophile. Refluxing trimellitic anhydride chloride and 1*H*,1*H*,2*H*,2*H*-perfluorooctan-1-ol, **15**, in dry THF led to formation of the desired ester **16** in low yield, along with several other compounds. Removal of the solvent led to the isolation of a brown oil that proved to have only limited solubility in a range of organic solvents. This insolubility hampered efforts to purify the mixture by both recrystallisation and silica chromatography, and probably arises as a consequence of ring opening polymerisation, and di- or tri-substitution, which lead to the formation of a mixture of highly fluorinated products.

The reaction was repeated, again in dry, degassed THF, but with less time at reflux. Analysis of the reaction mixture by GC-MS showed formation on an undesired product and so reaction was stopped prior to full conversion of the TMA-Cl. The side product arising has a mass consistent with the addition of two alcohol units to a single molecule of trimellitic anhydride chloride. However, the major component of the mixture was the ester **16**, isolated in 37 % yield.

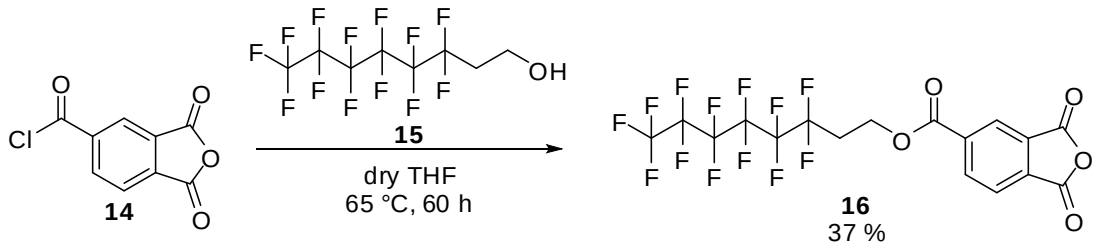

Figure 3.1: Reaction of trimellitic anhydride chloride with 1H,1H,2H,2H-perfluorooctan-1-ol

16 was isolated by washing of the crude reaction mixture with methanol and the low

yield is, in part, due to the partial solubility of fluorinated ester **16** in methanol. The NMR spectra of **16** shows no significant chemical shift differences from the ^{1}H and ^{19}F NMR spectra of the fluorinated alcohol **15**. Since NMR spectra of **16** are similar to the NMR spectra of the starting materials the reaction is best followed, and analysed, by mass spec techniques, in particular GC-MS.

The reaction was extended, on a similar 6 mmol scale, to include the larger C_8F_{17} homologue. As before, the reaction was performed in refluxing dry THF. The reaction was stopped and worked up after 23 hours due to the onset of side product formation observed by GC-MS. The reaction mixture was purified by removal of solvent and volatile components under vacuum, and by washing the crude solid obtained from this process with methanol to leave a white waxy solid. However, the isolated yield of **18** was 13 %, reflecting the incomplete reaction.

Unfortunately, reaction between the polyfluorinated decanol and trimellitic anhydride chloride performed at room temperature to minimise side reactions gave a significantly worse conversion, and no useful amount of perfluoroalkylated product were formed. However, larger scale reactions at reflux temperature gave 48 % yield of **18** as side product formation was less of a problem in larger scale reactions.

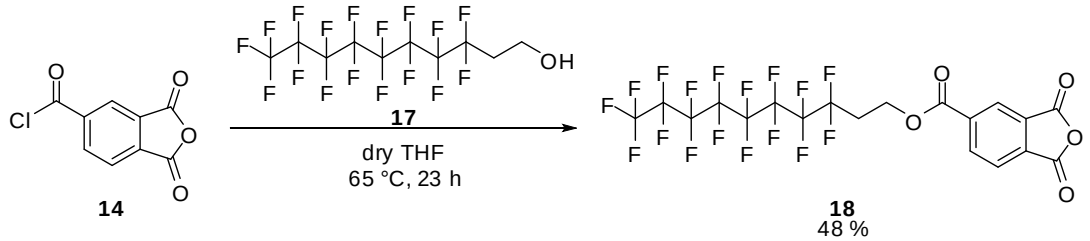

Figure 3.2: Initial conditions for esterification of an acid chloride by reaction with fluoroalcohol

Reactions were also extended to shorter perfluoroalkyl homologues, although the products of these reactions could not be isolated as pure products. GC-MS data shows the formation of the desired esters from reaction between **14** and lighter fluorinated alcohols, but the ester products are entirely miscible with alcohols and

could not be purified by washing with methanol, nor could they be purified by silica chromatography or recrystallisation.

To use **16** as a 'drop-in' additive in the synthesis of a polyester resin suitable for use in a powder coating approximately 100 g of **16** was needed for initial testing. This was achieved using a series of batch processes, with batches using between 75 and 100 mmol of acid chloride **14**. The key step to obtaining a pure product on this scale is to ensure full removal of solvent and volatile material before washing with methanol, because incomplete removal of solvent led to a golden coloured oil that was entirely miscible with methanol. Consequently, purification became very difficult. A further 120 gram quantity of **16** was produced, by a series of batch reactions, due to the promising nature of initial formulation testing with **16** in a resin for powder coatings.

Additionally, as a control experiment, to compare the effect of the fluorinated side chain attached to the diacid system in paint formulations, the non-fluorinated analogue **19** was synthesised by reaction of TMA-Cl, **14**, with 1-octanol in THF. A variety of conditions were investigated in order to optimise the reaction (Table 3.1). As with the fluorinated systems, the key step in purification is to ensure a dry solid before washing, although this was easier to achieve with this hydrocarbon system **19** than with the fluorinated systems **16** and **18**.

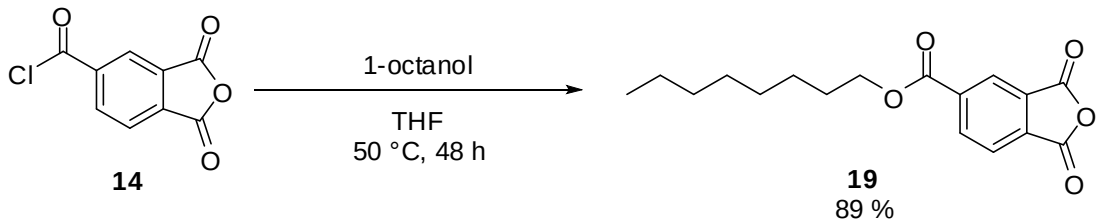

Figure 3.3: Reaction of trimellitic anhydride chloride and 1-octanol

*Table 3.1: Conditions used for the reaction between trimellitic anhydride chloride and 1-octanol, and extent of conversion to desired monoester **19***

Ratio TMA-Cl:1-Octanol (n:1)	Temp / °C	Reaction time / h	GC yield / %
1.06	65	48	72
1.10	65	91	77
0.71	65	116	60
1.00	55	48	94
1.00	50	48	96

As would be expected, an excess of alcohol (Table 3.1, entry 3) leads to a lower yield, due to the formation of greater amounts of di- and tri-substituted product. Lowering the temperature gives a large increase in crude yield, due to a lowering of side reactions at the anhydride functional group. After a brief optimisation of the reaction conditions this process was repeated several times to synthesise 120 g of **19** for incorporation into a powder coating system.

3.3 Stability of perfluoroalkylated TMA-ester 16 under polyester forming conditions

Prior to the attempted incorporation of the synthesised fluorinated ester **16** into a polymer paint resin it was necessary to check that the perfluoroalkyl unit is not liberated under the paint formulation conditions and, consequently, lost from the polyester linked resin that is created.

Model transesterification reactions were performed under similar conditions to those currently used for polyester synthesis, using equimolar amounts of NPG **20** (2,2-dimethyl-1,3-propanediol) and perfluoroalkylated TMA ester **16**, in the presence of a proprietary tin based catalyst marketed as BNT cat-210 (Figure 3.4). Transesterification was carried out independently at two separate temperatures, 200 °C, which is typical of the conditions used in polyester forming reactions featuring

TMA and NPG, and 150 °C, a high temperature that is below the boiling point of 1*H*,1*H*,2*H*,2*H*-perfluorooctan-1-ol to minimise evaporation of the perfluoroalkylated alcohol if, indeed, it is eliminated from the ester group.

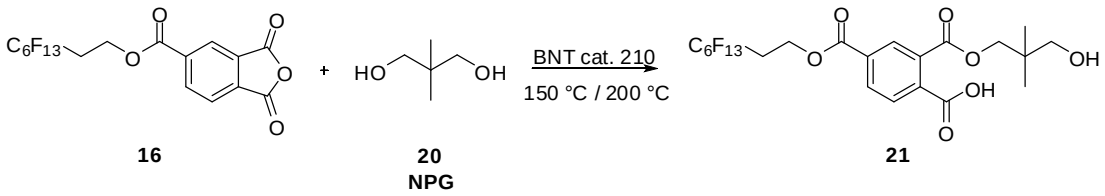

Figure 3.4: Conditions for model transesterification reaction

The ^{1}H NMR spectra of both 1*H*,1*H*,2*H*,2*H*-perfluorooctan-1-ol **15** and TMA-ester **16** were measured previously, and the shift for the alkyl protons at the *β*-carbon position differ, from 2.60 ppm for **16** to 2.35 ppm for the free alcohol **15** (Figure 3.5). This allows the relative amounts of **16** and any free perfluoroalkyl alcohol eliminated from the TMA-ester to be determined by comparison of NMR peak intensity.

Aliquots of the reaction mixture were taken every hour for eight hours and then again after 24 hours. All samples were analysed by ^{1}H and ^{19}F NMR spectroscopy, and several samples were also analysed by GC-MS. The GC trace of the reaction mixture showed only one peak, corresponding to **16**. Presumably, any oligomer or polymer formed is not volatile enough to pass down a GC column, and no free fluorinated alcohol was detected.

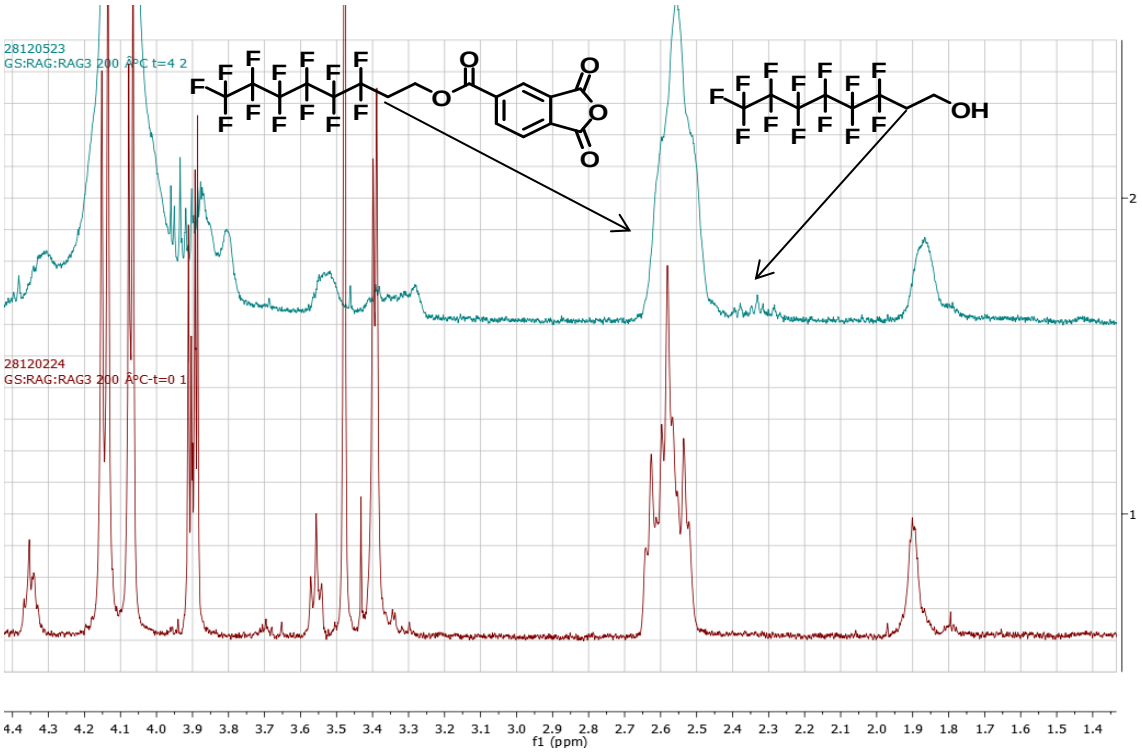

*Figure 3.5: ^{1}H NMR spectra of an equimolar amount of **16** and NPG (bottom) and overlay of NMR spectra after heating for four hours in the presence of a tin catalyst*

By a comparison of peak intensities in the ^{1}H NMR spectra of the model esterification reaction (Figure 3.5) it is possible to estimate the percentage of non-bonded 1*H*,1*H*,2*H*,2*H*-perfluorooctan-1-ol **15** relative to the amount of perfluoroalkyl moiety attached to **16** as part of an ester functional group. This ratio was calculated for reaction at both 150 °C and 200 °C from the ^{1}H NMR intensities at 2.60 and 2.35 ppm, and the ratio of free fluorinated alcohol to esterified alcohol can be estimated (Table 3.2). At higher temperature it appears that more 1*H*,1*H*,2*H*,2*H*-perfluorooctan-1-ol is liberated in the early time phase of the reaction, but the amount of free fluorinated alcohol then decreases over time, presumably as NPG is incorporated into the polyester backbone leaving the fluorinated alcohol as the only nucleophile which can react with any remaining free acid/anhydride groups. It is also possible the amount of non-bonded 1*H*,1*H*,2*H*,2*H*-perfluorohexan-1-ol falls due to evaporation at high temperature.

Table 3.2: Amount of free 1H,1H,2H,2H-perfluorooctan-1-ol as a percentage of the total amount of perfluoroalkyl moiety in transesterification reaction (Figure 3.4)

	% free fluoroalcohol	
Time / h	150 °C	200 °C
0	0.0	0.0
1	0.0	8.0
2	5.7	7.9
3	-	8.3
4	3.8	9.1
5	5.7	14.5
6	5.7	3.9
7	3.8	2.9

The data shown in table 3.2 suggests that **16** is sufficiently stable to the conditions used for polyester resin synthesis. While some fluoroalcohol is eliminated during the esterification reaction with NPG, this is minimal, and most of the fluoroalcohol formed is re-incorporated into the molecule by reaction with alternative carbonyl units, such as the anhydride ring. This might lead to a complex mixture being formed *in situ* but this does not matter for paint coating applications, which are generally poorly defined polymers of high polydispersity.

3.4 Synthesis of polyester resins bearing alkyl and perfluoroalkyl side chains

The synthesis of polyfluoroalkylated polyester resins for use in powder coatings were run as three stage processes. Stage one involved the melting and mixing of the hydroxyl functional components; NPG **20** (245 g), TMP **22** (2-ethyl-2-hydroxyethyl-propane-1,3-diol, 5 g) and water (40 g), with tin based BNT cat-210 (100 mg) and a limited amount of IPA **23** (isophthalic acid, 360 g) which gives a hydroxyl functional polyester (Figure 3.6). This was achieved by initially heating the reaction vessel to 150 °C and increasing the temperature to 230 °C in a step wise fashion over six

hours. After the reaction mixture became clear the temperature remained at 230 °C for a further 90 minutes before being lowered to 120 °C.

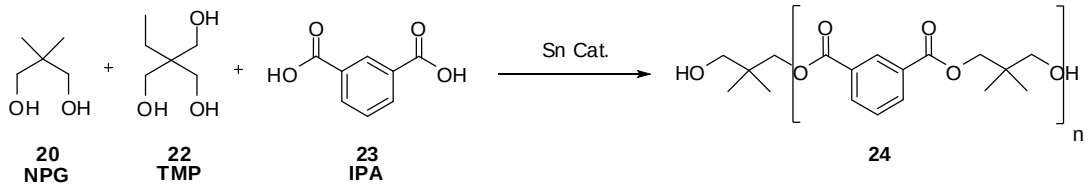

Figure 3.6: Scheme showing the first stage of the synthesis of polyester resins

Prior to commencement of the second stage, the amount of acid and hydroxyl groups in the polymer mixture were found by titration. The acid value was found using an AV2 (acid value 2) operating procedure in which approximately two grams of the reaction mixture is taken and cooled to room temperature. Upon cooling, the reaction mixture forms a brittle solid which is dissolved in 50 mL of a xylene:dowanol mixture and this solution titrated with a 0.1 M solution of potassium hydroxide in methanol using phenolphthalein (1 % in methanol) as indicator. The hydroxyl value cannot be determined by an acid-base titration and so the sample is first reacted with a mixture of butyl acetate, *para*-toluenesulfonic acid and acetic anhydride which creates one mole of acid functionality for every mole of alcohol reacted. The mixture is then titrated with 0.6 M potassium hydroxide in methanol. Acid and hydroxyl values are shown later for each polymer system formed.

Stage two consisted of increasing the temperature of the stirred reaction mixture to 150 °C and, subsequently, adding further quantities of IPA (9.88 g) and adipic acid **25** (7.51 g), combined with an appropriate quantity of NPG (5.9 g) to correct for a lack of OH functionality, as determined by a titration of the hydroxyl group performed as described above. After addition of these components, the temperature was increased, again in a stepwise fashion, over four hours, up to 230 °C and left at this elevated temperature for four hours. Subsequently, the mixture was heated to 120 °C for 16 hours. After this 16 hour period the temperature was raised to 190 °C and NPG (1.10 g) added to again correct for a lack of OH functionality determined by further titration, and estimation of free hydroxyl functionality, to give polymeric

system **26**.

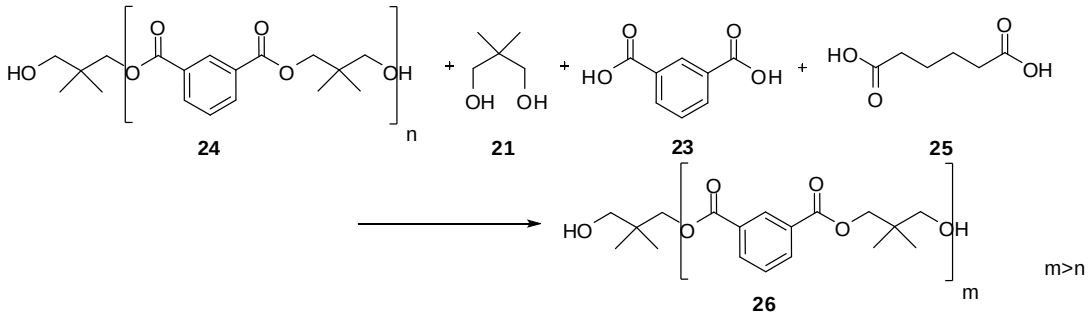

*Figure 3.7: Stage 2 for the synthesis of polyester resins end capped with **16** and **19***

Stage three was the addition of the TMA derived ester (**19** (67.2 g)) at 190 °C to end cap the previously hydroxyl functional polyester chain and give an acid functional polyester featuring a pendent side chain. This was achieved with a reaction time of 24 hours, the final 16 hours of which were spent at 120 °C.

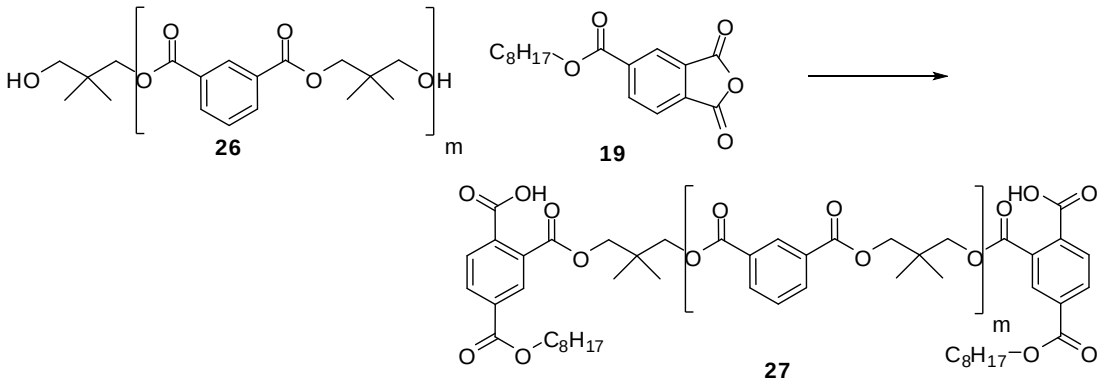

*Figure 3.8: Schematic for end capping of polyester chains with TMA derived anhydride system **19***

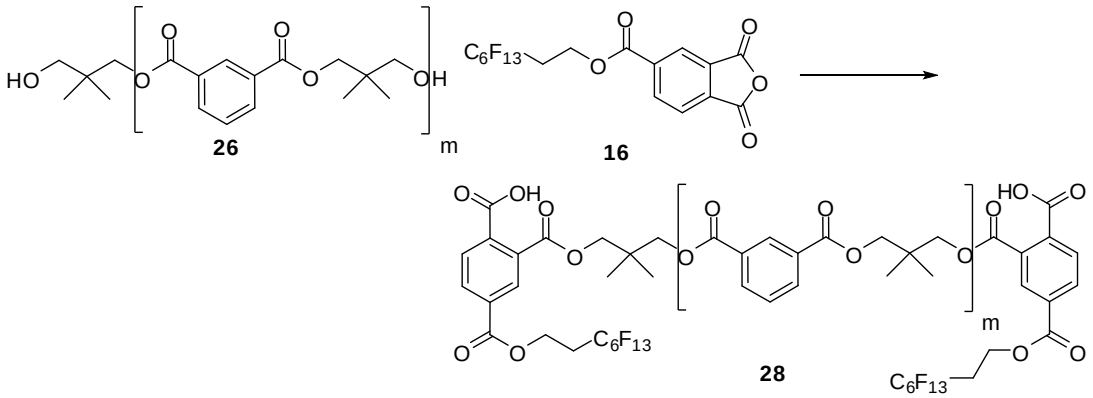

*Figure 3.9: Schematic for end capping of polyester chains with **16***

Two resins were synthesised, alkyl resin **27**, end capped with **19**, and polyfluoroalkyl resin **28**, end capped with **16,** over the course of four days.

3.4.1 Testing of a polyester resin synthesised for powder coatings

In section 3.4 two novel polyester resins **27** and **28** were synthesised with the aim of producing two new powder coating systems. This section discusses initial testing and characterisation performed for each resin.

One of the key properties for powder coatings is a low viscosity. As a simplification, it can be said that powder coatings lower the rate of corrosion of a coated metallic system by physically blocking attack of the substrate by reactive species, and by preventing the oxidation of the metal by forming a barrier to the removal of electrons from the system. For a coating to perform this task it must spread and cover the entire surface without defects such as air pockets, which can act as porous channels and aid flow of chemical agents such as water to the substrate surface. Low viscosity powder coatings provide better coverage as the flow of the coating occurs with lower force and generally leads to a smoother, more uniform coating with fewer defects. In designing resins for use in powder coating systems it is desirable to have a low viscosity but necessary to ensure the glass transition temperature is above room

temperature, and within a suitable operating window. Both resin **27** and resin **28** fit these criteria (Table 3.3).

Both resins are glassy, brittle solids at room temperature, as would be expected given that the glass transition temperatures, as measured by DSC, are significantly above ambient temperature (Table 3.3). While glass transition temperatures are slightly lower than that for polyester resins currently used in powder coating systems, the main criteria for a useful resin is that the resin is solid at room temperature but melts at easily accessible temperatures (T_g ~ 50 – 80 °C).

*Table 3.3: Data for polyester resins of the type shown in figures 3.8 and 3.9 end capped with **19** (**27**) and **16** (**28**)*

	Alkyl Resin **27**	Polyfluoroalkylated Resin **28**
AV2 / $mg.g^{-1}$	22.35	24.92
AV3 / $mg.g^{-1}$	27.03	29.25
Viscosity / p	22	13
OH_{value} / $mg.g^{-1}$	-16.76	-17.14
T_g / °C	47	51

The method of obtaining AV2 data was described above, and AV3 data is also found by a titration of the acid functionality. AV3 data is acquired by dissolving approximately 2.5 g of cooled final resin in 50 mL MEK:DMSO followed by addition of water (5 mL) which ring opens the anhydride ring forming two further acid groups. This mixture is then titrated with 0.6 M potassium hydroxide in methanol using a 3:1 mixture of thymol blue:cresol red dissolved in methanol (1 % w/v) as indicator. Any difference between the AV2 and AV3 values is therefore attributable to the extra acid groups formed from anhydride ring opening by water, and the amount of unreacted anhydride ring present can be calculated from the difference between AV2 and AV3.

The AV2 (acid value type 2) and AV3 (acid value type 3) values are similar for both resins **27** and **28** because the values were monitored during the synthesis, as described above, and corrections made to keep the values similar to both each other and to other standard polyester resins by addition of appropriate amounts of diol and IPA. Ideally, the difference in AV2 and AV3 values will be small, as this corresponds to a greater incorporation of the end capping group (either **16** or **19**). The hydroxyl value can be used as a measure of the extent of reaction of end groups as the value stays constant after complete reaction of all diol components. Values are commonly negative as they are referenced to a standard of distilled water.

GPC was performed on both resins to estimate the M_n and M_w of each sample. The alkyl resin **27** has a higher number and weight average molecular weight than the resin featuring pendent fluoroalkyl chains, **28**, and also a higher PDI, a measure of the heterogeneity of the size of polymer chains (Table 3.4). Resin **28** is more uniform in nature, with a slightly lower PDI indicative of a smaller range of masses of the polymer chains. This effect may be caused by the electron withdrawing effect of the perfluoroalkyl unit which lowers the reactivity of the terminal acid group and prevents addition of ring opened **16** adding to end capped polymer chains.

Table 3.4: Molecular weight data for polyester resins

Resin	Average M_n / $g.mol^{-1}$	Average M_w / $g.mol^{-1}$	Average PDI
Alkyl, **27**	5495.0	14857.5	2.70
Polyfluorinated, **28**	4601.5	10790.0	2.34

3.5 Synthesis of new powder coating systems

After analysis both resins, **27** and **28**, were processed to create powder coating systems. This involved grinding the resins into a powder and mixing with the other components, all of which are commonly used in powder coating systems, in the quantities shown in table 3.5. As can be seen in table 3.5 most of the mass of coating

comprises the polyester resin (**27** or **28**) while additives are either pigments (Titanium dioxide), organic molecules to aid flow by modifying viscosity (Primid XL522 **29**, and Benzoin **30**) or waxes.

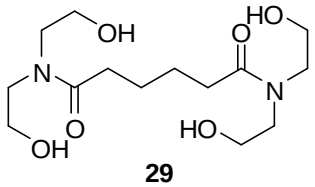

29

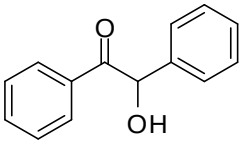

30

Table 3.5: Composition of powder resins synthesised from H-TMA and F-TMA

	Mass / g
Polyester resin (**27** or **28**)	655.7
Primid XL552 **29**	26.2
Benzoin **30**	3.0
Lanco Wax 1525MF	4.0
Byk LPG21191	10.0
Titanium dioxide	300.0
Total Mass	998.93

For both powder coating systems, this mixture of components was passed through a twin screw extruder, a process in which the powders are mixed and heated to form a homogenous paste. After cooling, the solidified pastes were broken into smaller pieces, ground further, and passed through a 45 Å sieve to give sufficiently fine powders for electrostatic coating of QUV-A aluminium panels. The aluminium panels were coated to a depth of approximately 65 μm and heated to 200 °C for exactly 15 minutes to cure the coating.

*Figure 3.10: Photos of coating samples bound onto Q-panels. From left to right: a current commercial coating (control), and powder coatings derived from **27** 'H-TMA' and **28** 'F-TMA'*

In addition to making test panels coated with powder coatings 'H-TMA' and 'F-TMA' derived from the novel resins **27** and **28** respectively, a set of aluminium panels were also coated with a currently used coating system as a control experiment. The powder coating used as a control is analogous to the powder coatings prepared from the novel polyester resins but end capped with trimellitic anhydride **13** and currently used as a commercial coating.

A range of tests currently used to assess powder coatings were performed with the focus on testing chemical stability, adhesion to the substrate and the gloss of the coating. Chemical stability is tested by a solvent rub in which a cloth dampened with MEK (methyl ethyl ketone) is rubbed back and forth over the coating 100 times, and the effect monitored by eye. All three coatings performed well and withstood the solvent rub without any smearing of the coating.

The crosshatch and reverse impact tests, in which a 1 Kg weight was dropped from 25 cm into the reverse of the test panels, were both assessed by eye. All three coating systems showed minor cracking of the coating upon deformation of the substrate

caused by the impact, with the perfluoroalkyl containing F-TMA coating showing the greatest degree of cracking. The F-TMA powder coating also performed worse after sticky tape was fixed to the sample and then peeled away, which is a further measure of adhesion between coating and substrate.

These trends are best observed by analysis of figure 3.11. A comparison of the dents in each coating, caused by the rear impact test, shows a loss of coating at the point of impact for F-TMA and H-TMA coatings whereas the control has not peeled off at the point of impact. The large difference in performance under the crosshatch test is apparent by comparing the points on each panel (Figure 3.11) where a grid has been scored into the powder coating. The F-TMA coated panel is completely uncoated at this point, whereas the other two coatings are intact, even after adhesion, and subsequent removal, of sticky tape.

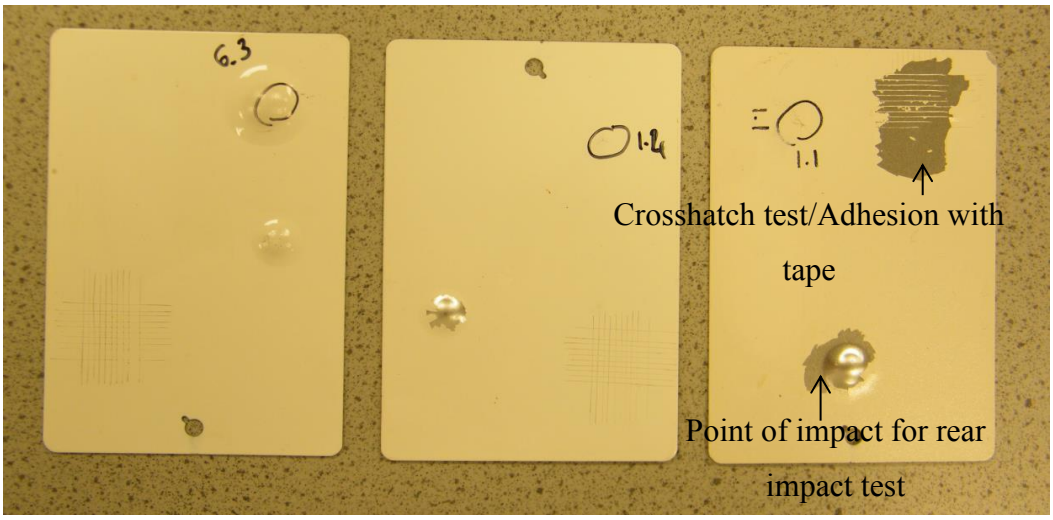

Figure 3.11: Photo of (L-R) control, H-TMA, F-TMA coatings after adhesion tests

Data from the Eriksson test (Table 3.6), in which a metal rod is mechanically forced into the rear of the test panel and the depth of penetration prior to the cracking of the coating is measured, correlates with the less qualitative reverse impact test described above in which it was noted that the unmodified control system had the greatest adhesion to the aluminium substrate. Between H-TMA and F-TMA, the two

modified coating systems, there is little difference but the currently used coating, used here as a control reference, performed significantly better than the modified coatings. The Eriksson test is a measure of the flexibility of a coating, and adding an alkyl chain to the polyester resin clearly reduces flexibility.

Table 3.6: Data from various tests on power coating systems; Control, H-TMA and F-TMA

			Control	H-TMA	F-TMA
Eriksson		Depth / mm	6.3	1.4	1.1
Gel test	Time for sample to gel / s	Run 1	139	74	83
		Run 2	126	70	77
		Run 3	123	65	88
Gloss test	% light reflected at angle	20 °	87.5	89.6	5.1
		60 °	97.0	100.2	33.3
		85 °	96.9	96.4	30.0

The gel test (Table 3.6) is performed by placing a sample of the resin used in each powder coating in a metal well heated to 200 °C. At such temperatures the resin melts to give a liquid, which is manually stirred and the time taken for the melted resin to gel is recorded as it is a measure of the reactivity of the resin. The gel test shows a similar pattern to the Eriksson test, the time taken for the resins to gel at 200 °C is similar for the two modified systems but the currently used system outperforms both. From the gel test it appears that addition of an alkyl or perfluoroalkyl side chain increases the reactivity of the resin.

The most interesting set of data observed, from the gloss test, shows the amount of light reflected from the coating surface at three different angles and always shows a maximum at 60 °. The two non-fluorinated powder coatings, the control and H-TMA, are broadly similar, and look similar to the eye, both being opaque, white coatings with a slight orange peel texture. The F-TMA coating is textured and thus scatters light making it visibly duller than the comparable non-fluorinated systems.

We can speculate that this morphology arises partly from phase separation of the perfluoroalkyl units.

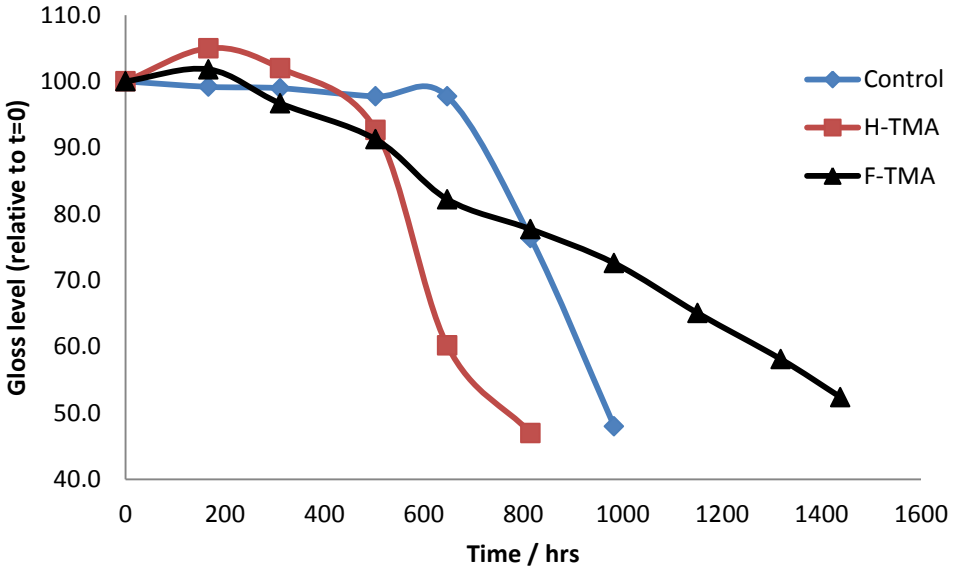

Figure 3.12: Change of gloss level over time for DP1918 and related powder coatings

Figure 3.12 shows that the F-TMA system undergoes gloss loss at a much slower rate, taking about 50 % longer to fall below the 50 % gloss loss threshold at which monitoring is stopped. While use of a resin featuring polyfluorinated pendent chains increases the lifetime of the coating, H-TMA coating shows a decrease in gloss retention relative to the control and so the increase in gloss retention is not merely due to the presence of an alkyl chain or a change in packing caused by incorporation of a side chain. However, table 3.6 showed that the F-TMA coating started with a low gloss level and this is an important caveat. At such low initial gloss levels the magnitude of gloss loss due to UV degradation can never be that great. Despite this, a coating system with the potential for greater gloss retention than the current commercial coating has been demonstrated, and would be of interest.

3.6 Conclusions

In this chapter it has been shown that fluorinated alcohols and 1-octanol can be

reacted with trimellitic anhydride chloride, **14**, under mild conditions to give ester products featuring a masked diacid as the major product. While the reaction is not entirely chemoselective, crude reaction mixtures are of reasonable purity and are easily purified further by washing with methanol. Use of these conditions and work-up procedure allowed **16**, **18** and **19** to be synthesised in a suitable quantity for powder coating synthesis (~ 100 g), through use of an iterative batch process.

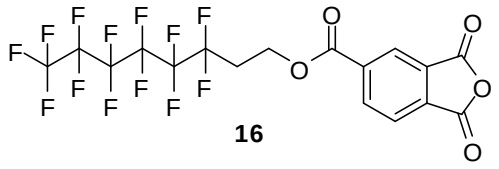

16

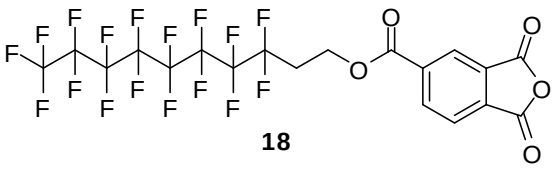

18

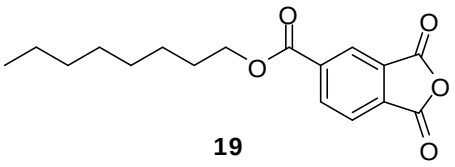

19

TMA derived esters **16** and **19** are capable of being incorporated into polyester resins suitable for powder coatings using current methodology, and IPA and NPG based polyester systems can be end capped creating novel powder coatings. Initial testing on these systems shows that these coating systems end capped with trimellitic anhydride with an attached alkyl (H-TMA coating) or perfluoroalkyl group (F-TMA coating) are less flexible than those that are end capped with TMA itself and thus fracture easier under an applied force. However, initial work on gloss retention under UV light shows that the incorporation of perfluoroalkyl units may prolong coating lifetime which would be a beneficial enhancement of powder coatings.

4. Synthesis of main chain perfluoroalkylated amines and epoxides for paint formulations

4.1 Introduction

In chapters two and three discussion focused on the creation of side chain fluorinated monomers from polyfluorinated iodides and polyfluorinated esters. In contrast, 2,2,3,3,4,4,5,5,-octafluorohexan-1,6-diol, along with difunctional derivatives such as 2,2,3,3,4,4,5,5-octafluorohexan-1,6-dimaine (Figure 4.1), should act as a main chain monomer as the perfluoroalkyl unit is part of the monomer backbone (Figure 2.4). Diepoxides and diamines are common monomers in paint coating formulations and, therefore, polyfluorinated diepoxides and polyfluorinated diamines could potentially be exploited as 'drop-in' monomers in a range of current formulations.

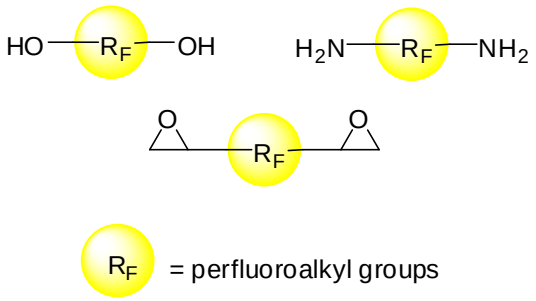

Figure 4.1: Main chain fluorinated monomers for use in paint formulations

While polyfluorinated alcohols are readily available as the products of telomerisation reactions, polyfluorinated epoxides and amines are either not commercially available or prohibitively expensive and, therefore, need to be synthesised from commercially available polyfluoroalcohol building blocks such as **31**. The synthesis of polyfluorinated epoxides from commercially available **31** are discussed in this chapter along with the synthesis of polyfluorinated diamines and related side chain perfluoroalkylated derivatives.

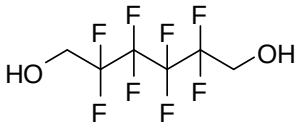

31

4.2 Gabriel synthesis of polyfluorinated diamines ($H_2NCH_2R_FCH_2NH_2$)

The Gabriel synthesis [1] is a method for the synthesis of amines by substitution of a leaving group, commonly a halide. This method has the advantages that it avoids the use of azide and amide reagents, which, while good nucleophiles, are highly toxic, and proceeds under mild conditions.

A literature precedent for the conversion of an alcohol connected to a perfluoroalkyl unit into an amine has been reported and provides a potentially useful method for the synthesis of perfluoroalkylated diamines for use in paint systems. [2, 3] The first step in a Gabriel synthesis is to convert the hydroxyl functionality into a leaving group by reaction with tosyl chloride **32**.

Following this method, we found that 2,2,3,3,4,4,5,5-octafluorohexane-1,6-diol **31** reacts with tosyl chloride under standard conditions, with the ditosylate product **33** isolated in 58 % yield after recrystallisation from methanol. In addition, the dimesylate compound **35** was synthesised to provide an analogue that is potentially more reactive than the ditosylate **33** towards nucleophiles in subsequent processes.

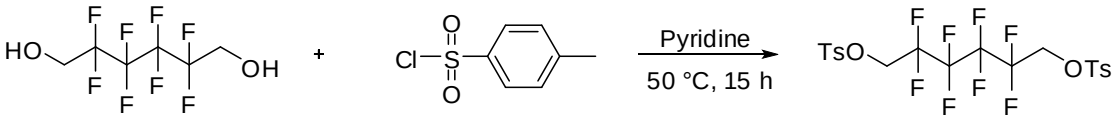

31 + **32** → **33** 58 %

Figure 4.2: Synthesis of a fluorinated ditosylate

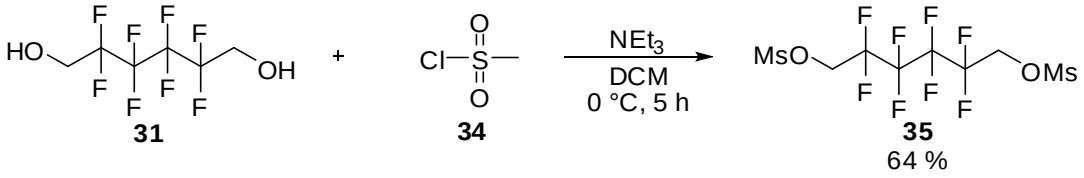

Figure 4.3: Synthesis of polyfluorinated dimesylate

In reactions between potassium phthalimide and either **33** or **35** (Table 4.1), performed in high boiling solvents, no sign of reaction was observed by ^{1}H NMR spectroscopy, ^{19}F NMR spectroscopy, or GC-MS. Given the low reactivity of these polyfluorinated electrophiles the more reactive ditriflate **37** was synthesised from 2,2,3,3,4,4,5,5-octafluorohexane-1,6-diol. Unusually for a triflate species **37** is crystalline and reasonably stable, which allowed a molecular structure of **37** to be obtained by X-ray crystallography (Figure 4.5).

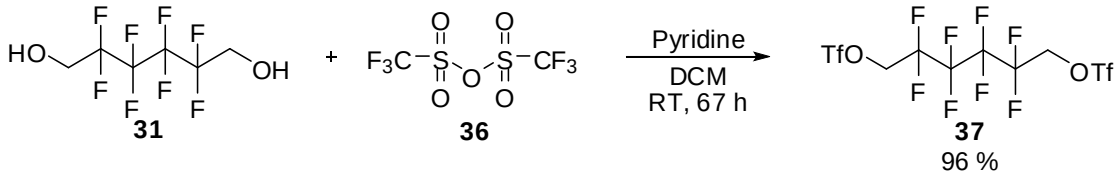

Figure 4.4: Synthesis of a fluorinated bistriflate

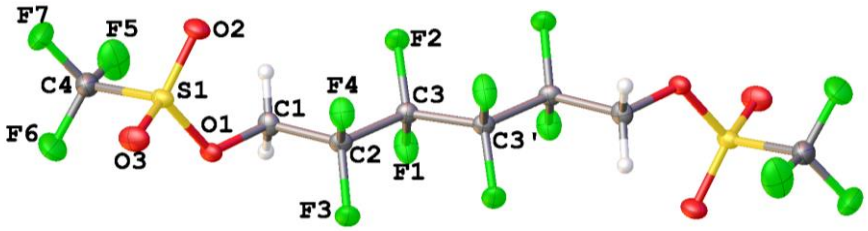

*Figure 4.5: Molecular structure of **37***

Table 4.1: Conditions attempted for reaction between potassium phthalimide and polyfluorinatedactivated electrophiles

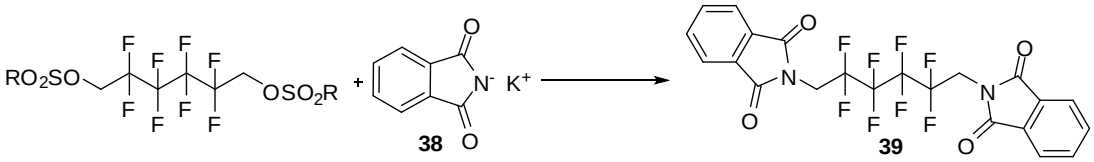

Electrophile	Solvent	Temperature / °C	Reaction time / h	Outcome of reaction
33	DMF	140	20	No reaction
33	DMF	150	5	No reaction
33	DMF	120	67	No reaction
33	HMPA	200	5	No reaction
33	DMPU	200	5	No reaction
33	DMPU	220	5	No reaction
33	DMPU	220	10	No reaction
35	DMF	80	18	No reaction
35	DMF	120	4	No reaction
37	DMF	100	20	**39** (91 %)

As can be seen from table 4.1, **37** was reacted with potassium phthalimide and, under relatively mild conditions, nucleophilic substitution led to isolation of desired **39** (Figure 4.6).

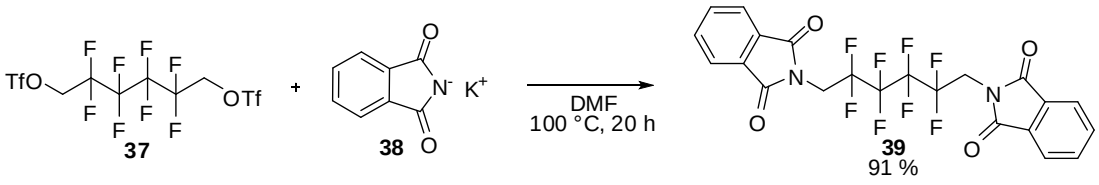

Figure 4.6: Reaction of fluorinated bistriflate with potassium phthalimide

In the final stage of the multi-step synthesis, perfluoroalkylated diphthalimide **39** was treated with hydrazine hydrate in refluxing ethanol. [4] A brief study into the optimal reaction conditions was performed and 2,2,3,3,4,4,5,5-octafluorohexane-1,6-diamine **40** was isolated in a 21 % yield.

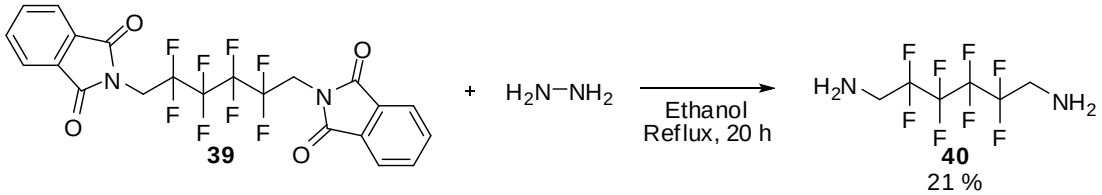

Figure 4.7: Conditions for hydrazinolysis of 2,2'-(2,2,3,3,4,4,5,5-octafluorohexane-1,6-diyl)diisoindoline-1,3-dione

The ^{1}H NMR spectrum of the polyfluorinated diamine **40** contains two peaks of equal peak intensity. This corresponds to **40** which has only two distinct proton environments due to the symmetrical nature of the molecule and, of the two peaks, one is a triplet of triplets, due to $^{3}J_{HF}$ and $^{4}J_{HF}$ coupling and the other peak is a broad singlet indicative of an amine group.

Whilst the main chain fluorinated diamine monomer **40** was successfully synthesised in low yield, the amount of diamine **40** produced was small (< 100 mg), much less than the quantity needed for satisfactory testing as a paint coating additive. Due to the difficulty in producing useful quantities of material this multi-step route was, unfortunately, considered unsuitable for the synthesis of **40** on the necessary scale and alternative approaches to main chain fluoroalkyl systems were investigated.

4.3 Two-step approach for the synthesis of fluorinated epoxy and diepoxy systems from fluorinated alcohol building blocks

Many polymer coating systems used by the protective coatings industry contain epoxy-amine functionality and so our research focused on the synthesis of potential 'drop-in' perfluoroalkylated epoxy systems as a means of synthesising paint coatings bearing main chain perfluoroalkyl units. Two approaches were taken towards these targets; the reaction of alcohols and allylic electrophiles to form ethers, with subsequent oxidation of the allylic double bonds (Route A, Figure 4.8) and reaction of fluorodiol with epichlorohydrin (Route B, Figure 4.8).

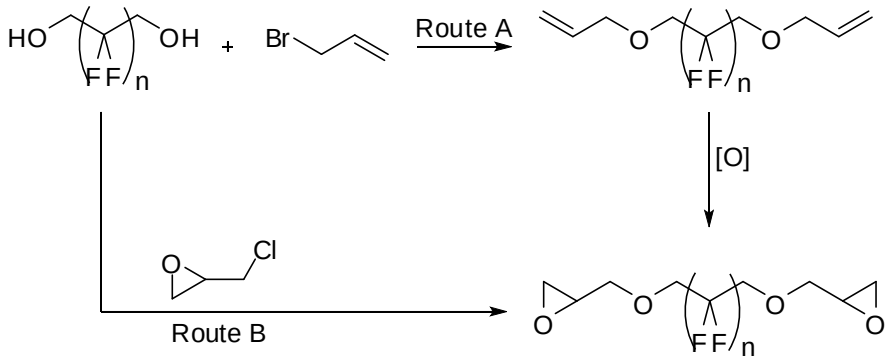

Figure 4.8: General approach for conversion of a fluorinated diol into fluorinated diepoxy monomer

4.3.1 Reaction of polyfluoroalcohols in the presence of strong base

Model reactions involving alcohols were performed. Processes featuring monofunctional systems are experimentally simpler than the corresponding processes involving difunctional systems and so our research in this area initially investigated the synthesis of polyfluorinated monoepoxy systems.

Preliminary work proceeded with model, powerful electrophiles; benzyl bromide, as a model for alkyl halide systems such as allyl bromide, and benzoyl bromide as a model for carbonyl systems so that the viability of polyfluorinated alkoxides as nucleophiles could be assessed. In both instances the desired reaction, nucleophilic substitution and addition-elimination, proceeded cleanly with no trace of side products (Figures 4.9 and 4.10).

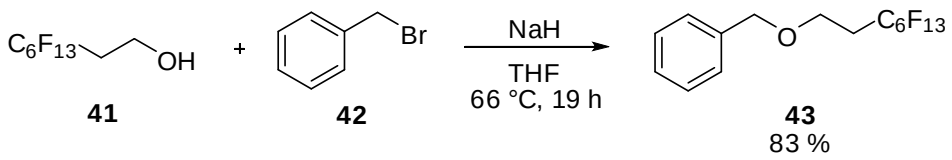

*Figure 4.9: Reaction of fluorinated alcohol **41** with benzyl bromide*

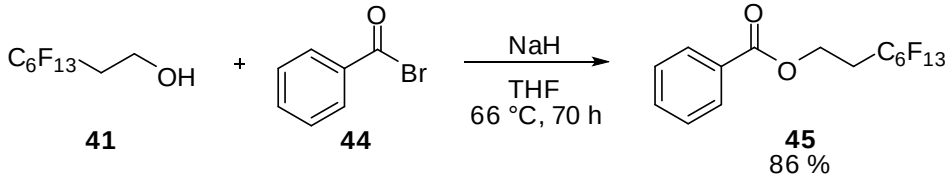

*Figure 4.10: Reaction of fluorinated alcohol **41** with benzoyl bromide*

After these initial successful exploratory reactions, reactions of perfluoroalkylated alcohols with allyl bromide (Table 4.2) were studied. In all reactions shown (Table 4.2), only a single product was isolated, and all products were 99+ % pure after a single wash with water.

Table 4.2: Reactions of perfluoroalkylated alcohols with allyl bromide in the presence of strong base

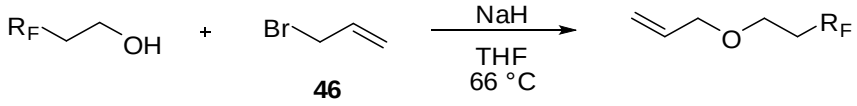

R_F	Reaction time / h	Product	Yield / %
C_2F_5	40	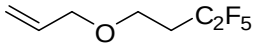 **47**	Not isolated
C_4F_9	69	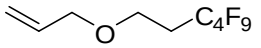 **48**	59
C_6F_{13}	70	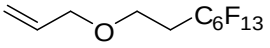 **49**	73
C_8F_{17}	41	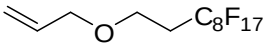 **50**	69

The C_2F_5 homologue, derived from 3,3,4,4,4-pentafluorobutan-1-ol, could not be isolated since allyl ether **47** is probably too volatile, and was lost due to evaporation from the reaction mixture. Analogues of these species, featuring CF_2H terminal units, were also synthesised using the same conditions giving a related class of polyfluorinated allyl species that could be used to compare the effect of a terminal CF_3 group with a terminal CF_2H group in paint coatings.

Table 4.3: Conditions for reaction of CF_2H terminal perfluoroalkylated alcohols with allyl bromide

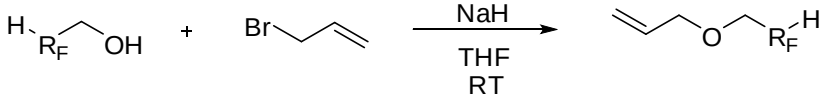

R_F	Reaction time / h	Product	Yield / %
C_4F_8	46	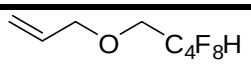 **51**	62
C_6F_{12}	68	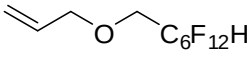 **52**	85

In attempts to create the bis(allyloxy) species derived from 2,2,3,3,4,4,5,5-octafluorohexane-1,6-diol **31**, three methods were attempted. One approach involved reaction of compound **33** with allyl alkoxide (Figure 4.11), but despite reflux for 44 hours no conversion was observed by ^{19}F NMR spectroscopy and 82 % of the ditosyl compound was later reclaimed from the reaction mixture.

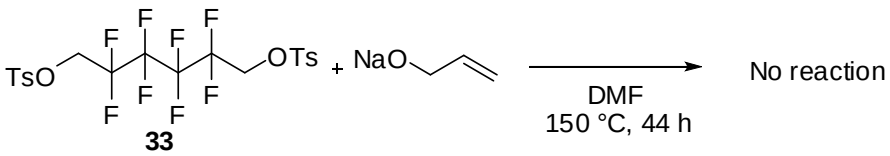

*Figure 4.11: Conditions for attempted reaction of allyl alkoxide with **33***

An alternative method investigated was a Mitsonobu coupling reaction of allyl alcohol with **31** in the presence of DIAD and triphenylphosphine. [5] However, the reaction gave no conversion, with ^{19}F NMR spectra showing that the only species present after 24 hours of reaction was the starting octafluorodiol.

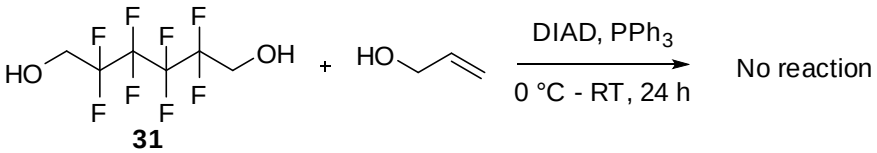

Figure 4.12: Attempted Mitsonubu reaction between fluorinated diol and allyl alcohol, resulting in no reaction

The final method investigated used the same sodium hydride mediated conditions as in tables 4.2 and 4.3. However, reaction of diol **31** in an excess of allyl bromide gave an insoluble gel from which no useful product could be isolated. Due to the formation of a gel in THF solution, the reaction was attempted in various other solvents (Table 4.4). Reactions performed in DMF show the necessity of base in enabling the reaction. Use of diethyl ether gave a much greater conversion than the other solvents screened, but separating bis(allyloxy) system **53** and the mono(allyoxy) **54** compound was not possible by either distillation or silica chromatography.

*Table 4.4: Variation of reaction solvents for conversion of **31** to bis(allyloxy) **53***

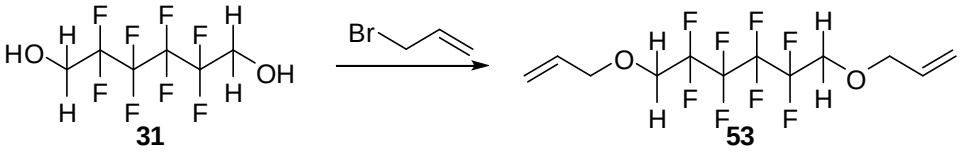

31 **53**

Solvent	Base	Reaction time / h	Reaction temp / °C	Conversion / %	Comments
THF	NaH	14	66	-	Gel formation
DMF	-	66	120	3	
DMF	NaH	66	125	68	
MeCN	NaH	22	82	71	
Et_2O	NaH	166	35	84	23 % isolated yield

While silica chromatography and distillation are not effective means of separating **53** and **54**, recrystallisation of a mixture of **53** and **54** in chloroform:hexane allowed the isolation of the desired bisallyloxy compound **53**, but in low yield (23 %). For testing in paint coating formulations around 40 g of the polyfluorinated bis(epoxide) are required, and such low yields in the first step of a two-step process are prohibitive due to the amount of material wasted. This suggests that in order to isolate a pure sample of **53** the reaction needs to reach full conversion which will be slow in diethyl ether. Ensuring full conversion makes separation of **53** and **54** unnecessary.

Consequently, the reaction was performed under more typical William ether synthesis conditions in acetone with potassium carbonate used as base (Figure 4.13).

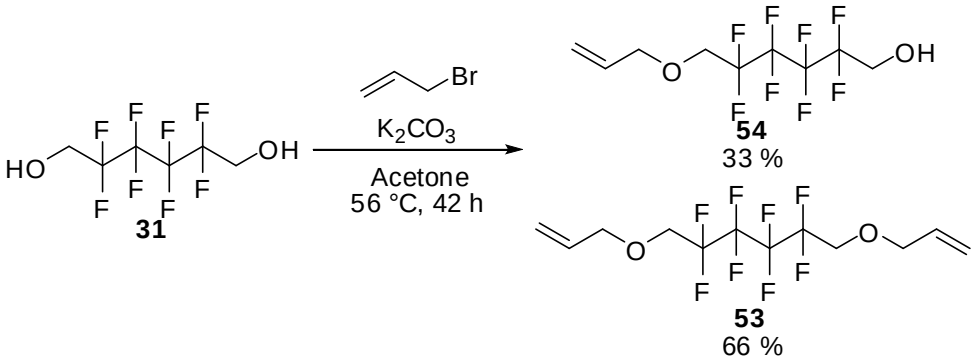

Figure 4.13: Ether synthesis in acetone

As with attempts using sodium hydride, mono- and di- allylated products were formed. Due to the difficulty in separation it is necessary to ensure full conversion which was achieved by using a large excess of allyl bromide and potassium carbonate. The mixture was followed by ^{19}F NMR spectroscopy allowing the extent of conversion to be monitored over time (Figure 4.14). ^{19}F NMR studies show that the surface area of potassium carbonate is an important factor in the rate of reaction, as reactions in which commercial anhydrous potassium carbonate was ground before use, to give a greater surface area:mass ratio, proceeded faster. As can be seen (Figure 4.14) the rate of reaction slows over time, which is typical of bimolecular reactions. However, the observed rate of reaction of the mono-allyloxy compound **54** appears to be slower than the rate of reaction of **31**.

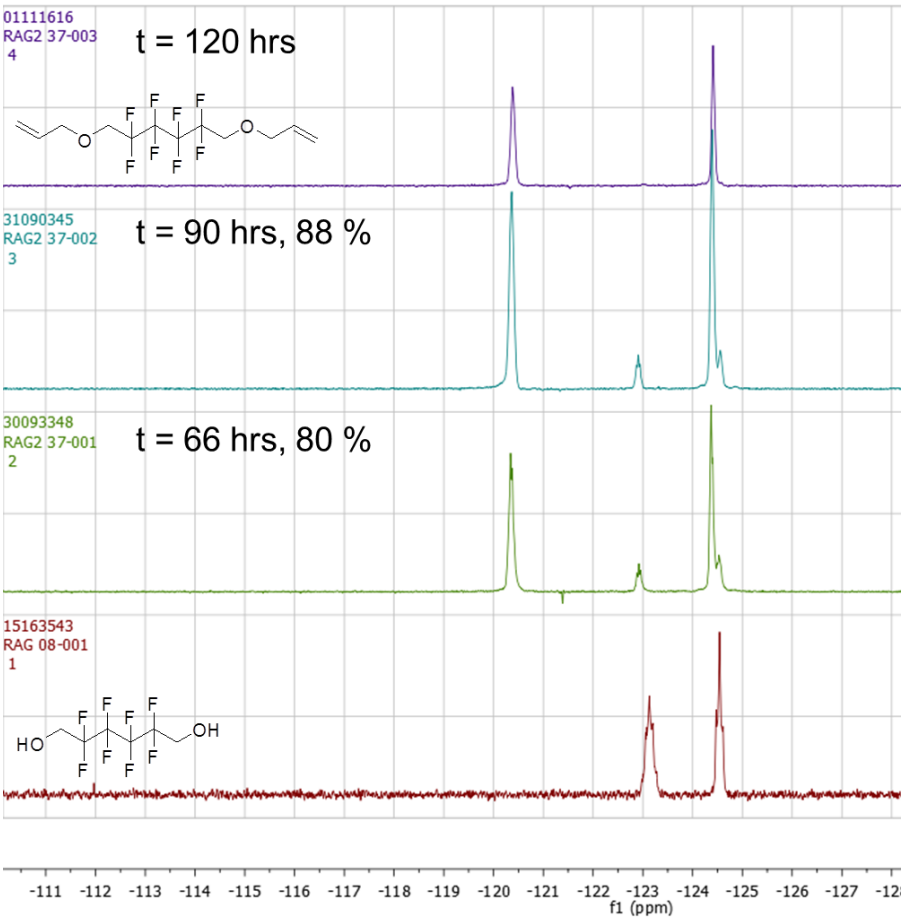

Figure 4.14: Overlay of ^{19}F NMR spectra showing conversion of a fluorinated diol to a fluorinated diallyl compound

4.3.2 Epoxidation of polyfluorinated alkenes

Following the synthesis of the allyloxy intermediates (Section 4.3.1) this section will discuss the formation of epoxide rings from polyfluorinated allyloxy species such as **53** by oxidation processes, following the strategy outlined in figure 4.8 (Route A).

4.3.2.1 Oxidation using *meta*-chloroperbenzoic acid as oxidant

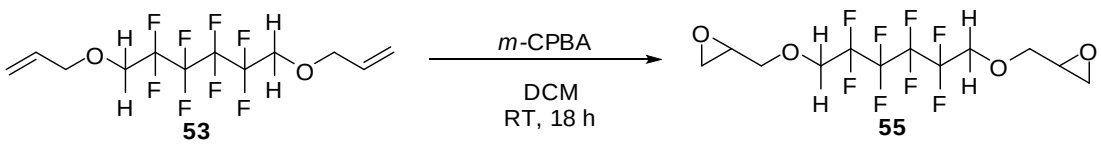

53 **55**

Figure 4.15: Reaction of polyfluorinated allyloxy ether with m-CPBA

M-CPBA is one of the most common reagents for forming an epoxide from an alkene. However, despite the use of an excess (1.5 equivalents) of *m*-CPBA only low conversion of **53** was observed, with **55** produced as part of a complex mixture of organic products.

As can be seen in figure 4.16, the crude product from reaction of **53** with *m*-CPBA contains several aromatic environments, evidence that both unreacted *m*-CPBA and 3-chlorobenzoic acid are present. Resonances at 5.8 ppm and 5.2 ppm, corresponding to the alkene unit of **53** are evidence of incomplete conversion of the starting material. There are also peaks in the ^{1}H NMR spectra (Figure 4.16) that cannot be assigned and, presumably, arise from side reactions and decomposition.

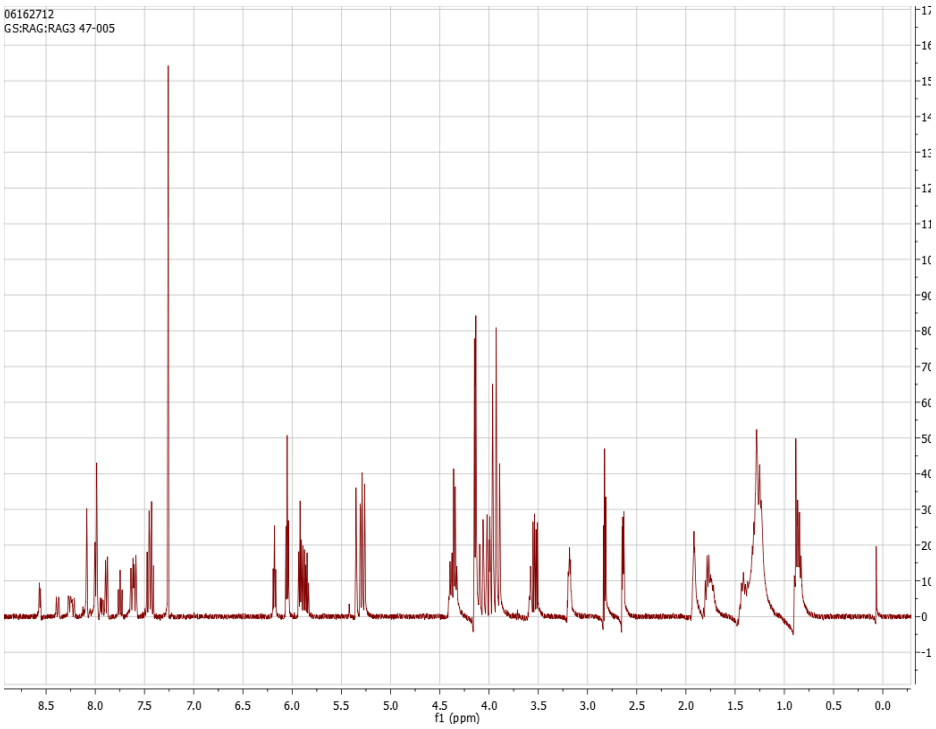

*Figure 4.16: ^{1}H NMR spectrum of the crude product from reaction of **53** with m-CPBA (Figure 4.15)*

Since the reaction of **53** with *m*-CPBA does not give full conversion, even with long reaction times, and also leads to formation of insoluble white material in a side reaction, it is not suitable as a method for the conversion of **53** to **55** or oxidation of other polyfluorinated alkenes. With reactions featuring alkenes and *m*-CPBA the alkene acts as a nucleophile, and it appears that the perfluoroalkyl unit of **53** lowers

the electron density at the alkene group slowing the reaction.

4.3.2.2 Epoxidation via chlorohydrin intermediate

An alternative method of epoxidation was performed in which the desired epoxide was formed via the corresponding chlorohydrin (Figure 4.17). Following conversion to the chlorohydrin, the chlorine is lost as a leaving group during ring closing nucleophilic attack from the adjacent hydroxyl oxygen atom to form the three membered epoxide ring.

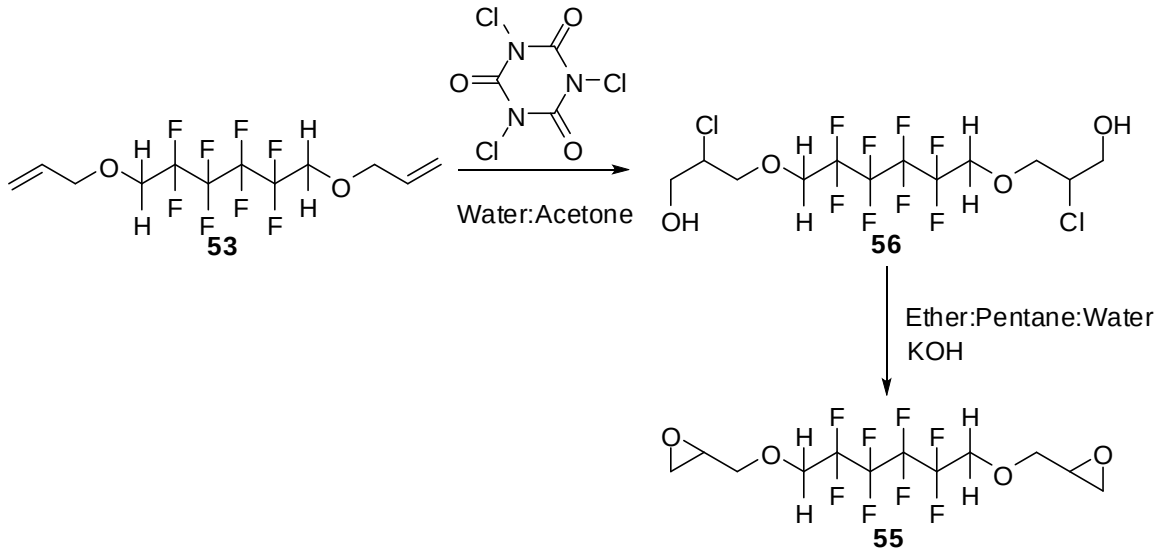

Figure 4.17: Proposed route to formation of epoxides via chlorohydrin intermediate[6]

We found that reaction of **53** with TCICA in aqueous acetone led to formation of **56** within 18 hours. The second step of the reaction involving base induced epoxidation was run for a further 18 hours, and the crude solid obtained recrystallised from hexane:ether (Figure 4.18).

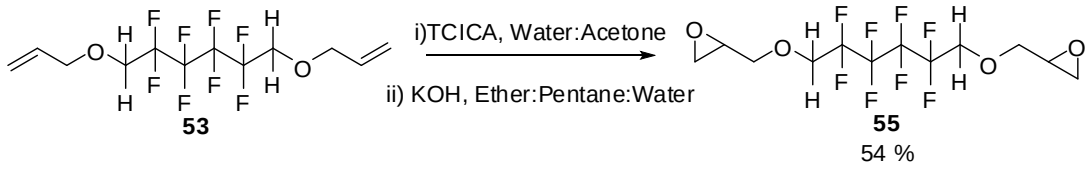

Figure 4.18: Two step conversion of a semi-fluorinated diallyl system to corresponding bisepoxide

While the route to **55** shown above (Figures 4.17 and 4.18) is a useful process it suffers from a long reaction time, and the necessity of separating the three products still present after recrystallisation. This route was not optimised due to concurrent studies into other oxidation methods.

4.3.2.3 Oxidation using HOF.MeCN as oxidant

Along with the more well-known reagents above, the use of HOF.MeCN, [7, 8] a reagent available in Durham, was examined in both flow and batch processes. Previous literature [7] has shown the 'HOF.MeCN' complex is a potent electrophilic oxygen source, and it is known to convert alkene bonds to epoxides. Substrates that undergo epoxidation upon reaction with HOF.MeCN include dodec-1-ene and both (E)- and (Z)-stilbene. [9]

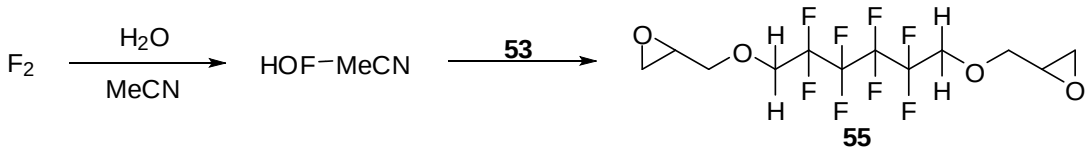

Figure 4.19: Scheme showing formation of hypofluorous acid complex and subsequent oxidation of allylic bonds

The 'HOF.MeCN' complex can be generated by passing 10 % fluorine gas, dissolved in nitrogen, through aqueous acetonitrile. [9] This process generates a solution containing HOF.MeCN into which the substrate is then injected. Following a short reaction time, usually in the order of minutes, the organic components can be extracted from the aqueous solution to give crude products. The reaction equipment is shown in figure 4.20, highlighting the key components consisting of tank cylinders

containing 10 % F_2/N_2 mixture from which the gas mixture flows into the reaction flask that has been filled with aqueous acetonitrile. The reaction flask also contains an outlet, for unreacted F_2 and waste gases, which is connected to a scrubber to prevent release of F_2 and HF to the environment.

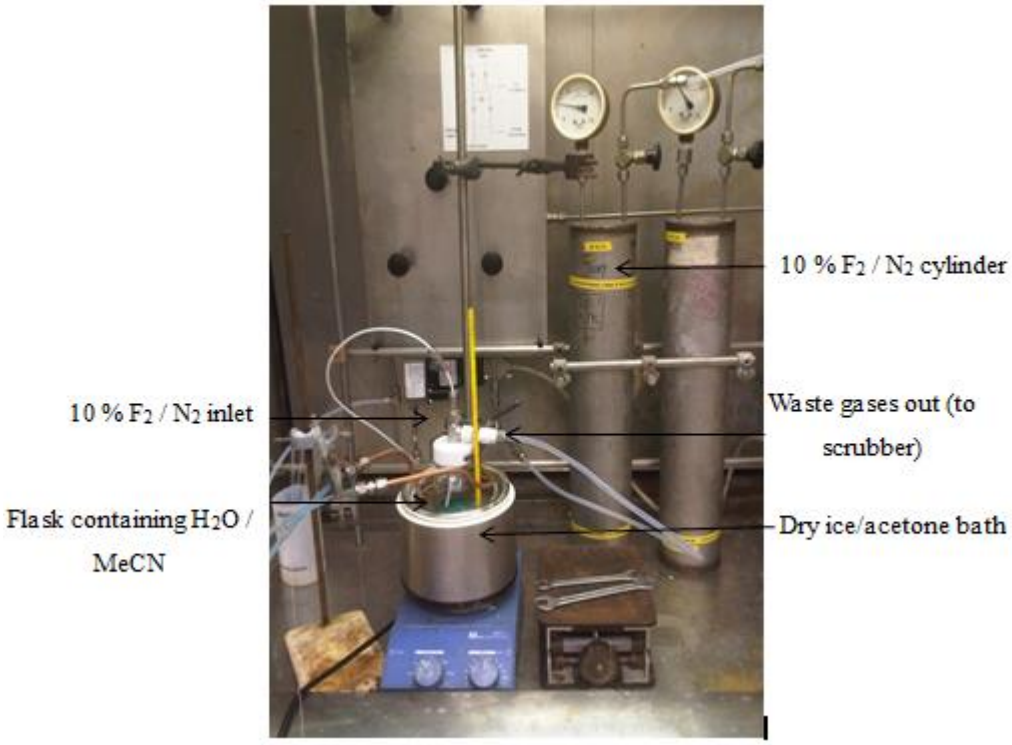

Figure 4.20: Set-up of equipment for batch oxidation using HOF.MeCN

The allyloxy systems (**49**, **52** and **53**) were oxidised by reaction with HOF.MeCN in a batch process (Figure 4.21).

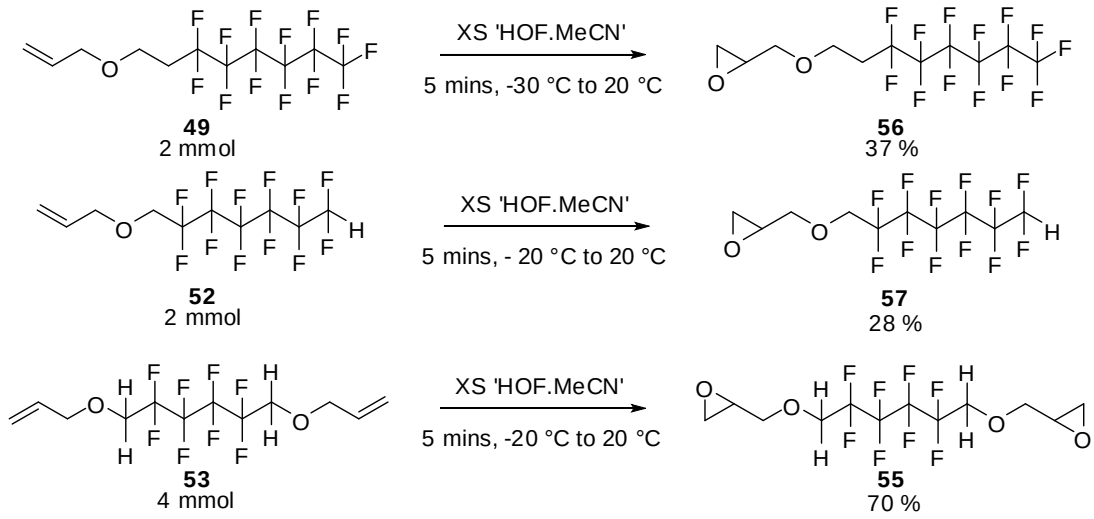

Figure 4.21: Oxidations of polyfluorinated alkenes using HOF.MeCN in a batch process

Reaction times for allylic species are generally on the order of minutes and achieve full conversion with 1.1 molar equivalents of oxidising agent. The ^{1}H NMR spectrum below (Figure 4.22), collected after reaction of **53** with HOF.MeCN (Figure 4.23), shows the complete absence of allyl peaks (5.86 ppm and 5.28 ppm) and the generation of five new peaks which correspond to the protons of the epoxide ring and adjacent site; full conversion was achieved.

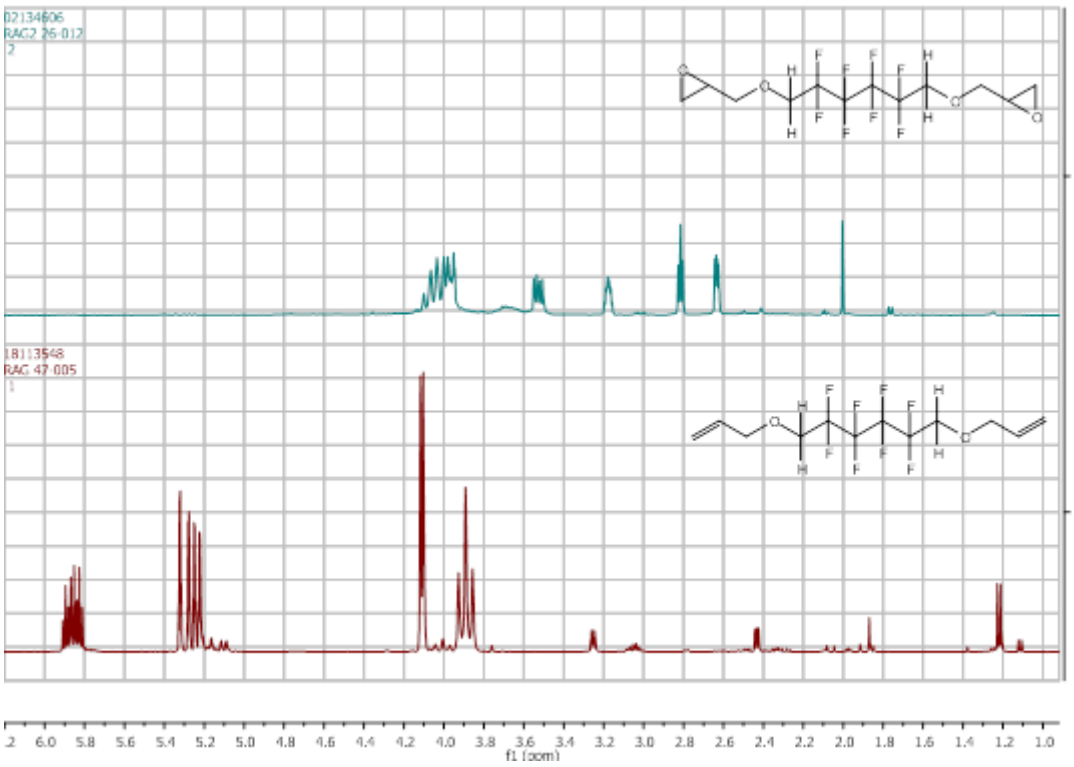

Figure 4.22: Overlay of ^{1}H NMR spectra for diallyl (bottom) and diepoxy (top) systems

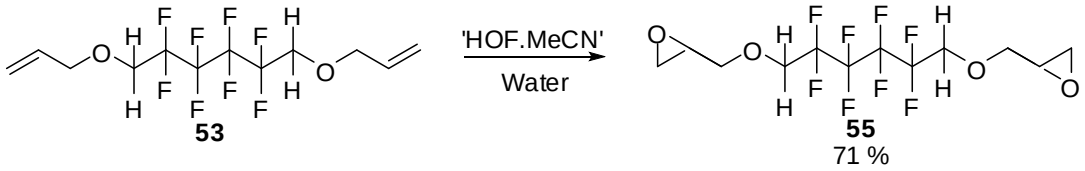

Figure 4.23: Scheme for reaction of fluorinated bis(allyloxy) system with hypofluorous acid in a batch process

Oxidation in a batch process proceeds cleanly with formation of only one product. However, the hypofluorous acid complex has a half-life in the order of hours, even at 0 °C, [7] which prevents a large quantity of the complex being generated. For this reason batches can only be reasonably small, and this is prohibitive in using a batch process for the oxidation of large quantities of perfluoroalkylated allylic compounds.

Therefore, the reaction was repeated in a flow process, where the 'HOF.MeCN' complex generated is reacted almost instantly. [9] As shown in the scheme below (Figure 4.24) the aqueous acetonitrile, injected with use of a syringe pump, and fluorine/nitrogen gas are mixed within the flow reactor which generates HOF.MeCN.

[10] To the flow of HOF.MeCN is added a solution of substrate dissolved in acetonitrile, again with use of a syringe pump to control the rate of addition. The length of time the solution is given to react is varied by amending the tubing path length prior to collection of all components in an aqueous solution of sodium bicarbonate which neutralises any hydrogen fluoride generated in the process. As with the batch process, the organic components are extracted from the collection vessel to isolate a crude product.

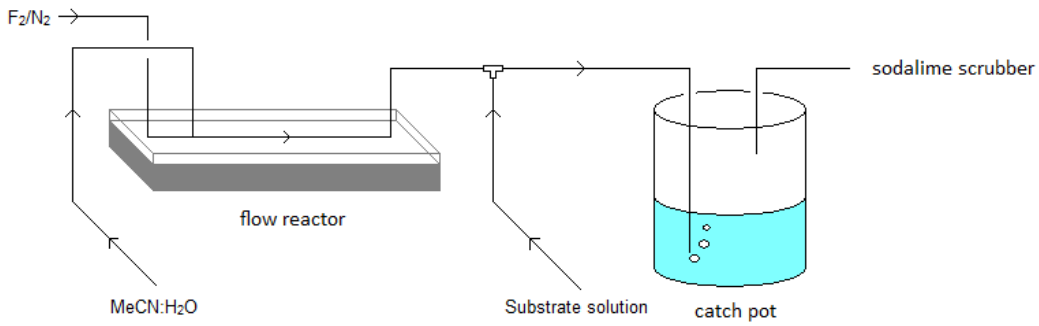

Figure 4.24: Schematic of HOF.MeCN generation and reaction in a flow process

As the flow process is more complex than a batch process, due to the increased number of variable parameters (rate of gas flow, rate of substrate addition, rate of aqueous acetonitrile addition, path length) the monoallyloxy product **52** was used as a model substrate before reaction of **53** to establish correct conditions.

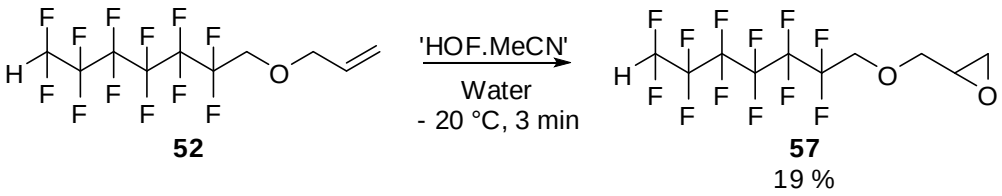

Figure 4.25: Epoxidation of fluorinated allyl system using hypofluorous acid

Epoxidation occurs rapidly when using hypofluorous acid in a flow process. Given the successful synthesis of **57**, the flow process was extended to include the bisallyloxy compound **53**. The oxidisation of **53** by HOF.MeCN in a flow process was optimised to obtain full conversion of the substrate, which was achieved with flow rates of 20 $mL.min^{-1}$ and 10 $mL.hour^{-1}$ for 10 % F_2 in nitrogen and 4:1

acetonitrile:water respectively. This solution was combined with addition of substrate, 1,6-bis(allyloxy)-2,2,3,3,4,4,5,5-octafluorohexane, **53**, at 9.9 mL.hour^{-1}. While 100 % of starting material was reacted, as shown by the absence of allyl peaks in the ^{1}H NMR spectrum of the crude product, the reaction forms a mixture of both mono and diepoxy products. However, following recrystallisation from chloroform-hexane the diepoxy species **55** was isolated as a clear oil in good yield.

^{1}H NMR spectra of the polyfluorinated bis(epoxy) product **55** (Figure 4.26) shows six major peaks due to the different magnetic environments.

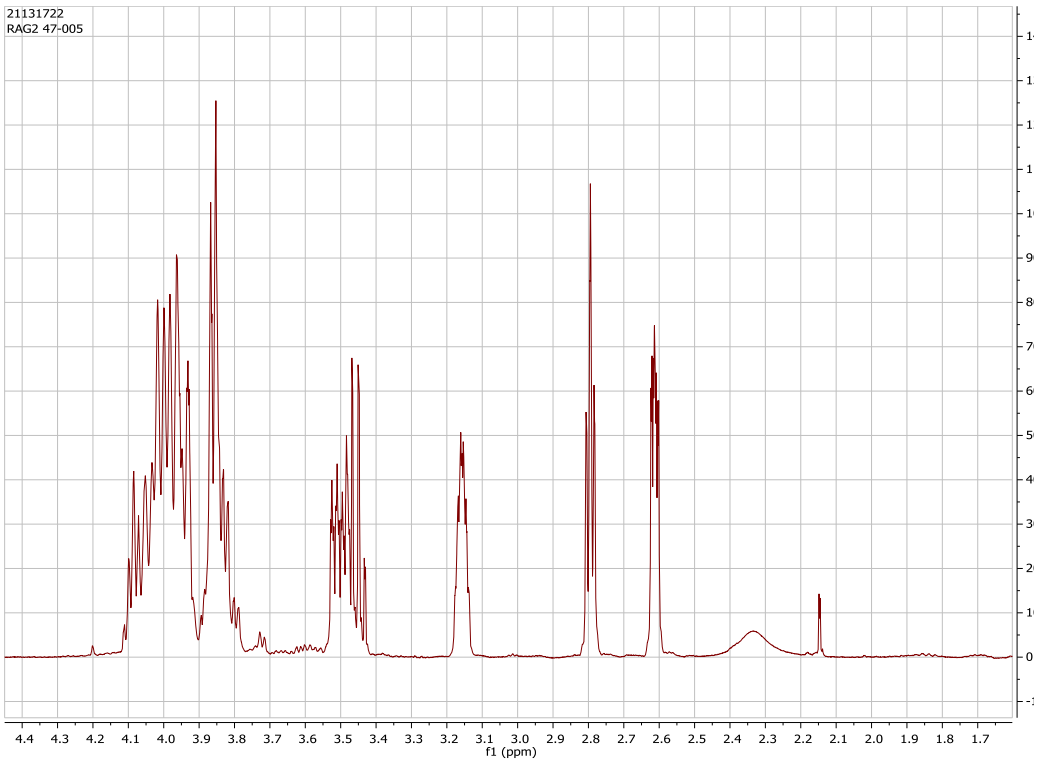

*Figure 4.26: ^{1}H NMR spectrum of **55** synthesised by oxidation of **53** using HOF.MeCN as oxidant in a flow process*

However, reactions featuring HOF.MeCN could not be performed on the scale necessary due to the refurbishment of the fluorine lab in 2013. Therefore, our research investigated route B (Figure 4.8) which forms polyfluorinated epoxide monomers for paint coatings from reaction of polyfluorinated alcohols and epichlorohydrin.

4.3.4. Reactions of polyfluorinated alcohols with epichlorohydrin

The reaction of epichlorohydrin with alcohols bearing a perfluoroalkyl unit was attempted under two different sets of conditions. The first was an extension of previous Williamson ether type conditions mediated by potassium carbonate, but using epichlorohydrin as solvent (Figure 4.27). Under these conditions, the desired product was formed, but with significant amounts of oligomeric product also observed.

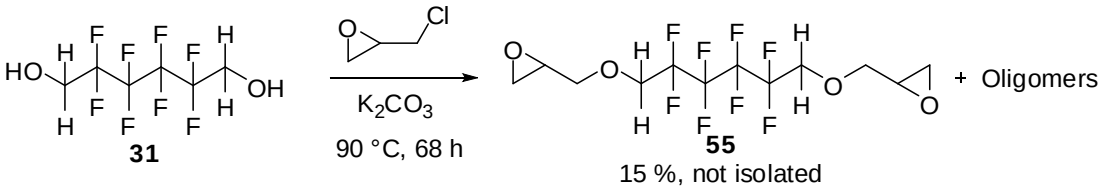

Figure 4.27: Conversion of polyfluorinated diol to polyfluorinated bis(epoxy) compound

The other conditions used were biphasic, [11] featuring a concentrated solution of aqueous sodium hydride, TBAB as phase transfer catalyst, and an excess of epichlorohydrin. The initial attempt of the biphasic conditions (Figure 4.28) gave a good yield of desired bis(epoxy) compound **55** with a short reaction time using reasonably mild conditions.

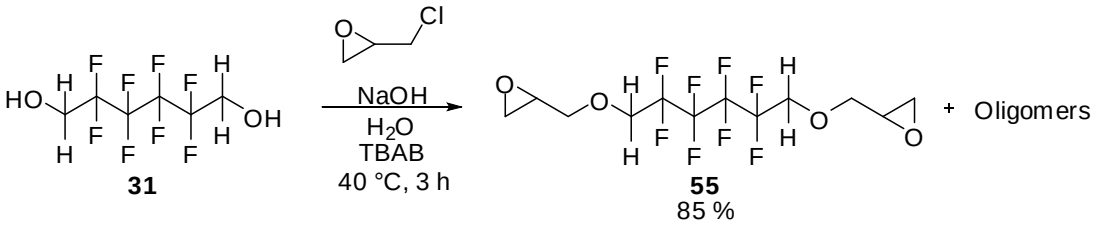

Figure 4.28: Biphasic reaction conditions for conversion of fluorinated diol into fluorinated diepoxide

Of the two methods (Figures 4.27 and 4.28) the biphasic conditions give the greatest yield of **55**, but did not give a pure product as a side reaction led to the formation of oligomeric material. High temperature distillation of the crude product arising from

the biphasic reaction was unsuccessful as a means of separating **55** and the oligomeric material, as the heat promoted ring opening of the epoxide functionality and led to the synthesis of more oligomeric material. However, vacuum distillation at low pressure allows removal of excess epichlorohydrin and other volatile material from the reaction mixture, leaving just **55** and small quantities of oligomeric material. In addition to mass-spec (ASAP) confirming the presence of both dimers and trimers of **55**, GPC (gel permeation chromatography) analysis of the product obtained from the biphasic reaction route (Figure 4.28) confirms that oligomers are present. GPC did not allow accurate calculation of either M_n or M_w as the sample has a refractive index lower than the standard (THF) which causes molecular weight calculations to be merely an estimate. Figure 4.29 shows one major peak and two smaller peaks corresponding to two impurities, both of higher mass which is consistent with formation of oligomers.

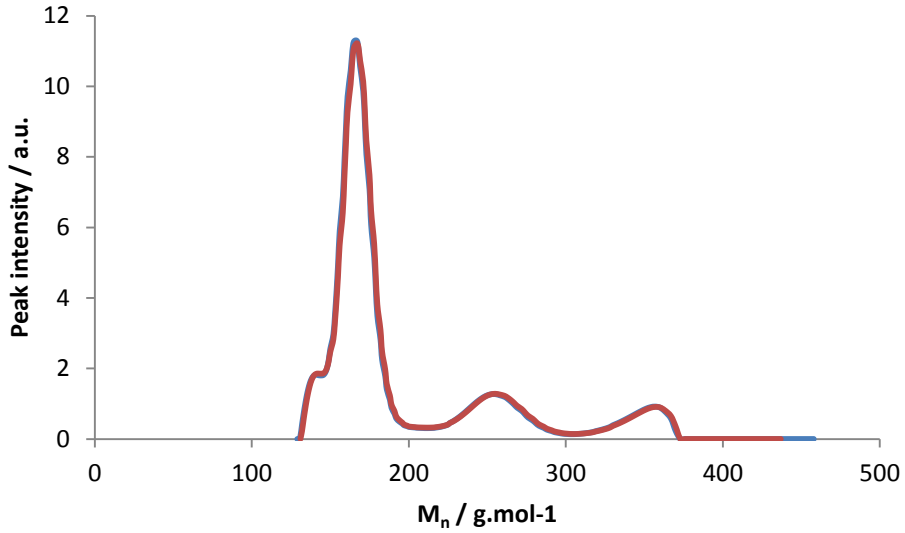

*Figure 4.29: Molecular weight distribution graph for **55** produced by epichlorohydrin method*

As the desired bis(epoxy) product and oligomeric material cannot be separated a range of conditions were screened (Table 4.5), with the aim of minimising oligomer formation.

*Table 4.5: Conditions screened for reaction of **31** with epichlorohydrin*

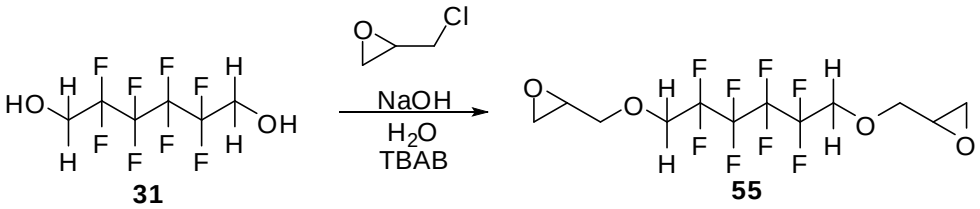

31 **55**

Temperature / °C	Time / h	Starting molar equivalents NaOH	% **55** in crude product
40	3.5	5	80
40	4.7	6	84
40	2.5	5	84
40	21.5	5	80
RT	48	2.2	85
RT	70	2.2	90
RT	164	2.1	95

The ^{1}H NMR spectra of the product from the reaction of **31** with epichlorohydrin are identical to the spectra of samples formed from the earlier two-step route (Figure 4.30) and reactions allowed the synthesis of in excess of 30 g of bis(epoxide) **55** per batch. This allowed facile generation of suitable quantities of fluorinated bis(epoxide) for testing as an additive in paint coating formulations.

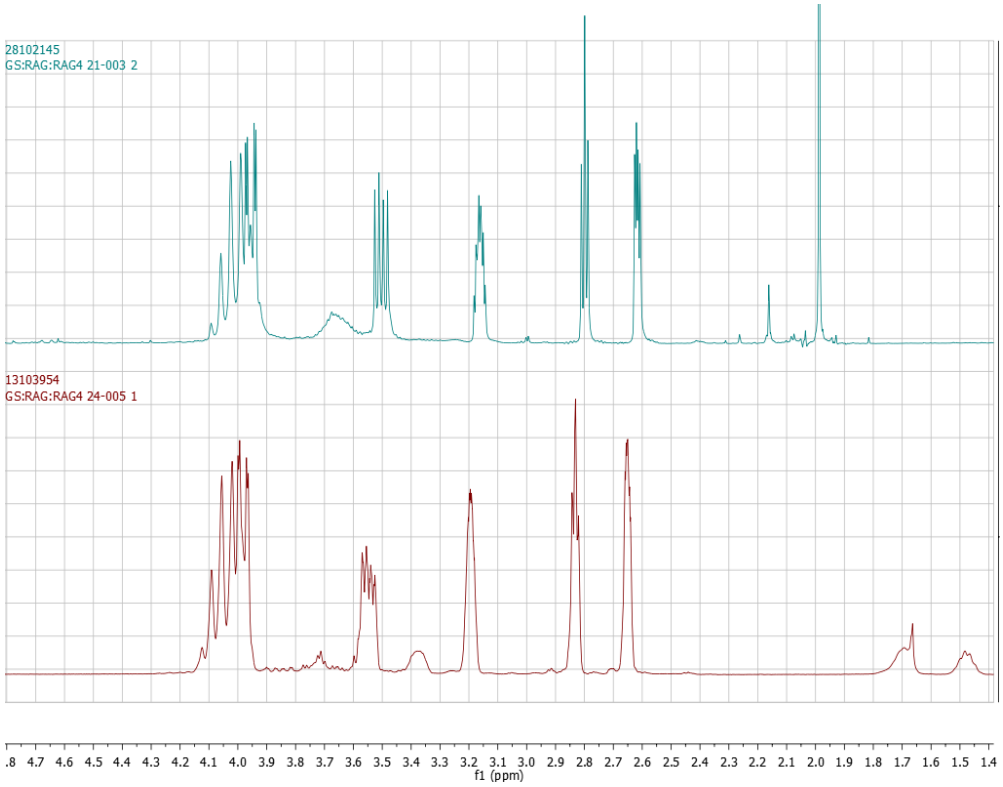

*Figure 4.30: Overlay of ^{1}H NMR spectra for **55** arising from; above, hypofluorous acid oxidation route and below, biphasic epichlorohydrin reaction conditions*

The scope of the reaction of epichlorohydrin with perfluoroalkylated alcohols was extended to incorporate the reaction of 1*H*,1*H*-perfluoroheptan-1-ol **58**. Synthesis of a monoepoxy product from **58** will give a side chain fluorinated monomer that can be used as a 'drop-in' additive in paint coating formulations and allow a direct comparison between the effect of main chain and side chain functional monomers in similar paint coatings.

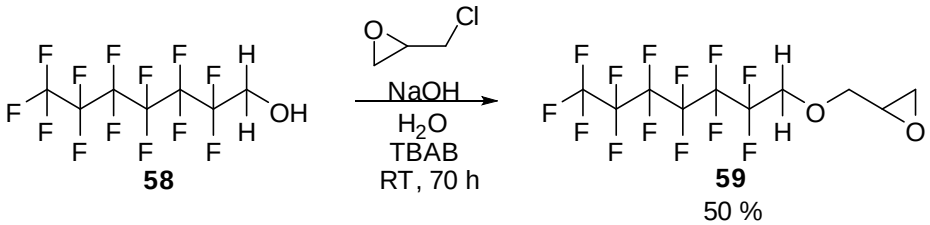

Figure 4.31: Conversion of fluorinated alcohol into fluorinated epoxide

Other than a shorter reaction time, conditions for the reaction of **58** with epichlorohydrin (Figure 4.31) were very similar to those used for the conversion of

the fluorinated diol **31**. Unlike **55**, the diepoxy compound, **59** can be purified by vacuum distillation allowing pure samples to be obtained as shown in the ^{1}H NMR spectrum of **59** (Figure 4.32).

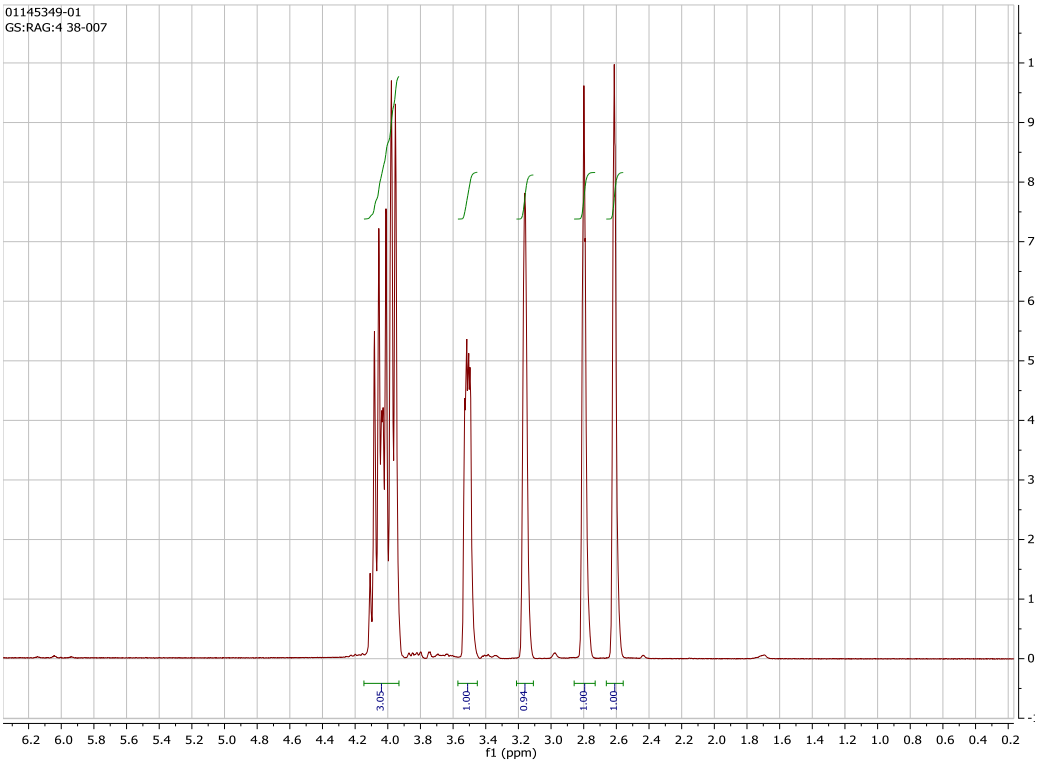

*Figure 4.32: ^{1}H NMR spectrum of **59***

4.4 Conclusions

In this chapter, two routes for the synthesis of perfluoroalkyl containing epoxy systems, which are potentially useful coating additives, were investigated. One route featured a two-step process, involving reactions between polyfluorinated alcohols and allyl bromide, followed by oxidation. Oxidation using hypofluorous acid in a batch process gave the greatest yields of epoxides from fluorinated allyl systems.

Novel fluorinated epoxides were synthesised on a larger scale by reaction of polyfluorinated alcohols with epichlorohydrin. Reactions of polyfluorinated alcohols with epichlorohydrin allowed synthesis of large quantities of both main and side chain fluorinated epoxides suitable for incorporation into paint coating formulations.

4.5 References to chapter 4

1. Gibson, M.S.; Bradshaw, R.W.; *Angew. Chem. Int. Ed.*, **1968**, 7, 919 – 930.

2. Wu, X.; Boz, E.; Sirkis, A.M.; Chang, A.Y.; Williams, T.J.; *J. Fluorine Chem.*, **2012**, 135, 292 – 302.

3. Velez-Herrera, P.; Ishida, H.; *J. Fluorine Chem.*, **2009**, 130, 573 – 580.

4. Ing, H.R.; Manske, R.H.F.; *J. Chem. Soc.*, **1926**, 129, 2348 – 2351.

5. Szabo, D.; Bonto, A.; Kovesdi, I.; Gomory, A.; Rabai, J.; *J. Fluorine Chem.*, **2005**, 126, 639 – 650.

6. Ye, J.; Wang, Y.; Chen, J.; Liang, X.; *Adv. Synth. Catal.*, **2004**, 346, 691 – 696.

7. Rozen, S.; Bareket, Y.; Kol, M.; *Tetrahedron*, **1993**, 49, 8169 – 8178.

8. Rozen, S.; Kol, M.; *J. Org. Chem.*, **1990**, 55, 5155 – 5159.

9. McPake, C.B.; Murray, C.B.; Sandford, G.; *Tetrahedron Lett.*, **2009**, 50, 1674 – 1676.

10. McPake, C.C.; *New Continuous flow methodology*. PhD thesis, Durham, December 2011.

11. Yi, W.; Feng, Z.; Zhang, Q.; Zhang, J.; Li, L.; Zhu, W.; Yu, X.; *Org. Biomol. Chem.*, **2011**, 9, 2413 – 2421.

5. Synthesis and testing of paint coatings derived from a polyfluorinated diol or epoxide

5.1 Introduction

In chapter 4 several epoxy monomers bearing a perfluoroalkyl unit were synthesised. Two systems, **55** and **59**, were synthesised on a multigram scale (110 g) to enable the inclusion of the perfluoroalkylated epoxide functional monomers into epoxy-amine coating formulations. The inclusion of such 'drop-in' perfluoroalkylated monomers will allow the effects of incorporating a perfluoroalkyl unit into an epoxy-amine paint coating to be assessed. The creation of paint coating systems incorporating these monomers, and relevant testing on these coatings, are detailed within this chapter. Also included is data for paint coatings modified by addition of **31**, the commercially available 2,2,3,3,4,4,5,5-octafluorohexane-1,6-diol, which was incorporated into polyurethane systems and also a polyester functional powder coating as a main chain perfluoroalkylated monomer. All synthesis and testing of paint coatings detailed in this chapter were performed at the AkzoNobel Felling site (Gateshead, UK) under the supervision of, primarily, Dr Doug Beaumont and Mr Laurent Mialon.

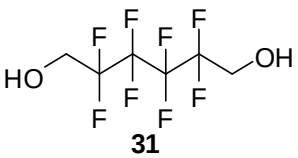

31

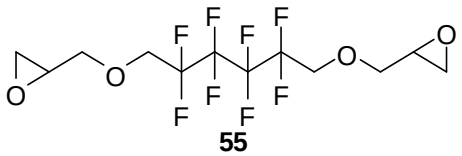

55

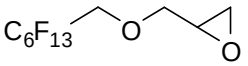

59

5.2 Paint coatings incorporating 2,2,3,3,4,4,5,5-octafluorohexane-1,6-diol 31

Polyfluorohexanediol **31** was incorporated into three distinct systems; a powder coating formulation composed of a polyester linked binder formed by reaction of IPA

(isophthalic acid) and hexane-1,6-diol, and two 'wet' coating systems featuring polyurethane linkages as part of the polymer network.

5.2.1 Modified acrylic polyurethane coating cured with polyisocyanate

5.2.1.1 Synthesis of modified acrylic polyurethane paint coating

The first paint system to be created was a modified version of an acrylic polyurethane coating comprising of, primarily, a hydroxyl functional acrylic resin. The standard coating 'base' comprises the hydroxyl functional acrylic resin and a pigment, either titanium dioxide or talc, dissolved in MEK (methyl ether ketone). The use of different pigmenting agents differentiates between a paint system used as a primer and one used as a finish coating. Exact quantities of components used to create the hydroxyl functional paint base are tabulated (Table 5.1).

Table 5.1: Formulation of paint bases containing an hydroxyl functional acrylic resin

Acrylic polyurethane - primer paint 'base' (A)	
Material	Quantity / g
Acrylic polyol	220
Talc	105
MEK	30

Acrylic polyurethane - finish paint 'base' (B)	
Material	Quantity / g
Acrylic polyol	220
Talc	105
MEK	30
Dibutyltin diacetate	0.070

To create the modified systems, the amount of hydroxyl functional acrylic paint base used was lowered, and supplementary hydroxyl functionality added in the form of either hexane-1,6-diol, as a hydrocarbon 'control' sample, or 2,2,3,3,4,4,5,5-octafluorohexane-1,6-diol. Both were added as a 50 weight per cent solution in MEK

(Tables 5.2 and 5.3). While hydroxyl functionality was provided by the small molecule diols, the equivalent weight of the diols is almost one-tenth that of the acrylic polyol bases and so the mass of diol in any given system is quite low. Following paint 'base' formulation and brief mixing each sample was cured with an isocyanate based curing agent, which consists primarily of **60**, a trimer formed by reaction of three hexamethylene-1,6-diisocyante units, along with some unreacted aliphatic hexamethylene-1,6-diisocyante. Table 5.2 and table 5.3 show the relative masses of diol and curing agent in primer and finish systems.

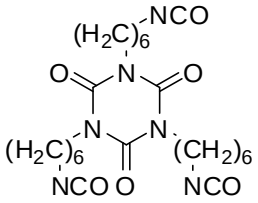

*Figure 5.1: **60**, the major component of the isocyanate based curing agent*

Table 5.2: Composition of coating systems based on acrylic polyurethane modified by addition of hexane-1,6-diol

Entry	OH functionality from hexanediol / %	Primer 'base' (A) / g	50 wt.% Hexanediol : MEK Solution / mg	Curing agent / g	PVC
1	0.0	35.1	-	4.5	22.7
2	0.1	35.0	2.5	4.5	22.7
3	1.0	34.7	25	4.5	22.7
4	10	35.1	272	5	21.9
5	50	31.2	2180	8	17.1

Entry	OH functionality from hexanediol / %	Finish 'base' (B) / g	50 wt.% Hexanediol : MEK Solution / mg	Curing agent / g	PVC
6	0.0	35.1	-	4.5	16.3
7	0.1	35.0	2.5	4.5	16.3
8	1.0	34.7	25	4.5	16.2
9	10	35.1	272	5	15.7
10	50	31.2	2180	8	12.3

PVC (Pigment Volume Concentration) = $V_p / (V_p + V_B)$

Table 5.3: Composition of acrylic urethane based coating systems modified by addition of 2,2,3,3,4,4,5,5-octafluorohexane-1,6-diol (Fluorodiol)

Entry	OH functionality from fluorodiol / %	Primer 'base' (A) / g	50 wt.% Fluorodiol : MEK Solution / mg	Curing agent / g	PVC
11	0.0	35.1	-	4.5	22.7
12	0.1	35.0	5.4	4.5	22.7
13	1.0	34.7	54	4.5	22.7
14	10	35.1	605	5	21.9
15	50	31.2	4530	7.5	16.8

Entry	OH functionality from fluorodiol / %	Finish 'base' (B) / g	50 wt.% Fluorodiol : MEK Solution / mg	Curing agent / g	PVC
16	0.0	35.1	-	4.5	16.3
17	0.1	35.0	5.4	4.5	16.3
18	1.0	34.7	54	4.5	16.2
19	10	35.1	605	5	15.7
20	50	31.2	4530	7.5	12.0

After a combination of all components, the 20 systems were mechanically stirred at

around 3000 rpm by a dispermat apparatus, and applied to test panels by means of a draw down bar, which is a steel or aluminium block with a raised base of 300 μm depth. After covering the substrate with the paint coating, the draw down bar is passed over the wet film coating removing all coating at a depth greater than the notch in the base. The finish systems were applied to four QUV-A aluminium panels with a wet film thickness of 300 μm. The primer systems were applied to a single QUV-A panel, at 300 μm wet film thickness, and to three Sa2.5 blasted steel panels at a wet film thickness of 400 μm. Sa2.5 refers to a grade of sandblasting in which the substrate has been blast cleaned until millscale, rust paint and foreign matter is completely removed. All coatings were allowed to cure in air at ambient temperature for a week prior to surface analysis.

5.2.1.2 Testing of modified acrylic polyurethane coating

The first measurement to be taken after curing was the dry film thickness (DFT) of the Sa2.5 steel panels which is calculated by measuring the conductivity when a current is passed through the coating using a handheld potentiometer manufactured by Cole-Parmer. For each panel a measure of the dry film thickness was taken at 12 points across the coating surface and an average calculated. Of the three Sa2.5 panels coated with each system, the two which had the most consistent paint coverage were chosen to be used in further tests, and the others discarded. Also discarded were all test panels coated in the paint system in which 50 % of the OH functionality was provided by the hexanediol, as at such concentrations the hexanediol is immiscible in the coating system and phase separation occurred.

Table 5.4: Average dry film thickness of coatings applied to Sa2.5 panels

	OH functionality from hexane-1,6-diol / %							
	0.0		0.1		1.0		10	
	A	B	A	B	A	B	A	B
Mean thickness of coating /μm	243.3	247.3	230.7	232.5	233.5	255.3	271.4	223.3

	OH functionality from 2,2,3,3,4,4,5,5-octafluorohexane-1,6-diol / %									
	0.0		0.1		1.0		10		50	
	A	B	A	B	A	B	A	B	A	B
Mean coating thickness /μm	243.3	247.3	241.3	244.4	270.5	221.2	220.4	214.3	220.1	248.3

Mean dry film thicknesses are all within a reasonably small 56 μm range. While the system cures with loss of solvent, leading to a reduction in the volume of the coating, the amount of solvent lost should be similar for each coating system. Monitoring of physical properties of coatings of vastly different film thicknesses does not allow for a good comparison as, of course, the protection afforded to the substrate is dependent on the thickness of the coating.

The coated blasted steel panels were placed in a Prohesion cabinet (C3 environment) [1] which is a form of accelerated weathering involving alternating salt spray and heat cycles mimicking an urban or industrial environment. [2] Typically, each cycle is an hour long, with the spray cycle performed at ambient temperature and the drying/heat cycle performed at 35 °C during which air at around 28 psi is added to aid drying. Samples were prepared by taping the edges of the panels, in order to avoid failure at points with thinner coating, and by drilling a hole through the coating to create a defect and expose the substrate surface.

The effect of the anti-corrosion test described above is monitored by eye and a slight difference in performance, in favour of coatings incorporating the main chain fluorinated diol over systems modified with hexane-1,6-diol was noticed. However, both are broadly similar to the unmodified commercial system. The hexanediol systems may have performed worse due to hexanediol precipitating out of solution before the curing reaction could occur. This would give an area that was hydrophilic, due to the free alcohol groups, which may channel water to the substrate surface by osmosis, resulting in a greater number of corrosion sites. Another reason for the similarity between the modified and unmodified systems could be due to the relatively low levels of diols added, even when 50 % of the OH functionality is provided by 2,2,3,3,4,4,5,5-octafluorohexane-1,6-diol the diol only accounts for around one-tenth of the coating mass.

A sample of each coating that had cured on the aluminium Q-panels was removed from the metal substrate and used to find the glass transition temperature of the coatings, by use of DSC (Table 5.5). Each sample was heated, at a rate of 20 °C.min^{-1}, cooled to – 50 °C, and then reheated under the same rate of heating. Data is taken from the 'reheated' second run as further curing can take place during the first heating. As pigmentation should not influence data acquired by DSC, tests were performed on only the primer system.

Table 5.5: Glass transition temperature of polyurethane linked coatings

OH functionality from diol	T_g / °C
0.0 %	58.5
0.1 % (Fluorodiol)	61.6
1.0 % (Fluorodiol)	63.6
10 % (Fluorodiol)	60.4
50 % (Fluorodiol)	51.4
0.1 % (Hexanediol)	61.2
1.0 % (Hexanediol)	62.2
10 % (Hexanediol)	62.9

Given potential measurement errors with the equipment used, a difference of less than 2 °C is not considered significant. Modification of the standard system by addition of small molecule diols increases the glass transition temperature slightly, although there are no significant differences in the T_g between the modified systems which are in the range 60 – 62 °C, with the exception of the system in which 50 % of the OH functionality arises from the fluorinated diol (51.4 °C). This change is likely indicative of a significant change in the polymer network, probably a reduction in the amount of crosslinking as this is known to reduce the T_g of polymers.

Modified primer and finish systems were both used to investigate the effect of modification upon surface energy, calculated by the OWRK method (Section 1.3.2.2) using two sessile drops. Surface energies are only affected by a few layers of atoms at the surface of a coating and can be used to assess the surface composition. Table 5.6 shows no difference in contact angle upon addition of the diols to the coating formulation. From this it can be surmised that the perfluoroalkyl region does not surface segregate to any great extent and nor does the hexanediol. FT-IR techniques that probe a surface to a depth of a few microns showed no obvious differences between systems, and no peak corresponding to the vibrational frequency of a C-F bond was noticeable for the coatings incorporating 2,2,3,3,4,4,5,5-octafluorohexane-

1,6-diol.

Table 5.6: Contact angle data for coating systems modified by incorporation of small molecule diols

Fluorinated coating system			Non-fluorinated coating system		
Amount of diol / % OH functionality	Contact angle water / °	Contact angle CH_2I_2 / °	Amount of diol / % OH functionality	Contact angle water / °	Contact angle CH_2I_2 / °
0.0	84.7	34.3	0.0	84.7	34.3
0.1	84.0	35.4	0.1	85.0	33.7
1.0	81.1	34.3	1.0	84.5	33.0
10	84.4	35.2	10	84.1	37.6
50	84.7	37.6	50	82.5	36.3

The final test on this isocyanate cured system investigated the effect of UV light on gloss and colour stability. Coated Q-panels were placed in a QUV cabinet which exposes the sample to alternating UV light and moisture. The gloss level of samples were periodically monitored by measuring the intensity of light reflected by the coating at incident angles of 20 °, 60 ° and 85 ° through use of a commercially available glossmeter (BYK Wavescan-II). This gloss level, monitored using intensity of light reflected, is compared with the initial gloss level before coatings were subjected to UV light (Figure 5.2). All systems are comparable, although it appears that gloss retention is amplified as the level of diol is increased, which holds for both the diol containing a perfluoroalkyl unit and the diol with a purely hydrocarbon backbone. Any conclusions from this are modified by the earlier statement that the system with 50 % OH from 2,2,3,3,4,4,5,5-octafluorohexane-1,6-diol likely has a different network structure, and so it cannot be assumed that the effect arises because of the incorporation of a perfluoroalkyl group. The data has a large standard deviation, due to a reasonably large difference between the gloss values of the two panels coated with each system, an effect which occurs as failure of the coatings materialises in a non-uniform manner. However, such data is encouraging, and is one

of the reasons an attempt was made to use the same perfluoroalkylated alcohol as an additive in a similar polyurethane system cured with an aliphatic isocyanate.

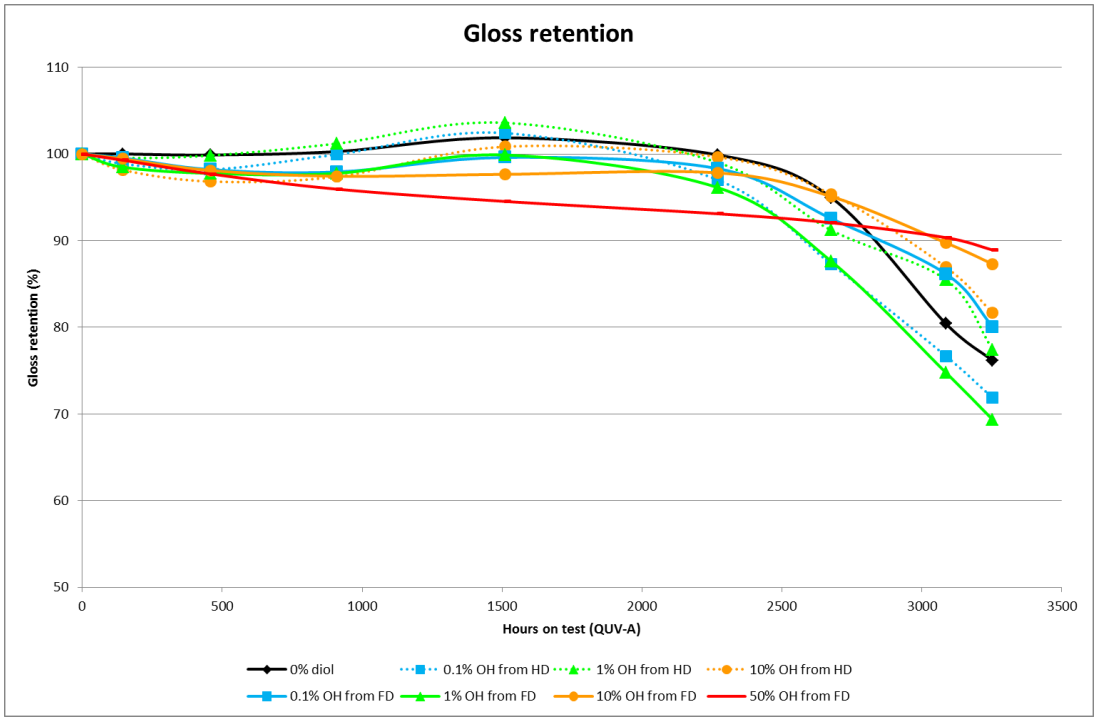

Figure 5.2: Graph of gloss retention for acrylic polyurethane based coatings

5.2.2 Polyester functional coating system cured with a polyester polyol

5.2.2.1 Synthesis of paint coating

In the system cured with **60** (Section 5.2.1) there was no difference in coating properties between the 'standard' system and systems incorporating small quantities (<10 %) of 2,2,3,3,4,4,5,5-octafluorohexane-1,6-diol. Therefore, an attempt at creating a similar coating derived from a commercial yacht paint coating, where gloss is one of the key marketable assets, used only high levels of additive. At higher loading, the polar hexanediol monomer was incompatible with the previous non-polar acrylic polyol system. The basic unit in the polyester polyurethane coating is a

polyol functional polyester, which should be more miscible with polar diols. Following the previous experimental procedure, the standard polyester polyurethane system was modified by addition of 2,2,3,3,4,4,5,5-hexane-1,6-diol ('F-diol') or hexane-1,6-diol, used as a control. Formulations of the modified coatings are given below (Table 5.7). The curing agent used (Figure 5.3) is an isocyanate based curing agent consisting of polymers formed through reaction of 1,6-hexamethylene diisocyanate with hydroxyl functional compounds.

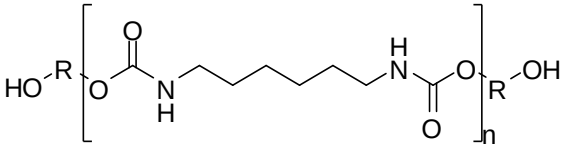

Figure 5.3: Structure of polyisocyanate based curing agent

Table 5.7: Formulation of polyester-polyurethane coatings modified by addition of a polyfluorodiol

OH functionality from fluorodiol **31** / %	Mass polyester urethane paint 'base'/ g	Mass fluorodiol / g	Mass isocyanate curing agent / g	Mass MAK / g	Total Mass / g
0	200	0.0	152.6	87.5	440.1
10	200	4.4	169.6	93.5	467.5
20	200	9.8	190.8	100	500.6
50	100	19.5	152.6	68	340.1

The coating systems were sprayed onto aluminium Q-panels that had previously been sanded and coated with an epoxy primer. Two coats of each system were applied to the respective test panels, with the second coat applied 25 minutes after the first. Subsequently, the panels were cured for two weeks under ambient conditions.

5.2.2.2 Testing of modified high gloss yacht coating

Testing of the panels was limited to UV testing and hardness, as previous tests (Section 5.2.1) had shown incorporation of 2,2,3,3,4,4,5,5-octafluorohexane-1,6-diol had little effect on surface properties such as surface energy. Microindentation hardness testing was performed in which a diamond tipped load was mechanically forced into the coating and both the force exerted on the panel and the depth of the indentation are measured. It is desirable for coatings to have a high microhardness so that they are not deformed by low energy impacts. Given that addition of either 2,2,3,3,4,4,5,5-octafluorohexane-1,6-diol or hexane-1,6-diol into the system lowers microhardness it is likely a network effect, caused by a lowering of crosslinking upon replacement of a polyol with a small molecule diol. At lower levels of diol addition the difference between H-diol (hexane-1,6-diol) and F-diol (2,2,3,3,4,4,5,5-octafluorohexane-1,6-diol) is negligible but at high levels of additive the difference is significant and is believed to arise from the decreased flexibility of the perfluoroalkyl unit relative to the alkyl unit of hexane-1,6-diol. A more flexible system will undergo greater deformation for a given force.

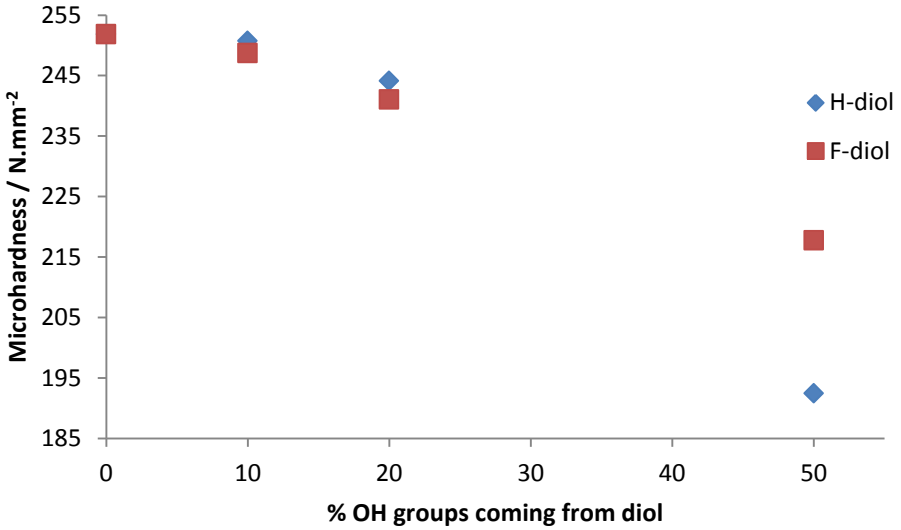

Figure 5.4: Microhardness of modified polyurethane system

Addition of diol causes a lowering in the gloss level of coatings but had little effect on the UV durability of the coatings. The graphs below (Figures 5.5 and 5.6) show the variation of colour (ΔE, formally a measure of the distance between two colours in a colour space) with time for each system, when subjected to accelerated weathering which includes a UV exposure cycle. All coatings give similar performance within the experimental error. The difference in colour retention between incorporating hexane-1,6-diol and 2,2,3,3,4,4,5,5-octafluorohexane-1,6-diol is marginal.

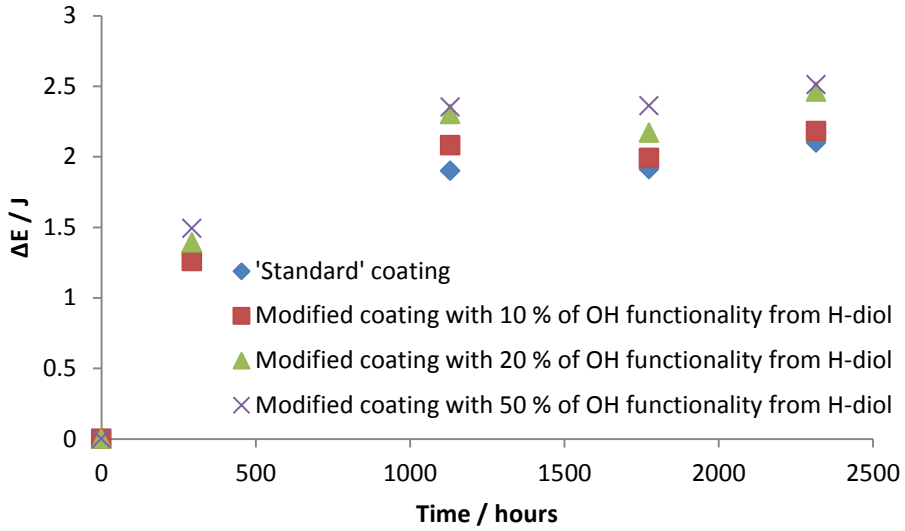

Figure 5.5: Variation of ΔE with time for polyester polyurethane coatings

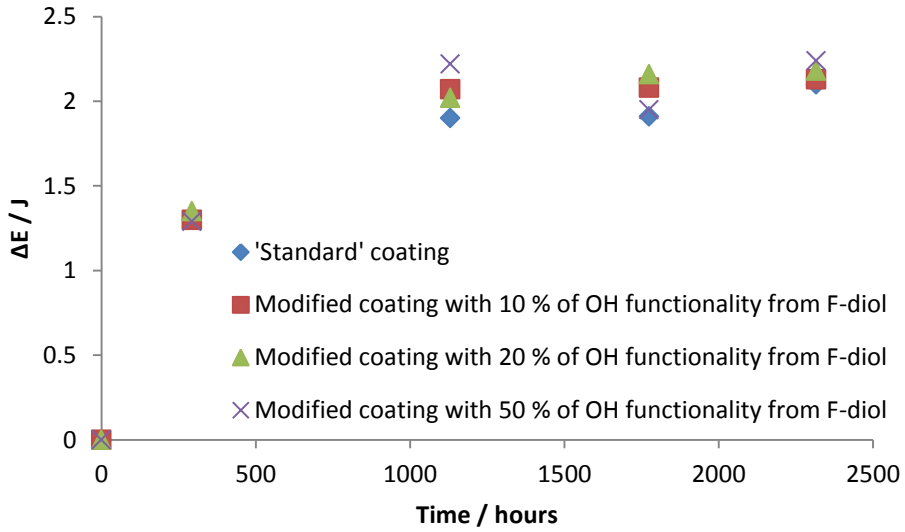

Figure 5.6: Variation of ΔE with time for polyester polyurethane coatings modified by inclusion of 2,2,3,3,4,4,5,5-octafluorohexane-1,6-diol

One possible interpretation of the data is to claim that the C-H alkyl backbone is not the weak point of the system. Altering the point at which the system initially undergoes degradation should have a large effect on the UV stability. Given that the H-diol and F-diol additives made little difference to the UV stability of the coating system it may be that degradation of the coating happens away from the hydrocarbon backbone at the site of monomer linkage. It should be noted that even when 50 % of the OH functionality was provided by 2,2,3,3,4,4,5,5-octafluorohexane-1,6-diol the mass of diol represents only 5.7 % of the mass of the coating system which is a small amount, and it is possible that addition of perfluoroalkylated diol in this quantity is below the level needed to see an improved effect.

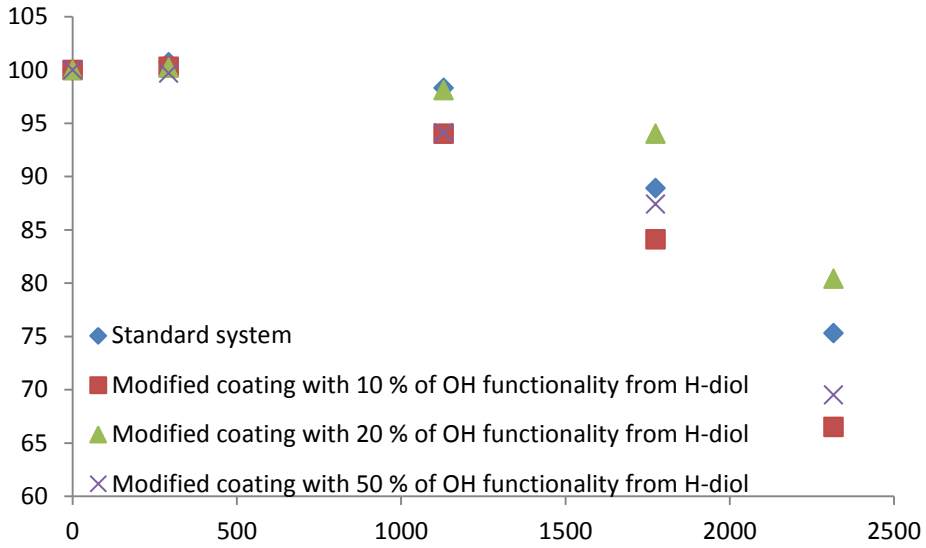

Figure 5.7: Change in gloss level for urethane coatings cured with aliphatic isocyanate

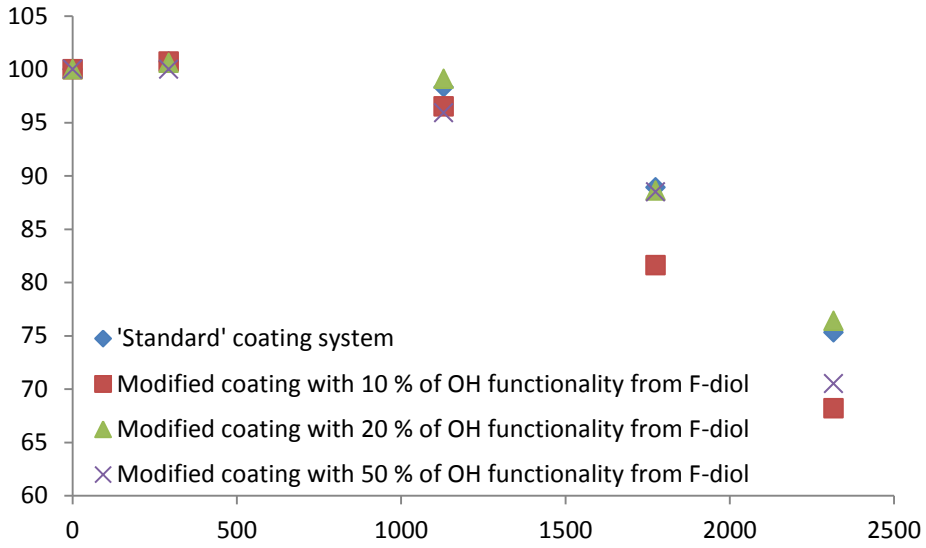

Figure 5.8: Change in gloss level for urethane coatings cured with aliphatic isocyante

Gloss levels were determined by use of a Sheen Tri-glossmaster taking five readings for each coated panel and calculating the mean gloss of the coating. The mean gloss level for each of the three panels coated with an identical paint coating was then averaged to give a value for each coating system. Gloss levels are a surface property, as light reflection is only relevant at the surface of the coating, and at these levels of diol addition the surface of the coatings are likely not sufficiently modified for any

difference in properties to be noticeable. The only change noticed for testing with these systems was data from microhardness testing which is a bulk property. Neither of the surface properties tested, gloss or colour, showed a significant difference upon modification by inclusion of 2,2,3,3,4,4,5,5-octafluorohexane-1,6-diol or inclusion of hexane-1,6-diol.

5.2.3 Modification of a polyester powder coating by inclusion of 2,2,3,3,4,4,5,5-octafluorohexane-1,6-diol

In addition to the two isocyanate cured wet paint systems above, a polyester based powder coating system incorporating 2,2,3,3,4,4,5,5-octafluorohexane-1,6-diol, **31**, was also produced. Polyester based powder coatings are a combination of materials, including waxes and primers, but the most important component is the resin synthesised from acid and alcohol functional monomers. 2,2,3,3,4,4,5,5-Octafluorohexane-1,6-diol was introduced as one such monomer, allowing creation of a polyester bearing perfluoroalkyl regions.

5.2.3.1 Synthesis of a polyester resin bearing perfluoroalkyl units

Among other components a standard polyester resin used in the coating industry contains two linear additives, hexane-1,6-diol and adipic acid, which both serve to increase the flexibility of the polymer backbone and trimethylolpropane which acts as a crosslinker. A novel analogue of this polyester was synthesised in which hexanediol was omitted, and replaced by an equivalent quantity of 2,2,3,3,4,4,5,5-octafluorohexane-1,6-diol.

Initially, the suitability of 2,2,3,3,3,4,4,5,5-octafluorohexane-1,6-diol as a monomer for inclusion into polyester systems was analysed by reaction with isophthalic acid (IPA), in the presence of a tin catalyst, operating at 180 °C in the melt. This was

performed to ascertain that the fluorinated diol would react with the difunctional acid at a reasonable rate and so be incorporated into a polyester resin. The extent of reaction was monitored by titration of the acid functionality and while the reaction between hexanediol and IPA is faster than the reaction between fluorinated hexanediol and IPA, both reactions proceed at a reasonable rate for polyester resin formulation.

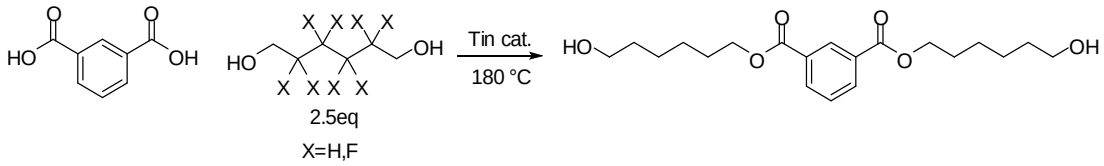

Figure 5.9: Test reaction between IPA and diols

Table 5.8: Extent of conversion for the reaction shown in figure 5.9

	4 Hours	8 Hours	24 Hours
X=H	93 %	98 %	-
X=F	33 %	-	98 %

Having ascertained that 2,2,3,3,4,4,5,5-octafluorohexane-1,6-diol is significantly reactive to be incorporated into a polyester network, the novel resin was synthesised. The perfluoroalkyl containing analogue of the standard resin contains the same components in the same starting ratio but includes 2,2,3,3,4,4,5,5-octafluorohexane-1,6-diol as a replacement for hexane-1,6-diol. Throughout the synthesis of modified fluorinated polyester resin acid values and hydroxyl values were monitored, by titration, and the amount of IPA and diol added were adjusted. In total the reaction ran for 74 hours, but due to laboratory practices the temperature was reduced from 230 °C - 240 °C to 150 °C overnight, so it should be possible to complete the reaction on a shorter time frame.

5.2.3.2 Testing of a novel polyester resin containing 2,2,3,3,4,4,5,5-octafluorohexane-1,6-diol

The fluorinated polyester resin synthesised was primarily analysed by NMR spectroscopy, as the easiest way to ascertain the presence of fluorine atoms in the polymer. The ^{1}H NMR spectra of the standard and fluorinated resins (Figure 5.10) show very little difference, which is to be expected as neither hexanediol nor fluorinated 2,2,3,3,4,4,5,5-octafluorohexane-1,6-diol are present in a large enough quantity to register a peak in the ^{1}H NMR spectra. Both proton NMR spectra show aromatic peaks arising from IPA regions and peaks at 4.3 ppm and 1.2 ppm arising from NPG domains. The ^{19}F NMR spectra (Figure 5.11) of the two resins are different, the standard resin contains no fluorinated monomer and no fluorine atoms are observed by ^{19}F NMR analysis as expected, while the ^{19}F NMR spectrum of the fluorinated polyester contains two peaks at δ = - 119.8 and δ = - 123.9, evidence that the symmetric fluorinated diol has been incorporated into the resin. Analysis of the resins by MALDI mass-spectrometry also shows significant similarities, with loss of the same repeating unit in each.

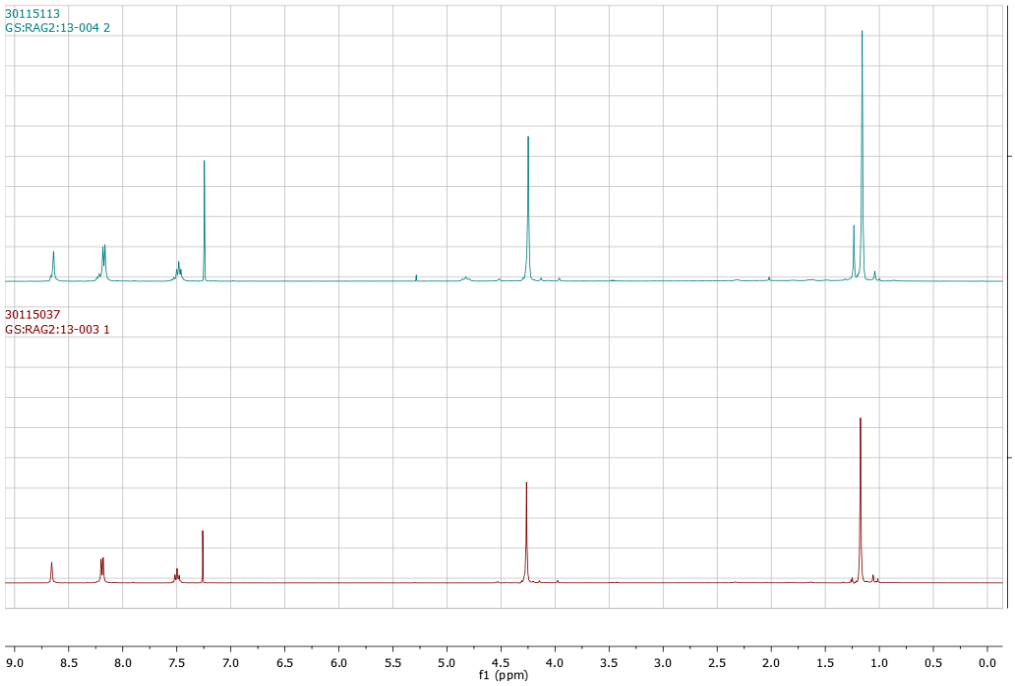

Figure 5.10: ^{1}H NMR spectra of the standard polyester resin (lower trace) and fluorinated polyester resin (upper)

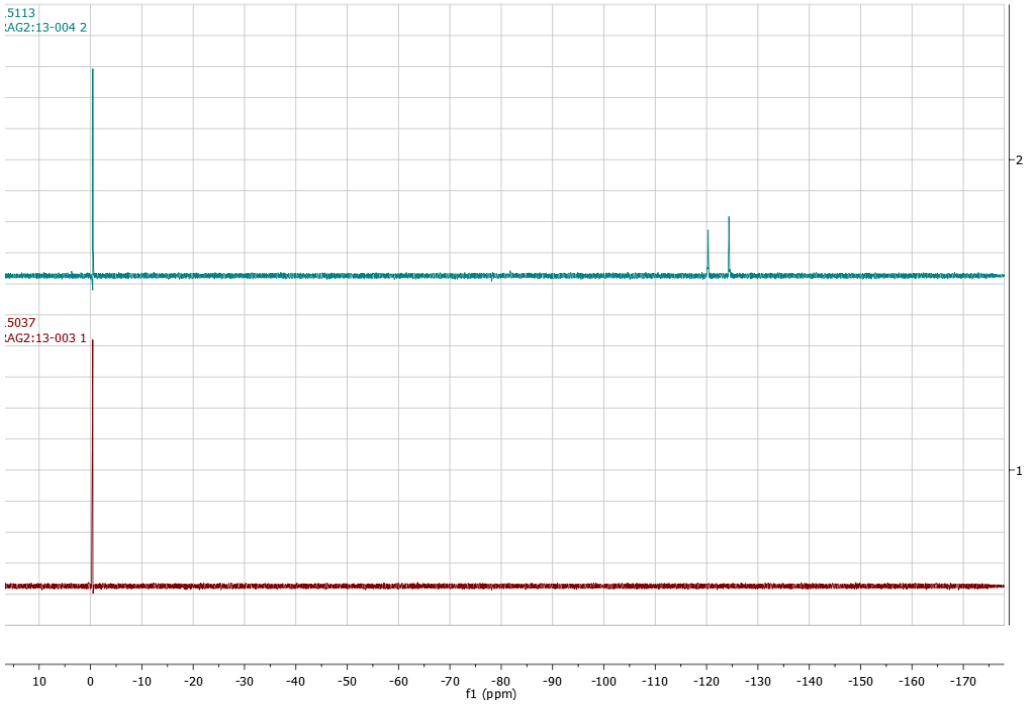

Figure 5.11: ^{19}F NMR spectra of the standard polyester resin (lower) and fluorinated polyester resin (upper)

Table 5.9: Data from initial testing of a standard polyester resin and a fluorinated analogue

Resin	Acid value / $mg.g^{-1}$	Hydroxyl value / $mg.g^{-1}$	T_g / °C	η_{200} / p
Standard Hydrocarbon polyester	25.1	-17.14	59 – 60	42.2
Fluorinated polyester	25.1	-20.90	54 – 55	31.9

From table 5.9 it can be seen that the two resins synthesised show little difference in either acid or hydroxyl values as these were monitored throughout the reaction and adjustments made, by adding more IPA or NPG, to keep the values close to the standard formulation. Larger differences are seen in the glass transition temperature and viscosities, with the incorporation of perfluoroalkyl regions leading to a lowering of both T_g and viscosity. For ease of process, resins are required to have a glass transition temperature above 50 °C, so that they exist as brittle solids and can be easily ground and extruded at temperatures above ambient conditions without undergoing a phase transition. While the T_g of the fluorinated polyester is lowered by inclusion of perfluoroalkyl regions the resin is still easily processed as a solid under standard operating procedures.

Both polyester resins were used to create powder coating systems. This process involved grinding the resins into a powder and mixing with other components in the quantities shown in the table below (Table 5.10). This mixture of components was then passed through a twin screw extruder, a process in which the powder is mixed and heated, to form a homogenous paste. After cooling, the solidified paste was broken into smaller pieces, ground further, and passed through a 45 Å sieve to give a sufficiently fine powder for electrostatic coating of QUV-A aluminium panels. The aluminium panels were coated to a depth of approximately 65 μm and cured by heating to 200 °C for exactly 15 minutes.

Table 5.10: Composition of powder coatings synthesised from polyester resins

Component	Mass / g
Polyester resin	655.7
Primid XL552	26.2
Benzoin	3.0
Lanco Wax 1525MF	4.0
Byk LPG21191	10.0
Titanium dioxide	300.0
Total Mass	998.93

Table 5.11: Data for powder coatings created from polyester resins. (F=Fail, P=Pass)

Resin used	Reverse impact test	Reverse impact and tape	MIBK solvent rub	Cross Hatch	M_n / $g.mol^{-1}$	M_w / $g.mol^{-1}$	Gloss (60 °) / Percentage light reflected
Standard	F	P	P	P	7268	13980	93.5
Fluorinated	F/P	P	P	P	7376	14436	91.5

Table 5.12: Surface energy data for powder coatings manufactured using standard and fluorinated polyester resins

Resin	Surface energy / $mJ.m^2$	Dispersive / $mJ.m^2$	Polar SE / $mJ.m^2$
Standard	43.33	40.86	2.47
Fluorinated	43.57	43.28	0.29

Both powder coatings have a glossy, white aspect due to the inclusion of titanium dioxide. The fluorine containing coating synthesised using the fluorinated polyester resin has a smoother texture and less ‘orange peel’ then the coating derived from the standard polyester resin, presumably as the fluorinated resin has a lower viscosity which enables a more even flow during the heat curing. Both the powder coatings perform to a similar standard with reverse impact, cross hatch and solvent rub tests (Table 5.11). Both coatings synthesised have similar number average and weight average molecular weights, which is expected given that the coatings are near

identical, and the fluorinated diol accounts for only around 5% of the total mass of the powder coating synthesised from the fluorinated polyester. As the molecular weight of the two coatings is similar, it can be implied that both coatings have a similar degree of polymerisation and, therefore, that differences in physical properties between the coatings are more likely to be due to the presence of the fluorinated domains than to differing network effects or conformations.

The most noticeable difference between the two powder coatings arises upon examination of the surface properties, and particularly the surface energy. Total surface energy differs little between the two coatings but the magnitude of polar and dispersive components shows a marked difference (Table 5.12). The coating manufactured using the resin with perfluoroalkyl domains has a much lower polar surface energy component, which is consistent with perfluoroalkyl groups being present at the surface.

In conclusion, a polyester resin modified by addition of a polyfluorinated diol has been synthesised and incorporated into a powder coating system. Testing on the powder coating system synthesised using the polyester resin is positive; it differs only slightly, and for the better, in both visible appearance and adhesion to the substrate when compared with the current standard coating synthesised from the unfluorinated resin. From the surface energy data (Table 5.12) it can be ascertained that some perfluoroalkyl domains in the fluorine containing powder coating have surface segregated causing a difference in polar surface energy to be observed.

5.3 Paint coatings incorporating polyfluorinated epoxide monomers

In addition to the use of 2,2,3,3,4,4,5,5-octafluorohexane-1,6-diol, **31**, as an additive in paint coating systems, two polyfluorinated epoxides, **55** and **59**, were also incorporated into a coating formulation and the effect on the physical properties of

the coating monitored. The additives, **55** and **59**, were incorporated into a coating usually derived from bisphenol-A and a phenalkamine curing agent (Figure 5.12).

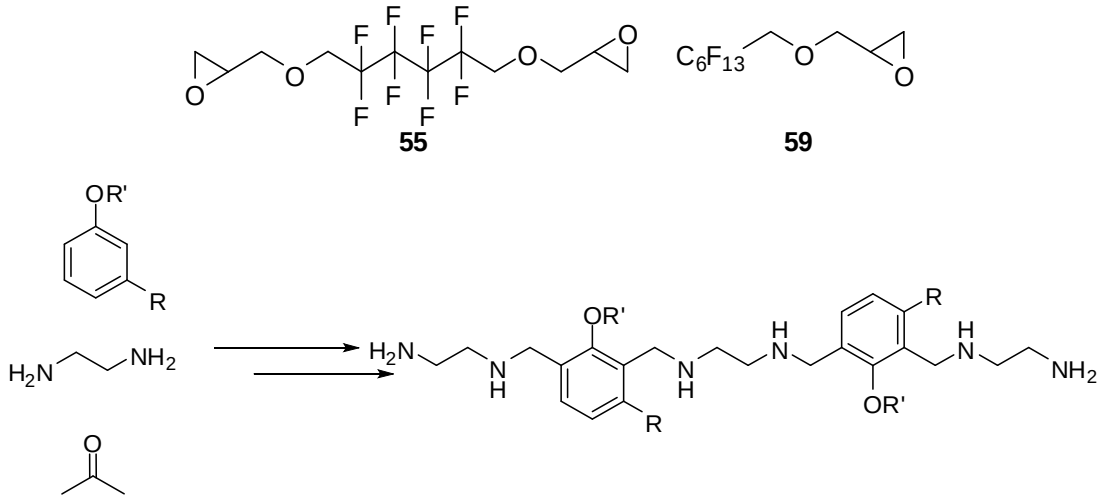

Figure 5.12: Formation of phenalkamine curing agent

Four paint 'bases' were created, which involved combining all components shown in table 5.13 prior to a stirring of the mixture at 3000 rpm for 15 min to ensure full mixing. Of the four paint 'bases' created, one is a formulation in which all epoxy functionality is from bisphenol-A and the other three 'bases' are modified systems in which either 10 % or 25 % of the EEW (epoxy equivalent weight) arises from use of aliphatic diepoxy monomer **55** or HDDGE **(**1,6-hexanediol diglycidyl ether). With 10 % EEW from **55** there is expected to be little or no change in the polymer network upon curing relative to the standard 100 % Bis-A formulation, but at 25 % EEW a change in the polymer network is possible and so HDDGE was introduced as a non-fluorinated analogue of **55** to produce a formulation with the same polymer network as a control experiment.

Table 5.13: Composition of pigmented paint bases

Paint 'base'	Mass bisphenol-A / g	Mass **55** / g	Mass HDDGE / g	Mass 4:1 Xylene: Butanol solution / g	Mass talc / g	Total mass / g	System EEW
100 % Bisphenol-A	70.0	-	-	37.6	92.2	199.8	577
75:25 Bis-A:**55**	40.0	13.5	-	28.0	68.6	149.9	568
90:10 Bis-A:**55**	47.8	5.3	-	28.1	68.8	150.0	571
75:25 Bis-A:HDDGE	40.9	-	9.8	28.7	70.5	149.9	555

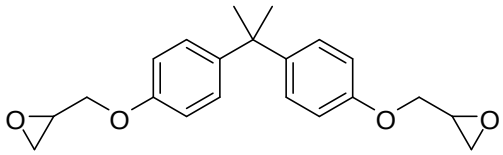

Bis-phenol A diglycidyl ether

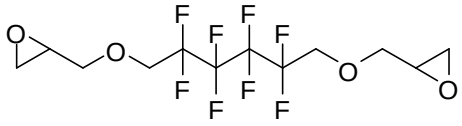

55

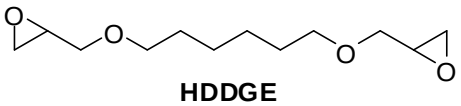

HDDGE

After standing overnight the four 'paint bases' shown in table 5.13 were cured into coatings (Table 5.14), and each applied to the following; two Sa2.5 blasted steel panels by means of a 400 μm draw down bar, two ST2 grade rusted steel panels applied by brush, and a single aluminium Q-panel applied by 400 μm draw down bar. After application the paint coatings were left to cure for one week under ambient conditions.

*Table 5.14: Composition of paint coatings incorporating **55** and **59***

System	Base	Additive	Mass base / g	Mass additive / g	Mass phenalkamine curing agent / g	Total mass / g	Epoxy functionality from additive / g
1	100 % Bis-A base	-	25	-	4.88	29.98	-
2	75:25 Bis-A:**55** base	-	25	-	4.95	29.95	-
3	90:10 Bis-A:**55** base	-	25	-	4.93	29.93	-
4	75:25 Bis-A:HDDGE base	-	25	-	5.07	30.07	-
5	100 % Bis-A base	**59**	25	0.93	5.13	31.06	5
6	100 % Bis-A base	BGE	25	0.30	5.13	30.43	5

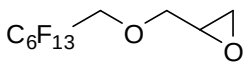

59

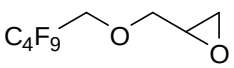

BGE

Six unpigmented ('clear') coating formulations were synthesised which have the same stoichiometry as the pigmented systems (Table 5.14), but omit the talc pigment from the paint 'base' (Table 5.13). Each of the six clear formulations was used to coat five plastic slides that had been pre-cleaned with acetone. Application of the unpigmented systems to the plastic slides was by use of a 300 μm draw down cube. Of the thirty slides coated, one slide for each distinct system was used to perform dry track testing, which is a measurement of the time taken for a coating to cure. Dry track testing (Table 5.15) was performed by loading the coated polymer slides onto a B.K. drying recorder which drags a metal pin through the coating system and from which two values are recorded; end of gel tear refers to the point at which the pin stops scoring through the whole coating and is somewhat analogous to the term 'touch dry' while end of track is the point at which the coating is fully cured and the

pin being dragged over the coating no longer leaves an indent. The dry track test was performed in an oven at a temperature of 23 °C and an atmosphere of 50 % relative humidity as use of these standard conditions allows comparison with other dry track testing data. The data from the dry track test (Table 5.15) shows little difference in curing time between systems. The time taken for both the end of gel tear and end of track are always within half an hour of the unmodified 'standard' system (system 1), in which all epoxide functionality arises from bisphenol-A.

Table 5.15: Results from dry track test

System	Paint base used	End gel tear / h	End of track / h
1	100 % Bis-A base	5.5	8.0
2	75:25 Bis-A:**55** base	5.5	7.5
3	90:10 Bis-A:**55** base	5.5	7.0
4	75:25 Bis-A:HDDGE base	6.0	8.0
5	100 % Bis-A with 5 % **59** additive	5.3	8.5
6	100 % Bis-A with 5 % BGE additive	5.5	8.5

The remaining slides coated with the unpigmented formulations, after one day curing at ambient temperature, were used to assess the water uptake of each coating. For this, three slides of each system were immersed in separate sealed glass jars of distilled water and the mass of the slide and coating measured periodically and referenced to the mass of the coated slide prior to immersion, with any gain in mass assumed to be due to incorporation of water into the coating film. All systems show a sharp increase in mass, before an equilibrium is reached at around five days (Figures 5.13 and 5.14). Before equilibrium is reached most coatings show a decrease in mass from the local maximum and it is impossible to differentiate between loss of absorbed water from the coating and loss of components of the paint coating, as both events cause a decrease in the mass of the coated slide. Small molecule diols and the phenalkamine curing agent are potentially soluble in water

and, if not bonded in the polymer network, are likely to leach out of the coating resulting in a mass decrease, relative to the mass before immersion. All systems, barring system 4, show a decrease from some local maximum after two days and it is likely that all paint coatings lose some molecules that did not chemically bond into the network during the curing process.

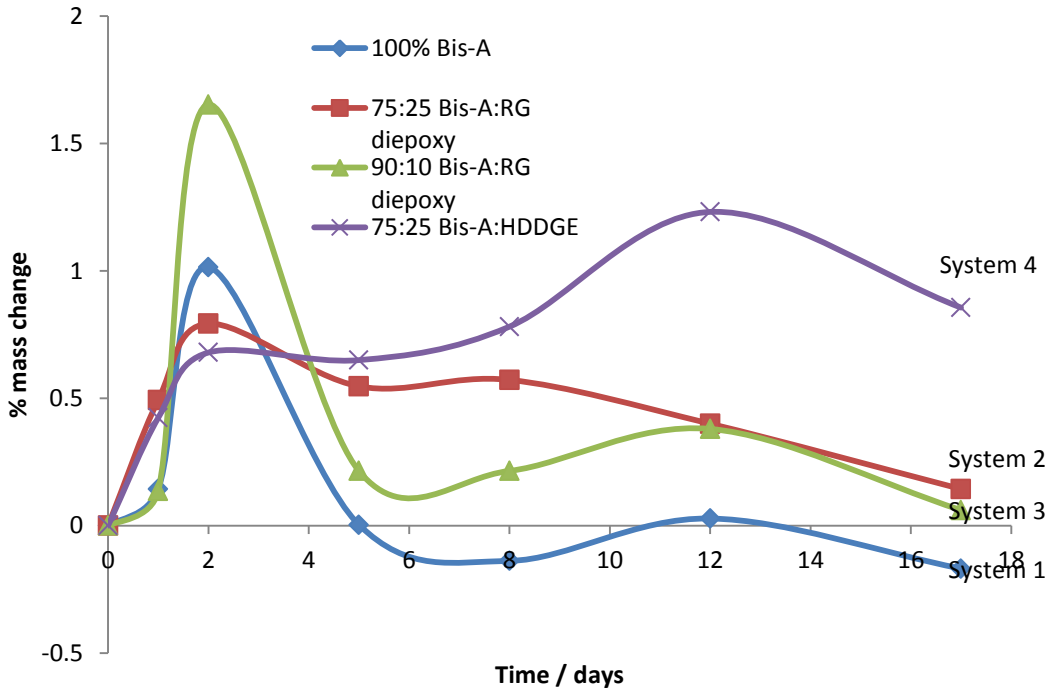

Figure 5.13: Mass change upon immersion in water for unpigmented coating systems

Figure 5.13 shows that system 3, the 90:10 Bis-A:fluorinated diepoxide system absorbs far more water in the initial phase than the unmodified system 1. Between the second and third data points (t=2 and t=5) system 3 then loses mass. As the loss of mass cannot be attributed entirely to absorbed water being released from the coating it must be assumed that some of the mass loss is due to leaching of organic molecules out of the coating, implying that they were not covalently bonded into the polymer network. There is also a large difference in relative mass change between the fluorine incorporating and non-fluorinated 75:25 (Bis-A:Aliphatic bisepoxide) coatings (systems 2 and 4). While the perfluoroalkyl region of **55** is hydrophobic so

too is the alkyl region of HDDGE and, therefore, such a large difference is probably not due to the difference in hydrophobicity between the aliphatic epoxide monomers. One theory for the difference in mass change between the fluorinated bis(epoxy) and HDDGE formulations is that fewer molecules of the polyfluorinated bisepoxide reacted into the polymer network, which would account for the greater leaching observed with this system. An alternative theory is that the coating incorporating the more rigid polyfluorinated bis(epoxy) species is itself more rigid, and so the coating featuring the polyfluoroalkylated bisepoxide swells less upon inclusion of water maintaining a smaller free volume than the corresponding non-fluorinated coating.

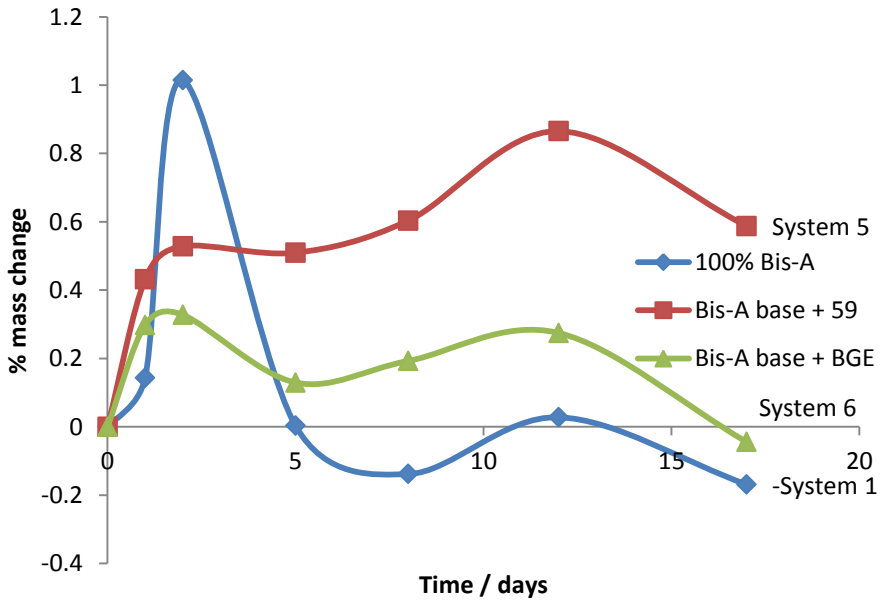

Figure 5.14: Mass change upon immersion in water for unpigmented coating systems featuring epoxide additives

The unpigmented coatings featuring mono-epoxy additives (systems 5 and 6) both show a smaller mass gain in the initial period than the unmodified 100 % Bis-A system (Figure 5.14), which is beneficial. However, system 5 continues to incorporate water over a much longer time period than any of the other coating formulations examined. As there is no mass loss between any two points in time the coating incorporating **59** (system 5) may leach fewer molecular components into the bulk solution. The coating incorporating BGE (system 6) shows a low absorption of

water into the coating in the first two days and also shows only a small mass loss.

Data on the glass transition temperature was also obtained from the unpigmented systems as pigmentation should not alter the T_g of a coating system. As with previous experiments used to find glass transition temperatures from DSC, samples were run once, in which a thermal event was seen around 40 – 45 °C. Samples were then reheated from – 50 °C to 250 °C at a rate of 20 °C.min^{-1} to obtain a better estimate of T_g. From the T_g data (Table 5.16) it is apparent that inclusion of small amounts of diepoxy (system 3) or monoepoxy (systems 5 and 6) derivatives make little change to the polymer backbone as the T_g is near identical for these systems. Addition of larger quantities of small molecule bis(epoxy) species causes a lowering in the T_g due to an increase in the flexibility of the system. This hypothesis is consistent with the observation that addition of HDDGE, which is more flexible than the perfluoroalkylated bis(epoxy) species **55**, causes a larger drop in the glass transition temperature than addition of **55**.

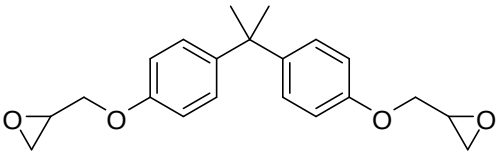

Bis-phenol A diglycidyl ether

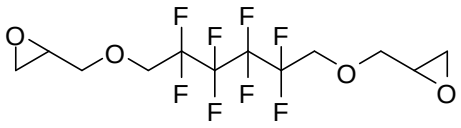

55

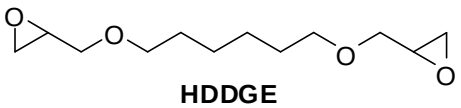

HDDGE

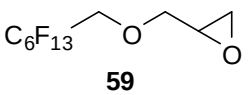

59

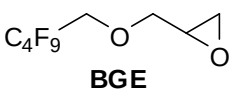

BGE

Table 5.16: T_g data obtained from DSC reheats for unpigmented coating systems

	Reheats	Glass transition / °C	
System	Description	Onset	Mid-point
1	100 % Bis-A	74.0	84.3
2	75:25 Bis-A:**55**	64.0	74.4
3	90:10 Bis-A:**55**	78.2	86.9
4	75:25 Bis-A:HDDGE	49.2	60.6
5	100 % Bis-A with 5 % **59** additive	75.1	86.1
6	100 % Bis-A with 5 % BGE additive	80.9	88.1

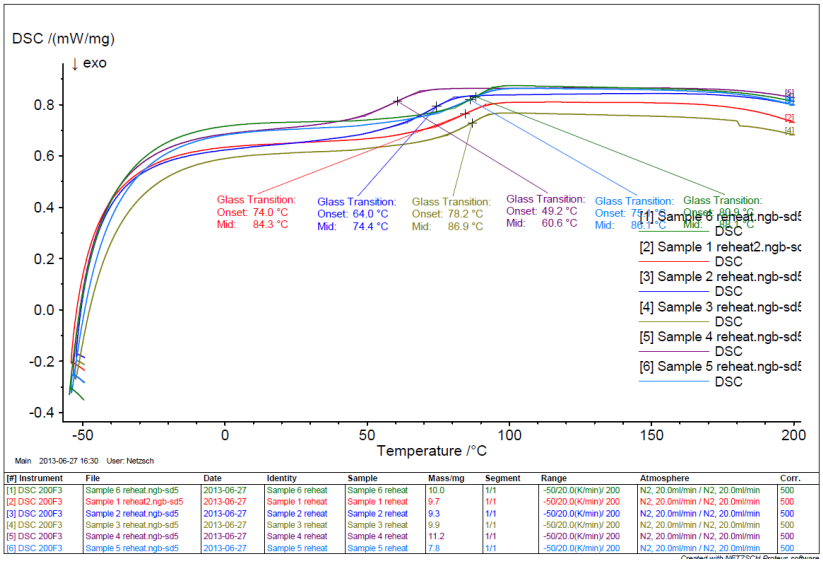

[#] Instrument	File	Date	Identity	Sample	Mass/mg	Segment	Range	Atmosphere	Corr.
[1] DSC 200F3	Sample 6 reheat.ngb-sd5	2013-06-27	Sample 6 reheat	Sample 6 reheat	10.0	1/1	-50/20.0(K/min)/ 200	N2, 20.0ml/min / N2, 20.0ml/min	500
[2] DSC 200F3	Sample 1 reheat2.ngb-sd5	2013-06-27	Sample 1 reheat	Sample 1 reheat	9.7	1/1	-50/20.0(K/min)/ 200	N2, 20.0ml/min / N2, 20.0ml/min	500
[3] DSC 200F3	Sample 2 reheat.ngb-sd5	2013-06-27	Sample 2 reheat	Sample 2 reheat	9.3	1/1	-50/20.0(K/min)/ 200	N2, 20.0ml/min / N2, 20.0ml/min	500
[4] DSC 200F3	Sample 3 reheat.ngb-sd5	2013-06-27	Sample 3 reheat	Sample 3 reheat	9.9	1/1	-50/20.0(K/min)/ 200	N2, 20.0ml/min / N2, 20.0ml/min	500
[5] DSC 200F3	Sample 4 reheat.ngb-sd5	2013-06-27	Sample 4 reheat	Sample 4 reheat	11.2	1/1	-50/20.0(K/min)/ 200	N2, 20.0ml/min / N2, 20.0ml/min	500
[6] DSC 200F3	Sample 5 reheat.ngb-sd5	2013-06-27	Sample 5 reheat	Sample 5 reheat	7.8	1/1	-50/20.0(K/min)/ 200	N2, 20.0ml/min / N2, 20.0ml/min	500

Figure 5.15: DSC traces for epoxy functional paints cured with a phenalkamine curing agent

Contact angles, obtained using a sessile drop method, with 4 µL drops of water and 1.4 mL drops of diiodomethane, were measured for the six systems and the total surface energy of each system is similar. Addition of small bis(epoxy) functional molecules appears to increase the contact angle of water on the surface of the coating, and the effect is marginally greater for inclusion of **55** than HDDGE (samples 2 and 4), corresponding to a lowering of the polar surface energy. The contact angle of system 5, which incorporates the fluorinated mono-epoxy molecule **59**, is by far the lowest observed with these systems and could well be indicative of

perfluoroalkyl domains surface segregating. This is significant as system 6 shows no difference from system 1, the standard 100 % Bisphenol-A coating, and, therefore, the lowering of contact angle in system 5 is not due to a reorientation of the polymer network caused by inclusion of a mono-epoxy molecule but is attributable to the presence of perfluoroalkylated groups in the surface

Table 5.17: Surface energy data for epoxy systems cured with a phenalkamine curing agent

	Average contact angle / °				
Sample	Diiodomethane	Water	Dispersive SE / $mN.m^{-1}$	Polar SE / $mN.m^{-1}$	Total SE / $mN.m^{-1}$
1	41.5	54.7	27.6	22.0	49.6
2	43.7	62.8	28.2	16.3	44.6
3	45.1	54.5	25.7	23.3	48.9
4	39.9	60.9	29.8	16.8	46.6
5	59.4	37.9	30.5	17.5	47.9
6	41.5	54.2	27.5	22.4	49.9

As with the other wet paint systems, IR spectroscopy of these coatings, when bonded onto aluminium panels, showed no major differences between coating systems. For the blasted steel panels (Sa 2.5), dry film thicknesses were measured, by measurement of conductivity using a handheld potentiometer manufactured by Cole-Parmer. All panels had dry film thicknesses between 110 and 146 μm and were tested for corrosion under accelerated weathering conditions. The change to the coating and test panel can be observed visually, figure 5.16 shows the appearance prior to test while later photos (Figures 5.17 and 5.18) show various patches of rust and a blistering of the coatings after weathering. For each coating system, two coated panels were subjected to testing, labelled as System X-1 and X-2 where the initial number (X = 1-6) refers to the coating system described above (Table 5.14).

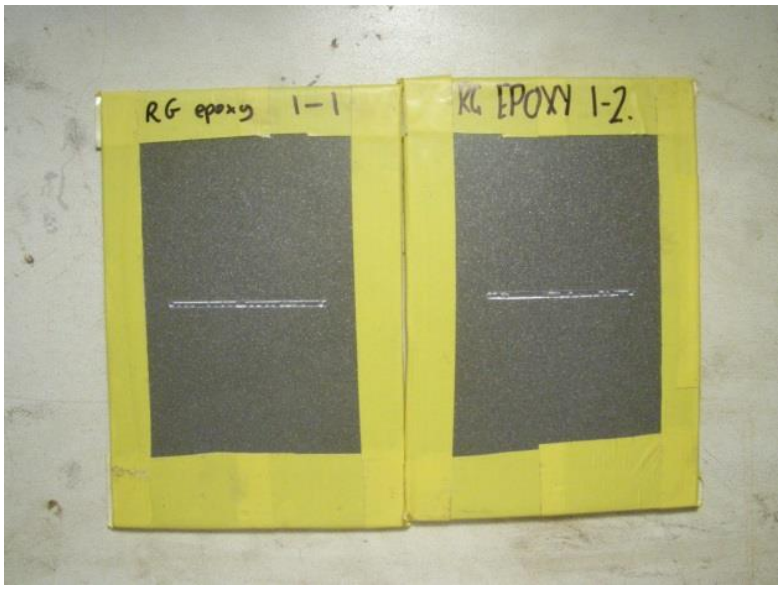

Figure 5.16: Coated Sa2.5 panel prior to accelerated weathering

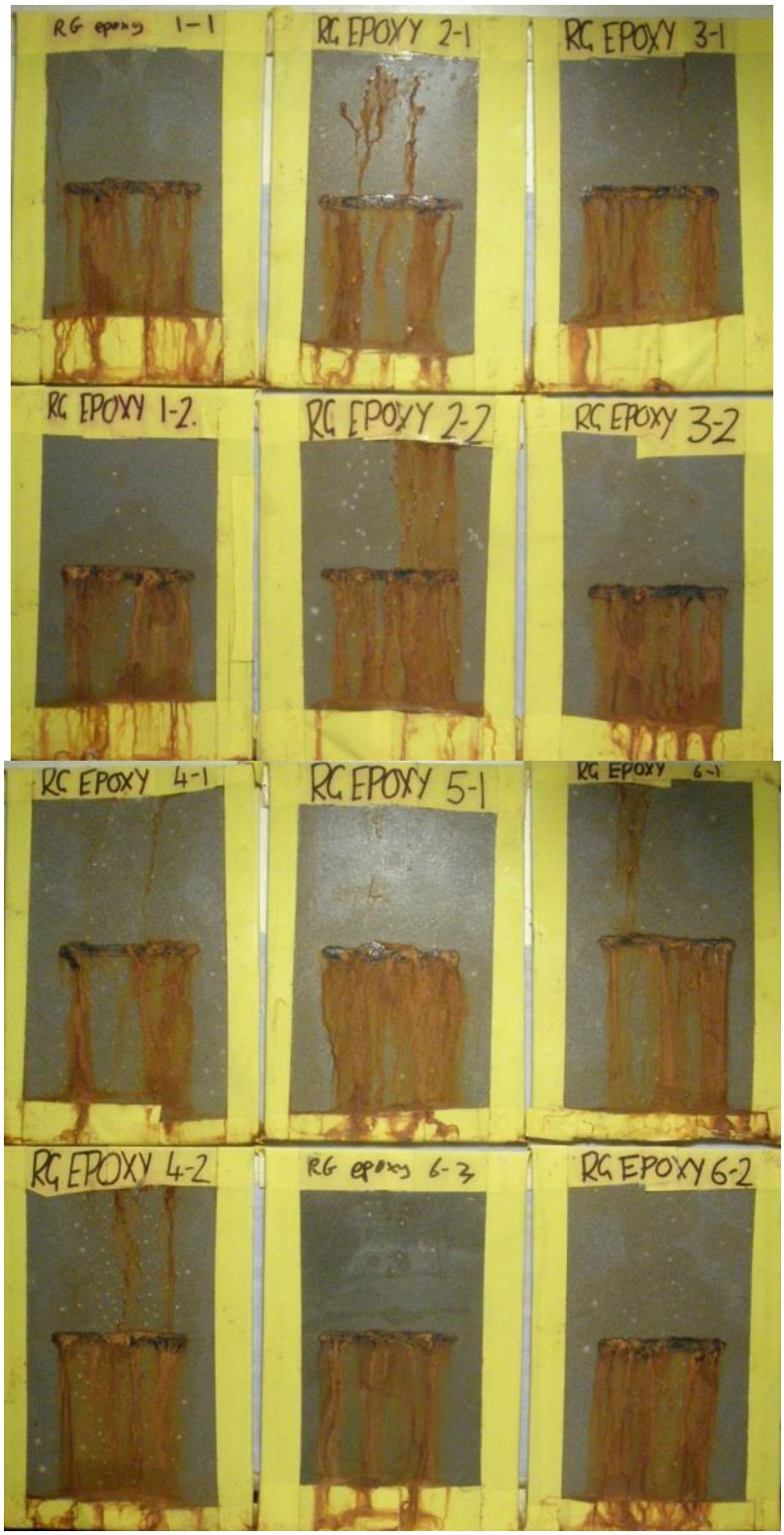

Figure 5.17: Coated Sa2.5 panels after four weeks on test

Figure 5.18: Coated Sa2.5 panels after 12 weeks on test

All coatings were scored horizontally to create a defect in the coating and give a site for rust formation. From figure 5.17 it is evident that systems 2, 3 and 4 all show significant blistering, with the effect lessened for system 3, the least modified of the three systems. At this time point the remaining systems show signs of blistering, but are mostly intact. In figure 5.18, taken eight weeks later, all coatings apart from 1-1 and 1-2 (system 1) have failed due to blistering or delamination. The unmodified system (system 1) is the most robust and shows the lowest amount of blistering and fewer substrate defects when compared with all the modified systems.

Anti-corrosive testing was also performed on the coated ST2 rusted panels. Failures in the coating occurred faster than for coatings on the blasted steel panels, due to a combination of less adhesion and an already degraded substrate. Table 5.18 illustrates the same trend as figures 5.17 and 5.18, with system 2 providing the least protection to the metallic substrate. From a comparison between systems 5 and 6 it is apparent that addition of fluorinated mono-epoxide creates a paint coating that is less protective than addition of a non-fluorinated system, although both perform worse than the unmodified system using bisphenol-A. The minor modification to system 3 has little effect on the protective coating but also showed little effect to other physical properties such as surface energy and glass transition temperature and so has not created an improved paint coating.

Table 5.18: Assessment of ST2 panels coated with epoxy paint systems

Sample	System	Performance (weeks)											
		1	2	3	4	5	6	7	8	9	10	11	12
RG epoxy 1-1	Bis-A	5	5	5	5	5	5	5	5	5	5	5	3
RG epoxy 1-2	Bis-A	5	4	4	4	4	4	4	4	4	4	4	4
RG epoxy 2-1	75:25 Bis-A:RG epoxy	5	3	3									
RG epoxy 2-2	75:25 Bis-A:RG epoxy	5	4	3									
RG epoxy 3-1	90:10 Bis-A:RG epoxy	5	5	5	5	5	5	4	4	4	4	4	3
RG epoxy 3-2	90:10 Bis-A:RG epoxy	5	4	4	4	4	4	4	4	4	4	4	3
RG epoxy 4-1	75:25 Bis-A:HDDA	5	4	4	4	4	4	4	4	4	4	4	3
RG epoxy 4-2	75:25 Bis-A:HDDA	5	3	3	3	3	3	3	3	3	3	3	3
RG epoxy 5-1	Bis-A + 5wt% RG mono	5	3	3	3								
RG epoxy 5-2	Bis-A + 5wt% RG mono	5	4	4	3								
RG epoxy 6-1	Bis-A + 5wt% BGE	5	4	4	4	4	4	3					
RG epoxy 6-2	Bis-A + 5wt% BGE	5	5	5	5	5	4	3					

Key	
5	Film intact
4	Film intact but some concerns/uncertainty
3	Failure due to small blistering or delamination
2	Failure due to large blistering or cracking
1	Widespread failure - delamination/blistering etc.

This concluded the testing of coatings synthesised from epoxy functional monomers. In conclusion, addition of polyfluorinated epoxides **55** and **59** seemed to show little difference to quantifiable physical properties such as T_g and water uptake but gave much worse performance as protective coatings under accelerated weathering conditions in comparison to standard coatings.

5.4 References to chapter 5

1. International Paint; *ISO 12944, Protect your assets in three easy steps,* Technical report for customers.
2. Cremer, N.D.; *Prohesion compared to salt spray and outdoors: cyclic methods of accelerated corrosion testing*, Technical report for C. & W. Technical equipment Ltd.: Shropshire, England, 1989.

6. Metal mediated perfluoroalkylation

6.1 Introduction

Polyfluorinated alkyl building blocks of the type used in the previous chapters are useful starting materials for the synthesis of organic systems containing perfluoroalkyl groups. In contrast, perfluoroalkylating agents for trifluoromethylation are commonly used on a research and pharmaceutical scale for the addition of trifluoromethyl moieties to existing organic systems.

Expansion of such trifluoromethylating systems to incorporate larger perfluoroalkyl moieties would allow for the synthesis of organic molecules bearing larger perfluoroalkyl units. As this approach is different to the building block approach explored previously it should allow for the creation of different classes of novel perfluoroalkyl monomers through late stage fluorination.

Copper mediated trifluoromethylation, as demonstrated by, among others, Hartwig, [1] is a route for the synthesis of trifluoromethylated aromatic systems from aryl iodides and aryl bromides. It appears that yields for reactions of **60**, [phen]Cu(CF_3), with aromatic halides are independent of the electronic character of the aromatic iodides (Figure 6.1) allowing a range of trifluoroaryl systems to be prepared.

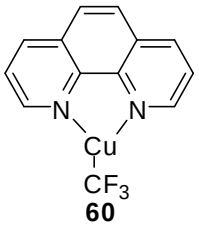

60

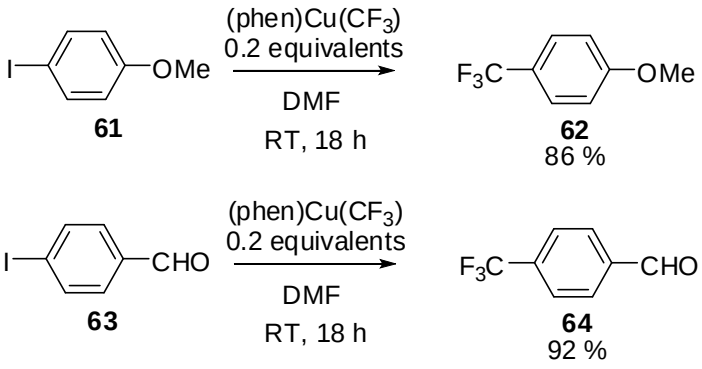

*Figure 6.1: Trifluoromethylation of aromatic iodides using **60** [1]*

From figure 6.1 it can be seen that **60** reacts with aromatic iodides under mild conditions and in high yield. The mechanism of the reaction is currently unknown, although it has been demonstrated that the reaction of **60** with aromatic halides does not proceed via a free radical intermediate. [1, 2]

60 has been synthesised via two different methods, one of which is shown in figure 6.2 below. However, this synthesis needs to be performed in a dry and inert atmosphere. An alternative method for the formation of **60**, is the *in situ* generation in standard laboratory conditions (Figure 6.3). Reactions of *in situ* generated **60** with aromatic iodides give comparable yields to the reaction of pre-formed **60**. Copper reagent **60** is commercially available but, at the moment, prohibitively expensive for use on the scale required for the synthesis of 'drop-in' additives for paint formulations. In contrast, the *in situ* route to **60** uses cheap reagents (copper chloride, 1,10-phenanthroline and potassium *tert*-butoxide) and, while it does require an inert atmosphere of nitrogen or argon, requires no special handling or equipment

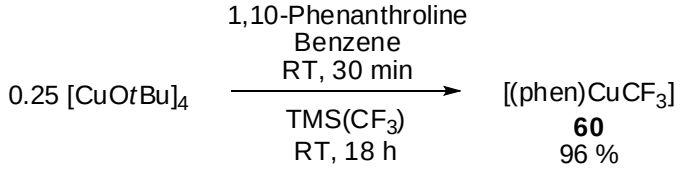

*Figure 6.2: Air sensitive process for the synthesis of **60***

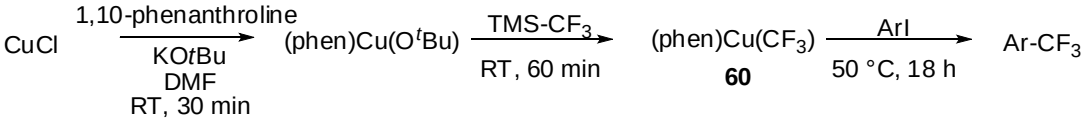

*Figure 6.3: In situ conditions for the synthesis and reaction of **60***

In addition, the larger (phen)Cu(C_3F_7) reagent has been isolated via the same route as (phen)Cu(CF_3) (Figure 6.2), and gives comparable perfluoroalkylation yields to reactions of **60** (Figure 6.4). [1] However, the use of larger homologues ($R_F > C_3F_7$) has not been reported in the literature.

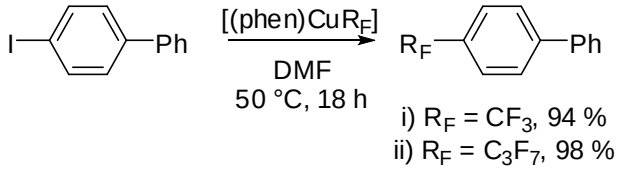

Figure 6.4: Reaction of copper-perfluoroalkyl reagents

In the synthesis of **60**, the Ruppert-Prakash reagent, **65** [3] was used as a source of trifluoromethyl anion. **65** is a well-documented reagent for the addition of a trifluoromethyl unit to carbonyl groups and was first synthesised by Ruppert through a condensation reaction between bromotrifluoromethane and trimethylsilyl chloride, mediated by HMPA (Figure 6.5). [4]

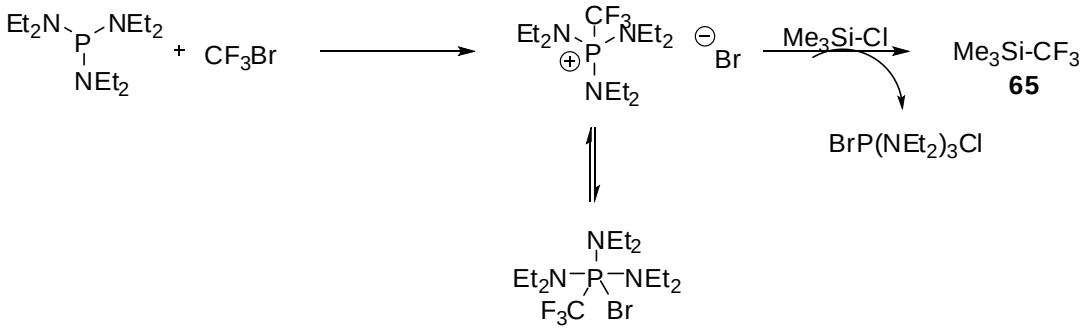

Figure 6.5: Synthesis of Ruppert-Prakash reagent [4]

Trifluoromethytrimethylsilane, **65**, is reasonably stable and can be stored almost indefinitely under ambient conditions in the absence of moisture. In the presence of fluoride ion, the trifluoromethyl group is liberated from **65** and the pseudo-anion

adds to carbonyl groups (Figure 6.6). While a range of fluoride sources have been used, and all give similar yields, TBAF is the most common source of fluoride initiator due to the commercial availability of TBAF as a solution in THF and the ease of handling a liquid compared to other solid fluoride sources. [5]

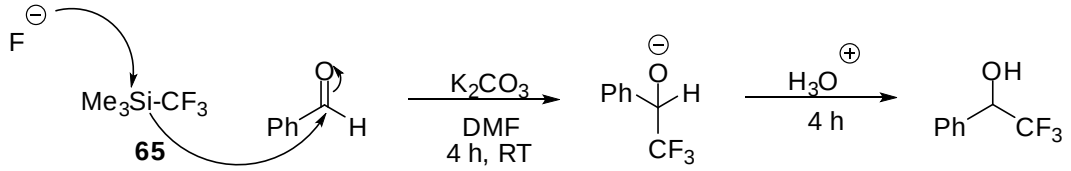

Figure 6.6: Fluoride mediated reaction of the Ruppert-Prakash reagent with benzaldehyde [5]

Compound **66**, the pentafluoroethyl homologue of the Ruppert-Prakash reagent, is also reported in literature, [3] formed in an analogous reaction to **65** using a larger perfluoroalkyl halide such as 1-bromoperfluoroethane. However, there are few reported perfluoroalkylation reactions using perfluoroalkyl silanes larger than **66**, leaving scope for the development of a new perfluoroalkylating reagent.

$Me_3Si{-}C_2F_5$

66

Another potential method of adding perfluoroalkyl units to existing organic systems is by cross-metathesis. Cross metathesis of alkenes, using molybdenum, tungsten or ruthenium catalysts such as **67**, is a versatile technique for the creation of new carbon-carbon double bonds as the reaction is tolerant to a range of functional groups. [6] While the literature contains many examples of olefin metathesis, including reactions with electron deficient alkenes, very few metathesis reactions of fluorinated alkenes have been reported, [7] and so metathesis of polyfluorinated alkenes offers a potential route to novel perfluoroalkyl containing monomers.

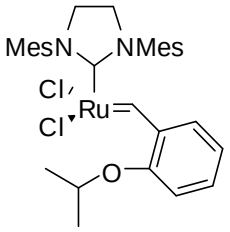

67

The major advantage of **67** over other metathesis catalysts is the enhanced air and moisture stability enabling the use of **67** outside of a glove box environment. [8] Reactions mediated by **67** are postulated to proceed via the Chauvin mechanism and, therefore, give a thermodynamic mixture of products. Cross metathesis reactions of α-alkenes give seven possible products, two stereoisomers for both homodimers, ethene and the crossmetathesis product. Under standard conditions ethene evaporates from the reaction mixture, both preventing the reverse reaction and eliminating one product from the crude mixture. In the absence of the reverse crossmetathesis process, reactions mediated by **67** are kinetically controlled and, consequently, the product mixture is usually simpler than that shown in figure 6.7 as the (*Z*)-isomers are not easily formed. This is illustrated in figure 6.8, in which only two products were identified, both showing (*E*) isomerisation.

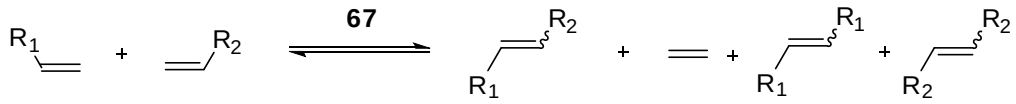

*Figure 6.7: Model reaction of substituted α-alkenes mediated by **67***

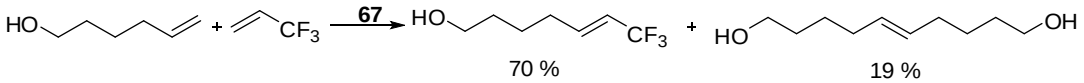

*Figure 6.8: Cross metathesis of a fluorinated alkene, mediated by **67***

6.2 Copper based trifluoromethylation

Before we attempted the synthesis and application of copper mediated perfluoroalkylation we decided to check the applicability of the trifluoromethylation

process by purchasing **60** and repeating literature conditions for the reaction of **60** and 1-bromo-4-iodobenzene (Figure 6.9). [1] Desired product **69** was isolated in a 49 % yield and the extent of reaction can be monitored by ^{19}F NMR which shows the formation of an aryl bound trifluoromethyl group at – 63.3 ppm as the reaction proceeds.

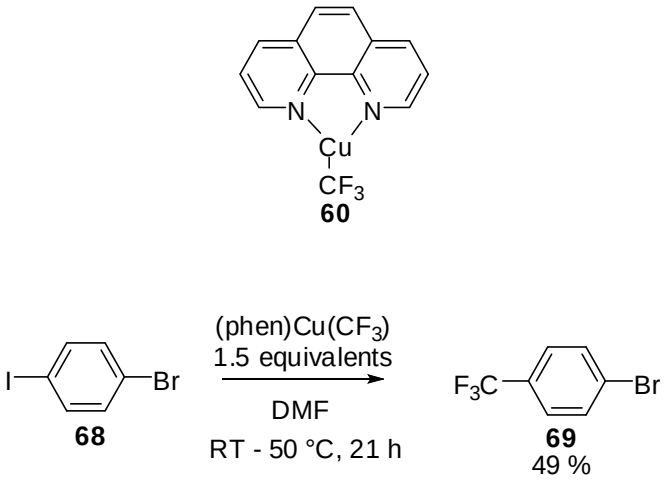

*Figure 6.9: Reaction of 1-bromo-4-iodobenzene with **60**, a (trifluoromethyl)copper complex*

While commercially available perfluoroalkyl copper reagent **60** proceeds in good yield it is too expensive (£151 / g) for use in paint formulations and so attempts at generating **60** *in situ* were performed using copper(I) chloride, potassium *t*-butoxide, 1,10-phenanthroline, and $TMSCF_3$ following literature procedures. [1]

In situ synthesis of **60** and subsequent trifluoromethylation of 1-bromo-4-iodobenzene was attempted several times (Table 6.1). Reactions were initially performed in DMF, following the literature procedure, as DMF is suggested to help stabilise the copper reagent **60**. However, reactions performed in DMF were unsuccessful and no trace of either **60** or **69** was observed by either ^{19}F NMR or GC-MS. Therefore, further reactions were performed using acetonitrile as solvent but attempts at synthesising **69** in acetonitrile were also unsuccessful. HMPA was used as an additive to stabilise **60** [9] but again, no sign of trifluoromethylation was observed.

*Table 6.1: Reaction conditions for the reaction of 1-bromo-4-iodobenzene using in-situ generated **1***

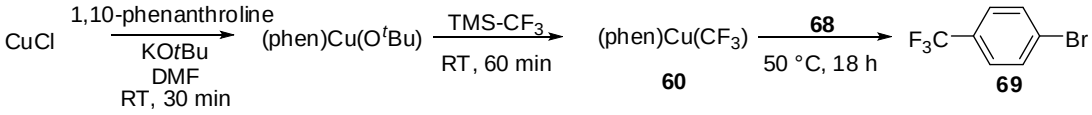

Attempt	Solvent	Time (Post ArI addition)	Additive	Ratio CuCl:TMS-CF_3	% Ar-CF_3 (**69**)
1	Wet DMF	18	-	1	0
2	DMF	18	-	1	0
3	DMF	67	-	1	0
4	DMF	16	HMPA	1	0
5	MeCN	20	HMPA	1	0
6	MeCN	20	-	1	0
7	DMF	42	-	0.5	0

Our attempts to generate a copper trifluoromethylation reagent failed, and the necessity of an extremely low oxygen/low moisture environment is probably required. Given the failure to synthesise **60** in 'normal' conditions, no attempts at synthesising a larger analogue of **60** such as (phen)Cu(C_6F_{13}) were attempted.

6.3 Metathesis of polyfluoroalkyl alkenes

Initial investigations into the metathesis of perfluoroalkyl alkenes reacted 1*H*,1*H*,2*H*-perfluorooct-1-ene **3** with styrenes as representative model aromatic alkenes, adapting related literature processes. Styrene, and *o*-substituted styrenes, are useful model systems as they are generally slower to homodimerise than aliphatic alkenes and, therefore, formation of undesired products should be minimised. [10] A tenfold excess of perfluoroalkylated alkene **3** was used to further minimise homodimerisation of the styrene component. Despite this, reaction of styrene

derivatives and **3**, mediated by HG-II, **67**, mainly gave homodimer products (Table 6.2).

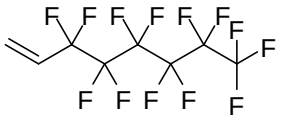

*Table 6.2: Outcome of reaction of **3** with substituted styrenes in the presence of HG-II (**67**)*

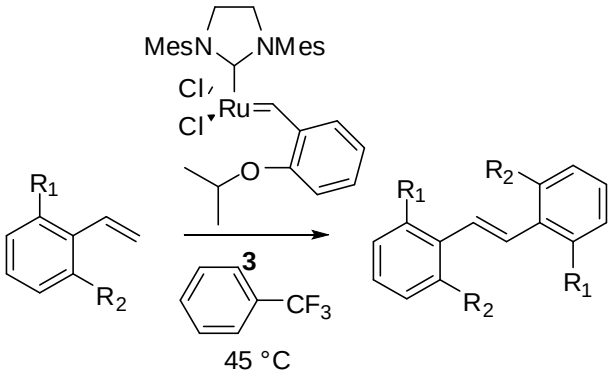

R_1	R_2	Time of reaction / h	Isolated yield of homodimer / %	Compound number
H	H	69	56	**70**
Cl	H	67	50	**71**
Me	H	70	62	**72**
Cl	Cl	121	No reaction	-

The reaction of styrenes, mediated by **67** (Table 6.2) gave grey-green solids, which after recrystallisation in ethanol afforded white crystals suitable for XRD (Figure 6.10). The molecular structure obtained by XRD shows that the E isomer is the preferred conformation at the double bond as expected. It is unclear whether 2,6-dichlorostyrene does not undergo dimerisation due to the steric bulk of the additional chlorine or whether the electron density of the alkene is too low to promote homodimerisation.

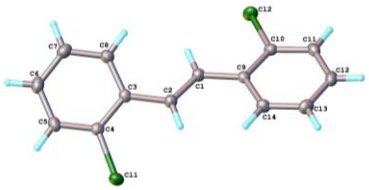

Figure 6.10: Molecular structure of 2,2'-dichlorostilbene

Following the results in table 6.2 our research switched to metathesis reactions of perfluoroalkyl alkenes with aliphatic α-alkenes. Reaction of 1-octene and 1*H*,1*H*,2*H*-perfluorooct-1-ene led to the formation of both the desired crossmetathesis product **73**, and the homodimer of 1-octene, **74**, in a 93.5:6.5 ratio (Figure 6.11). No dimerisation of 1*H*,1*H*,2*H*-perfluorooct-1-ene was observed. **73** was isolated in a 22 % yield from the crude reaction mixture by extraction into a perfluorinated solvent. ^{1}H NMR spectroscopy of **73** is consistent with two alkene resonances in a 1:1 ratio.

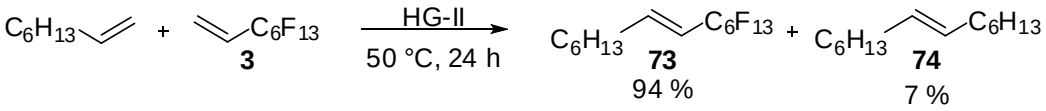

*Figure 6.11: Reaction of **3** with 1-octene*

Further metathesis reactions featuring **3** and other α-alkenes were attempted (Table 6.3).

*Table 6.3: Outcome of reactions between 1H,1H,2H-perfluorooct-1-ene **3** and α-alkenes*

Alkene	Conditions	Catalyst loading / mol%	Conversion to crossproduct / %	Conversion to homodimer / %
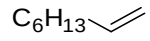	45 °C, 24 h	5	94	6
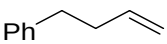	45 °C, 67 h	5	0	8
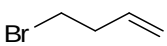	45 °C, 68 h	5	0	100
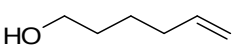	45 °C, 5 h	10	0	0
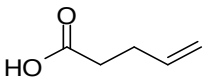	50 °C, 24 h	10	0	0

Reaction of 4-bromobut-1-ene in the presence of **67** led to formation of homodimer (*E*)-1,6-dibromohex-3-ene, **75**, which was isolated in 34 % yield (Figure 6.12). For entries four and five (Table 6.3) catalyst loading was increased with the aim of increasing the rates of reaction but no metathesis products (either dimers or cross-products) were observed for reactions featuring either hex-5-en-1-ol or pent-4-enoic acid in the presence of **67** and **3**.

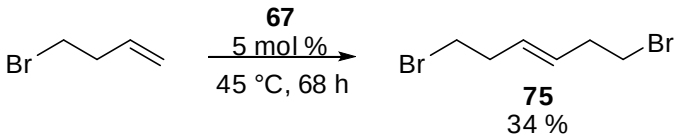

*Figure 6.12: Homodimerisation of 4-bromobut-1-ene in the presence of **67***

From the above data (Table 6.3) it appears that functionalised α-alkenes do not undergo cross metathesis with 1*H*,1*H*,2*H*-perfluorooct-1-ene in the presence of **67** due to the low reactivity of the polyfluorinated alkene. The low reactivity is probably a mixture of electronic effects, the low electron density at the alkene, and steric effects, with the rigid perfluoroalkyl unit hindering addition of the alkene to the ruthenium centre. The low reactivity is evidenced by the lack of homodimerisation of **70** under these conditions, which contrasts with hydrocarbon alkenes. As a consequence of the low reactivity, metathesis of 1*H*,1*H*,2*H*-perfluorooct-1-ene with α-alkenes was not pursued further due to time constraints but the successful reaction of 1*H*,1*H*,2*H*-perfluorooctene with 1-octene shows some promise.

6.4 Reactions of perfluoroalkylated trimethylsilane derivatives

Before the attempted synthesis of a perfluoroalkylated silane, reactions of **65** and **66** with aldehydes were carried out to establish the necessary conditions for reactions of such perfluoroalkylation reagents with representative electron rich and electron deficient aromatic aldehydes (Table 6.4).

Table 6.4: Yield of addition of R_F units to substituted benzaldehydes

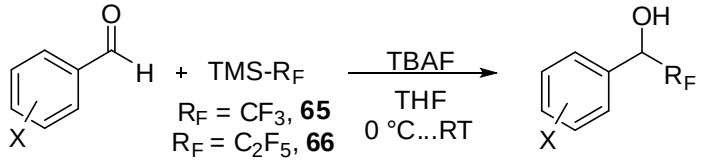

TMS-R_F	Aldehyde	Time / h	Product	Isolated yield / %
65	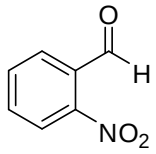	2	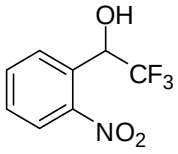 **76**	66
65	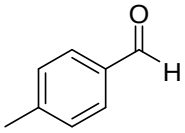	2	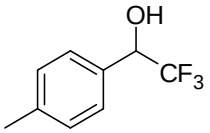 **77**	51
66	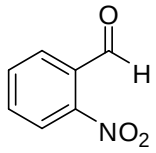	4	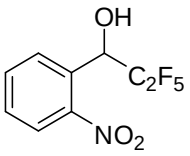 **78**	53
66	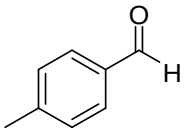	4	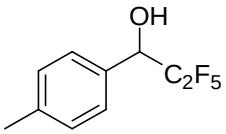 **79**	59

Table 6.4 indicates that reactions proceed in good yield independent of the electronic character of the carbonyl group. Despite the use of cold temperatures, reactions are experimentally easy to perform and the addition of perfluoroalkyl groups to aldehydes leads to formation of alcohols, a monomeric functionality. Therefore, synthesis of a larger analogue of **65** and **66** was attempted.

The first attempted synthesis of a silane bearing a larger perfluoroalkyl group used

conditions analogous to those used for the creation of the Ruppert-Prakash reagent (Figure 6.13). [4] Under the reaction conditions shown, conversion to **81** was 80 %, as analysed by ^{19}F NMR spectroscopy. However, **81** and **82** could not be easily separated.

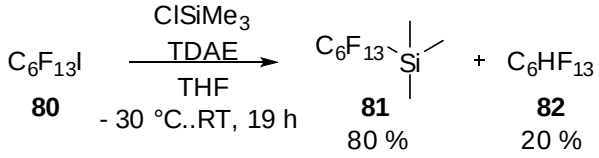

Figure 6.13: Synthesis of perfluoroalkylated TMS

Table 6.5: Conditions for synthesis of perfluoroalkylated TMS

$C_6F_{13}I$ / mmol	TDAE / mmol	Solvent	Temperature / °C	Reaction time / h	Crude yield **81** / %
10	12	THF	- 30	2	80
10	12	Tetraglyme	- 30	3	50
10	24	Tetraglyme	- 20	3	58
10	12	THF	- 20	3	68
10	12	Tetraglyme	- 30	2	65

As can be seen from table 6.5 the reaction shows little dependence on solvent between THF and tetraglyme. However, the reaction is moisture sensitive as the perfluoroalkyl anion generated by reduction of **80** reacts faster with water than with trimethylsilyl chloride leading to competing formation of **82**.

As it proved impossible to easily separate **81** and **82** attempts were made to react **81** *in situ*. Addition of TBAF and 4-methylbenzaldehyde to solutions containing **81** and **82** did not lead to perfluoroalkylation of the aldehyde despite long reaction times far in excess of those used in earlier reactions for trifluoromethylation (Table 6.4). It appears, from ^{19}F NMR spectroscopy data, from TBAF does not liberate the perfluorohexyl group from **81** under the attempted conditions reflecting the larger steric bulk of the perfluorohexyl group relative to the trifluoromethyl group.

6.5 Direct addition of perfluoroalkyl anions to carbonyl groups

As a consequence of the failure to isolate **81**, the focus of our research switched to the investigation of perfluoroalkylation of organic molecules by addition of other perfluoroalkyl anion sources to carbonyl groups. Initially, model reactions featuring monofunctional aldehydes and monofunctional ketones were attempted to assess the reactivity of the perfluoroalkyl anion generated by reaction of perfluorohexyl iodide, **80**, with TDAE. These model reactions were performed using an adapted version of a literature procedure for trifluoromethylation. [12]

Table 6.6: Reactions of substituted aromatic aldehydes/ketones with $C_6F_{13}I$

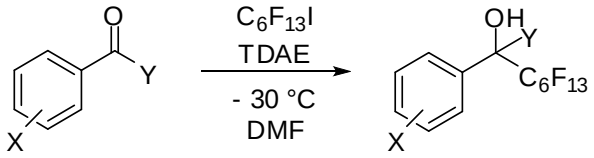

X	Y	Reaction time /h	Yield / %	Compound number
2-NO_2	H	2	60	**83**
4-Me	H	5	48	**84**
4-Me	Me	21	No reaction	-
4-Cl	Me	20	No reaction	-

Addition of a tridecafluorohexyl unit to 2-nitrobenzaldehyde and 4-methylbenzaldehyde is lower yielding than for addition of trifluoromethyl or a pentafluoroethyl group (Table 6.4) due to the greater stability of the larger perfluoroalkyl anion. The reaction is easily followed by ^{1}H NMR spectroscopy which shows the disappearance of the aldehyde proton ($\delta \approx 10.5$ ppm) and appearance of a peak at 5.05 ppm corresponding to the C*H*OH proton which exhibits a coupling constant consistent with a $^3J_{HF}$ coupling. While addition of a tridecafluorohexyl group to aldehydes proceeds in good yield, in contrast, no product is observed for the reaction of ketones under these conditions.

Since conditions for the direct addition of a perfluorohexyl group to simple aromatic aldehydes have been established, the reaction was extended to more complicated aldehyde systems. Under similar conditions to those used above isophthalaldehyde was reacted with 1-iodoperfluorohexane **80**. Addition of two perfluoroalkyl units to isophthalaldehyde would generate a perfluoroalkylated diol that is potentially a useful monomer.

Table 6.7: Conditions used for the reaction of 1-iodoperfluorohexane with isophthalaldehyde

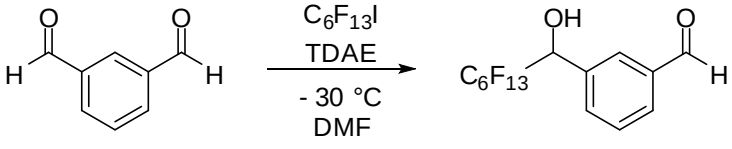

85 **86**

Ratio $C_6F_{13}I$:Isophthalaldehyde	Maximum temperature	Reaction time / h	Solvent	Crude yield of **86** / %
2.4	Ambient	2	DMF	60
4.8	Ambient	46	DMF	28
0.1	Ambient	24	DMF	32
20	Ambient	24	DMF	22
20	50	114	DMF	44
20	50	42	MeCN	56

In all reactions, no trace of the desired diaddition product was observed with initial attempts leading to monoaddition product **86**. The third attempt, which used a large excess of isophthalaldehyde, led to formation of oligomeric product arising from reaction of the alcohol group of **86** with the aldehyde functionality of isophthalaldehyde. Further attempts, using both a greater excess of perfluoroalkyl iodide and more forcing conditions, gave incomplete conversion to **86** and no evidence for diaddition of tridecafluorohexyl units to isophthalic acid was observed by ^{1}H NMR, ^{19}F NMR and GC-MS. It can be concluded that diaddition of a perfluorohexyl group to isophthalaldehyde is non-trivial due to incomplete reactions

leading to oligomerisation and the need for harsh conditions to push the reaction to full conversion. However, this route offers possibilities for monomer formation given appropriate development.

6.6 Conclusions

In this chapter a range of techniques for the addition of perfluoroalkyl groups to organic systems were explored with the aim of synthesising monomers that could be added to current paint coating formulations as 'drop-in' additives.

Whilst model copper based trifluoromethylation proceeds with **60** the reagent is too expensive for large scale use, and attempts to generate **60** *in situ* proved unsuccessful. To overcome the need for expensive metal reagents the utility of metathesis catalyst **67** was investigated. Almost all the metathesis reactions attempted in section 6.3 showed either no reaction whatsoever or homodimerisation of the non-fluorinated alkene, as a consequence of the greater reactivity of the non-fluorinated alkene relative to 1*H*,1*H*,2*H*-perfluorohex-1-ene.

Subsequent work investigated reaction of perfluoroalkyl anion reagents generated from silyl reagents and by reduction of 1-iodoperfluorohexane. **81**, perfluorohexyltrimethylsilane, was successfully synthesised but could not be isolated from side products such as 1H-perfluorohexane. Some techniques showed promise for further research, but such work was not performed as part of this thesis due to time constraints.

6.7 References to chapter 6

1. Morimoto, H.; Tsubogo, T.; Litvinas, N.D.; Hartwig, J.F.; *Angew. Chem. Int. Ed.*, **2011**, 50, 3793 – 3798.

2. Enemaerke, R.J.; Christensen, T.B.; Jensen, H.; Daasbjerg, K.; *J. Chem. Soc.*, *Perkin Trans. 2*, **2001**, 1, 1620 – 1630.

3. Prakash, G.S.K.; Yudin, A.K.; *Chem. Rev.*, **1997**, 97, 757 – 786.

4. Ruppert, I.; Schlich, K.; Volbach, W.; *Tetrahedron Lett.*, **1984**, 25, 2195 – 2198.

5. Cheng, H.; Pei, Y.; Leng, F.; Li, J.; Liang, A.; Zou, D.; Wu, Y.; Wu, Y.; *Tetrahedron Lett.*, **2013**, 54, 4483 – 4486.

6. Chatterjee, A.K.; Morgan, J.P; Scholl, M.; Grubbs, R.H.; *J. Am. Chem. Soc.*, **2000**, 122, 3783 – 3784.

7. Imhof, S.; Randl, S.; Blechert. S.; *Chem. Comm.*, **2001**, 1692 – 1693.

8. Vougioukalakis, G.C.; Grubbs, R.H.; *Chem. Rev.*, **2010**, 110, 1746 – 1787.

9. Wiemers, D.M.; Burton, D.J.; *J. Am. Chem. Soc.*, **1986**, 108, 832 – 834.

10. Chatterjee, A.K.; Tae-Lim, C.; Sanders, D.P.; Grubbs, R.H.; *J. Am. Chem. Soc.*, **2003**, 125, 11360 – 11370.

11. Pauff, S.M.; Miller, S.C.; *J. Org. Chem.*, **2013**, 78, 711 – 716.

12. Petrov. V.A.; *Tetrahedron Lett.*, **2001**, 42, 3267 – 3269.

7. Experimental section

7.1 General

NMR Spectroscopy: Proton, carbon and fluorine nuclear magnetic resonance spectra (^{1}H NMR, ^{13}C NMR, ^{19}F NMR) were recorded on a Bruker Advance-400 spectrometer (^{1}H NMR, 400 MHz; ^{13}C NMR 101 MHz; ^{19}F NMR 376 MHz), a Varian Inova-500 spectrometer (^{1}H NMR, 500 MHz; ^{13}C NMR 127 MHz; ^{19}F NMR 188 MHz), Varian VNMRS-600 spectrometer (^{1}H NMR, 600 MHz; ^{13}C NMR 151 MHz; ^{19}F NMR 564 MHz) or Varian VNMRS-700 spectrometer (^{1}H NMR, 700 MHz; ^{13}C NMR 151 MHz; ^{19}F NMR 658 MHz) with solvent reference as the internal standard (^{1}H NMR, $CHCl_3$ at 7.26 ppm; ^{13}C NMR, $CDCl_3$ at 77.36 ppm; ^{19}F NMR, $CFCl_3$ at 0.00 ppm). ^{1}H, ^{13}C and ^{19}F spectroscopic data are reported as follows: chemical shift, integration, multiplicity (s = singlet, d = doublet, t = triplet, q = quartet, sept = septet, m = multiplet), coupling contants (Hz) and assignment.

Mass spectrometry: GC-MS analysis was performed on a Trace-MS device (Thermo-Finnegan corporation) operating in electron impact ionisation (EI^+) mode and ASAP analysis was achieved with a Xevo QtoF mass spectrometer (Waters Limited, UK) equipped with an atmospheric solids analysis probe.

Elemental analysis: C, H and N analyses were collected with an Exeter Analytical CE-440 Elemental Analyser.

IR: Infra-Red spectra were recorded on a Perkin Elmer Spectrum RX1 fitter with an ATR attachment.

X-ray analysis: All crystallographic data was recorded with a Rigaku R-axis SPIDER IP diffractometer equipped with Cryostream (Oxford Cryosystems) low-temperature device at 120 K with graphite-monochromated MoK_α-radiation ($\lambda = 0.71073$ Å).

Melting point analysis: Melting points were measured with a Gallenkamp apparatus at atmospheric pressure and are uncorrected.

Microwave: All microwave irradiated reactions were heated in a Biotage Initiator^{TM} Sixty microwave using a 0.5 – 2.0 mL, 2 – 5 mL or 10 – 20 mL microwave vial fitted with a Biotage magnetic follower and sealed with a Reseal^{TM} Septum. The microwave was set to heat at constant temperature, as specified in the relevant experimental procedure, and each reaction was timed from the point at which the temperature had been reached. After the reaction time had expired, the microwave vial and its contents were cooled to 45 °C by an external flow of nitrogen gas. Reactions involving DMF or DMSO as solvent were heated to the target temperature using the 'very high' irradiation mode. Reactions involving acetonitrile and THF were heated using the 'high' irradiation mode and those reactions using toluene as solvent were heated using the 'normal' irradiation mode.

Chemicals and solvent: Unless otherwise stated, commercially available reagents were used without purification. An Innovative Technology Inc. Solvent Purification System fitted with a Metrohm 831 Karl Fischer Coulometric Titrator was used to dry MeCN, DMF, THF and toluene whilst anhydrous DMSO was purchased from Sigma-Aldrich. Hexanes, DCM and Chloroform were purchased from Fischer and used without further purification. Flash column chromatography was carried out using Fluorochem Silicagel LC60A (40 – 63 μm). FC3280 (perfluorooctane) was provided by 3M.

7.2 Experimental to Chapter 2

Reaction of 1*H*,1*H*,2*H*,2*H*-perfluorooctyl iodide with nucleophiles

Method 1: Tetrabutylammonium bromide (171 mg, 0.53 mmol), 1*H*,1*H*,2*H*,2*H*-perfluorooctyl iodide (776 mg, 1.64 mmol) and 1-octanol (415 mg, 3.19 mmol) were combined in DMF (20 mL). This mixture was heated to 50 °C for 10 minutes after which potassium hydroxide (90.1 mg, 1.61 mmol) was added. Subsequently, the mixture was heated to 70 °C for 90 minutes. Evaporation of solvent gave *1H,1H,2H-perfluorooct-1-ene* (522 mg, 92 %) as a colourless liquid; b.p. 105 – 107 °C [lit. 106 – 107 °C] [1], HRMS (ESI^+) Found $[M-H]^+$ 345.0034, $C_8H_2F_{13}$ requires 345.0027; ^1H NMR (400 MHz, $CDCl_3$): δ 5.92 – 5.84 (1H, m, $CHCF_2$), 5.63 – 5.55 (1H, m, CH_2), 5.49 – 5.40 (1H, m, CH_2); ^{19}F (658 MHz, $CDCl_3$): δ -81.2 (3F, t, $^4J_{FF}$ 9.9, CF_3), -114.5 (2F, s, CF_2), -122.1 (2F, s, CF_2), -123.3 (2F, s, CF_2), -123.7 (2F, s, CF_2), -126.4 (2F, s, CF_2); *m/z* (ESI) 345.0 (100 %, $[M-H]^+$).

Method 2: Tetrabutylammonium bromide (208 mg, 0.64 mmol), 1*H*,1*H*,2*H*,2*H*-perfluorooctyl iodide (1.51 mg, 3.18 mmol) and ethylene glycol (201 mg, 3.24 mmol) were combined in DMF (20 mL). This mixture was heated to 50 °C for 10 minutes after which potassium hydroxide (278 mg, 4.95 mmol) was added. Subsequently, the mixture was heated to 70 °C for 90 minutes. Evaporation of solvent left *1H,1H,2H-perfluorooct-1-ene* (943 mg, 86 %) as a colourless liquid; physical and spectral data as above.

Method 3: To a flask containing imidazole (272 mg, 4.0 mmol) was added dry ethyl acetate (50 mL) and 1*H*,1*H*,2*H*,2*H*-perfluorooctyl iodide (762 mg, 1.61 mmol). This solution was heated for 5 days at 75 °C and the mixture was washed with water (2 x 20 mL). Evaporation of the organic solvent gave *1H,1H,2H-perfluorooct-1-ene* (188 mg, 34 %) as a colourless liquid; physical and spectral data as above.

Method 4: Amine (0.5 mmol) and 1*H*,1*H*,2*H*,2*H*-perfluorooctyl iodide (237 mg, 502 μmol) were combined in THF (2 mL) and heated to 100 °C under microwave conditions

for 40 minutes. Evaporation of solvent left *1H,1H,2H-perfluorooct-1-ene* as a colourless liquid; physical and spectral data as above.

By use of method 4 ethylamine was reacted with 1*H*,1*H*,2*H*,2*H*-perfluorooctyl iodide producing *ethanaminium iodide* (66 %) as a white solid which was isolated by filtration but not purified further; ^{1}H NMR (400 MHz, D_2O); 3.41 – 3.34 (2H, m, NCH_2), 1.64 – 1.58 (3H, m, CH_3); *m/z* 172.1 (100 %, $[M\text{-}H]^+$)

By use of method 4 isopropylamine was reacted with 1*H*,1*H*,2*H*,2*H*-perfluorooctyl iodide producing *propan-2-aminium iodide* (60 %) as a white solid which was isolated by filtration but not purified further; ^{1}H NMR (400 MHz, D_2O); 4.02 – 3.96 (1H, m, NCH), 1.68 – 1.65 (6H, m, CH_3); *m/z* 186.0 (100 %, $[M\text{-}H]^+$)

By use of method 4 diisopropylamine was reacted with 1*H*,1*H*,2*H*,2*H*-perfluorooctyl iodide producing *diisopropylammonium iodide* (27 %) as an off white white solid which was isolated by filtration but not purified further; ^{1}H NMR (400 MHz, D_2O); 4.01 – 3.97 (1H, m, NCH), 1.69 – 1.65 (6H, m, CH_3); *m/z* 228.0 (100 %, $[M\text{-}H]^+$)

By use of method 4 triethylamine was reacted with 1*H*,1*H*,2*H*,2*H*-perfluorooctyl iodide producing *triethylammonium iodide* (24 %) as a white solid which was isolated by filtration but not purified further; ^{1}H NMR (400 MHz, D_2O); 3.43 – 3.37 (2H, m, NCH_2), 1.60 – 1.52 (3H, m, CH_3); *m/z* 228.0 (100 %, $[M\text{-}H]^+$)

1-Methyl-3-(1*H*, 1*H*, 2*H*, 2*H*-perfluorooctyl)-imidazolium iodide, 6

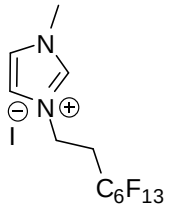

6

Method 1: *N*-Methylimidazole (0.200 g, 2.52 mmol) and 1*H*, 1*H*, 2*H*, 2*H*-perfluorooctyl iodide (1.006 g, 2.12 mmol) were dissolved in degassed toluene (5 mL) and the mixture was heated to 110 °C for 24 hours to give an oily precipitate. The solvent was evaporated and the residue recrystallised from acetonitrile:toluene to give *1-methyl-3-(1H, 1H, 2H, 2H-perfluorooctyl) imidazolium iodide* (498 mg, 42 %) as a white solid; m.p. 91.1 – 93.0 °C; Anal calc. for $C_{12}H_{10}N_2F_{13}I$: C 25.90 %, H 1.81 %, N 5.04%. Found: C 25.75 %, H 1.77 %, N 5.04 %; ^{1}H NMR (600 MHz, $(CD_3)_2CO$): δ 9.66 (1H, s, NCHN), 7.93 (1H, s, NCH), 7.71 (1H, s, NCH), 4.78 (2H, t, $^{3}J_{HH}$ 7.10, NCH_2), 3.99 (3H, s, CH_3), 3.12 - 3.03 (2H, m, CH_2CF_2); ^{13}C (151 MHz, $(CD_3)_2CO$): δ 137.90 (NCN), 135.0 – 118.0 (13C, m, CF_2, CF_3 (overlapping)), 123.91 ($N(CH_2)CH$), 122.83 ($N(CH_3)CH$), 41.88 (s, CH_3), 37.2 (NCH_2), 31.27 (t, $^{2}J_{CF}$ 20.9, CH_2CF_2); ^{19}F (564 MHz, $(CD_3)_2CO$): δ -81.67 – -81.74 (3F, m, CF_3), -114.25 (2F, s, CF_2), -122.42 (2F, s, CF_2), -123.43 (2F, s, CF_2), -123.97 (2F, s, CF_2), -126.78 (2F, s, CF_2); *m/z* (ESI^+) 429.2 (100 %, $[M-I]^+$).

Method 2: *N*-Methyl imidazole (82.8 mg, 1.01 mmol) and 1*H*,1*H*,2*H*,2*H*-perfluorooctyliodide (1.94 g, 4.08 mmol) were combined in toluene (2 mL) and heated to 100 °C for 30 minutes under microwave irradiation. Evaporation of solvent yielded a dark oil that was twice recrystallised from acetonitrile:toluene to give *1-methyl-3-(1H, 1H, 2H, 2H-perfluorooctyl)-imidazolium iodide* (173 mg, 40 %) as a white solid; physical and spectral data as above

1-(3,3,4,4,5,5,6,6,7,7,8,8,8-Tridecafluorooctyl)pyridinium iodide, 7

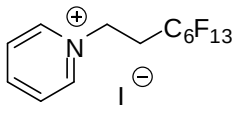

7

1*H*, 1*H*, 2*H*, 2*H*-Perfluoroctyl iodide (2.00 g, 4.19 mmol) and pyridine (380 μg, 480 μmol) were added to degassed toluene (10 mL) and the mixture refluxed for six days at which point a solid precipitate had formed. After evaporation of toluene the resulting solid was taken up in DCM (20 mL) and washed with water (2 x 10 mL). DCM was evaporated to give an impure yellow/orange solid which was washed with toluene to give *1-(3,3,4,4,5,5,6,6,7,7,8,8,8-tridecafluorooctyl)pyridinium iodide* (220 mg, 83 %) as a yellow/orange powder; m.p. 233.2 – 235.0 °C [lit 234 – 236 °C] [2]; Anal calc. for $C_{13}H_9F_{13}NI$: C 28.2 %, H 1.64 %, N 2.53%. Found: C 27.91 %, H 1.55 %, N 2.35 %; ^{1}H NMR (600 MHz, $(CD_3)_2CO$): δ 9.63 (2H, d, $^3J_{HH}$ 7.1, ArH), 8.84 (1H, t, $^3J_{HH}$ 7.7, ArH), 8.35 (2H, t, $^3J_{HH}$ 6.9, ArH), 5.43 (2H, t, $^3J_{HH}$ 7.2, NCH_2), 3.43 (2H, tt, $^3J_{HF}$ 19.1, $^3J_{HH}$ 7.4, CH_2CF_2); ^{13}C (151 MHz, $(CD_3)_2CO$): δ 146.74 (NCHCH*C*H), 145.83 (NCH), 135.0 – 118.0 (13F, m, CF_2, CF_3 (overlapping)), 128.50 (NCH*C*H), 53.67 (CH_2N), 31.74 (t, $^2J_{CF}$ 21.1, *C*H_2CF_2); ^{19}F (564 MHz, $(CD_3)_2CO$): δ -81.71 – -81.74 (3F, m, C*F*$_3$), -113.65 (2F, s, CF_2), -122.40 (2F, s, CF_2), -123.44 (2F, s, CF_2), -123.91 (2F, s, CF_2) -126.80 (2F, s, CF_2); *m/z* (ESI^+) 426.1 (100 %, $[M-I]^+$).

N-(3,3,4,4,5,5,6,6,7,7,8,8,8-Tridecafluorooctyl)aniline, 8

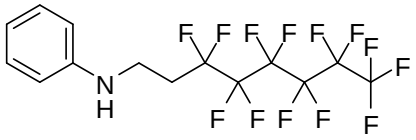

8

1*H*, 1*H*, 2*H*, 2*H*-Perfluoro-1-iodooctane (2.00 g, 4.22 mmol) was added dropwise to aniline (1.61 g, 17.2 mmol) heated to 90 °C. Subsequently, the temperature was raised to 140 °C for 20 hours. Upon cooling, aqueous sodium hydroxide (2M, 100 ml) was added and the organic components extracted into diethyl ether (3 x 40 mL). The organic layer was washed with water (3 x 15 mL) and dried over magnesium sulphate to give a liquid which was purified by distillation to give *N-(3,3,4,4,5,5,6,6,7,7,8,8,8-tridecafluorooctyl)aniline* (1.23 g, 69 %) as an oil; b.p 124 – 126 °C (9.7 mbar); HRMS (ESI) Found $[M]^+$ 439.0591, $C_{14}H_{10}F_{13}N$ requires 439.0606; ^{1}H NMR (700 MHz, $CDCl_3$): δ 7.34 – 7.30 (2H, m, NCCHC*H*), 6.89 (1H, t, $^3J_{HH}$ 7.3, NCCHCHC*H*), 6.72 (2H, dd, $^3J_{HH}$ 8.6, $^4J_{HH}$ 1.0, NCCH), 3.77 (1H, s, NH), 3.59 (2H, t, $^3J_{HH}$ 7.2, NCH_2), 2.50 – 2.39 (2H, m, CH_2CF_2); ^{13}C (176 MHz, $CDCl_3$): δ 147.1 (N*C*CH), 135.0 – 118.0 (13F, m, CF_2, CF_3 (overlapping)), 129.5 (NCCH*C*H), 118.2 (NCCHCH*C*H), 112.9 (NC*C*H), 35.8 (CH_2NH), 30.7 (t, $^2J_{CF}$ 14.1, *C*H_2CF_2); ^{19}F (658 MHz, $CDCl_3$): δ -81.4 (3F, t, $^4J_{FF}$ 9.9, CF_3), -114.2 (2F, s, CF_2), -122.1 (2F, s, CF_2), -123.2 (2F, s, CF_2), -123.8 (2F, s, CF_2), -126.5 (2F, s, CF_2); *m/z* (GC-MS) 440.3 (20 %, $[M]^+$), 106.3 (100).

(4,4,5,5,6,6,7,7,8,8,9,9,9-Tridecafluorononyloxy)benzene, 10

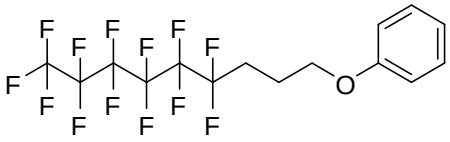

10

Anhydrous potassium carbonate (512 mg, 3.70 mmol), 4,4,5,5,6,6,7,7,8,8,9,9,9-tridecafluorononyl iodide (259 mg, 531 µmol) and phenol (62 mg, 658 µmol) were

combined in acetonitrile (16 mL) and heated to 82 °C for 21 hours after which the mixture was cooled to room temperature and washed with water (20 mL). The organic components were extracted with DCM (3 x 15 mL), dried over magnesium sulfate, and volatile components were evaporated to give *(4,4,5,5,6,6,7,7,8,8,9,9,9-tridecafluorononyloxy)benzene* (188 mg, 78 %) as a white semi-crystalline solid; m.p. 38.5 – 40.0 °C; HRMS (ASAP) Found $[M]^+$ 454.0606, $C_{15}H_{11}F_{13}O$ requires 454.0602; ^{1}H NMR (700 MHz, CD_3OD): δ 7.24 (2H, t, $^3J_{HH}$ 7.0, OCCHC*H*), 6.93 – 6.87 (3H, m, OCC*H*, OCCHCHC*H*), 4.02 (2H, t, $^3J_{HH}$ 6.0, CH_2O), 2.35 (2H, tt, $^3J_{HF}$ 19.3, $^3J_{HH}$ 8.1, CH_2CF_2), 2.04 (2H, m, C*H*$_2$CH$_2$O), ^{13}C (151 MHz, $(CD_3)_2O$): δ 158.7 (O*C*CH), 135.0 – 118.0 (13F, m, CF_2, CF_3 (overlapping)), 129.3 (OCCH*C*H), 120.6 (OCCHCH*C*H), 114.4 (OC*C*H), 65.9 (CH_2O), 27.4 (t, $^2J_{HF}$ 22.1, *C*H$_2$CF$_2$), 20.2 (*C*H$_2$CH$_2$O); ^{19}F (658 MHz, CD_3OD): δ -82.48 (3F, s, C*F*$_3$), -115.5 (2F, s, CF_2), - 123.0 (2F, s, CF_2), - 123.9 (2F, s, CF_2), - 124.5 (2F, s, CF_2), - 127.4 (2F, s, CF_2); *m/z* (ASAP) 454.1 (100 %, $[M]^+$).

N-(4,4,5,5,6,6,7,7,8,8,9,9,9-Tridecafluorononyl)aniline, 11

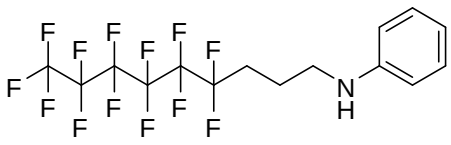

11

Anhydrous potassium carbonate (415 mg, 3.00 mmol), 4,4,5,5,6,6,7,7,8,8,9,9,9-tridecafluorononyl iodide (254 mg, 520 µmol) and aniline (510 mg, 5.48 mmol) were combined in acetonitrile (15 mL) and heated to 82 °C for 47 hours after which the mixture was cooled to room temperature and washed with water (30 mL). Organic compounds were extracted into diethyl ether (3 x 15 mL) and the organic washings were combined and dried over magnesium sulfate. Evaporation of volatile components left a yellow oil further purified by distillation under reduced pressure which left *N-(4,4,5,5,6,6,7,7,8,8,9,9,9-tridecafluorononyl)aniline* as a light yellow oil (148 mg, 63 %); b.p. >200 °C; HRMS (ASAP) Found $[M]^+$ 454.0856, $C_{15}H_{13}F_{13}N$ requires 454.0840; ^{1}H NMR (700 MHz, $CDCl_3$): δ 7.17 (2H, dt, $^3J_{HH}$ 26.4, 8.0, NCCHCH), 6.77 – 6.73 (1H, m, NCCHCHC*H*), 6.69 – 6.63 (2H, m, NCCH), 3.24 (2H, t, $^3J_{HH}$ 6.9,

CH_2N), 2.25 – 2.19 (2H, m, $CF_2CH_2CH_2$), 1.96 – 1.92 (2H, m, CF_2CH_2); ^{13}C (176 MHz, ($CDCl_3$): δ 158.7 (N*C*CH), 135.0 – 118.0 (13F, m, CF_2, CF_3 (overlapping)), 129.3 (NCCH*C*H), 120.6 (NCCHCH*C*H), 114.4 (NC*C*H), 65.9 (CH_2O), 27.4 (t, $^2J_{HF}$ 22.1, *C*H_2CF_2), 20.0 (*C*H_2CH_2N); ^{19}F (658 MHz, $CDCl_3$): δ -81.50 (3F, s, CF_3), -114.6 (2F, s, CF_2), - 122.4 (2F, s, CF_2), - 123.4 (2F, s, CF_2), - 123.9 (2F, s, CF_2), - 126.7 (2F, s, CF_2); *m/z* (ASAP) 454.1 (100 %, $[M]^+$) 453.1 (75).

4,4,5,5,6,6,7,7,8,8,9,9,9-Tridecafluoro-*N,N*-diisopropylnonan-1-amine, 12

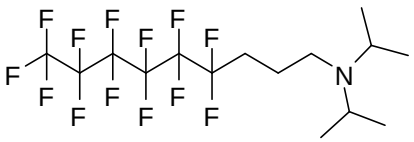

12

4,4,5,5,6,6,7,7,8,8,9,9,9-Tridecafluorononyl iodide (556 mg, 1.14 mmol), diisopropylamine (2.45 g, 24.2 mmol) and potassium carbonate (521 mg, 3.77 mmol) were combined in acetonitrile (15 mL) and heated to 82 °C for 24 hours after which the reaction mixture was cooled to room temperature. Following cooling, the mixture was washed with water (40 mL) and the organic components extracted with diethyl ether (3 x 15 mL). The organic fractions were combined and dried over magnesium sulfate before evaporation. The crude product was taken up in diethyl ether (20 mL) and washed with water (5 x 20 mL) before drying under vacuum to leave *4,4,5,5,6,6,7,7,8,8,9,9,9-tridecafluoro-N,N-diisopropylnonan-1-amine* (362 mg, 69 %) as a colourless oil; b.p. > 200 °C; HRMS (ASAP) Found $[M+H]^+$ 462.1459, $C_{15}H_{21}F_{13}N$ requires 462.1466; ^1H NMR (600 MHz, $CDCl_3$): δ 2.99 (2H, sept, $^3J_{HH}$ 6.6, C*H*$(CH_3)_2$), 2.49 (2H, t, $^3J_{HH}$ 6.9, CH_2N), 2.11 – 2.09 (2H, m, C*H*$_2CH_2N$), 1.67 (2H, quin, $^3J_{HH}$ 6.0, CH_2CF_2), 0.99 (6H, d, $^3J_{HH}$ 6.6, (C*H*$_3)_2CH$); ^{13}C (151 MHz, $CDCl_3$): δ 135.0 – 118.0 (13F, m, CF_2, CF_3 (overlapping)), 47.5 (*C*H$(CH_3)_2$), 43.5 (CH_2N), 28.4 (t, $^2J_{CF}$ 22.7, *C*H_2CF_2), 20.7 (*C*H_2CH_2N), 20.6 (CH_3); ^{19}F (564 MHz, $CDCl_3$): δ -81.4 (3F, t, $^4J_{FF}$

10.0, C*F*$_3$), -114.3 (2F, s, CF_2), - 122.5 (2F, s, CF_2), - 123.4 (2F, s, CF_2), - 124.1 (2F, s, CF_2), - 126.7 (2F, s, CF_2); *m/z* (ASAP) 462.1 (80 %, $[M+H]^+$), 446.1 (100), 391.3 (76).

7.3 Experimental to Chapter 3

3,3,4,4,5,5,6,6,7,7,8,8,8-Tridecafluorooctyl-1,3-dioxo-1,3-dihydroisobenzofuran-5-carboxylate, 16

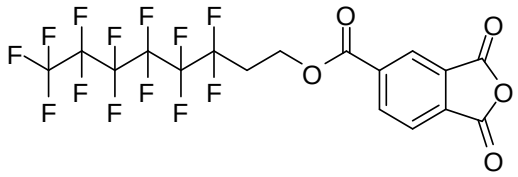

16

Trimellitic anhydride chloride (14.98 g, 75.4 mmol), dry THF (150 mL) and 1*H*, 1*H*, 2*H*, 2*H*-perfluorooctan-1-ol (23.49 g, 64.5 mmol) were combined under an atmosphere of argon. The resulting mixture was heated to 65 °C for 48 hours and then cooled to room temperature and stirred for a further 48 hours. THF was evaporated to leave a white residue which was washed with methanol (450 mL) to leave a white powder that was further dried *in vacuo* to give *3,3,4,4,5,5,6,6,7,7,8,8,8-tridecafluorooctyl 1,3-dioxo-1,3-dihydroisobenzofuran-5-carboxylate* (18.11 g, 47 %) as a white powder; m.p. 98.3 – 99.9 °C; Anal calc. for $C_{17}H_7F_{13}O_5$: C 37.94 %, H 1.31 %. Found: C 38.19 %, H 1.35 %,; HRMS (ASAP) Found $[M+H]^+$ 539.0153, $C_{17}H_8F_{13}O_5$ requires 539.0164; ^{1}H NMR (700 MHz, $(CD_3)_2CO$): δ 8.62 (1H, dd, $^3J_{HH}$ 7.9, $^4J_{HH}$ 1.4, ArH), 8.55 (1H, dd, $^4J_{HH}$ 1.3, $^5J_{HH}$ 0.8, ArH), 8.25 (1H, dd, $^3J_{HH}$ 7.9, $^5J_{HH}$ 0.7, ArH), 4.80 (2H, t, $^3J_{HH}$ 6.1, CH_2OCO), 2.94 (2H, tt, $^3J_{HF}$ 19.2, $^3J_{HH}$ 6.1, CF_2CH_2); ^{13}C (176 MHz, $(CD_3)_2CO$): δ 166.6 (C=O), 162.2 (C=O), 162.1 (C=O), 136.8 (Ar), 136.7 (Ar), 135.0 – 118.0 (13F, m, CF_2, CF_3 (overlapping)), 135.1 (Ar), 132.2 (Ar), 125.8 (Ar), 125.7 (Ar) 57.9 (*C*H_2-O-C=O), 29.9 (t, $^2J_{CF}$ 21.2, *C*H_2CF_2); ^{19}F (564 MHz, $(CD_3)_2CO$): δ -81.72 (3F, t, $^4J_{FF}$ = 10.1, CF_3), -113.93 (2F, s, CF_2), -122.41 (2F, s, CF_2), -123.43 (2F, s, CF_2), -124.10 (2F, s, CF_2), -126.79 (2F, s, CF_2); *m/z* (ASAP) 539.0 (100 %, $[M+H]^+$).

3,3,4,4,5,5,6,6,7,7,8,8,9,9,10,10,10-Heptadecafluorodecyl-1,3-dioxo-1,3-dihydroisobenzofuran-5-carboxylate, 18

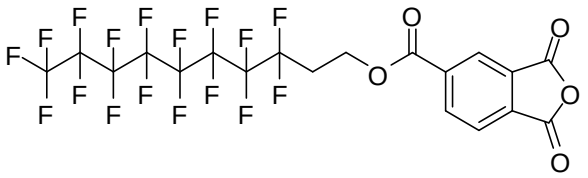

18

Trimellitic anhydride chloride (15.114g, 72.0 mmol) and 1*H*,1*H*,2*H*,2*H*-perfluoro-1-decanol (32.00 g, 69.0 mmol) were combined in THF (150 mL) and heated to 65 °C for 137 hours. Following evaporation of THF, the mixture was washed with methanol (400 mL) which afforded *3,3,4,4,5,5,6,6,7,7,8,8,9,9,10,10,10-heptadecafluorodecyl 1,3-dioxo-1,3-dihydroisobenzofuran-5-carboxylate* (20.7 g, 47 %) as a white solid; m.p. 117.9 – 119.3 °C; Anal calc. for $C_{19}H_7F_{17}O_5$: C 35.76 %, H 1.11 %, N 0.00 %. Found: C 35.65 %, H 1.09 %, N 0.00 %; HRMS (ASAP) Found $[M+H]^+$ 639.0104, $C_{19}H_8F_{17}O_5$ requires 639.0100; ^{1}H NMR (600 MHz, $(CD_3)_2CO$): δ 8.61 (1H, dd, $^3J_{HH}$ 7.9, $^4J_{HH}$ 1.4, ArH), 8.55 (1H, m, ArH), 8.25 (1H, dd, $^3J_{HH}$ 7.9, $^5J_{HH}$ 0.7, ArH), 4.80 (2H, t, $^3J_{HH}$ 6.1, CH_2OCO), 2.95 (2H, tt, $^3J_{HF}$ 19.2, $^3J_{HH}$ 6.1, CF_2CH_2); ^{13}C (151 MHz, $(CD_3)_2CO$): δ 163.6 (C=O), 162.3 (C=O), 162.2 (C=O), 136.8 (Ar), 136.7 (Ar), 135.1 (Ar), 135.0 – 118.0 (18F, m, CF_2, CF_3 (overlapping)), 132.2 (Ar), 125.8 (Ar), 125.7 (Ar) 57.9 (*C*-O-C=O), 29.9 (t, $^2J_{CF}$ 21.4, *C*H_2CF_2); ^{19}F (564 MHz, $(CD_3)_2CO$): δ -81.73 (3F, m, $^4J_{FF}$ 10.1), -113.95 (2F, pm, $^4J_{FF}$ 15.7, CF_2), -122.19 (2F, s, CF_2), -122.46 (4F, s, CF_2, CF_2), -123.29 (2F, s, CF_2), -124.07 (2F, s, CF_2), -126.77 (2F, s, CF_2); *m/z* (ASAP) 639.0 (100 %, $[M+H]^+$). The process was repeated a further three times and the products combined to give (87.31 g, 48 % (average)).

Octyl 1,3-dioxo-1,3-dihydroisobenzofuran-5-carboxylate, 19

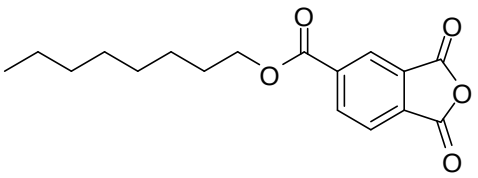

19

1-Octanol (12.36 g, 94.9 mmol) was added to a solution of trimellitic anhydride chloride (20.033 g, 94.7 mmol) in THF (125 mL). The resulting solution was heated to 55 °C for 48 hours before the evaporation of volatile components which gave a green oil. Evaporation gave *octyl 1,3-dioxo-1,3-dihydroisobenzofuran-5-carboxylate* (25.2 g, 87 %) as a low melting light green solid; m.p. 26.7 – 28.8 °C; HRMS (ASAP) Found $[M+H]^+$ 305.1390, $C_{17}H_{21}O_5$ requires 305.1389; ^{1}H NMR (700 MHz, ($CDCl_3$): δ 8.63 (1H, s, CC*H*C), 8.56 (1H, d, $^3J_{HH}$ 7.9, ArH), 8.10 (1H, d, $^3J_{HH}$ 7.8, ArH), 4.40 (2H, t, $^3J_{HH}$ 6.7, CH_2OCO), 1.83 – 1.78 (2H, m, CH_2CH_2O), 1.48 – 1.23 (10H, m, CH_2CH_2); ^{13}C (176 MHz, $(CD_3)_2CO$): δ 164.1 (C=O), 162.0 (C=O), 161.9 (C=O), 138.1 (Ar), 137.2 (Ar), 134.4 (Ar), 131.7 (Ar), 126.9 (Ar), 126.0 (Ar) 66.8 (C-O-C=O), 31.9 (*C*H_2CH_2), 29.3 (*C*H_2CH_2), 29.3 (*C*H_2CH_2), 28.7 (*C*H_2CH_2), 22.8 (*C*H_2CH_2), 14.2 (*C*H_3CH_2); *m/z* (ASAP) 305.1 (100 %, $[M+H]^+$), 193.0 (30).

H-TMA, 27

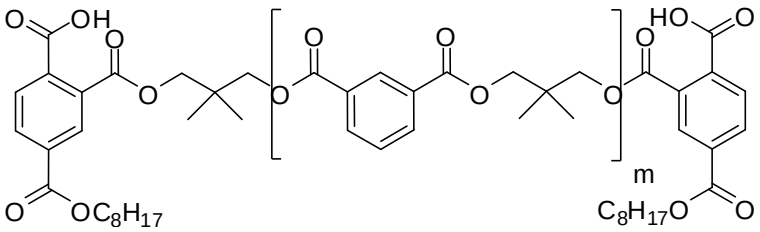

27

Neopentyl glycol (245.0 g, 2.35 mol), trimethylolpropane (5.0 g, 37.3 mmol), isophthalic acid (359.8 g, 2.17 mol), water (40.0 g, 2.22 mol) and a tin catalyst, BNT-cat 210 (103 mg) were combined at a temperature of 150 °C. After addition of all

components, the temperature was raised to 230 °C over six hours. After the mixture became visibly clear the temperature was held at 230 °C for a further 90 minutes before being lowered to 120 °C for 15 hours. The temperature was then elevated to 150 °C, and after two hours isophthalic acid (9.9 g, 59.6 mmol), adipic acid (7.5 g, 51.3 mmol) and neopentyl glycol (5.9 g, 56.7 mmol) were added and the temperature raised to 230 °C over a four hour period. After three hours temperature was again lowered to 120 °C, for 17 hours, before neopentyl glycol (1.1 g, 10.6 mmol) was added and the temperature raised to 190 °C. After a further two hours, octyl 1,3-dioxo-1,3-dihydroisobenzofuran-5-carboxylate (67.2 g, 221.1 mmol) was added. After 24 hours the mixture was allowed to cool to room temperature to give *H-TMA* (468.2 g) as a glassy solid which was analysed without any further purification.

F-TMA, 28

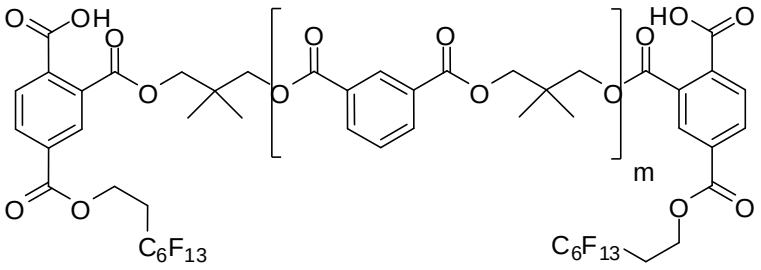

28

Neopentyl glycol (175.0 g, 1.68 mol), trimethylolpropane (3.6 g, 26.8 mmol), isophthalic acid (257.0 g, 1.55 mol), water (40.0 g, 2.22 mol) and a tin catalyst, BNT cat-210 (100 mg) were combined at 150 °C after which the temperature was raised to 230 °C over six hours. The mixture was left at 230 °C for 90 minutes after clarity was observed and then cooled to 120 °C for 14 hours before the temperature was elevated to 150 °C for two hours. Isophthalic acid (7.9 g, 47.5 mmol), adipic acid (5.6 g, 38.3 mmol) and neopentyl glycol (3.5 g, 33.6 mmol) were added and the temperature set to 230 °C for five hours, and then 120 °C for 17 hours. Subsequently, isophthalic acid (3.0 g, 18.1 mmol) and adipic acid (1.9 g, 13.0 mmol) were added and the temperature raised to 210 °C for 26 hours before addition of 3,3,4,4,5,5,6,6,7,7,8,8,8-tridecafluorooctyl-1,3-dioxo-1,3-dihydroisobenzofuran-5-carboxylate (92.1 g, 171.2 mmol). After two

hours, neopentyl glycol (0.9 g, 8.6 mmol) was added, with a further quantity of neopentyl glycol (1.3 g, 12.5 mmol) added one hour later. One hour after the final addition of neopentyl glycol the mixture was cooled to room temperature to give *F-TMA* (208 g) as a brown glassy solid which was analysed without any further purification.

Preparation of H-TMA powder coating from polyester resin 27

Polyester resin **27** (655.7 g), primid XL552 (26.2 g, 819 mmol), benzoin (3.0 g, 14.1 mmol), lanco wax 1525MF (4.0 g), Byk LPG21191 (10.0 g) and titanium dioxide (300 g, 3.76 mol) were combined and ground manually. The mixture was then twice passed through a twin screw extruder to form a homogeneous paste. The white paste was ground, using a commercial coffee grinder, and passed through a 106 μm mesh sieve. The resulting powder was electrostatically spray coated onto QUV-A aluminium panels to a depth of 60 – 80 Å and the coated aluminium panels baked for 15 minutes at 200 °C to give QUV-A panels coated with H-TMA for sample testing.

Preparation of F-TMA powder coating from polyester resin 28

Polyester resin **28** (655.7 g), primid XL552 (26.2 g, 819 mmol), benzoin (3.0 g, 14.1 mmol), lanco wax 1525MF (4.0 g), Byk LPG21191 (10.0 g) and titanium dioxide (300 g, 3.76 mol) were combined and ground manually. The mixture was then twice passed through a twin screw extruder to form a homogeneous paste. The white paste was ground, through use of a commercial coffee grinder, and passed through a 106 μm sieve. The resulting powder was electrostatically spray coated onto QUV-A aluminium panels to a depth of 60 – 80 Å and the coated aluminium panels baked for 15 minutes at 200 °C to give QUV-A panels coated with F-TMA for sample testing.

7.4 Experimental to Chapter 4

2,2,3,3,4,4,5,5-Octafluorohexane-1,6-ditosyl, 33

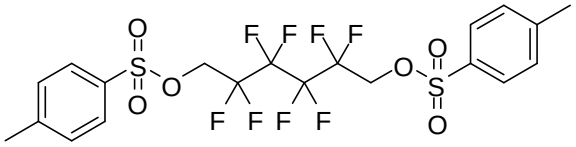

33

A solution of 2,2,3,3,4,4,5,5-octafluoro-1,6-hexanediol (2.5 g, 9.54 mmol) and *p*-toluenesulfonyl chloride (4.30 g, 22.5 mmol) in pyridine (15 mL) was heated to 50 °C for 16 hours. Cold water (10 mL) was added and the precipitate filtered and recrystallised from methanol to yield *2,2,3,3,4,4,5,5-octafluorohexane-1,6-ditosyl* (2.917 g, 58 %) as a white solid; m.p. 136.3 – 137.4 °C; HRMS (ESI) Found $[M+Na]^+$ 593.0333, $C_{20}H_{18}O_6F_8S_2Na$ requires 593.0315. ^{1}H NMR (700 MHz, $(CD_3)_2CO$): δ 7.87 (4H, d, $^3J_{HH}$ 8.3, $CHCSO_3$), 7.52 (4H, d, $^3J_{HH}$ 8.1, C*H*CCH_3), 4.74 (4H, t, $^3J_{HH}$ 13.3, CH_2CF_2), 2.47 (6H, s, CH_3); ^{13}C (176 MHz, $(CD_3)_2CO$): δ 147.61 (CSO_3), 133.59 (*C*CH_3), 131.74 (*C*$HCCH_3$), 129.53 (C*H*CSO_3), 65.83 (t, $^2J_{CF}$ 27.2, *C*H_2CF_2), 22.17 (CH_3); ^{19}F (658 MHz, $(CD_3)_2CO$): δ -120.16 (2F, s, CF_2CH_2), -123.81 (2F, t, $^3J_{HF}$ 14.9, CF_2CF_2); *m/z* (GC-MS) 571.0 (48 %, $[M]^+$), 415.1 (100).

2,2,3,3,4,4,5,5-Octafluorohexane-1,6-diyl dimethanesulfonate, 35

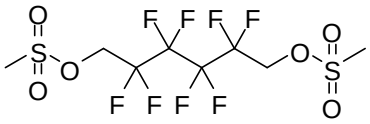

35

Mesyl chloride (1.92 g, 16.8 mmol) and triethyl amine (1.70 g, 16.8 mmol) in dry DCM (50 mL) were cooled to 0 °C, with stirring, and 2,2,3,3,4,4,5,5-octafluorohexane-1,6-diol (2.04 g, 7.78 mmol) was added. After five hours at 0 °C, and after further cooling to -5 °C for several hours a white solid precipitated and was collected by filtration

(2.281 g). The solid was dissolved in DCM (20 mL) and washed with water (2 x 10 mL). Evaporation of the organic layer gave *2,2,3,3,4,4,5,5-octafluorohexane-1,6-diyl dimethanesulfonate* (2.067 g, 64 %) as a white solid; m.p. 69.7 – 70.7 °C; Anal calc. for $C_8H_{10}F_8S_2O_6$: C 23.00 %, H 2.41 %, N 0.00 %, Found: C 22.91 %, H 2.37 %, N 0.00 %; HRMS (ESI) Found $[M+H]^+$ 418.9861, $C_8H_{11}O_6F_8S_2$ requires 418.9869; ^{1}H NMR (500 MHz, $(CD_3)_2CO$): δ 4.93 (2H, t, $^3J_{HF}$ 13.6, CH_2CF_2), 3.33 (3H, s, CH_3); ^{13}C (127 MHz, $(CD_3)_2CO$): δ 64.45 (t, $^2J_{CF}$ 26.2, CH_2CF_2), 37.27 (CH_3); ^{19}F (188 MHz, $CDCl_3$): δ -124.52 (2F, s, CF_2CF_2), - 128.00 (2F, t, $^4J_{FF}$ 14.8, CH_2CF_2); *m/z* (GC-MS) 387.9 (100 %, $[M - 2CH_3]^+$).

2,2,3,3,4,4,5,5-Octafluorohexane-1,6-diyl bis(trifluoromethanesulfonate), 37

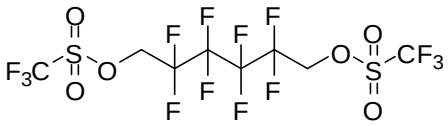

37

2,2,3,3,4,4,5,5-Octafluorohexane-1,6-diol (2.869 g, 10.9 mmol) and pyridine (1.96 g, 24.8 mmol) were stirred, at room temperature, in DCM (200 mL) under an atmosphere of argon for 40 minutes after which triflic anhydride (5.70 g, 20.2 mmol), dissolved in DCM (100 mL), was added dropwise over 75 minutes. Following the addition of triflic anhydride, the reaction was stirred for 67 hours after which the reaction was washed with water (3 x 100 mL) and saturated sodium bicarbonate solution (2 x 100 mL). Subsequently, the organic layer was dried over magnesium sulfate and DCM evaporated to give *2,2,3,3,4,4,5,5-octafluorohexane-1,6-diyl bis(trifluoromethanesulfonate)* (5.40 g, 94.0 %) as white crystals which were further dried under vacuum; m.p. 52.1 – 53.9 °C; Anal calc. for $C_8H_4F_{14}S_2O_6$: C 18.27 %, H 0.77 %, N 0.00 %. Found: C 18.32 %, H 0.81 %, N 0.00 %; ^{1}H NMR (500 MHz, $(CD_3)_2CO$): δ 5.48 (4H, t, $^3J_{HF}$ 12.9, CH_2O); ^{13}C (151 MHz, $(CD_3)_2CO$): δ 118.4 (q, , $^1J_{CF}$ 318.2, CF_3), 110.9 (m, CF_2), 109.1 (m, CF_2), 69.2 (t, $^2J_{CF}$ 27.7, CH_2); ^{19}F (564 MHz, $(CD_3)_2CO$): -74.6 (3F, s, CF_3), -120.4 (2F, s, CF_2), -123.6 (2F, s, CF_2); *m/z* (ASAP) 526.9 (42 %, $[M+H]^+$), 225.0 (100).

2,2'-(2,2,3,3,4,4,5,5-Octafluorohexane-1,6-diyl)diisoindoline-1,3-dione, 39

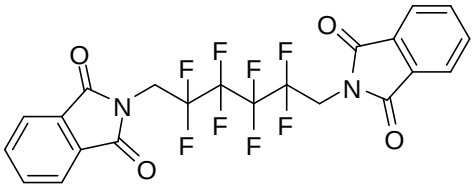

39

2,2,3,3,4,4,5,5-Octafluorohexane-1,6-diyl bis(trifluoromethanesulfonate) (1.000 g, 1.90 mmol) was dissolved in DMF (75 mL) in an atmosphere of argon. To this solution was added potassium phthalimide (875 mg, 4.72 mmol) and the resulting mixture heated to 100 °C for 20 hours. Subsequently, the mixture was cooled to room temperature and saturated brine solution (80 mL) was added leading to formation of a white precipitate which was collected by filtration. The filtrand was stirred in chloroform (400 mL) and refiltered to isolate *2,2'-(2,2,3,3,4,4,5,5-octafluorohexane-1,6-diyl)diisoindoline-1,3-dione* (915 mg, 91 %) as a white solid; m.p. 260.2 – 261.2 °C; Anal calc. for $C_{22}H_{12}F_8N_2O_4$: C 50.78 %, H 2.32 %, N 5.38 %. Found: C 50.78 %, H 2.26 %, N 5.38 %; HRMS (ASAP) Found $[M+H]^+$ 521.0754, $C_{22}H_{13}F_8N_2O_4$ requires 521.0748; ^{1}H NMR (600 MHz, $(CD_3)_2CO$): δ 7.96 (4H, q, $^3J_{HH}$ 3.0, C*H*CHC), 7.93 (4H, q, $^3J_{HH}$ 3.0, CHCC(O)), 4.48 (4H, t, $^3J_{HF}$ 16.1, NCH_2), ^{13}C (151 MHz, $(CD_3)_2CO$): δ 166.7 (C=O), 134.8 (*C*HCHC), 131.8 (*C*CO), 123.5 (*C*HCC(O)), 37.4 (NCH_2); ^{19}F (564 MHz, $(CD_3)_2CO$): δ -116.6 – -115.4 (4F, m, CF_2CH_2), -123.9 – -122.7 (4F, m, CF_2CF_2); *m/z* (ASAP) 521.0 (100 %, $[M+H]^+$).

2,2,3,3,4,4,5,5-Octafluorohexane-1,6-diamine, 40

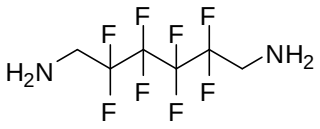

40

Hydrazine monohydrate (1.03 g, 20.6 mmol) was added, by syringe, to a flask containing 2,2'-(2,2,3,3,4,4,5,5-octafluorohexane-1,6-diyl)diisoindoline-1,3-dione (444 mg, 852 µmol) and ethanol (100 mL). The resulting mixture was refluxed for 20 hours and the flask cooled to 5 °C to promote formation of an off white precipitate which was separated by filtration. The ethanol filtrate was reduced *in vacuo* to yield a white solid (355 mg) which was further purified by stirring in chloroform (50 mL) for 90 minutes after which a white precipitate was removed by filtration. The chloroform solution was evaporated to give *2,2,3,3,4,4,5,5-octafluorohexane-1,6-diamine* (46 mg, 21 %) as a yellow solid; m.p. 44.7 – 46.4 °C; ^{1}H NMR (700 MHz, CD_3Cl): δ 3.25 (4H, t, $^{3}J_{HH}$ 15.7, CH_2); ^{13}C NMR (176 MHz, CD_3Cl): δ 43.05 (t, $^{2}J_{CF}$ 24.0, CH_2NH_2); ^{19}F (658 MHz, CD_3Cl): δ -122.3 – -120.8 (4F, m, CF_2CH$_2$), -124.4 – -123.5 (4F, m, CF_2CF$_2$); *m/z* (GC-MS) 261.1 (100 %, $[M+H]^+$).

((3,3,4,4,5,5,6,6,7,7,8,8,8-Tridecafluorooctyloxy)methyl)benzene, 43

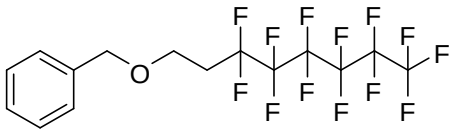

43

Sodium hydride (101 mg, 4.23 mmol) was placed under an inert atmosphere, washed with hexanes (2 x 10 mL) and taken up in dry THF (30 mL). After 15 minutes of stirring 1*H*, 1*H*, 2*H*, 2*H*-perfluorooctan-1-ol (1.01 g, 2.78 mmol) was added prior to an additional 15 minutes of stirring. Subsequently, benzyl bromide (518 mg, 3.03 mmol)

was added and the mixture refluxed for 19 hours over which time a precipitate formed which was removed by filtration. The filtrate was condensed to give a liquid that was purified by silica chromatography (DCM) to give *((3,3,4,4,5,5,6,6,7,7,8,8,8-tridecafluorooctyloxy)methyl)benzene* (1.05 g, 83 %) as a colourless liquid; HRMS (ESI) Found $[M]^+$ 453.0511, $C_{15}H_{11}F_{13}O$ requires 453.0524; ^{1}H NMR (600 MHz, $CDCl_3$): δ 7.29 – 7.17 (5H, m, ArH), 4.44 (2H, s, CCH_2O), 3.66 (2H, t, $^3J_{HH}$ 6.8, OCH_2CH_2), 2.40 – 2.28 (2H, m, CH_2CF_2); ^{13}C (151 MHz, $CDCl_3$): δ 136.6 (OCH_2C), 127.8 (CH_2CCHCH), 127.5 ($CH_2CCHCHCH$), 126.7 (CH_2CCH), 61.1 (CH_2CH_2O), 32.4 ($ArCH_2O$), 30.6 (t, $^2J_{CF}$ 21.6, CH_2CF2); ^{19}F (564 MHz, $CDCl_3$): δ -81.39 (3F, t, $^4J_{FF}$ 9.9, CF_3), -113.8 (2F, s, CF_2), -122.4 (2F, s, CF_2), -123.3 (2F, s, CF_2), -124.2 (2F, s, CF_2), -126.7 (2F, s, CF_2); *m/z* (GC-MS) 453.1 (100 %, $[M-H]^+$).

3,3,4,4,5,5,6,6,7,7,8,8,8-Tridecafluorooctyl benzoate, 45

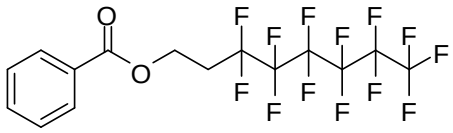

45

1*H*, 1*H*, 2*H*, 2*H*-Perfluorooctan-1-ol (2.02 g, 5.54 mmol) was added to sodium hydride (187 mg, 7.79 mmol) in an inert atmosphere and the mixture stirred for ten minutes before addition of dry THF (40 mL). After a further 30 minutes of stirring benzoyl bromide (958 mg, 5.6 mmol) was added and the mixture refluxed for 70 hours. The solvent was evaporated and the mixture purified by silica chromatography (DCM) to give *3,3,4,4,5,5,6,6,7,7,8,8,8-tridecafluorooctyl benzoate* (2.23 g, 86 %) as a pink liquid; b.p > 250 °C; IR (cm^{-1}): 1726 (C=O), 1190 (C-O); Anal calc. for $C_{15}H_9F_{13}O_2$: C 38.48 %, H 1.94 %, N 0.00 %. Found: C 38.31 %, H 1.92 %, N 0.00 %; HRMS (ESI) Found [M+H] 469.0482, $C_{15}H_{10}F_{13}O_2$ requires 469.0473; ^{1}H NMR (700 MHz, $CDCl_3$): δ 8.05 (2H, d, $^3J_{HH}$ 8.2, C(O)CC*H*), 7.58 (1H, t, $^3J_{HH}$ 7.4, C*H*CHCHC), 7.45 (2H, t, $^3J_{HH}$ 7.7, C(O)CCHC*H*), 4.63 (2H, t, $^3J_{HH}$ 6.4, OCH_2), 2.65 – 2.56 (2H, m, CH_2CF_2); ^{13}C (176 MHz, $CDCl_3$): δ 166.1 (C=O), 135.0 – 118.0 (13F, m, CF_2, CF_3 (overlapping)),133.2 (*C*HCHCHC), 129.6 (*C*C(O)), 129.5 (*C*HCC(O)), 128.4

(*C*HCHCC(O)), 56.7 (*C*-O-C=O), 30.6 (t, $^{2}J_{CF}$ 21.8, *C*H_2CF2); ^{19}F (658 MHz, $CDCl_3$): δ -81.36 (3F, t, $^{4}J_{FF}$ 10.1, CF_3), -113.96 (2F, s, CF_2), -122.29 (2F, s, CF_2), -123.31 (2F, s, CF_2), -124.00 (2F, s, CF_2), -126.60 (2F, s, CF_2); *m/z* (GC-MS) 467.9 (22 %, $[M]^+$), 105.3 (100).

6-(Allyloxy)-1,1,1,2,2,3,3,4,4-nonafluorohexane, 48

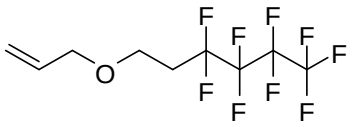

48

A 60 % Sodium hydride dispersion in mineral oil (722 mg, 30.1 mmol) was added to a two necked flask which was subjected to a vacuum and purged with argon. The sodium hydride was washed with hexane (2 x 12 mL), following which dry THF (20 mL) and 1*H*, 1*H*, 2*H*, 2*H*-perfluorohexan-1-ol (1.43 g, 5.42 mmol) were added. After fifteen minutes allyl bromide (715 mg, 5.91 mmol) was added and the solution stirred at room temperature for a further 69 hours to give a yellow solution. The yellow solution was washed with water (40 mL) and extracted with diethyl ether (3 x 10 mL). Solvent was evaporated to give *6-(allyloxy)-1,1,1,2,2,3,3,4,4-nonafluorohexane* (960 mg, 59 %) as a colourless liquid; b.p. 67 – 71 °C; HRMS (ASAP) Found $[M-H]^+$ 303.0426, $C_{11}H_8F_{13}O$ requires 303.0431; ^{1}H NMR (600 MHz, $CDCl_3$): δ 5.86 (1H, ddt, $^{3}J_{HH}$ 16.2, 10.4, 5.6, C*H*CH_2), 5.26 (1H, d, $^{3}J_{HH}$ 16.2, C*H*$_2$CH), 5.17 (1H, d, $^{3}J_{HH}$ 10.5, C*H*$_2$CH), 4.00 (2H, d, $^{3}J_{HH}$ 5.4, CHC*H*$_2$O), 3.72 – 3.64 (2H, m, OC*H*$_2$CH$_2$), 2.45 – 2.33 (2H, m, CH_2CF_2); ^{13}C (151 MHz, $CDCl_3$): δ 134.0 (*C*H), 117.2 (*C*H_2CH), 72.0 (*C*H_2CF_2), 61.8 (O*C*H_2CH$_2$), 31.5 (O*C*H_2CH); ^{19}F (564 MHz, $CDCl_3$): δ -81.53 – -81.45 (3F, m, CF_3), -113.9 (2F, s, CF_2), -124.9 (2F, s, CF_2), -126.4 (2F, s, CF_2); *m/z* (GC-MS) 304.2 (100 %, $[M]^+$).

8-(Allyloxy)-1,1,1,2,2,3,3,4,4,5,5,6,6-tridecafluorooctane, 49

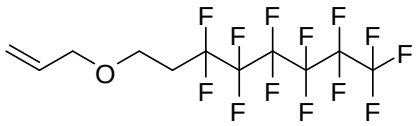

49

A 60 % Sodium hydride dispersion in mineral oil (420 mg, 4.1 mmol) was washed with hexane (2 x 15 mL) under an atmosphere of argon. The sodium hydride was then taken up in dry THF (25 mL) and 1*H*, 1*H*, 2*H*, 2*H*-perfluorooctan-1-ol (1.98 g, 5.44 mmol) added to the solution. After fifteen minutes, allyl bromide (1.20 g, 9.94 mmol) was added and the solution stirred at room temperature for a further 69 hours to give a yellow solution. The yellow solution was washed with water (40 mL) and organic components were extracted into DCM (3 x 30 mL). DCM and volatiles were evaporated to give *8-(allyloxy)-1,1,1,2,2,3,3,4,4,5,5,6,6-tridecafluorooctane* (1.612 g, 73 %) as a brown liquid; b.p. 62 – 63 °C (9.6 mbar); Anal calc. for $C_{11}H_9F_{13}O$: C 32.69 %, H 2.24 %, N 0.00 %. Found: C 32.91 %, H 2.19 %, N 0.00 %; HRMS (ESI) Found $[M-H]^+$ 403.0371, $C_{11}H_8F_{13}O$ requires 403.0368; ^{1}H NMR (600 MHz, $CDCl_3$): δ 5.89 (1H, ddt, $^3J_{HH}$ 16.1, 10.6, 5.6, C*H*CH_2), 5.32 – 5.18 (2H, m, C*H*$_2$CH), 4.00 (2H, d, $^3J_{HH}$ 5.6, CHC*H*$_2$O), 3.72 (2H, t, $^3J_{HH}$ 6.9, OC*H*$_2$$CH_2$), 2.46 – 2.36 (2H, m, CH_2CF_2); ^{13}C (151 MHz, $CDCl_3$): δ 135.0 – 118.0 (13F, m, CF_2, CF_3 (overlapping)), 134.0 (CH), 117.2 (*C*H_2CH), 72.0 (*C*H_2CF_2), 61.8 (O*C*$H_2$$CH_2$), 31.5 (O*C*$H_2$CH); ^{19}F (564 MHz, $CDCl_3$): δ -81.43 – -81.47 (3F, m, CF_3), -113.9 (2F, s, CF_2), -122.4 (2F, s, CF_2), -123.4 (2F, s, CF_2), -124.2 (2F, s, CF_2), -126.7 (2F, s, CF_2); *m/z* (GC-MS) 404.2 (82 %, $[M]^+$).

10-(Allyloxy)-1,1,1,2,2,3,3,4,4,5,5,6,6,7,7,8,8-heptadecafluorodecane, 50

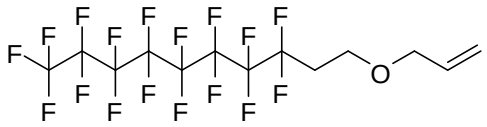

50

A 60 % dispersion of sodium hydride in mineral oil (990 mg, 24.8 mmol) was washed with hexane (3 x 15 mL) before addition of THF (75 mL) and 1*H*,1*H*,2*H*,2*H*-perfluoro-1-decanol (4.789g, 10.3 mmol). After fifteen minutes of stirring at room temperature allyl bromide (4.9 g, 40.5 mmol) was added and the mixture stirred for a further 41 hours. Subsequently, the mixture was washed with water (150 mL) and the organic components extracted into DCM (3 x 15 mL). The combined DCM extractions were condensed under vacuum to give an orange liquid that was distilled to give *10-(allyloxy)-1,1,1,2,2,3,3,4,4,5,5,6,6,7,7,8,8-heptadecafluorodecane* (3.59 g, 69 %) as a clear liquid; b.p. 75 – 77 °C (7.9 mbar); HRMS (ESI) Found $[M-H]^+$ 503.0319, $C_{13}H_8F_{17}O$ requires 503.0304; ^{1}H NMR (700 MHz, $CDCl_3$): δ 5.95 – 5.82 (1H, m, C*H*CH_2), 5.33 – 5.15 (2H, m, C*H*$_2$CH), 4.01 (2H, dt, $^3J_{HH}$ 5.6, 1.4, CHC*H*$_2$O), 3.72 (2H, t, $^3J_{HH}$ 6.9, OC*H*$_2$CH$_2$), 2.48 – 2.35 (2H, m, CH_2CF_2); ^{13}C (151 MHz, $CDCl_3$): δ 134.0 (CH), 117.3 (*C*H_2CH), 72.1 (*C*H_2CF_2), 61.8 (OCH_2CH$_2$), 31.4 (OC*H*$_2$CH); ^{19}F (658 MHz, $CDCl_3$): δ -81.4 (3F, t, $^4J_{FF}$ 13.2, CF_3), -113.9 (2F, s, CF_2), -122.4 (2F, s, CF_2), -123.4 (2F, s, CF_2), -124.2 (2F, s, CF_2), -126.7 (2F, s, CF_2); *m/z* (ASAP) 504.0 (23 %, $[M]^+$), 503.0 (100).

5-(Allyloxy)-1,1,2,2,3,3,4,4-octafluoropentane, 51

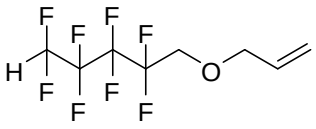

51

A 60 % dispersion of sodium hydride in mineral oil (904 mg, 22.6 mmol) was washed with hexane (3 x 10 mL) under an atmosphere of argon and taken up in dry THF (40 mL). 2,2,3,3,4,4,5,5-Octafluoro-1-pentanol (4.00 g, 16.39 mmol) was added and the resulting solution stirred for 15 minutes after which allyl bromide (2.80 g, 23.1 mmol) was added. The mixture was stirred at room temperature for 24 hours after which a further portion of sodium hydride dispersion in mineral oil (118 mg, 2.95 mmol) and additional allyl bromide (1.40 g, 11.6 mmol) were added. The mixture was stirred for another 22 hours after which water (40 mL) was added and the organic compounds extracted into diethyl ether (3 x 20 mL). The organic washings were dried over anhydrous magnesium sulfate. After separating the solid magnesium sulfate by filtration the remaining THF solution was distilled to obtain *5-(allyloxy)-1,1,2,2,3,3,4,4-octafluoropentane* (2.748 g, 62 %) as a colourless liquid; b.p. 147.1 – 149.7 °C; HRMS (ASAP) Found $[M\text{-}H]^+$ 271.0356, $C_8H_7F_8O$ requires 271.0369; ^{1}H NMR (700 MHz, $CDCl_3$): δ 6.03 (1H, tt, $^2J_{HF}$ 52.0, $^3J_{HF}$ 5.5, HCF_2CF_2), 5.90 – 5.81 (1H, m, CH_2CHCH_2), 5.34 – 5.19 (2H, m, $CHCH_2$), 4.10 (2H, d, $^3J_{HH}$ 5.7, OCH_2CH), 3.89 (2H, t, $^3J_{CF}$ 13.9, CH_2CF_2); ^{13}C (176 MHz, $CDCl_3$): δ 132.9 (CH), 118.5 (CH_2CH), 66.3 (t, $^2J_{CF}$ 25.5, OCH_2CF_2), 25.4 (OCH_2CH); ^{19}F (658 MHz, $CDCl_3$): δ -120.3 (2F, s, CF_2), -126.3 (2F, s, CF_2), -131.0 (2F, s, CF_2), -138.0 (2F, s, CF_2); *m/z* (ASAP) 271.0 (100 %, $[M\text{-}H]^+$).

7-(Allyloxy)-1,1,2,2,3,3,4,4,5,5,6,6-dodecafluoroheptane, 52

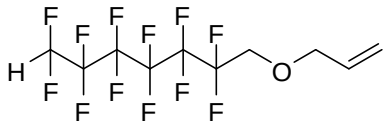

52

A 60 % dispersion of sodium hydride in mineral oil (8.14 g, 203.5 mmol) was washed with hexane (3 x 15 mL) under an atmosphere of argon before addition of THF (150 mL). To this solution was added 2,2,3,3,4,4,5,5,6,6,7,7-dodecafluoroheptan-1-ol (40.48 g, 121.9 mmol). Subsequently, the mixture was stirred for 15 minutes before addition of allyl bromide (23.8 g, 196.7 mmol) and further stirring at room temperature for 68 hours. Water (400 mL) was added and the organic components extracted into diethyl ether (3 x 150 mL). The diethyl ether was dried over magnesium sulfate and evaporated to give *7-(allyloxy)-1,1,2,2,3,3,4,4,5,5,6,6-dodecafluoroheptane* (38.7 g, 85.3 %) as a clear oil; b.p. 94.0 – 96.1 °C (25.1 mbar); HRMS (ASAP) Found $[M\text{-}H]^+$ 371.0286, $C_{10}H_7F_{12}O$ requires 271.0305; ^{1}H NMR (600 MHz, $CDCl_3$): δ 6.02 (1H, tt, $^2J_{HF}$ 51.9, $^3J_{HF}$ 5.2, H*C*F_2CF_2), 5.91 – 5.85 (1H, m, CH_2CHCH_2), 5.34 – 5.25 (2H, m, CHCH_2), 4.13 (2H, m, OCH_2CH), 3.92 (2H, t, $^3J_{HF}$ 14.0, CH_2CF_2); ^{13}C (151 MHz, $CDCl_3$): δ 135.0 – 119.4 (12F, m, CF_2, CF_3 (overlapping)), 132.9 (CH), 118.3 (*C*H_2CH), 73.3 (O*C*H_2CH), 66.4 (t, $^2J_{CF}$ 25.5, O*C*H_2CF_2); ^{19}F (564 MHz, $CDCl_3$): δ -120.0 – -120.8 (2F, m, CF_2), -122.6 (2F, m, CF_2), -123.9 (4F, m, CF_2) -130.0 (2F, m, CF_2), -137.7 (2F, d, $^2J_{HF}$ 50.8, CF_2H); *m/z* (ASAP) 371.0 (100 %, $[M\text{-}H]^+$).

1,6-Bis(allyloxy)-2,2,3,3,4,4,5,5-octafluorohexane, 53

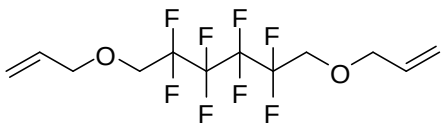

53

2,2,3,3,4,4,5,5-Octafluorohexane-1,6-diol (5.034 g, 19.2 mmol), potassium carbonate (8.412 g, 60.9 mmol) and allyl bromide (28.00 g, 231.4 mmol) were dissolved in

acetone (150 mL). The mixture was refluxed for 120 hours, with further addition of allyl bromide (14.00 g, 115.7 mmol) after 66 hours, and potassium carbonate (3.488 g, 25.2 mmol) after 90 hours. After cooling the mixture was washed with water (150 mL), with organic components extracted into DCM (3 x 50 mL) and dried over magnesium sulfate. Evaporation of solvent from the organic layer led to formation of a brown solid, which was recrystallised from hexane. The recrystallised material was washed with acetone, and the filtrate dried *in vacuo* to leave *1,6-bis(allyloxy)-2,2,3,3,4,4,5,5-octafluorohexane* (2.844 g, 43 %) as a colourless oil; HRMS (ASAP) Found $[M-H]^+$ 341.0785, $C_{12}H_{14}F_7O_2$ requires 341.0788; ^{1}H NMR (400 MHz, $CDCl_3$): δ 5.82 (1H, ddt, $^3J_{HH}$ 17.2, 10.3, 5.7, OCH_2CH), 5.24 – 5.14 (2H, m, $CHCH_2$), 4.07 – 3.98 (2H, m, OCH_2CH), 3.85 (2H, t, $^3J_{HF}$ 13.2, CF_2CH_2); ^{13}C NMR (101 MHz, $CDCl_3$): δ 132.1 (CH), 117.6 (CH_2CH), 72.4 (CF_2CH_2, CH_2CH); ^{19}F (376 MHz, $CDCl_3$): δ - 120.4 (2F, s, CF_2CH_2); -124.4 (2F, s, CF_2CF_2); *m/z* (ASAP) 341.0 (82 %, $[M-H]^+$), 279.1 (100).

2,2'-(2,2,3,3,4,4,5,5-Octafluorohexane-1,6-diyl)bis(oxy)bis(methylene)dioxirane, 55

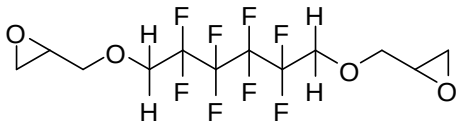

55

Method 1: Sodium hydroxide flakes (8.054 g, 201.4 mmol), tetra-*n*-butylammonium bromide (1.707 g, 5.30 mmol), 2,2,3,3,4,4,5,5-octafluorohexane-1,6-diol (25.016, 95.4 mmol), water (5.20 g, 288.9 mmol) and (±)epichlorohydrin (118.1 g, 1.28 mol) were combined in a flask fitted with a drying tube. The resulting mixture was stirred at room temperature for 26 hours before addition of further (±)epichlorohydrin (59.1 g, 638.8 mmol). Following this the mixture was stirred for 73 hours and sodium hydroxide (807 mg, 20.2 mmol) added prior to 20 hours of stirring and addition of a further portion of sodium hydroxide (821 mg, 20.5 mmol). After 70 hours of stirring, the mixture was filtered. The filtrate was washed with water (20 mL) and the organic components extracted into DCM (2 x 15 mL). The DCM layer was purified by vacuum distillation to

remove both DCM and epichlorohydrin (26-28 °C, 18.2 mbar), leaving *2,2'-(2,2,3,3,4,4,5,5-octafluorohexane-1,6-diyl)bis(oxy)bis(methylene)dioxirane* (33.2 g, 93.1 %) as a grey oil; HRMS (ASAP) Found $[M+H]^+$ 375.0836, $C_{12}H_{15}F_8O_4$ requires 375.0843; ^{1}H NMR (400 MHz, $CDCl_3$): δ 4.07 – 3.94 (3H, m, C*H*$_2$CF$_2$, CHC*H*$_2$O), 3.55 – 3.50 (1H, m, CHC*H*$_2$O), 3.19 – 3.15 (1H, m, C*H*CH$_2$O) 2.83 – 2.80 (1H, m, C*H*$_2$(O)CH), 2.64 – 2.61 (1H, m, C*H*$_2$(O)CH); ^{13}C NMR (101 MHz, $CDCl_3$): δ 73.2 (*C*H$_2$CH), 68.6 (t, $^2J_{CF}$ 24.2, *C*H$_2$CF$_2$), 50.6 (CH$_2$*C*H), 43.9 (CH*C*H$_2$O); ^{19}F (376 MHz, CD_3Cl): δ -120.1 (4F, s, CF$_2$CH$_2$), -123.9 (4F, m, C*F*$_2$CF$_2$CH$_2$); *m/z* (ASAP) 375.1 (100 %, $[M+H]^+$), 357.1 (50), 301.1 (46).

Method 2: 1,6-Bis(allyloxy)-2,2,3,3,4,4,5,5-octafluorohexane (2.536 g, 7.42 mmol) was dissolved in a 1:5 mixture of water:acetone and stirred. To this solution was added trichloroisocyanuric acid (1.811 g, 7.79 mmol) prior to further stirring at ambient temperature for 18 hours. After addition of DCM (30 mL) the reaction mixture was filtered and the filtrate washed with sodium sulfate (2 x 20 mL) and water (20 mL). Removal of the organic solvent *in vacuo* gave a yellow oil to which was added pentane (22 mL), diethyl ether (22 mL), water (10 mL) and potassium hydroxide (1.133 g, 20.2 mmol). After 18 hours of stirring at ambient temperature the reaction mixture was washed with water (2 x 10 mL) and dried over sodium sulfate. Removal of the organic solvent gave *2,2'-(2,2,3,3,4,4,5,5-octafluorohexane-1,6-diyl)bis(oxy)bis(methylene) dioxirane* (1.493 g, 53.8 %) as a colourless oil; physical and spectral analysis as above.

Method 3: A mixture of 1:4 F_2:N_2 was passed through a solution of 1:9 water:acetonitrile (20 mL) cooled to – 20 °C at a rate of 30 mL min^{-1} for 60 minutes, after which the flask was purged with nitrogen for two minutes. To this flask was added 1,6-bis(allyloxy)-2,2,3,3,4,4,5,5-octafluorohexane (1.364 g, 3.99 mmol) dissolved in acetonitrile (2 mL) and the mixture left to react for five minutes, before addition of saturated aqueous sodium bicarbonate (45 mL) and extraction of the organic components into DCM (2 x 10 mL). The DCM layer was dried over anhydrous magnesium sulfate and reduced *in vacuo* to leave *2,2'-(2,2,3,3,4,4,5,5-octafluorohexane-1,6-diyl)bis(oxy)bis(methylene) dioxirane* (1.052 g, 70.4 %) as a colourless oil; physical and spectral analysis as above.

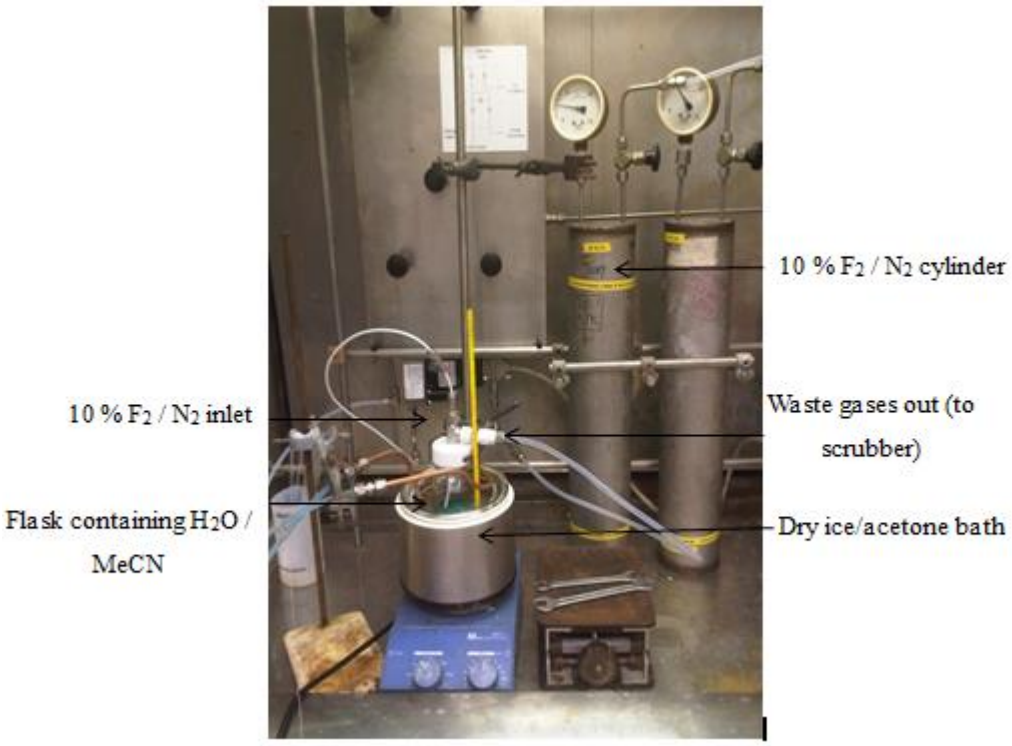

2-((3,3,4,4,5,5,6,6,7,7,8,8,8-Tridecafluorooctyloxy)methyl)oxirane, 56

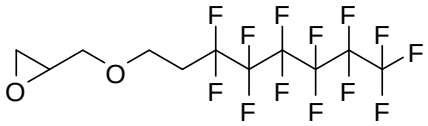

56

A mixture of 1:4 F_2:N_2 was passed through a solution of 1:9 water:acetonitrile (20 mL) cooled to – 35 °C at a rate of 30 mL min^{-1} for 30 minutes. Subsequently, the flask was purged with nitrogen for two minutes. To this flask was added 8-(allyloxy)-1,1,1,2,2,3,3,4,4,5,5,6,6-tridecafluorooctane (807 mg, 2.00 mmol) dissolved in acetonitrile (2 mL). Following three minutes of stirring the mixture was warmed to room temperature, and saturated aqueous sodium bicarbonate solution (20 mL) added before extraction of the organic components into DCM (2 x 10 mL). Evaporation of the DCM left *2-((3,3,4,4,5,5,6,6,7,7,8,8,8-tridecafluorooctyloxy)methyl)oxirane* (307 mg,

37 %) as a clear oil; HRMS (ASAP) Found $[M+H]^+$ 421.0477, $C_{11}H_{10}O_2F_{13}$ requires 421.0473; ^{1}H NMR (400 MHz, $CDCl_3$): δ 3.83 – 3.74 (3H, m, CH_2CH_2O, $CHCH_2O$), 3.37 (1H, dd, $^2J_{HH}$ 11.6, $^3J_{HH}$ 5.9, $CH_2(O)CH$), 3.16 – 3.12 (1H, m, $CH_2(O)CH$), 2.80 (1H, dd, $^3J_{HH}$ 5.0, 4.2, $CHCH_2O$), 2.62 – 2.60 (1H, m, $CH(O)CH_2$), 2.48 – 2.35 (2H, m, CH_2CF_2); ^{13}C NMR (101 MHz, $CDCl_3$): δ 135.0 – 118.0 (13F, m, CF_2, CF_3 (overlapping)), 71.9 (OCH_2CH), 63.3 (OCH_2CH_2), 50.8 (CH_2CH), 44.1 ($CH(O)CH_2$), 32.1 – 30.8 (m, CH_2CF_2); ^{19}F (376 MHz, $CDCl_3$): δ -81.0 (3F, s, CF_3), -113.6 (2F, s, CF_2), -122.0 (2F, s, CF_2), -123.0 (2F, s, CF_2), -123.8 (2F, s, CF_2), -126.3 (2F, s, CF_2); *m/z* (ASAP) 421.0 (100 %, $[M+H]^+$).

2-((2,2,3,3,4,4,5,5,6,6,7,7-Dodecafluoroheptyloxy)methyl)oxirane, 57

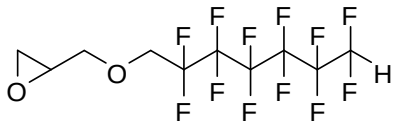

57

Method 1: A mixture of 1:4 F_2:N_2 was passed through a solution of 1:9 water:acetonitrile (20 mL) cooled to – 20 °C at a rate of 40 mL min^{-1} for 60 minutes, after which the flask was purged with nitrogen for two minutes. To this mixture was added 7-(allyloxy)-1,1,2,2,3,3,4,4,5,5,6,6-dodecafluoroheptane (778 mg, 2.09 mmol) dissolved in acetonitrile (2 mL). Following five minutes of stirring the mixture was warmed to room temperature, and saturated aqueous sodium bicarbonate solution (40 mL) added before extraction of the organic components into DCM (3 x 10 mL). Evaporation of the DCM left *2-((2,2,3,3,4,4,5,5,6,6,7,7-dodecafluoroheptyloxy)methyl)oxirane* (208 mg, 26 %) as a clear oil; HRMS (ASAP) Found $[M+H]^+$ 389.0403, $C_{10}H_9O_2F_{12}$ requires 389.0411; ^{1}H NMR (600 MHz, $CDCl_3$): δ 6.04 (1H, tt, $^2J_{HF}$ 54.2, $^3J_{HF}$ 5.2, HCF_2), 4.11 – 3.93 (3H, m, CF_2CH_2O, $CHCH_2O$), 3.51 (1H, dd, $^2J_{HH}$ 11.9, $^3J_{HH}$ 6.0, $CH_2(O)CH$), 3.17 – 3.15 (1H, m, $CH_2(O)CH$), 2.80 (1H, t, $^3J_{HH}$ 4.5, $CHCH_2O$), 2.63 – 2.61 (1H, m, CH_2CF_2); ^{13}C NMR (126 MHz, $CDCl_3$): δ 73.3 (OCH_2CH), 68.3 (t, $^2J_{CF}$ 120.1, CH_2CF_2), 50.6 (CH_2CH), 43.7

(CH(O)CH_2); ^{19}F (564 MHz, $CDCl_3$): δ -120.1 (2F, s, CF_2), -122.4 (2F, s, CF_2), -123.7 (4F, s, CF_2) -129.8 (2F, s, CF_2), -137.4 (2F, d, $^2J_{HF}$ 51.9, CF_2H); *m/z* (ASAP) 389.0 (100 %, $[M+H]^+$).

Method 2: Fluorine (16 mmol), as a 10 % mixture in nitrogen, was pushed through a microreactor along with a 1:4 methanol:water mixture (10 mL) and 7-(allyloxy)-1,1,2,2,3,3,4,4,5,5,6,6-dodecafluoroheptane (779 mg, 2.09 mmol) dissolved in 1:1 DCM:MeCN (10 mL). The products were collected in water (30 mL). After completion of the reaction saturated aqueous sodium hydrogen carbonate (30 mL) was added to the collection vessel and the organic components extracted into DCM (3 x 10 mL). Evaporation of DCM gave *2-((2,2,3,3,4,4,5,5,6,6,7,7-dodecafluoroheptyloxy)methyl)oxirane* (151 mg, 19 %) as a clear oil; physical and spectral data as above

2-((2,2,3,3,4,4,5,5,6,6,7,7,7-Tridecafluoroheptyloxy)methyl)oxirane, 59

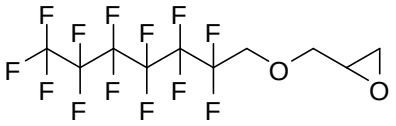

59

Sodium hydroxide flakes (3.010 g, 75.2 mmol), tetra-*n*-butylammonium bromide (1.208 g, 3.74 mmol), water (2.00 g, 111.1 mmol), 1*H*,1*H*,2*H*,2*H*-perfluoroheptan-1-ol (24.5 g, 70.0 mmol) and (±)epichlorohydrin (70.8 g, 76.5 mol) were combined in a flask fitted with a drying tube. The resulting mixture was stirred at room temperature for 79 hours, after which the mixture was washed with water (40 mL) and organics extracted into DCM (3 x 10 mL). The organic layer was dried over magnesium sulfate prior to vacuum distillation which led to isolation of *2-((2,2,3,3,4,4,5,5,6,6,7,7,7-tridecafluoroheptyloxy)methyl)oxirane* (8.00 g, 28 %) as a colourless liquid; b.p. 66.0 – 70.0 °C (6.7 mbar); HRMS (ASAP) Found $[M+H]^+$ 407.0308, $C_{10}H_8O_2F_{13}$ requires 407.0317; ^1H NMR (500 MHz, $CDCl_3$): 4.11 - 3.89 (3H, m, CF_2CH_2O, $CHCH_2O$), 3.51

– 3.47 (1H, m, CH_2(O)CH), 3.17 – 3.10 (1H, m, CH_2(O)CH), 2.81 - 2.72 (1H, m, CHCH_2O), 2.61 – 2.55 (1H, m, CHCH_2O); ^{13}C NMR (126 MHz, $CDCl_3$): δ 135.0 – 118.0 (13F, m, CF_2, CF_3 (overlapping)), 73.3 (OCH_2CH), 68.3 (t, $^2J_{CF}$ 25.6, CH_2CF_2), 50.6 (CH_2CH), 43.7 (CH(O)CH_2); ^{19}F (376 MHz, $CDCl_3$): δ -81.2 (3F, s, CF_3), -120.3 (2F, s, CF_2), -122.7 (2F, s, CF_2), -123.3 (4F, s, CF_2) -123.9 (2F, s, CF_2), -126.7 (2F, s, CF_2); *m/z* (ASAP) 407.0 (95 %, $[M+H]^+$), 389.0 (100), 377.0 (92).

7.5 Experimental to Chapter 5

Acrylic polyurethane

To paint 'bases' created by combining and stirring a hydroxyl functional acrylic (220 g, EW 1046 $gmol^{-1}$), talc (105 g, 277 mmol), methyl ethyl ketone (30 g, 416 mmol) and dibutyltin diacetate (70 mg, 199 μmol, 0.1 mol %) was added a polyisocyanate curing agent (4.5 g, EW 195 $gmol^{-1}$). The resulting mixture was stirred at 3000 rpm for 15 minutes and degassed under vacuum before application to test panels.

Fluorinated polyester resin

Neopentyl glycol (480.5 g, 4.61 mol), 2,2,3,3,4,4,5,5-octafluorohexane-1,6-diol (134 g, 51.1 mmol), trimethylolproane (11.1 g, 82.7 mmol) and BNT-cat 210 (500 mg) were combined with water (62.6 g, 3.48 mol) and heated to 85 °C. Once all the solid components had melted isophthalic acid (785.2 g, 4.73 mol) was added and the temperature raised to 150 °C for 15 minutes, after which the temperature was raised by 10 °C every 30 minutes up to 200 °C. After 60 minutes at 200 °C, by which time the solution was clear, the temperature was increased to 230 °C for 150 minutes, before being lowered to 150 °C overnight. After 17 hours the temperature was raised to 180 °C and neopentyl glycol (5.8 g, 55.7 mmol), 2,2,3,3,4,4,5,5-octafluorohexane-1,6-diol (1.6 g, 6.1 mmol) and isophthalic acid (109.6 g, 660.0 mmol) added and the temperature increased in 10 °C increments every 30 minutes up to a maximum of 230 °C. After four hours the temperature was again lowered to 150 °C. After 15 hours the temperature was set to 190 °C and a further quantity of both neopentyl glycol (2.9 g, 27.8 mmol) and

2,2,3,3,4,4,5,5-octafluorohexane-1,6-diol (0.8 g, 3.05 mmol) added. Immediately after addition of further diol the temperature was raised directly to 230 °C for six hours before lowering the temperature to 150 ° for 15 hours. After a further two hours at 230 °C the mixture was cooled to give the *fluorinated polyester resin* as a brown tinted glassy solid used without further purification.

Preparation of aluminium panels coated with a powder coating prepared from a novel fluorinated polyester resin

Fluorinated polyester resin (655.7 g), primid XL552 (26.2 g, 819 mmol), benzoin (3.0 g, 14.1 mmol), lanco wax 1525MF (4.0 g), Byk LPG21191 (10.0 g) and titanium dioxide (300 g, 3.76 mol) were combined and ground manually. The mixture was then twice passed through a twin screw extruder to form a homogeneous paste. The white paste was ground, through use of a commercial coffee grinder, and passed through a 106 μm sieve. The resulting powder was electrostatically spray coated onto QUV-A aluminium panels to a depth of 60 – 80 Å and the coated aluminium panels baked for 15 minutes at 200 °C.

Epoxy-amine functional systems

To a 25 g aliquot of a paint 'base' created by combining and stirring Bisphenol-A blend (70 g, EW 202 $gmol^{-1}$), talc (92.2 g, 243 mmol) and a 4:1 xyxlene:butanol mixture (37.6 g) was added a phenalkamine curing agent (4.9 g, EW 125 $gmol^{-1}$). The resulting mixture was stirred at 3000 rpm for 15 minutes to ensure full dispersion before application to test panels.

Application of 'wet' paint coatings to Sa2.5 steel panels/QUV-A panels

An aliquot of wet paint coating was placed onto sandblasted steel panels, cleaned to grade Sa2.5 or QUV-A panels pre-cleaned with acetone. The paint coating was then

spread over the surface of the metal panel through use of a draw-down bar (100 – 500 µm). The coated panels were then left to cure in air, under ambient conditions, for seven days before testing. Between four and eight panels were coated with each coating system.

Testing and analysis of coated panels

QUV-A data was found by placing coated aluminium panels into a QUV cabinet operating at 365 nm. The atmosphere within the cabinet altered between high humidity (> 100 % relative humidity) and high temperature (> 150 °C) with each cycle lasting four hours. Samples were monitored by eye for visual signs of blistering and peeling of the paint coating.

Surface gloss levels were found through use of a BYK Wavescan-II machine. For each coated panel a minimum of five readings at each angle (20 °, 60 °, 85 °) were performed and values averaged. The mean gloss value for each panel was then averaged with all other panels coated with the same coating to give the values reported.

Surface energies were found using a commercially available goniometer and a two-drop method (diiodomethane, water) with twenty readings taken per panel and one panel of each coating system tested. Values reported are based on the mean value of all ten contact angles for each liquid type.

Coated blasted steel panels were prepared for Prohesion testing by taping the edges of the panels and drilling a small circular hole in the coating. Taped panels were then placed in a Prohesion cabinet (C3 environment) alternating salt spray and heat cycles. Each cycle was an hour long, with the spray cycle performed at ambient temperature and the drying/heat cycle performed at 35 °C during which air at around 28 psi is added to aid drying.

The dry film thickness of samples on steel and aluminium panels was found by using a pre-calibrated Cole-Palmer handheld potentiometer. 12 measurements were taken for

each panel, and the mean of the twelve values reported as the DFT for the panel. Resin viscosity measurements were performed on a commercially available viscometer, with the heating unit set to 200 °C.

Water uptake was found by immersing plastic slides covered to a wet film thickness of 300 µm in water after one day of curing. The mass of the coated slide was measured periodically and referenced to the mass before immersion, giving a percentage change in mass as a function of time.

Adhesion of powder coatings was measured by two methods. Application of a 245 N force to the rear of a coated QUV-aluminium panel by dropping a 1 Kg weight from a height of 25 cm. The panel was then checked by eye for cracking and deformation of the substrate. Subsequently, a piece of masking tape was placed over the area and removed to observe adhesion of the powder coating to the aluminium surface. Adhesion was also investigated using the crosshatch test in which a test panel was scratched with a scalpel to create two perpendicular series of five lines 1 mm apart. Masking tape was used to cover the area and then peeled off to assess the adhesion of the coating to the surface.

7.6 Experimental to Chapter 6

1-Bromo-4-(trifluoromethyl)benzene, 69

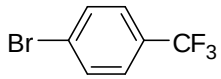

69

Under an inert atmosphere 1-bromo-4-iodobenzene (145 mg, 513 µmol) and 1,10-phenanthroline ligated (trifluoromethyl)copper (i) complex [(phen)$CuCF_3$] (267 mg, 854 µmol) were combined, dissolved in dry DMF (2.5 mL) and subsequently heated to 50 °C for 21 hours. After cooling to ambient temperature the solution was diluted with diethyl ether (20 mL) and passed through a celite pad which was washed with a further

portion of diethyl ether (20 mL). The combined filtrate was washed with 1 M HCl (20 mL), saturated aqueous sodium hydrogen carbonate (20 mL), brine (20 mL) and dried over sodium sulfate before evaporation of the filtrate which left *1-bromo-4-(trifluoromethyl)benzene* (57 mg, 50 %) as a light brown liquid; HRMS (ASAP) Found $[M]^{\cdot}$ 223.9194, $C_7H_4BrF_3$ requires 223.9448; ^{1}H NMR (600 MHz, $CDCl_3$): δ 7.63 (2H, d, $^3J_{HH}$ 8.4, CHCBr), 7.50 (2H, d, $^3J_{HH}$ 8.4, $CHCCF_3$); ^{13}C NMR (151 MHz, $CDCl_3$): δ 132.1 (*C*HCBr), 130.1 (*C*CF_3), 126.9 (*C*$HCCF_3$), 126.1 (CBr), 124.1 (CF_3); ^{19}F (564 MHz, $CDCl_3$): δ - 63.3 (3F, s, CF_3); *m/z* (GC-MS) 223.9 (100 %, [M]).

(*E*)-Stilbene, 70

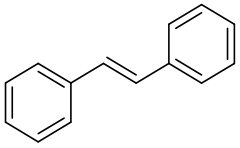

70

Styrene (454 mg, 4.36 mmol) and 3,3,4,4,5,5,6,6,7,7,8,8,8-tridecafluorooct-1-ene (15.01 g, 43.4 mmol) were combined under an atmosphere of argon. To this mixture was added Hoveyda-Grubbs 2nd generation catalyst (12 mg, 19.2 µmol) dissolved in benzyl trifluoride (3.57 g, 24.4 mmol). The resulting solution was heated to 45 °C for 69 hours after which it was reduced *in vacuo* to give a grey/green powder purified by recrystallisation from ethanol to give *stilbene* (220 mg, 56 %) as a white powder; m.p. 122.8 – 124.4 °C [lit. 122 – 125 °C] [3]; HRMS (ASAP) Found $[M]^+$ 180.0941, $C_{14}H_{12}$ requires 180.0939; ^{1}H NMR (400 MHz, $((CD_3)_2SO)$: δ 7.54 (1H, d, $^3J_{HH}$ 8.1, CHC*H*C), 7.38 (1H, t, $^3J_{HH}$ 7.7, C*H*CHC), 7.27 (1H, t, $^3J_{HH}$ 7.6, C*H*CHCHC), 7.26 (1H, s, C=CH); ^{13}C NMR (101 MHz, $((CD_3)_2SO)$: δ 137.5 (*C*CH=CH), 129.2 (CCHC*H*), 128.9 (C=CHCC*H*), 128.1 (C*H*CHCHC), 127.0 (C=*C*); *m/z* (ASAP) 181.1 (100 %, $[M+H]^+$), 180.1 (54).

(*E*)-1,2-Bis(2-chlorophenyl)ethene, 71

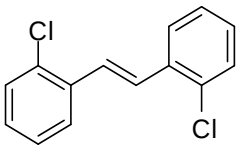

71

2-Chlorostyrene (659 mg, 4.77 mmol) and 3,3,4,4,5,5,6,6,7,7,8,8,8-tridecafluorooct-1-ene (15.01 g, 43.4 mmol) were combined under an atmosphere of argon. To this mixture was added Hoveyda-Grubbs 2nd generation catalyst (13 mg, 20.8 µmol) dissolved in benzyl trifluoride (2.56 g, 23.2 mmol). The resulting solution was heated to 45 °C for 67 hours after which it was reduced *in vacuo* to give a green solid, purified by recrystallisation from ethanol to give *1,2-bis(2-chlorophenyl)ethene* (299 mg, 50 %) as green tinted needle shaped crystals; m.p. 98.3 – 99.2 °C [lit. 98.5 – 99.0 °C] [4]; HRMS (ASAP) Found $[M]^+$ 248.0172, $C_{14}H_{10}Cl_2$ requires 248.0160; ^{1}H NMR (700 MHz, $((CD_3)_2SO)$: δ 7.86 (1H, d, $^3J_{HH}$ 7.6, CHCCl), 7.51 (1H, d, $^3J_{HH}$ 7.8, CC*H*CH), 7.48 (1H, s, C=CH), 7.40 (1H, t, $^3J_{HH}$ 7.4, C*H*CHC), 7.36 (1H, t, $^3J_{HH}$ 7.6, C*H*CHCCl); ^{13}C NMR (176 MHz, $((CD_3)_2SO)$: δ 134.7 (*C*Cl), 132.8 (CCl*C*C=C), 130.1 (*C*HCCl), 128.1 (*C*HCHCCl), 127.8 (*C*HCHC), 127.6 (C=C); *m/z* (ASAP) 249.0 (100 %, $[M+H]^+$).

(*E*)-1,2-Dio-tolylethene, 72

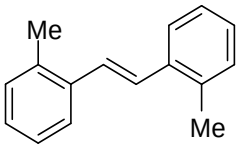

72

2-Methylstyrene (503 mg, 4.25 mmol) and 3,3,4,4,5,5,6,6,7,7,8,8,8-tridecafluorooct-1-ene (15.01 g, 43.4 mmol) were combined under an atmosphere of argon. To this mixture was added Hoveyda-Grubbs 2nd generation catalyst (12 mg, 19.2 µmol) dissolved in benzyl trifluoride (2.05 g, 18.6 mmol). The resulting solution was heated to 45 °C for 70 hours after which it was reduced *in vacuo* to give a grey solid, purified by

recrystallisation from ethanol to give *1,2-dio-tolylethene* (272 mg, 62 %) as silver/grey needle shaped crystals; m.p. 80.3 – 81.5 °C [lit. 75 – 77 °C] [5]; HRMS (ASAP) Found $[M]^+$ 208.1269, $C_{16}H_{16}$ requires 208.1252; ^{1}H NMR (700 MHz, $CDCl_3$): δ 7.60 (1H, d, $^3J_{HH}$ 7.4, C*H*CCH=CH), 7.24 – 7.22 (1H, m, C*H*CHCHCMe), 7.21 (1H, s, C=CH) 7.20 (1H, d, $^3J_{HH}$ 7.0, C*H*CHCMe), 7.19 (1H, d, $^3J_{HH}$ 7.1, C*H*CMe), 2.48 (3H, s, CH_3); ^{13}C NMR (176 MHz, $CDCl_3$): δ 136.8 (*C*CH=C), 135.8 (CMe), 130.3 (*C*HCHCMe), 128.0 (*C*HCMe), 127.5 (*C*HCHCC=C), 126.2 (C=C), 125.5 (*C*HCC=C), 19.9 (CH_3); *m/z* (ASAP) 209.1 (100 %, $[M+H]^+$), 179.1 (31).

(*E*)-1,1,1,2,2,3,3,4,4,5,5,6,6-Tridecafluorotetradec-7-ene, 73

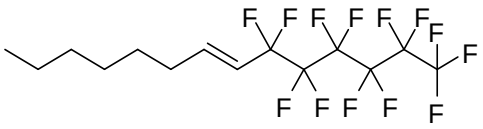

73

1*H*,1*H*,2*H*-Perfluorooct-1-ene (43.68 g, 12.6 mmol) and 1-octene (1.50 g, 13.4 mmol) were combined under an atmosphere of argon. To this was added Hoveyda-Grubbs 2nd generation catalyst (36 mg, 0.5 mol% loading) and the temperature was raised to 50 °C for 24 hours after which the flask was cooled to room temperature and reduced *in vacuo* to give a viscous green liquid. The liquid was taken up in chloroform (10 mL) and the fluorinated component of the mixture extracted into FC3280 (10 mL) which, when reduced, gave *(*E*)-1,1,1,2,2,3,3,4,4,5,5,6,6-tridecafluorotetradec-7-ene* (1.220 g, 22 %) as a colourless liquid; HRMS (ASAP) Found $[M-H]^+$ 429.0891, $C_{14}H_{14}F_{13}$ requires 429.0888; ^{1}H NMR (600 MHz, $CDCl_3$): δ 6.44 – 6.39 (1H, m, CH_2CH), 5.60 (1H, dt, $^3J_{HH}$ 15.5, $^3J_{HF}$ 12.1, $CHCF_2$), 2.22 – 2.18 (2H, m, CH_2CH), 1.46 (2H, p, $^3J_{HH}$ 7.3, $CH_2CH_2CH_2$), 1.35 – 1.28 (6H, m, CH_2), 0.90 (3H, t, $^3J_{HH}$ 6.8, CH_2CH_3); ^{13}C NMR (151 MHz, $CDCl_3$): δ 143.3 ($CHCH_2$), 117.1 (t, $^2J_{CF}$ 22.7, $CHCF_2$), 33.2 (t, $^4J_{CF}$ 12.8, CH_2CH), 28.9 (CH_2), 28.2 (CH_2), 22.7 (CH_2), 14.0 (CH_3); ^{19}F (564 MHz, $CDCl_3$): δ -81.5 (3F, s, CF_3), -111.8 (2F, s, CF_2), -122.1 (2F, s, CF_2), -123.4 (2F, s, CF_2), -124.1 (2F, s, CF_2), -126.7 (2F, s, CF_2); *m/z* (ASAP) 429.1 (25 %, $[M-H]^+$), 391.1 (85), 226.2 (100).

(*E*)-1,6-Dibromohex-3-ene, 75

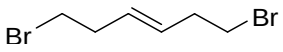

75

To a flask filled with argon was added 3,3,4,4,5,5,6,6,7,7,8,8,8-tridecafluorooct-1-ene (7.9 g, 22.9 mmol), 4-bromo-1-butene (293 mg, 2.17 mmol) and a solution of Hoveyda-Grubbs second generation catalyst (14 mg, 22.3 µmol) dissolved in benzyltrifluoride (1 mL). This mixture was heated to 45 °C from 68 hours after which the mixture was cooled to room temperature and reduced *in vacuo* to leave *(*E*)-1,6-dibromohex-3-ene* (179 mg, 34 %) as a dark oil; HRMS (ASAP) Found $[M+H]^+$ 242.9218, $C_{10}H_{11}Br_2$ requires 242.9207; ^{1}H NMR (400 MHz, $CDCl_3$): δ 5.55 – 5.53 (1H, m, CH_2CH), 3.38 (2H, t, $^3J_{HH}$ 7.0, CH_2Br), 2.60 – 2.56 (2H, m, CH_2CH); ^{13}C NMR (101 MHz, $CDCl_3$): δ 130.0 ($CHCH_2$), 35.9 (CH_2CH), 32.5 (CH_2Br); *m/z* (ASAP) 240.1 (100 %, $[M+H]^+$).

2,2,2-Trifluoro-1-(2-nitrophenyl)ethanol, 76

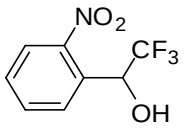

76

2-Nitrobenzaldehyde (7.732 g, 51.2 mmol) was dissolved in dry THF (60 mL) and cooled to 0 °C. To this solution was added both trifluoromethyltrimethylsilane (8.66 g, 60.9 mmol) and tetrabutylammounium fluoride (131 mg, 500 µm) before further stirring for two hours during which time the mixture warmed to ambient temperature. Siloxy compounds were hydrolysed with HCl and the solution taken up in diethyl ether (150 mL). The ether extract was washed with water (3 x 50 mL) and brine (3 x 50 mL) before being dried over anhydrous magnesium sulfate. Diethyl ether was evaporated to leave *2,2,2-trifluoro-1-(2-nitrophenyl)ethanol* (7.45 g, 66 %) as a brown oil; IR (cm^{-1}): 3504 (O-H), 1526 (NO_2); HRMS (ASAP) Found $[M-OH]^+$ 204.0255, $C_8H_5NO_2F_3$ requires 204.0272; ^{1}H NMR (700 MHz, $CDCl_3$): δ 7.98 (1H, d, $^3J_{HH}$ 8.2, $CHNO_2$), 7.95

(1H, d, $^{3}J_{HH}$ 7.9, C*H*CHC), 7.71 (1H, t, $^{3}J_{HH}$ 7.7, C*H*CHCNO$_2$), 7.56 (1H, t, $^{3}J_{HH}$ 8.4, C*H*CC(OH), 6.16 (1H, q, $^{3}J_{HF}$ 6.2, C*H*(OH)CF$_3$), 3.60 (1H, s, CHO*H*); ^{13}C NMR (176 MHz, CDCl$_3$): δ 148.5 (*C*NO$_2$), 133.9 (*C*CNO$_2$), 130.4 (*C*HCHCNO$_2$), 129.5 (*C*HCNO$_2$), 129.0 (*C*HCC(OH)), 125.0 (C*H*CHC), 124.0 (q, $^{1}J_{CF}$ 282.6, CH*C*F$_3$), 66.9 (q, $^{2}J_{CF}$ 32.8, *C*HCF$_3$); ^{19}F (376 MHz, CDCl$_3$): δ -77.9 (3F, d, $^{3}J_{HH}$ 7.7, CF$_3$); *m/z* (ASAP) 221.0 (18 %, [M]$^+$), 204.0 (100).

2,2,2-Trifluoro-1-p-tolylethanol, 77

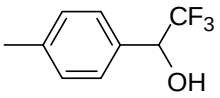

77

4-Methylbenzaldehyde (1.22 g, 10.2 mmol) was dissolved in dry THF (15 mL) and cooled to 0 °C. To this solution was added both trifluoromethyltrimethylsilane (1.73 g, 12.1 mmol) and tetrabutylammounium fluoride (26.2 mg, 100 µm) before stirring for two hours during which time the mixture warmed to ambient temperature. Siloxy compounds were hydrolysed with HCl and the solution taken up in diethyl ether (75 mL). The ether extract was washed with water (2 x 50 mL) and brine (2 x 50 mL) before drying over anhydrous magnesium sulfate. Diethyl ether was evaporated to leave *2,2,2-trifluoro-1-p-tolylethanol* (986 mg, 51 %) as a red oil; IR (cm^{-1}): 3380 (O-H); HRMS (ASAP) Found [M-OH]$^+$ 173.0511, C$_9$H$_8$F$_3$ requires 173.0578; ^{1}H NMR (600 MHz, CDCl$_3$): δ 7.37 (2H, d, $^{3}J_{HH}$ 7.9, C*H*CC(OH)), 7.23 (2H, d, $^{3}J_{HH}$ 7.9, C*H*CCH$_3$), 4.95 (1H, q, $^{3}J_{HF}$ 7.9, C*H*(OH)CF$_3$)), 2.40 (3H, s, Ar-CH$_3$); ^{13}C NMR (151 MHz, CDCl$_3$): δ 139.6 (*C*CH(OH)CF$_3$), 131.3 (*C*CH$_3$), 129.4 (*C*HCCH$_3$), 127.4 (*C*HCCHCF$_3$), 123.5 (q, $^{1}J_{CF}$ 282.0, CF$_3$), 72.8 (q, $^{2}J_{CF}$ 31.7, *C*H(OH)CF$_3$), 21.3 (Ar-CH$_3$); ^{19}F (564 MHz, CDCl$_3$): δ - 78.8 (3F, d, $^{3}J_{FH}$ 6.9, CF$_3$); *m/z* (ASAP) 190.1 (21 %, [M]$^+$), 173.1 (55).

2,2,3,3,3-Pentafluoro-1-(2-nitrophenyl)propan-1-ol, 78

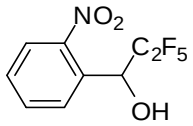

78

2-Nitrobenzaldehyde (7.345 g, 48.6 mmol) was dissolved in dry THF (60 mL) and cooled to 0 °C. To this solution was added both pentafluoroethyltrimethylsilane (11.68 g, 60.8 mmol) and tetrabutylammounium fluoride (130 mg, 500 µm) before stirring for two hours during which time the mixture warmed to ambient temperature. Siloxy compounds were hydrolysed with HCl and further THF (150 mL) added. The solution was diluted with diethyl ether (200 mL) and washed with water (50 mL) and brine (3 x 50 mL) before drying over anhydrous magnesium sulfate. Diethyl ether was evaporated to leave *2,2,3,3,3-pentafluoro-1-(2-nitrophenyl)propan-1-ol* (6.89 g, 53 %) as a brown oil; IR (cm^{-1}): 3496 (O-H), 1526 (NO_2); HRMS (ASAP) Found $[M\text{-}OH]^+$ 254.0240, $C_9H_5NO_2F_5$ requires 254.0240; ^1H NMR (600 MHz, $CDCl_3$): δ 8.00 (1H, d, $^3J_{HH}$ 8.2, $CHNO_2$), 7.99 (1H, d, $^3J_{HH}$ 7.8, C*H*CHCC(OH)), 7.72 (1H, t, $^3J_{HH}$ 7.6, C*H*CHCNO$_2$), 7.56 (1H, t, $^3J_{HH}$ 7.8, C*H*CC(OH)), 6.36 (1H, dd, $^3J_{HF}$ 18.7, 3.3, C*H*(OH)CF_2), 3.56 (1H, s, CHO*H*); ^{13}C NMR (151 MHz, $CDCl_3$): δ 148.5 (CNO_2), 133.9 (*C*HCNO$_2$), 130.4 (*C*HCHCNO$_2$), 130.1 (*C*HCNO$_2$), 129.0 (*C*HCC(OH)), 125.0 (*C*HCHC), 65.6 (dd, $^2J_{CF}$ 29.0, 21.1, *C*HCF_3); ^{19}F (564 MHz, $CDCl_3$): δ - 82.4 (3F, s, CF_3), - 119.5 (1F, d, $^2J_{FF}$ 282.2, CH(OH)CF_2), - 131.4 (1F, d, $^2J_{FF}$ 282.2 CH(OH)CF_2); *m/z* (ASAP) 271.0 (21 %, $[M]^+$), 254.0 (75), 239.2 (34).

2,2,3,3,3-Pentafluoro-1-p-tolylpropan-1-ol, 79

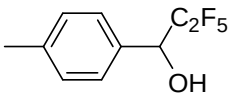

79

4-Methylbenzaldehyde (1.24 g, 10.3 mmol) was dissolved in dry THF (15 mL) and cooled to 0 °C. To this solution was added both trifluoromethyltrimethylsilane (2.728 g, 14.2 mmol) and tetrabutylammounium fluoride (26.2 mg, 100 µm) before stirring for three and a half hours during which time the mixture warmed to ambient temperature. Siloxy compounds were hydrolysed with HCl and the solution taken up in diethyl ether (75 mL). The ether extract was washed with water (2 x 50 mL) and brine (2 x 50 mL) before drying over anhydrous magnesium sulfate. Diethyl ether was evaporated to leave *2,2,3,3,3-pentafluoro-1-p-tolylpropan-1-ol* (1.435 g, 59 %) as an orange oil; IR (cm^{-1}): 3404 (O-H); HRMS (ASAP) Found $[M\text{-}OH]^+$ 223.0541, $C_{10}H_8F_5$ requires 223.0546; ^1H NMR (600 MHz, $CDCl_3$): δ 7.35 (2H, d, $^3J_{HH}$ 8.0, C*H*CC(OH)), 7.24 (2H, d, $^3J_{HH}$ 7.9, C*H*CCH_3), 5.05 (1H, dd, $^3J_{HF}$ 16.7, 7.6, C*H*(OH)CF_2)), 2.40 (3H, s, ArCH_3); ^{13}C NMR (151 MHz, $CDCl_3$): δ 139.9 (*C*CH(OH)CF_3), 131.1 (*C*CH_3), 129.5 (*C*HCCH_3), 127.9 (C*H*CCHCF_3), 72.0 (dd, $^2J_{CF}$ 27.8, 22.4, *C*H(OH)CF_2), 21.3 (ArCH_3); ^{19}F (564 MHz, $CDCl_3$): δ - 81.4 (3F, s, CF_3), - 122.18 (1F, d, $^2J_{FF}$ 276.4, C*F*$_2$CF_3), - 129.35 (1F, d, $^2J_{FF}$ 276.4, C*F*$_2$CF_3); *m/z* (ASAP) 223.1 (50 %, $[M\text{-}OH]^+$).

Tridecafluorohexyltrimethylsilane, 81

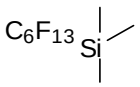

81

TDAE (2.00 g, 9.98 mmol) was dissolved in THF (20 mL) and cooled to -20 °C. To this was added a pre-mixed solution of 1-iodoperfluorohexane (5.35 g, 12.0 mmol) and trimethylsilyl chloride (1.08 g, 10.0 mmol). The reaction mixture was stirred for 2 hours over which time the reaction was allowed to warm to ambient temperature. The mixture

was distilled at 9.6 mbar to give tridecafluorohexyltrimethylsilane (3.90 g, 80 %) as an impure colourless liquid; HRMS (ASAP) Found $[M-H]^+$ 391.0192, $C_9H_8F_{13}Si$ requires 391.0188; ^1H NMR (400 MHz, $CDCl_3$): 0.23 (9H, s, CH_3); ^{19}F (376 MHz, $CDCl_3$): δ - 81.26 (3F, t, $^4J_{FF}$ 10.3, CF_3), -122.1 (2F, s, CF_2), - 121.9 (2F, s, CF_2), - 123.1 (2F, s, CF_2), - 126.4 (2F, s, CF_2), - 127.7 (2F, s, CF_2), *m/z* (ASAP) 391.0 (100 %, $[M-H]^+$).

2,2,3,3,4,4,5,5,6,6,7,7,7-Tridecafluoro-1-(2-nitrophenyl)heptan-1-ol, 83

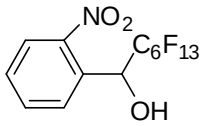

83

To a flask filled with argon was added tetrakis(dimethylamino)ethylene (8.18 g, 40.8 mmol) and dry DMF (40 mL). After cooling to - 30 °C a solution of 2-nitrobenzaldehyde (6.022 g, 39.8 mmol) and perfluorohexyl iodide (20.6 g, 46.2 mmol) in dry DMF (25 mL) was added and the mixture kept at between - 30 °C and - 20 °C for five hours after which the mixture was warmed to ambient temperature and water (75 mL) added. Fluorinated compounds were eluted with FC3280 (3 x 20 mL) and the fluorocarbon layer then reduced *in vacuo* to give a brown oil purified by silica chromatography (DCM as eluent) to afford *2,2,3,3,4,4,5,5,6,6,7,7,7-tridecafluoro-1-(2-nitrophenyl)heptan-1-ol* (262 mg, 1.4 %) as a colourless oil; HRMS (ASAP) Found $[M-OH]^+$ 454.0080, $C_{13}H_5F_{13}NO_2$ requires 454.0113; ^1H NMR (700 MHz, $CDCl_3$): 8.05 (1H, d, $^3J_{HH}$ 8.2, $CHNO_2$), 7.98 (1H, d, $^3J_{HH}$ 8.2, C*H*CHC), 7.75 (1H, t, $^3J_{HH}$ 7.6, C*H*CHCNO_2), 7.60 (1H, t, $^3J_{HH}$ 7.8, C*H*CC(OH)), 6.49 (1H, d, $^3J_{HF}$ 19.6, C*H*(OH)), 2.96 (1H, s, C(OH)); ^{13}C NMR (151 MHz, $CDCl_3$): δ 148.6 (CNO_2), 133.5 (*C*HCNO_2), 130.3 (*C*HCHCNO_2), 130.2 (*C*HCNO_2),128.9 (*C*HCC(OH)), 125.0 (*C*HCHC), 65.9 (*C*(OH)CF_2); ^{19}F (376 MHz, $CDCl_3$): δ - 81.26 (3F, t, $^4J_{FF}$ 10.3, CF_3), - 115.9 (1F, d, $^2J_{CF}$ 284.2, CH(OH)C*F*$_2$), -122.1 (2F, s, CF_2), - 121.9 (2F, s, CF_2), - 123.3 (2F, s, CF_2), - 126.6 (2F, s, CF_2), - 127.5 (1F, s, CF_2), *m/z* (ASAP) 454.0 (100 %, $[M-OH]^+$).

2,2,3,3,4,4,5,5,6,6,7,7,7-Tridecafluoro-1-p-tolylheptan-1-ol, 84

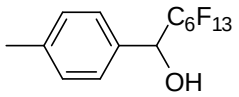

84

To a solution of tetrakis(dimethylamino)ethylene (3.96 g, 19.8 mmol) in dry DMF (20 mL) was added a mixture of 4-methylbenzaldehyde (2.85 g, 23.7 mmol) and perfluorohexyl iodide (9.28 g, 20.8 mmol) at - 30 °C. Following two hours of stirring at - 30 °C the solution was warmed to ambient temperature and stirred for a further 22 hours after which the reaction was quenched with 10 % HCl (20 mL) and the organic components extracted into DCM (3 x 20 mL). The DCM layer was washed with 10 % HCl (2 x 10 mL) and aqueous sodium thiosulfate (2 x 10 mL) before drying over magnesium sulfate. The organic layer was reduced *in vacuo* to give a yellow liquid purified by silica chromatography using DCM as eluent to give *2,2,3,3,4,4,5,5,6,6,7,7,7-tridecafluoro-1-p-tolylheptan-1-ol* (1.25 g, 60 %) as a white solid; HRMS (ASAP) Found $[M\text{-}OH]^+$ 423.0415, $C_{14}H_8F_{13}$ requires 423.0418; ^{1}H NMR (700 MHz, $CDCl_3$): δ 7.35 (2H, d, $^3J_{HH}$ 7.8, C*H*CC(OH)), 7.23 (2H, d, $^3J_{HH}$ 7.4, C*H*CCH_3), 5.17 (1H, dd, $^3J_{HF}$ 17.2, 3.8, C*H*(OH)CF_2)), 2.40 (1H, s (br), OH), 2.38 (3H, s, ArCH_3); ^{13}C NMR (176 MHz, $CDCl_3$): δ 139.9 (*C*CH(OH)CF_3), 131.2 (*C*CH_3), 129.5 (*C*HCCH_3), 128.0 (*C*HCCHCF_3), 72.4 (dd, $^2J_{CF}$ 28.8, 22.2, *C*H(OH)CF_2), 21.4 (ArCH_3); ^{19}F (564 MHz, $CDCl_3$): δ - 80.8 (3F, s, CF_3), - 118.1 (1F, d, $^1J_{CF}$ 283.3, CH(OH)CF_2), -122.2 (2F, s, CF_2), - 122.0 (2F, d, $^1J_{CF}$ 123.9, CF_2), - 122.8 (2F, d, $^1J_{CF}$ 136.5, CF_2), - 125.9 (2F, s, CF_2), - 126.2 (1F, s, CF_2); *m/z* (ASAP) 423.0 (100 %, $[M\text{-}OH]^+$).

References to chapter 7

1. Benefice-Malouet, S.; Blancou, H.; Calas, P.; Commeyras, A.; *J. Fluorine Chem.*, **1988**, 39, 245 – 260.

2. Quagliotto, P.; Barolo, C.; Barbero, N.; Barni, E.; Compari, C.; Fisicaro, E.; Viscardi, G.; *Eur. J. Org. Chem.*, **2009**, 19, 3167 – 3177.

3. Bluhm, H.F.; Donn, H.V.; Zook, H.D.; *J. Am. Chem. Soc.*, **1955**, 77, 4406 – 4407.

4. L'Ecuyer, P.; Turcotte, F.; Giguere, J.; Olivier, C.A.; Roberge, P.; *Can. J. Res., Section B: Chemical Sciences*, **1948**, 26, 70 – 71.

5. Xiao, X.; Lin, D.; Tong, S.; Luo, H.; He, Y.; Mo, H.; *Synlett*, **2011**, 12, 1731 – 1734.

8. Appendix

8.1 Crystallographic data

	2,2,3,3,4,4,5,5-Octafluorohexane-1,6-diyl bis(trifluoromethanesulfonate)
Identification code	11srv205
Empirical formula	$C_8H_4O_6F_{14}S_2$
Formula weight	526.23
Temperature/K	120
Crystal system	monoclinic
Space group	$P2_1/c$
a/Å	5.7159(2)
b/Å	9.1517(2)
c/Å	15.9169(5)
α/°	90.00
β/°	95.487(3)
γ/°	90.00
Volume/Å^3	828.80(4)
Z	2
ρ_{calc}mg/mm^3	2.109
m/mm^{-1}	0.501
F(000)	516
Crystal size/mm^3	0.59 × 0.11 × 0.06
2Θ range for data collection	5.14 to 60°
Index ranges	$-8 \le h \le 8$, $-12 \le k \le 12$, $-22 \le l \le 22$
Reflections collected	11055
Independent reflections	2412[R(int) = 0.0350]
Data/restraints/parameters	2412/0/144
Goodness-of-fit on F^2	1.040
Final R indexes [I>=2σ (I)]	R_1 = 0.0329, wR_2 = 0.0802
Final R indexes [all data]	R_1 = 0.0405, wR_2 = 0.0851
Largest diff. peak/hole / e Å^{-3}	0.504/-0.393

	(4,4,5,5,6,6,7,7,8,8,9,9,9-tridecafluorononyloxy)benzene
Identification code	12srv146
Empirical formula	$C_{15}H_{11}OF_{13}$
Formula weight	454.24
Temperature/K	120
Crystal system	monoclinic
Space group	$P2_1/c$
a/Å	28.5289(17)
b/Å	5.2551(3)
c/Å	11.1999(6)
α/°	90.00
β/°	97.016(5)
γ/°	90.00
Volume/Å^3	1666.55(16)
Z	4
ρ_{calc}mg/mm^3	1.810
m/mm^{-1}	0.212
F(000)	904.0
Crystal size/mm^3	0.3864 × 0.2638 × 0.046
2Θ range for data collection	5.76 to 57°
Index ranges	$-36 \leq h \leq 38$, $-5 \leq k \leq 7$, $-14 \leq l \leq 15$
Reflections collected	9326
Independent reflections	4205[R(int) = 0.0654]
Data/restraints/parameters	4205/0/306
Goodness-of-fit on F^2	1.057
Final R indexes [I>=2σ (I)]	R_1 = 0.0701, wR_2 = 0.1133
Final R indexes [all data]	R_1 = 0.1342, wR_2 = 0.1407
Largest diff. peak/hole / e Å^{-3}	0.45/-0.30

	(*E*)-1,2-bis(2-chlorophenyl)ethene
Identification code	13srv011
Empirical formula	$C_{14}H_{10}Cl_2$
Formula weight	249.12
Temperature/K	120
Crystal system	orthorhombic
Space group	Pbcn
a/Å	13.1270(3)
b/Å	11.6022(3)
c/Å	15.0696(3)
α/°	90.00
β/°	90.00
γ/°	90.00
Volume/Å^3	2295.15(9)
Z	8
ρ_{calc}mg/mm^3	1.442
m/mm^{-1}	0.531
F(000)	1024.0
Crystal size/mm^3	0.339 × 0.2291 × 0.1267
2Θ range for data collection	5.4 to 57.98°
Index ranges	$-17 \leq h \leq 17$, $-15 \leq k \leq 15$, $-20 \leq l \leq 20$
Reflections collected	34466
Independent reflections	3048[R(int) = 0.0731]
Data/restraints/parameters	3048/0/185
Goodness-of-fit on F^2	1.050
Final R indexes [I>=2σ (I)]	R_1 = 0.0358, wR_2 = 0.0868
Final R indexes [all data]	R_1 = 0.0508, wR_2 = 0.0962
Largest diff. peak/hole / e Å^{-3}	0.34/-0.24